Universidad de Oviedo

Universidad de Oviedo

Departamento de Biología Funcional

Programa de Doctorado "Investigación en Cáncer"

Mecanismos moleculares de daño y reparación durante la lesión pulmonar asociada a ventilación mecánica.

Tesis Doctoral

Adrián González López

Oviedo 2013

Universidad de Oviedo

Universidad de Oviedo

Departamento de Biología Funcional

Programa de Doctorado "Investigación en Cáncer"

Mecanismos moleculares de daño y reparación durante la lesión pulmonar asociada a ventilación mecánica.

Tesis Doctoral

Adrián González López

Oviedo 2013

ÍNDICE

ABREVIATURAS

αα	animoácido/s
ADN	ácido desoxirribonucleico
ADNc	ADN copia
ARN	ácido ribonucleico
CC16	proteína de células Clara
cmH_2O	centímetros de agua
DTNBP1	proteína de unión a distrobrevina-1
EGF	factor de crecimiento epidérmico
FiO_2	fracción inspirada de oxígeno
GSK3β	glicógeno sintasa kinasa-3β
HGF	factor de crecimiento de hepatocitos
IFN-γ	interferón gamma
IL	interleucina
kDa	kilodalton/s
KGF	factor de crecimiento de queratinocitos
LIX	quimiocina CXC inducida por Lipopolisacárido
MAPK	proteína quinasa activada por mitógeno
MCP-1	proteína quimiotáctica de monocitos-1
min	minutos
MIP-2	proteína inflamatoria de macrófagos-2
mmHg	milímetros de mercurio
PaO_2	presión arterial de oxígeno
RAGE	receptor de compuestos de glicosilación avanzada
TNFα	factor de necrosis tumoral alfa
SDS	dodecílsulfato de sodio
TGFβ	factor de crecimiento transformante beta

ABSTRACT

Acute respiratory distress syndrome (ARDS) is a lung injury condition with multiple etiologies characterized by an inflammatory process, increased alveolar permeability that generates a protein-rich pulmonary edema, hypoxia and increased work of breathing. Forty-five years after its formal description, pathogenetic mechanisms underlying ARDS are still largely unknown and the main strategy to maintain proper gas exchange is mechanical ventilation. However, this supportive treatment itself can cause lung damage. As a result of this, hospital mortality associated with this syndrome remains around 50% and almost all survivors face a significant decline in their quality of life, including different levels of residual lung disease, brain dysfunction and physical dependence.

Matrix metalloproteinases (MMPs) are a family of enzymes capable of processing a large number of extracellular matrix components. Among them, MMP-8 has a remarkable importance due to its capacity to perform a wide variety of functions that go far beyond processing structural elements of the extracellular matrix, like modulating the inflammatory response by interacting with different cyto- and chemokines. Also different MMPs have been implicated in repair and fibrosis processes after injury in various tissues.

The overall aim of the present thesis is to identify the role of MMP-8 during the different stages of ARDS, to establish a murine model to investigate the molecular mechanisms involved in lung repair after induced lung injury and to study the causes of brain dysfunction observed in patients undergoing mechanical ventilation.

Using mice genetically modified lacking MMP-8, we have shown that this metalloproteinase plays a dual and complex role, highly orchestrated over time. It has a proinflammatory role in the early hours of ventilator induced lung injury by facilitating the recruitment of neutrophils. However, in a model of endotoxemia prevents medium term leukocyte influx and promotes its clearance from lung parenchyma by modulating chemoattractans as S100A8 and S100A9. We have also shown that MMP-8 plays a deleterious role in the development of pulmonary fibrosis through IL-10 cleavage *in vivo*, which once processed loses its antifibrotic properties.

The establishment of a model of lung repair after VILI has allowed us to demonstrate that this type of injury is potentially reversible in a short period of time. The repair process depends on both an adequate and sufficient inflammatory response and an extracellular matrix remodelling. Regarding the latter, we found that MMP-2 promotes lung repair by facilitating epithelial migration, necessary for alveolar restoration.

Finally, we have identified a mechanisms whereby mechanical ventilation triggers neuronal excitotoxicity into the hippocampus, as a result of a hyperdopaminergic state in response to vagal signalling. These events trigger the activation of a Dysbindin-1C dependent system aimed to compensate the excess of dopamine release by removing their membrane cell receptors. This pathophysiological mechanism, supported by histological studies of brain autopsies from patients submitted to mechanical ventilation, could be a framework to explain the development of neuropsychological disorders in patients undergoing mechanical ventilation.

RESUMEN

El síndrome de distrés respiratorio agudo (SDRA) es un cuadro de lesión pulmonar con múltiples etiologías, caracterizado por un proceso inflamatorio con permeabilidad alveolar incrementada que genera un edema pulmonar rico en proteínas, hipoxia y un aumento del trabajo respiratorio. Cuarenta y cinco años después de su descripción oficial, los mecanismos patogenéticos del SDRA siguen siendo, en gran medida, desconocidos y sólo se dispone de tratamiento de soporte, siendo la ventilación mecánica la principal estrategia para el mantenimiento del intercambio gaseoso. Sin embargo, el uso de ventilación con presión positiva puede causar por sí mismo daño pulmonar. Como consecuencia de todo lo anterior, la mortalidad hospitalaria asociada a este síndrome permanece entorno al 50% y la práctica totalidad de los supervivientes se enfrentan a una importante merma en su calidad de vida, incluyendo distintos niveles de afectación pulmonar residual, disfunción cerebral y dependencia física.

Las metaloproteasas de matriz extracelular (MMPs) son una familia de enzimas capaces de procesar un gran número de componentes de la matriz extracelular. Dentro de ellas destaca la MMP-8, que es capaz de llevar a cabo una variedad de funciones que van más allá del procesamiento de los elementos estructurales de la matriz extracelular, modulando la respuesta inflamatoria mediante su interacción con distintas cito- y quimiocinas. También se han implicado diferentes MMPs en los procesos de reparación y fibrosis después de la lesión en distintos tejidos.

Dentro de este marco, se ha propuesto la presente Tesis Doctoral con el fin de identificar el papel de MMP-8 durante las distintas fases del SDRA, establecer un modelo que permita investigar los mecanismos moleculares implicados en la reparación pulmonar tras la lesión inducida por la ventilación mecánica (VILI) y estudiar las causas de la disfunción cerebral observada en pacientes sometidos a ventilación mecánica.

Utilizando ratones modificados genéticamente, deficientes en MMP-8, hemos demostrado que esta metaloproteasa juega un papel dual complejo y altamente orquestado en el tiempo. MMP-8 presenta un carácter pro-inflamatorio durante las

primeras horas del daño pulmonar inducido por ventilación mecánica facilitando el reclutamiento inicial de neutrófilos. Sin embargo, en un modelo de endotoxemia evita la llegada masiva de leucocitos a medio plazo y promueve su aclaramiento del parénquima pulmonar mediante su interacción con los potentes agentes quimiotácticos S100A8 y S100A9. Hemos demostrado también que MMP-8 juega un papel deletéreo durante el desarrollo de la fibrosis pulmonar mediante el procesamiento de IL-10 *in vivo*, que una vez procesada pierde sus propiedades antifibróticas.

El establecimiento de un modelo de reparación pulmonar tras el VILI nos ha permitido demostrar que este tipo de lesión es potencialmente reversible en un corto periodo de tiempo y que el proceso de reparación depende tanto de una adecuada y suficiente respuesta inflamatoria como del remodelado de la matriz extracelular. En lo concerniente a lo segundo, hemos mostrado que MMP-2 es capaz de promover la reparación pulmonar facilitando la migración epitelial necesaria para la reconstitución alveolar.

Finalmente, se ha identificado un mecanismo mediante el cual la ventilación mecánica desencadena procesos de excitotoxicidad neuronal en el hipocampo, como resultado de un estado de hiperdopaminergia en respuesta a una señalización vagal. Estos hechos desencadenan la activación de un sistema dependiente de disbindina-1C, encargado de compensar el exceso en la liberación de dopamina mediante la retirada de sus receptores de la membrana celular. Este mecanismo fisiopatológico, avalado por los estudios histológicos de autopsias cerebrales de pacientes sometidos a ventilación mecánica, podría servir para explicar el desarrollo de alteraciones neuropsicológicas en pacientes sometidos a ventilación mecánica.

INTRODUCCIÓN

El Síndrome de Distrés Respiratorio Agudo (SDRA).

Los pulmones conforman la superficie epitelial más extensa del organismo y se caracterizan por una estructura distribuida de alta complejidad. Se organizan como una monocapa de células epiteliales alineadas en forma de tubos que se ramifican hasta llegar a cada uno de los aproximadamente 480 millones de alveolos pulmonares (Ochs y col., 2004) que, en conjunto con el endotelio subyacente, actúan de interfase hematogaseosa. Los alveolos están formados principalmente por dos tipos celulares: los neumocitos tipo I, de morfología aplanada, que cubren la mayor parte de su superficie actuando de fina barrera frente al medio externo pero que permiten el intercambio gaseoso, y los neumocitos tipo II, de morfología cuboidal, que mediante una serie de funciones entre las que se encuentra su transdiferenciación a neumocitos tipo I ayudan a mantener la correcta función alveolar. También podemos identificar otros tipos celulares como macrófagos alveolares residentes con funciones de defensa y fibroblastos encargados de producir elementos de la matriz extracelular (ME). Ante cualquier agresión a este sistema, es de vital importancia el restablecimiento de la estructura capilar y la barrera epitelial del alveolo con el fin de restaurar la correcta difusión de gases y evitar así que tipos celulares intersticiales como los fibroblastos puedan invadir y colapsar los espacios alveolares.

Al proceso inflamatorio causado por el daño directo o indirecto del alveolo pulmonar se le conoce como síndrome de distrés respiratorio agudo (SDRA). Este síndrome se caracteriza por presentar hipoxemia arterial progresiva, disnea y un marcado incremento en el trabajo respiratorio. Documentado y hasta cierto punto descrito antes de 1900, en el último siglo el SDRA ha sido conocido por diversos nombres que incluyen: shock pulmonar, pulmón húmedo, pulmón de Da-Nang, atelectasia congestiva, síndrome del pulmón rígido y síndrome del pulmón blanco, por mencionar algunos. Durante la Segunda Guerra Mundial, Weed y McAfee fueron los primeros en informar de que soldados que habían sufrido shock traumático presentaban fallo respiratorio como consecuencia del mismo (Weed FW, 1927). Pero no fue hasta 1967 cuando Ashbaugh y colaboradores finalmente acuñaron el término de síndrome de distrés respiratorio agudo (Ashbaugh y col., 1967). En su estudio

describien el curso hospitalario de 12 pacientes críticos con diferente etiología que desarrollaron un repentino fallo respiratorio agudo con características fisiopatológicas muy similares. Todos estos pacientes presentaban síntomas de taquipnea, hipoxemia, resistencia refractaria a la oxigenación mediante soporte ventilatorio normal, cianosis, disminución de la distensibilidad pulmonar e infiltrado bilateral difuso en la radiografía del tórax.

En 1994 la conferencia del consenso americano-europeo introduce la definición de SDRA que ha sido utilizada hasta 2011 (Bernard y col., 1994). En ella se definió el SDRA como "un síndrome inflamatorio con permeabilidad incrementada que se asocia a un abanico de anormalidades clínicas, radiológicas y fisiológicas que no pueden ser explicadas, pero pueden coexistir, con el fallo cardiaco", incluyendo los criterios diagnóstico mostrados en la **Tabla 1**. Esta definición incluía el término daño pulmonar agudo (DPA) reservado para pacientes con severidad moderada con índice de oxigenación arterial (PaO_2/FiO_2) entre 200 y 300 mm Hg. En 2011, dentro del marco del Congreso de la Sociedad Europea de Medicina Intensiva realizado en Berlín (Ranieri y col., 2012) se propuso una nueva clasificación que eliminaba el término DPA y subdividía el SDRA en tres categorías mutuamente excluyentes basadas esencialmente en el grado de hipoxia (**Tabla 1**). En lo que respecta a esta tesis, nos referiremos indistintamente al daño pulmonar y al SDRA.

Ninguna de estas definiciones contempla la etiología del síndrome, sin embargo, una gran variedad de desórdenes clínicos pueden subyacer al SDRA. Se dividen entre aquellos derivados de una causa de lesión directa (pulmonares), más predecibles y con un periodo de latencia corto, y aquellos derivados de una causa indirecta (extrapulmonares) donde la respuesta inflamatoria sistémica suele tener un papel protagonista. Entre las pulmonares la más común es la neumonía con una incidencia del 42% (Villar y col., 2011). Otras causas de SDRA, de origen pulmonar, incluyen la aspiración de contenido gástrico, la ventilación mecánica, inhalación de sustancias tóxicas, traumatismos y el ahogamiento (Atabai and Matthay, 2002). La causa por excelencia de SDRA extrapulmonar es la sepsis abdominal con una incidencia del 31% (Villar y col., 2011), aunque también puede desencadenarse por

politraumatismos, quemaduras, embolia grasa provocada por fractura de huesos largos, shock hemorrágico, pancreatitis aguda y sobredosis de estupefacientes, entre otros. Independientemente de la causa, el SDRA converge en una patogénesis común caracterizada por un daño epitelial y endotelial del pulmón, que provoca un aumento de la permeabilidad alveolar, la invasión de un edema rico en proteínas procedentes del torrente sanguíneo y una respuesta inflamatoria aguda.

Tabla 1. Criterios de clasificación del SDRA.

Criterio de DPA y SDRA según el consenso americano-europeo (1994)				
	Tiempo	Oxigenación (PaO_2/FiO_2)	Radiografía de tórax	Presión enclavamiento arteria pulmonar
DPA	Comienzo agudo	≤300 mm Hg	Infiltrados bilaterales	≤18 mm Hg o sin evidencias de hipertensión en aurícula izquierda
SDRA	Comienzo agudo	≤200 mm Hg	Infiltrados bilaterales	≤18 mm Hg o sin evidencias de hipertensión en aurícula izquierda

Criterio de SDRA según la congreso de Berlín (2011)			
	Leve	*Moderado*	*Grave*
Tiempo de inicio	Inicio en menos de una semana desde el diagnóstico de la causa predisponente o aparición de un nuevo deterioro de los síntomas respiratorios.		
Imagen torácica	Opacidades bilaterales no explicables por derrame, atelectasias o nódulos.		
Origen del edema	Fallo respiratorio no explicable completamente por una insuficiencia cardiaca o la sobrecarga de líquidos.		
Hipoxemia (PaO_2/FiO_2)	200-300 mm Hg	100-200 mm Hg	<100 mm Hg

Cuarenta y cinco años después de la descripción oficial de este síndrome, la mortalidad de SDRA permanece elevada, generando un tremendo coste tanto humano como económico. Con una incidencia anual en España de 7,2 casos por cada 100.000 habitantes, la mortalidad hospitalaria ronda entre el 43 y el 48% (Villar y col., 2011). Si a eso le sumamos que un 56% de los pacientes que sobreviven a la estancia hospitalaria fallecen en el plazo de un año y que el 91% sufre algún tipo de dependencia funcional, es fácil concluir que el SDRA supone un importante problema sanitario (Cheung y col., 2006; Unroe y col., 2010).

Fisiopatología y patogénesis del SDRA.

La respuesta pulmonar ante una agresión precisa, en primer lugar, de la transducción de una señal de alarma a una respuesta bioquímica. Para ello es necesario un sistema capaz de detectar que el tejido se encuentra inmerso en un proceso patológico y de desencadenar respuestas fisiológicas primarias destinadas a frenarlo. Este sistema de alarma son los denominados patrones moleculares asociados al daño (DAMPS) que se dividen en dos familias. Cuando son de naturaleza exógena se denominan patrones moleculares asociados a patógenos o PAMPs. Constituyen este grupo un conjunto de moléculas de origen microbiológico, evolutivamente conservadas y con características similares que hacen posible la detección de un amplio abanico de especies patógenas mediante receptores tipo TLR (del inglés *Toll-like receptor*); la presencia de este tipo de receptores en el pulmón es elevada debido a su continua exposición al medio externo. Cuando son de naturaleza endógena son denominadas alarminas. En esta clase se incluyen un conjunto de moléculas estructuralmente diferentes, liberadas en respuesta al daño tisular por células en muerte no programada y por células inflamatorias locales (en el tejido pulmonar neumocitos y macrófagos alveolares, respectivamente), que activan y reclutan células del sistema inmune mediante su unión a receptores tipo TLR, IL-1R, RAGE (del inglés *Receptor of Advanced Glycation Endproducts*) (Bianchi, 2007). El reconocimiento de estos patrones moleculares mediante cualquiera de estas vías converge en la activación del factor nuclear-κB (NFκB). La translocación al núcleo de los factores de transcripción constituyentes de esta ruta induce la expresión de genes necesarios para perpetuar la respuesta inmune innata.

La activación de los macrófagos alveolares tras el reconocimiento de estas señales de daño tisular lleva a la producción de mediadores inflamatorios: 1) Prostaglandinas que producen vasodilatación provocando un descenso del flujo sanguíneo. 2) Citoquinas proinflamatorias como IL-1 y TNFα que actúan aumentando la permeabilidad de células endoteliales de los vasos cercanos mediante la expresión de P-selectina, E-selectina, moléculas de adhesión intercelular (ICAM-1) y de adhesión vascular (VCAM-1), facilitando así la migración transendotelial de los leucocitos. 3)

Quimiocinas como LIX y MIP-2 (en ratones) o IL-8 y MCP-1 (en humanos) que se encargan de "dirigir" la migración.

La vasodilatación y aumento de la permeabilidad vascular inducida por la activación de macrófagos, unida a la destrucción celular, especialmente de los neumocitos tipo I, produce una salida de plasma hacia el espacio intersticial y alveolar que inactiva el surfactante pulmonar. La aparición en el pulmón de un edema rico en proteínas, la infiltración neutrofílica, la destrucción del tapizado celular del alveolo y la consecuente formación de membranas hialinas ricas en fibrina, fibronectina y restos celulares (Simon R.H, 1992) son características definitorias de lo que se conoce típicamente como fase exudativa del SDRA (**Figura 1**) y se traducen en el cuadro histopatológico denominado daño alveolar difuso. Las autopsias de los pacientes fallecidos durante esta fase muestran unos pulmones rígidos, rojo-azulados y pesados debido a la hemorragia y a la formación de edema (Tomashefski, 2000).

El infiltrado inflamatorio durante las primeras horas está constituido esencialmente por leucocitos polimorfonucleares neutrófilos. Esta población celular representa entre el 60-70% del total de leucocitos circulantes (Stefanidakis and Koivunen, 2006) y responde rápidamente a las quimiocinas, especialmente del grupo CXC. Normalmente entran en apoptosis una vez que llegan al tejido infiltrado, de tal manera que al cabo de unas horas son progresivamente reemplazados por monocitos, que no sólo sobreviven en los tejidos, sino que proliferan dando lugar a macrófagos. No obstante, en algunos casos las poblaciones leucocitarias pueden variar. Por ejemplo, en infecciones por Pseudomonas los neutrófilos se reclutan de forma continua durante varios días, mientras que en infecciones virales la respuesta principal es de estirpe linfoide. Pero este corto tiempo de respuesta, tan favorable a la hora de responder ante una agresión, tiene su precio sobre la integridad y funcionalidad alveolar. En un primer momento la vasodilatación y el edema pulmonar, favorecidos por los macrófagos residentes en el pulmón, producen un aumento en la viscosidad sanguínea debido al aumento en la concentración de glóbulos rojos. La caída del flujo sanguíneo provoca un fenómeno denominado "marginación" en el cual los leucocitos salen más fácilmente del centro del vaso hacia los laterales e interaccionan con el

endotelio vascular, primero mediante interacciones débiles de tipo selectina en las cuales el leucocito "rueda" sobre la superficie del vaso y seguidamente a través de la unión de integrinas con ICAM-1 y VCAM del endotelio, formándose una unión más fuerte denominada "arresto" que lleva al leucocito hacia los sitios preferentes de migración transendotelial. En ese punto se inicia migración, que puede ser de dos tipos: paracelular a través de las uniones entre las células endoteliales; o transcelular mediante orgánulos vesículo-vacuolares (Woodfin y col., 2010).

Después de atravesar el endotelio y antes de llegar al espacio alveolar, el leucocito se encuentra con la membrana basal. Esta matriz extracelular compacta y altamente organizada se compone principalmente por cuatro familias de glicoproteínas (Lamininas, isoformas de colágeno tipo IV, nidógeno y proteoglicanos de heparán sulfato) (Korpos y col., 2009) y recubre la monocapa de células endoteliales separando los vasos sanguíneos del tejido intersticial. Puede influir directamente en el reclutamiento leucocitario hacia tejido inflamado a través de distintas señales de su composición molecular, o indirectamente mediante su potencial para unir y presentar citoquinas o factores quimiotácticos. El único modo que tienen los neutrófilos de cruzar esta barrera es a través de la degradación proteolítica mediante la liberación de metaloproteasas de matriz extracelular (MMPs) (Wolf y col., 2003). Además, estos enzimas facilitan la permeabilización vascular a través de la digestión de proteínas de unión entre células endoteliales (Reijerkerk y col., 2006), contribuyendo aun más al daño de la estructura pulmonar.

A esta fase exudativa le sigue la denominada fase proliferativa del SDRA (Ware and Matthay, 2000), en la que el organismo trata de llevar al pulmón al estado anterior a la lesión mediante la eliminación y retirada de los neutrófilos, la reabsorción del edema, y la reconstrucción del epitelio alveolar favoracida por la síntesis de colágeno. Los fenómenos de reparación inherentes a esta fase serán discutidos en profundidad en una sección posterior.

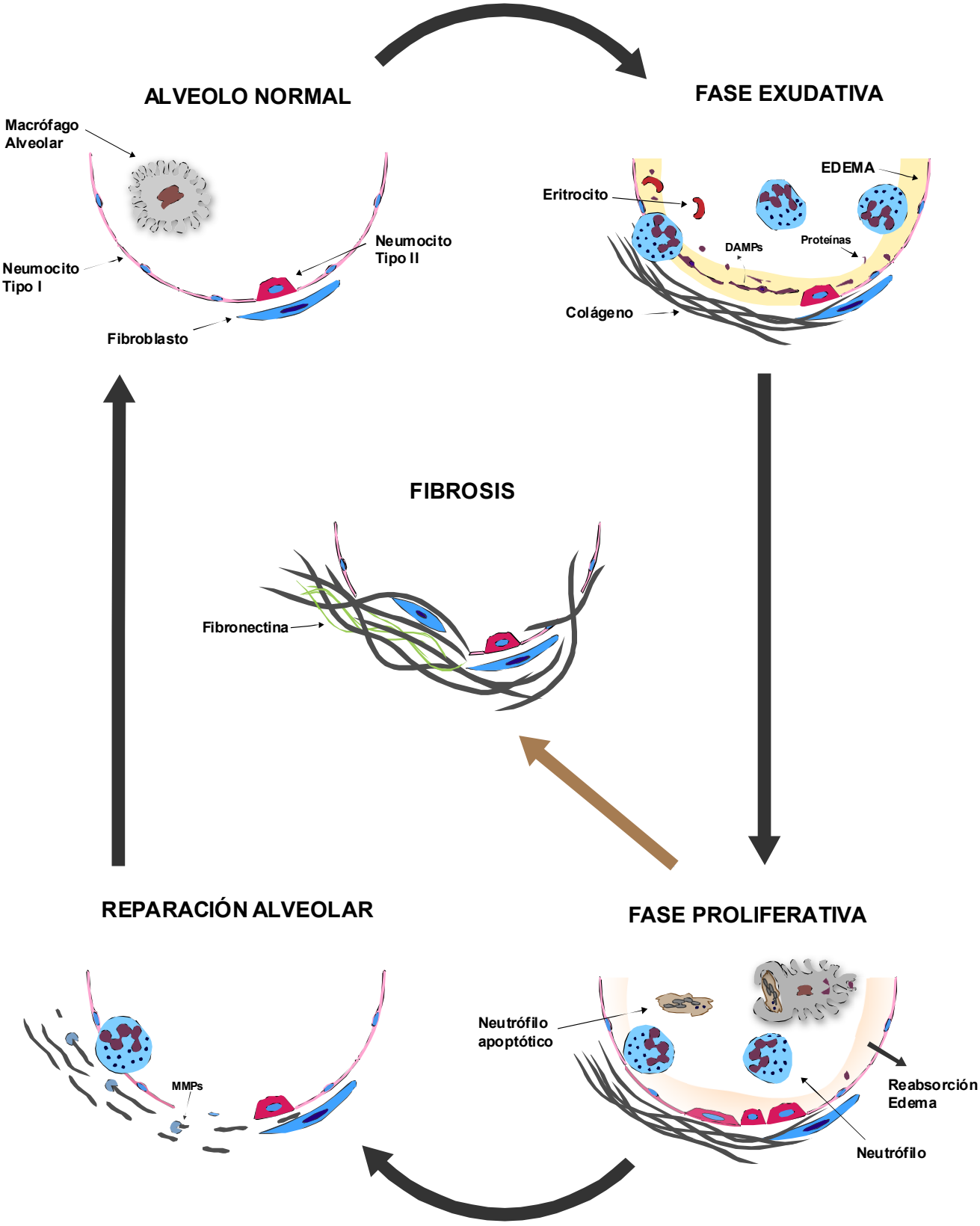

Figura 1. Fases del síndrome de distrés respiratorio agudo.

Daño pulmonar asociado a ventilación mecánica.

La ventilación mecánica es la piedra angular del tratamiento del SDRA en las unidades de cuidados intensivos (UCI) siendo, junto con el tratamiento de la enfermedad subyacente, la principal terapia para mantener un adecuado intercambio gaseoso. Aunque prácticamente todos los pacientes con SDRA reciben ventilación mecánica, este soporte vital dista enormemente de ser inocuo, ya que se asocia a una mortalidad entorno al 50% (Chertcoff y col., 2011). Desde hace tiempo es sabido que la ventilación mecánica "*per se*" puede inducir lesión en un pulmón sano e incluso empeorar una condición lesiva preexistente, a este fenómeno se le conoce como daño pulmonar asociado a la ventilación mecánica (VALI) (No-authors-listed, 2000). Este círculo vicioso de lesión - ventilación - VALI – lesión (**Figura 2**) complica la resolución del SDRA y hace que la ventilación mecánica llegue a ser, en los casos más severos, una causa relevante del mismo.

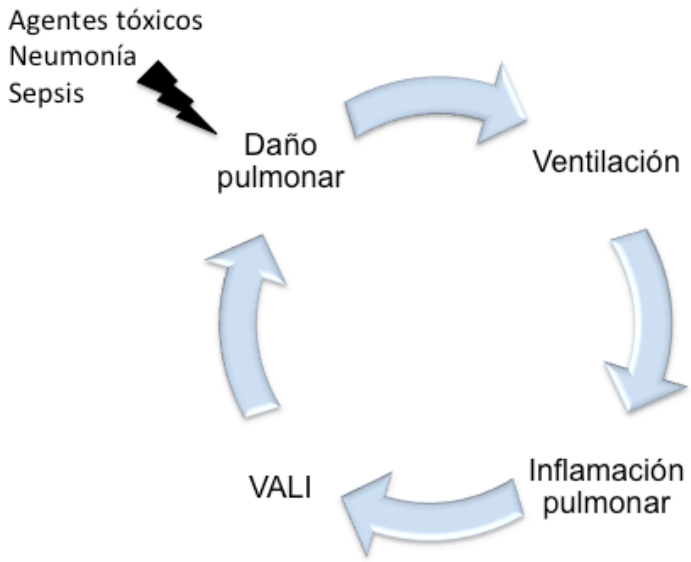

Figura 2. Esquema del daño pulmonar asociado a la ventilación mecánica.

La variedad de estudios llevados a cabo sobre el VALI así como sobre su homólogo en experimentación animal el VILI (del inglés *ventilator induced lung injury*) han permitido estudiar los mecanismos causantes del daño durante la ventilación mecánica y clasificarlos en tres categorías:

Volutrauma/Barotrauma: Referido a la relación existente entre el daño pulmonar y la sobredistensión alveolar generada por los volúmenes y presiones procedentes del ventilador mecánico al final de la inspiración. Los trabajos iniciales de Webb y Tierney, en los que ratas sometidas a ventilación con presiones elevadas presentaban un importante edema tanto perivascular como alveolar (Webb and Tierney, 1974), demostraron que la sobredistensión pulmonar podía dañar el parénquima. Estudios posteriores llevaron a la idea aceptada hoy día de que un alto volumen corriente durante la ventilación produce fenómenos de sobredistensión con riesgo de rotura de las paredes alveolares. Basándose en este hecho la práctica clínica se ha dirigido hacia la utilización de volúmenes corrientes bajos, en lo que se ha denominado como "ventilación protectora". El empleo de estas estrategias de ventilación se ha traducido en una mejora sustancial de la supervivencia en pacientes con SDRA (Montgomery y col., 1985; Ranieri y col., 1999; No-authors-listed, 2000) y en una menor incidencia de daño pulmonar tras la ventilación en pacientes con pulmones sanos. El problema de la sobredistensión se agrava cuando el pulmón sometido a ventilación presenta una lesión previa. La distribución heterogénea de las zonas de lesión lleva a la coexistencia de alveolos sanos y zonas de colapso alveolar (atelectasia). En estos casos incluso la utilización de estrategias de ventilación con bajos volúmenes corrientes es problemática, ya que la distribución de la ventilación se dirige preferentemente a los alveolos sanos, más compilantes, y genera sobredistensión de los mismos. En último término, este fenómeno se traduce en un aumento del daño pulmonar (Gattinoni y col., 1987; Terragni y col., 2007).

Atelectrauma: Referido a la lesión pulmonar causada por las variaciones cíclicas de la aireación de alveolos colapsados durante la ventilación. La causa mecánica de este proceso es el descenso de las presiones en la vía aérea durante la espiración por debajo de las presiones de cierre. Por lo tanto se asocia al empleo de una ventilación

con un bajo volumen teleespiratorio, más que por un bajo volumen corriente (Muscedere y col., 1994). En la práctica clínica se ha intentado llegar a un equilibrio que evite, en la medida de lo posible, tanto la sobredistensión alveolar como el atelectrauma, utilizando la denominada presión espiratoria final positiva (PEEP). Así una PEEP apropiada mantendría el pulmón parcialmente inflado al final de la espiración, consiguiendo evitar el estrés de cierre y reapertura de los alveolos colapsados. El ajuste del volumen corriente y de la PEEP han sido hasta la fecha los únicos procedimientos que han demostrado sobradamente su capacidad para disminuir el VALI. Sin embargo, la eficacia en el ajuste de los parámetros ventilatorios parece llegar a su límite (Curley y col., 2005; Meade y col., 2008; Bein y col., 2013) lo que hace necesario el desarrollo de otro tipo de aproximaciones para atenuar el VALI.

Biotrauma: Este mecanismo de lesión hace referencia a la liberación de mediadores inflamatorios en el pulmón ventilado y su posterior difusión sistémica. Se caracteriza por la llegada del infiltrado neutrofílico y la producción de citoquinas proinflamatorias, entre otras moléculas (Tremblay y col., 1997). La hipótesis del biotrauma viene soportada por estudios que muestran un aumento de infiltrado y liberación de citoquinas proinflamatorias tanto en lavados broncoalveolares como en plasma de pacientes sometidos a ventilación mecánica, fenómeno que se ve atenuado con el uso de estrategias de ventilación protectoras y PEEP (No-authors-listed, 2000; Imanaka y col., 2001); y por el hecho de que la mayoría de los pacientes con SDRA que fallecen, no lo hacen a causa del fallo respiratorio sino por una disfunción orgánica múltiple (MODS) (Slutsky and Tremblay, 1998), lo que podría explicarse por una descompartimentalización de la inflamación causada por la pérdida de la permeabilidad del endotelio local (Imai y col., 2003). A la traducción de los estímulos físicos, causados por la ventilación mecánica, en una respuesta bioquímica y molecular como la observada durante el biotrauma se le conoce como mecanotransducción. La conversión de fuerzas físicas externas en una señal que module la expresión génica o la estructura celular juega un papel importante en el desarrollo del VALI. Aunque se desconocen con exactitud los procesos exactos de la mecanotransducción, si se han identificado múltiples vías sensibles al estiramiento como canales de iones (Naruse and Sokabe, 1993), receptores de integrina encargados de transmitir las fuerzas

presentes en el intersticio pulmonar al interior celular (Taniguchi y col., 2010) o la quinasa de adhesión focal cuya activación aumenta la expresión de P-selectina facilitando el reclutamiento (Bhattacharya y col., 2003). Así mismo, cuando los mecanismos de reparación de membrana se ven superados por la magnitud de las fuerzas de sobredistensión originadas por la ventilación mecánica, la disrupción generada provoca la entrada de calcio al interior celular que actúa como sensor de daño y dispara la activación de rutas de señalización dependientes de NFκB y Fos (Grembowicz y col., 1999). El biotrauma contribuye a la persistencia del estado inflamatorio que se asocia con un peor pronóstico de los pacientes con SDRA (Meduri y col., 1995; Headley y col., 1997). Es por ello que la mayoría de las estrategias llevadas a cabo en modelos experimentales de ventilación mecánica se han basado en tratar de minimizar el daño inicial interfiriendo la respuesta inflamatoria pulmonar. Sin embargo, aunque muchas han obtenido resultados prometedores, su traslado a la práctica clínica ha tenido resultados decepcionantes (Uhlig and Uhlig, 2004).

Todos estos estudios sugieren que los mecanismos moleculares desencadenados durante el SDRA y el VILI son idénticos, e involucran la liberación de mediadores inflamatorios, infiltración neutrofílica y remodelado de la matriz extracelular. Es necesario estudiar el papel que juegan las MMPs específicas en dichos procesos para entender los mecanismos subyacentes al daño.

Reparación pulmonar.

Durante el desarrollo de la presente tesis doctoral nos interesamos también por el proceso de reparación pulmonar tras el daño inducido por la ventilación mecánica, que ha empezado a ser objeto de estudio hace apenas cinco años. En 2008, Nin y colaboradores publicaron un primer estudio al respecto (Nin y col., 2008). Sometieron a ratas de la cepa Sprague-Dawely a ventilación mecánica lesiva durante una hora, restableciendo luego su respiración espontanea y dejándolas recuperar. Los estudios histológicos mostraron una reducción significativa de la congestión capilar, el

edema intersticial, la necrosis de neumocitos tipo I y la formación de membranas hialinas tras veinticuatro horas de recuperación, alcanzando la normalidad tras 72 horas. Los mediadores inflamatorios mostraron un patrón similar. Esta rápida reversión del VILI tras el restablecimiento de la respiración espontanea nos animó a ahondar más en el estudio de los procesos de reparación tras el VILI.

Tras el daño pulmonar, este órgano, que en condiciones normales presenta una tasa de recambio celular y remodelado de matriz extracelular bajos, tiene que repararse lo más rápido posible. La reabsorción del edema, la regulación de la respuesta inflamatoria, en la que tiene un papel importante la eliminación del infiltrado neutrofílico, y la reconstrucción del epitelio alveolar son los aspectos claves de lo que clásicamente se conoce como fase proliferativa del SDRA (**Figura 1**) (Ware and Matthay, 2000).

La eliminación del exudado alveolar se produce principalmente por un sistema de transporte vectorial de iones a través de canales de sodio del epitelio alveolar (ENaC, *Epithelial Na Channel*) presentes en neumocitos tipo I y II. El sodio entra por la membrana apical de las células epiteliales alveolares y sale a través de su membrana basolateral gracias a la acción de la bomba Na+/K+ ATPasa (Crandall and Matthay, 2001) (**Figura 3**). Los modelos animales deficientes en ENaC muestran una mayor susceptibilidad a la formación de edemas y un aclaramiento deficiente del mismo (Hummler y col., 1996; Egli y col., 2004). El cloruro y el agua siguen al transporte de sodio a través de rutas transcelulares y paracelulares para mantener la neutralidad osmótica y electroquímica de la membrana epitelial alveolar. El transporte de agua se realiza a favor de gradiente y viene facilitado por los canales denominados acuaporinas (AQP). Cuatro miembros de la familia de las acuaporinas (AQP-1, -3, -4 y -5) han sido identificados en el pulmón (Effros y col., 1997; Kreda y col., 2001; Williams, 2003). Su ausencia mediante delección génica en ratones reduce drásticamente el transporte de agua osmóticamente activo (Bai y col., 1999), no obstante cuando estos animales son sometidos a modelos de lesión pulmonar, no se observa ni un incremento en la formación de edema ni una deficiencia en su aclarado, probablemente debido a que la

misma afectación en la permeabilidad pulmonar causante del edema, favorezca enormemente el transporte paracelular (Song y col., 2000).

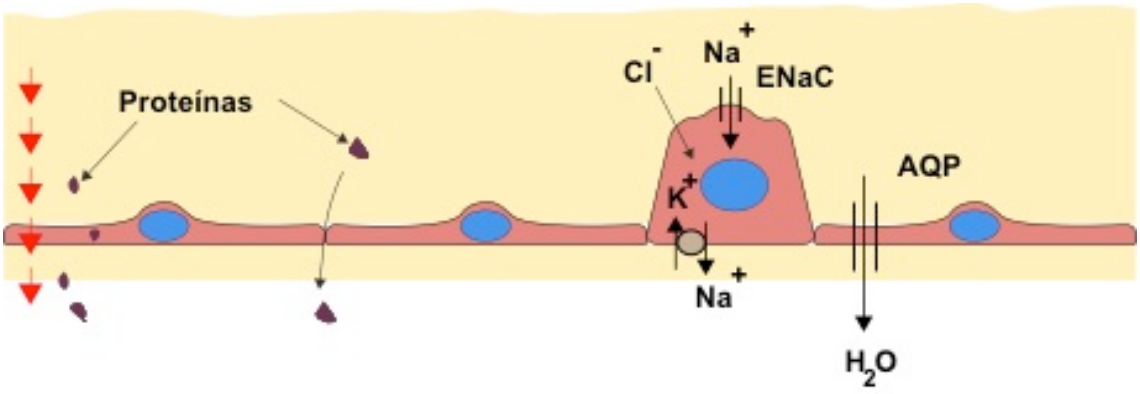

Figura 3. Mecanismos de reabsorción del edema pulmonar.

La eliminación del infiltrado neutrofílico que ha favorecido el estado inflamatorio de la fase exudativa y el bloqueo de los distintitos metabolitos liberados por el mismo (enzimas proteolíticos, citoquinas, mieloperoxidasa, acido araquidónico, leucotrienos y especies reactivas de oxígeno y de nitrógeno), es un paso más para el restablecimiento de la homeostasis tisular. Tres factores están implicados en la eliminación de los neutrófilos: 1) Su apoptosis, que se ha observado relacionada a la desaparición de factores estimulantes como G-CSF y GM-CSF (del inglés, *granulocyte y granulocyte-monocyte stimulating factor*, respectivamente) (Matute-Bello y col., 1997; Lesur y col., 2000), 2) su eliminación inocua del alveolo mediante fagocitosis y 3) el cese de su reclutamiento que se consigue gracias a la síntesis de inhibidores de la quimiotaxis de neutrófilos como el CC16 (Geerts y col., 2001) y autoanticuerpos anti IL-8 (Fudala y col., 2008).

Contrarrestar los productos liberados por los neutrófilos mediante compuestos que podrían denominarse protectores es también importante para facilitar la reparación. Así por ejemplo, la elastasa de neutrófilos, presente en niveles elevados en lavados broncoalveolares de pacientes con SDRA (Gando y col., 1997), capaz de inducir apoptosis epitelial (Suzuki y col., 2005), es contrarrestada mediante antiproteínas como la α1-antitripsina o la α2-macroglobulina, liberadas en respuesta a citoquinas proinflamatorias (Fowler AA, 1982). Algunas citoquinas antiinflamatorias como IL-10

son liberadas durante la respuesta proinflamatoria como un mecanismo de retroalimentación negativa para disminuir la expresión de mediadores proinflamatorios (Parsons, 1998). El balance entre mediadores pro- y antiinflamatorios es por tanto de vital importancia para limitar el daño tisular durante el SDRA.

Finalmente, la regeneración de la estructura alveolar requiere el recubrimiento celular de las zonas denudadas. Esta función viene dada por la proliferación de células progenitoras, su migración sobre la matriz extracelular que ha sido sintetizada a modo de cicatriz y su transdiferenciación en neumocitos tipo I. Se ha calculado que el porcentaje de células que entran en fase S del ciclo celular tras el daño pulmonar es 10 veces superior al que ocurre en condiciones normales (Reynolds y col., 2000). A nivel alveolar, los neumocitos tipo II han sido clásicamente considerados la única población celular depositaria de esta función, tanto en condiciones normales (Dobbs y col., 1985; Isakson y col., 2001; Rawlins y col., 2007) como tras el daño pulmonar (Zahm y col., 1991; Panos y col., 1995; Rawlins y col., 2007). Sin embargo, siguen apareciendo evidencias que ponen a prueba su papel como única fuente de recambio celular y la identificación exacta de los progenitores alveolares es aun objeto de discusión. Recientes estudios *in vitro* han mostrado que incluso los neumocitos tipo I poseen capacidades proliferativas y de plasticidad fenotípica (Qiao y col., 2008; Gonzalez y col., 2009). Los grandes avances en el conocimiento sobre las células madre llevados a cabo durante los últimos años se han traducido en la identificación de este tipo celular pluripotente como población residente en el tejido pulmonar (Kubo, 2011; Banerjee and Henderson, 2012; Hoffman and Ingenito, 2012), aunque su caracterización exacta aun es objeto de estudio. También se ha propuesto que las células madre derivadas de la medula ósea son capaces de llegar al pulmón a través del torrente sanguíneo y diferenciarse a células epiteliales (Sage y col., 2008; Yilmaz y col., 2012). Sin embargo, los estudios al respecto se han centrado más en su posible uso terapéutico (D'Agostino y col., 2010; dos Santos y col., 2012; Waszak y col., 2012; Xu y col., 2012) que en clarificar su papel en el proceso de reparación fisiológico. Los resultados obtenidos parecen apuntar no sólo a sus propiedades proliferativas, sino también hacia su papel de regulación de la respuesta inmune mediante la liberación de factores de crecimiento como EGF, KGF y HGF (Chen y col., 2008; Curley y col., 2012), los cuales

actúan como potentes mitógenos de neumocitos tipo II (Lindsay, 2011) incrementando la síntesis de surfactante (Raaberg y col., 1992), promueven la migración celular (Albaiceta y col., 2008) y la producción de citoquinas de clase Th2, de naturaleza antiinflamatoria (Panoskaltsis-Mortari y col., 2000). Una de las mayores expectativas en el campo de la reparación pulmonar es el desarrollo de modelos y métodos que permitan examinar los mecanismos de reparación epitelial directamente en el pulmón.

Una vez finalizada la fase proliferativa, la cicatriz de colágeno que ha servido de andamiaje celular y alveolar debe ser retirada para recuperar una difusión y una elasticidad adecuadas. Si este proceso no se resuelve de manera adecuada, el paciente entra en la denominada fase fibrótica del SDRA, caracterizada por un depósito excesivo de tejido conectivo tanto en el septo como en el espacio alveolar. Los mecanismos que impiden la correcta resolución de la fase proliferativa son aun objeto de estudio, pero la capacidad proteolítica de las MMPs parece ser de nuevo un elemento clave en este proceso. El estudio concreto del papel de estos enzimas en el transcurso del SDRA, tanto en la modulación de la respuesta inmune como en la resolución de la fibrosis ha sido abordado en la presente tesis.

Metaloproteasas de Matriz extracelular.

Las metaloproteasas de matriz extracelular (MMPs) conforman una familia de al menos 25 endopeptidasas pertenecientes a la superfamilia de las metzincinas. Estos enzimas son capaces de hidrolizar enlaces peptídicos a través un ataque nucleofílico mediado por una molécula de agua polarizada, gracias a un átomo de zinc localizado en su centro activo. Se sintetizan como zimógenos, con un dominio propéptido (≈80αα) que contiene un residuo de cisteína que interacciona con el átomo de zinc presente en el centro activo, y que ha de ser modificado o eliminado mediante otras MMPs o Serín-proteasas para que el enzima sea activo. Contienen también un péptido señal que las dirige hacia su secreción o a ser ancladas a la membrana celular. El patrón estructural general de las MMPs consiste en el propéptido anteriormente

mencionado, un dominio catalítico (≈170αα), un péptido de unión de longitud variable y un dominio hemopexina (≈200αα) que confiere especificidad por el sustratos. Aunque existen variaciones de este patrón que llevan a diferentes grupos de clasificación (**Tabla 2**), todas ellas presentan características similares e incluso se superponen en la especificidad de sustratos. Su expresión en tejidos adultos es normalmente baja, estando sujeta a un férreo control, principalmente a nivel transcripcional mediante vías de señalización como NFκB, MAPK, STATs y Smad, que una vez estimuladas regulan regiones promotoras de los genes de MMPs. Otros niveles de regulación de las MMPs incluyen regulación epigenética, post-transcripcional, y la inhibición de MMPs activas por inhibidores endógenos como los TIMPs (del inglés *Tissue Inhibitor of MetalloProteinases)* (Fanjul-Fernandez y col., 2010).

En un principio se creyó que la acción de las MMPs se restringía únicamente al remodelado y degradación de la matriz extracelular ya que son capaces, colectivamente, de degradar todos sus componentes. Estudios posteriores revelaron su capacidad de degradar una amplia variedad de sustratos como quimiocinas, citoquinas, moléculas de adhesión, inhibidores, receptores de superficie, factores de coagulación o factores de crecimiento (Stamenkovic, 2003). Esta variedad de sustratos les confiere una gran diversidad funcional en procesos biológicos como el embarazo, el desarrollo embrionario, la reabsorción ósea, la angiogénesis, la cicatrización, y patológicos como la artritis reumatoide, esclerosis múltiple, enfermedad periodontal o el desarrollo tumoral (Lopez-Otin and Bond, 2008). En los últimos años, la identificación de nuevos sustratos y el uso de animales deficientes en MMPs especificas, han demostrado su implicación en la regulación del proceso inflamatorio (Manicone and McGuire, 2008) ayudando en unos casos a proteger frente a la patología desencadenante del mismo o incluso contribuyendo a ella cuando su expresión está desregulada.

Tabla 2. Clasificación de las MMPs

Clasificación	Subgrupo	MMPs
Arquetipo	Colagenasas	MMP-1 (a y b), **MMP-8** y MMP-13
	Estromalisinas	MMP-3 y MMP-10
	Otras MMPs	MMP-12, MMP-19, MMP-20 y MMP-27
Gelatinasas	Gelatinasas	MMP-2 y MMP-9
Matrilisinas	Matrilisinas	MMP-7 y MMP-26
Activadas por furinas	Secretadas	MMP-11, MMP-21 y MMP-28
	Transmembrana tipo I	MT1- MMP, MT2- MMP, MT3- MMP y MT6- MMP
	Ancladas a GPI	MT4- MMP y MT6- MMP
	Transmembrana tipo II	MMP-23A y MMP-23B

El procesamiento de citoquinas pro- y anti-inflamatorias por parte de las MMPs lleva a tanto cambios en su actividad, como ocurre en la activación de IL-1β y TGFβ, como en su biodisponibilidad, por ejemplo liberando TNFα de su anclaje a la superficie celular y de TGFβ de sus depósitos en la ME (Van Lint and Libert, 2007). Sin embargo, la influencia de las MMPs en la progresión del proceso inflamatorio no se limita únicamente al procesamiento de citoquinas sino también al de quimiocinas y a la modulación de su gradiente, influenciando así el tráfico leucocitario y definiendo sus poblaciones. La proteólisis de quimiocinas puede tener efectos diversos y opuestos, inactivándolas (Van den Steen y col., 2003), aumentando su potencial quimiotáctico (Balbin y col., 2003; Tester y col., 2007) o generando un derivado antagónico de la misma capaz de unirse a su receptor pero no de inducir quimiotaxis (McQuibban y col., 2002). En este sentido, cabe destacar el importante papel de MMP-8 tanto en el reclutamiento inicial de leucocitos como en el posterior aclaramiento de los mismos mediante el procesamiento de quimiocinas CXC como son LIX (en ratones) o IL-8 (en humanos).

Con una estructura de metaloproteasa arquetipo como la descrita anteriormente, MMP-8 se engloba junto con MMP-1 y MMP-13, dentro del subgrupo de las colagenasas, dada su capacidad de escindir la triple cadena polipeptídica de colágeno a 3/4 de distancia del extremo N-terminal. Aunque MMP-8 degrada los tres

tipos de colágeno intersticial se diferencia de las otras colagenasas en su mayor afinidad por el colágeno tipo I., de tal manera que los ratones deficientes en MMP-8 solo mantienen un 8% de su capacidad colagenolítica tipo I unida a membrana (Owen y col., 2004). Este enzima es sintetizada principalmente durante la maduración del neutrófilo dentro de la médula ósea, se almacena dentro de gránulos como proteína latente (pro-MMP-8, 85kDa) y es liberada cuando se produce la activación del neutrófilo. Sin embargo, también se expresa en menor medida en otros tipos celulares como macrófagos, células epiteliales, queratinocitos, células endoteliales, fibroblastos, miofibroblastos, células musculares y condrocitos entre otros (Van Lint and Libert, 2006). Una vez liberada, MMP-8 ha de ser activada por oxidación mediante especies reactivas de oxígeno (ROS) generadas por el propio neutrófilo, o mediante degradación proteolítica por distintas proteasas incluida la propia forma activada de MMP-8. Además de la forma secretada, MMP-8 también se puede encontrar anclada a la membrana, siendo esta forma la de mayor actividad colagenolítica y la más resistente a los inhibidores TIMP-1 y TIMP-2 (Owen y col., 2004).

La observación de niveles elevados de esta MMP en enfermedades crónicas inflamatorias ha llevado al estudio de su papel durante el procesos inflamatorio. Un modelo experimental de carcinogénesis inducida mostró que ratones deficientes en MMP-8 presentaban una mayor susceptibilidad al desarrollo de tumores de piel. En estos animales se identificó una respuesta anómala en la aparición y posterior resolución del infiltrado neutrofílico, consistente en un retraso inicial en el reclutamiento leucocitario y una posterior acumulación crónica de polimorfonucleares (Balbin y col., 2003). Se han identificado varios mecanismos moleculares que podrían ser responsables de esta respuesta. Por un lado, MMP-8 es capaz de procesar diferentes Quimiocinas, así el procesamiento de la quimiocina LIX mediado por MMP-8 genera una forma más bioactiva (Tester y col., 2007), mientras que el procesamiento de MIP-1α genera una forma inactivada de la misma (Quintero y col., 2010). Estudios posteriores en modelos experimentales similares demostraron que parte de este efecto podría estar asociado con una menor apoptosis de neutrófilos, posiblemente mediada por un aumento de IL4 (Gueders y col., 2005; Gutierrez-Fernandez y col., 2007). La variedad en los mecanismos implicados hace que el papel de MMP-8 en el

tráfico de leucocitos sea complejo. El tipo de estímulo, tejido y el momento en que juega su papel parecen ser especialmente relevantes en la acción de esta MMP. Así, ratones deficientes en MMP-8 sometidos a un modelo de inflamación hepático inducido por TNF/Galactosamina (Van Lint y col., 2005) muestran un menor infiltrado de neutrófilos que se corresponde con una mayor supervivencia, mientras que en modelos de cierre de heridas (Gutierrez-Fernandez y col., 2007) e inflamación pulmonar aguda inducida por LPS suministrado intratraquealmente (Owen y col., 2004) el infiltrado es mayor. Parece por tanto adecuado ahondar más en el papel de esta MMP en una patología inflamatoria como es la lesión pulmonar, en la que es esencial la regulación de los procesos de reestructuración tisular tanto en las fases tempranas como en fases más tardías encaminadas a la recuperación de la homeostasis.

Efectos de la ventilación mecánica en el cerebro.

La aparición de desórdenes neuropsicológicos en los pacientes ingresados en las unidades de cuidados intensivos tales como niveles alterados de conciencia, inatención, desorientación, alucinaciones, psicosis y alteraciones psicomotoras, del habla, del estado de ánimo o de los ciclos sueño-vigilia, se han hecho más evidentes a medida que la medicina intensiva ha conseguido reducir los índices de mortalidad y los supervivientes tienen que enfrentarse a las posibles secuelas de los tratamientos recibidos. Así, se calcula que hasta un 80% de los pacientes ingresados en las unidades de cuidados intensivos presentan algún tipo de disfunción cerebral que va desde el delirio hasta el deterioro cognitivo prolongado (Vasilevskis y col., 2011; Jones and Pisani, 2012). Ambos procesos parecen estar relacionados, de tal manera que la duración del primero es un factor predictivo de la gravedad del segundo (Girard y col., 2010). Varios estudios muestran aumentos de un 20% en la estancia hospitalaria y de un 10% en la mortalidad por día de delirio (Ely y col., 2004; Pun and Ely, 2007), además de mayores tasas de reintubación y de un aumento del 40% en los costes hospitalarios (Milbrandt y col., 2004). Aquellos pacientes que sobreviven a su estancia hospitalaria presentan alteraciones estructurales cerebrales durante varios meses (Girard y col., 2010; Morandi y col., 2012). Aproximadamente el 60% se enfrentan a un deterioro

cognitivo en un periodo de 6 años (Girard y col., 2010), lo que supone una importante disminución en su calidad de vida y un incremento en los gastos extrahospitalarios asociados al tratamiento.

Varios estudios observacionales han identificado diversos factores que predisponen a la aparición de estas alteraciones neurológicas, tales como hipocalcemia, hipotensión o hipertensión, fiebre, hiperbilirubinemia, anemia, acidosis metabólica, incremento en los enzimas hepáticos, tabaquismo, el uso de sedantes y su vía de administración, diabetes, privación de sueño con desbalance de melatonina o el alcoholismo (Figueroa-Ramos y col., 2009). Sin embargo, el soporte ventilatorio se presenta como uno de los factores de riesgo más relevantes, incrementando en un 60% su incidencia en pacientes (Ely y col., 2001; Cavallazzi y col., 2012) y asociándose a una mayor mortalidad (Ely y col., 2004). Pese a su importancia y a que algunos estudios preliminares muestran la activación de distintas aéreas cerebrales en modelos animales de VILI (Quilez y col., 2011), todavía no se ha podido establecerse la relación causal entre la ventilación mecánica y el delirio. Se han propuesto, no obstante, algunas hipótesis al respecto. La primera de ellas relaciona el delirio con el daño isquémico de regiones sensibles a la hipoxia como el hipocampo, encargado de integrar la información sensorial y consolidarla en la memoria y cuya disfunción ha sido asociada con diversos desórdenes del comportamiento (Neves y col., 2008; Kuljeet SA, 2012). Esta hipótesis es apoyada por un estudio en el que se identificaron lesiones patológicas, atribuibles normalmente a hipoxia, en autopsias cerebrales de pacientes con delirio (Gunther y col., 2012) y por estudios experimentales en modelos de encefalopatía mediada por sepsis (Semmler y col., 2007). Sin embargo, la mayoría de los pacientes que fallecen en el transcurso del SDRA no lo hacen a causa de la hipoxemia debida al fallo respiratorio, sino por una disfunción orgánica múltiple. Como comentamos anteriormente, las presiones positivas utilizadas durante la ventilación mecánica desencadenan respuestas biológicas a través de fenómenos de mecanotransducción que producen la liberación de una amplia variedad de mediadores. La segunda hipótesis propone que la salida de estos mediadores a la circulación sistémica y su entrada en el cerebro a través de la barrera hematoencefálica, que puede estar comprometida por la presencia de MMPs en la

circulación sanguínea (Agrawal y col., 2006; Schubert-Unkmeir y col., 2010), o a través de los órganos circunventriculares o el plexo coroideo (Dantzer, 2001), podría provocar una respuesta inmune con reclutamiento leucocitario y alterar la homeostasis cerebral (D'Mello y col., 2009). La tercera hipótesis propone un desbalance en los niveles de neurotransmisores, concretamente una disminución en los niveles de acetilcolina y un aumento en los de dopamina. Aunque esta hipótesis está bastante aceptada, debido a la evidencia clínica de la mejoría en pacientes tratados con antipsicóticos como haloperidol (Jacobi y col., 2002), hasta la fecha no existen evidencias experimentales que la avalen. Es por ello que dentro del contexto de esta hipótesis, nos pareció interesante explorar la posible implicación del nervio vago, vía de comunicación neural entre el cerebro y los pulmones, en la disfunción cerebral asociada a la ventilación mecánica.

OBJETIVOS

Teniendo en cuenta los antecedentes descritos anteriormente, el objetivo principal de esta Tesis Doctoral es la identificación de mecanismos moleculares implicados en el establecimiento y resolución del SDRA, así como la búsqueda de estrategias encaminadas al tratamiento de los desórdenes neurológicos causados por el mismo.

En concreto, se plantearon los siguientes objetivos:

- Estudiar la implicación de MMP-8 en el desarrollo de las distintas fases del daño pulmonar mediante el empleo de un modelo murino deficiente en dicha metaloproteasa.

- Investigar los mecanismos moleculares implicados en la reparación pulmonar tras la lesión inducida por la ventilación mecánica.

- Estudiar las causas de la disfunción cerebral observada en pacientes sometidos a ventilación mecánica.

MATERIALES Y MÉTODOS

Modelos animales

Animales de experimentación

Los ratones de la cepa C57BL6 de 8-12 semanas de edad, tanto de genotipo normal (*Mmp8*$^{+/+}$) como deficientes en la metaloproteasa de matriz extracelular MMP-8 (*Mmp8*$^{-/-}$) fueron cedidos amablemente por el Dr. López Otín del Departamento de Bioquímica y Biología Molecular de la Universidad de Oviedo. Estos animales se generaron a partir de un fondo mixto C57BL6/129Sv (Balbin y col., 2003) y fueron posteriormente retrocruzados con C57BL6 durante al menos 8 generaciones para obtener un fondo genético puro. Todos los animales fueron genotipados mediante la extracción de ADN de la cola y realización de una reacción en cadena de la polimerasa (PCR). Los ratones de la cepa CD1 fueron criados en el Bioterio de la Facultad de Medicina de la Universidad de Oviedo.

Previo al estudio, los animales fueron mantenidos en condiciones libres de patógenos, sometidos a ciclos de 12 horas de luz/oscuridad, bajo condiciones ambientales de temperatura y humedad controladas y con acceso libre a alimento y agua. Los experimentos se realizaron tanto en el Bioterio como en el Área de Fisiología del Departamento de Biología Funcional de la Universidad de Oviedo. Todos los experimentos se realizaron de acuerdo con las guías vigentes sobre el uso de animales de experimentación. El estudio fue aprobado por el Comité de Etica de Experimentación Animal de la Universidad de Oviedo.

Modelo de VILI y modelo de VILI-Reparación

Los ratones se anestesiaron con una combinación de Ketamina 80 mg/kg (Ketolar, Parke-Davis Grupo Pfizer) y Xylacina 25 mg/kg (Rompun, Bayer) administrada por vía intraperitoneal. Se les realizó una traqueotomía previa conexión al ventilador mecánico (Dräger Evita 2 Dura-Neoflow, Alemania) insertando un catéter de 20G y fijándolo con seda para evitar fugas de aire. Los ratones se colocaron sobre una

almohadilla calefactora para mantener una apropiada temperatura corporal y recibieron cargas de volumen de 200 µl de solución Ringer-Lactato al inicio del experimento y cada dos horas para evitar la hipotensión. Los animales se sometieron a una ventilación mecánica en modo de control de presión utilizando una de las siguientes estrategias:

- Ventilación lesiva o de presión elevada: Presión inspiratoria pico (PIP) 25 cmH_2O, presión positiva al final de la expiración (PEEP o ZEEP) 0 cmH_2O, frecuencia respiratoria 50 resp/min, fracción inspirada de oxígeno (F_IO_2) 50%, relación tiempos inspiratorio/espiratorio (I:E) 1:1.

- Ventilación protectora o de presión baja: Presión inspiratoria pico (PIP) 15 cmH_2O, presión positiva al final de la expiración (PEEP) 2 cmH_2O, frecuencia respiratoria 100 resp/min, fracción inspirada de oxígeno F_IO_2 50%, relación tiempos inspiratorio/espiratorio (I:E) 1:1.

Los parámetros de ventilación fueron escogidos para conseguir la normocapnia basándose en experimentos previos. Se realizaron pausas inspiratorias al inicio del experimento para excluir posibles fugas de aire. La ventilación mecánica se mantuvo durante 2 horas (**Artículo 1**), tras las cuales se realizó una laparotomía con extracción de sangre arterial de la aorta para medición de pH y presiones de gases (PaO_2, $PaCO_2$) en sangre en un gasómetro *NPT7 (Radiometer*, Copenhague, Dinamarca). Como controles basales se utilizaron ratones en respiración espontánea no traqueotomizados. Para llevar a cabo el modelo de VILI-reparación (**Artículo 5**) se combinaron las estrategias descritas con diferentes tiempos de ventilación, generándose seis grupos experimentales que se detallan a continuación:

	Tiempo de ventilación (min)	
Grupo	Presión elevada	Presión baja
Basal	0	0
Lesión	90	0
Reparación	90	240
Control 90 min	0	90
Control 330 min	0	330
Estudio mortalidad	Hasta la muerte	0

Para el estudio de la afectación a nivel cerebral causada por la ventilación mecánica (**Artículo 6**) se optó por el uso de una PIP de 12 y 20 cmH_2O para la ventilación a baja y alta presión respectivamente. Se añadió también un grupo de ratones tratados con haloperidol (0,5 mg/Kg) treinta minutos antes de ser sometidos a ventilación mecánica con alta presión durante 90 min o sometidos a una vagotomía bilateral cervical inmediatamente antes de la ventilación.

Modelo de endotoxemia

Animales de ambos genotipos (*Mmp8*$^{+/+}$ y *Mmp8*$^{-/-}$) se dividieron de forma aleatoria en dos grupos experimentales. En los del grupo control se inyectaron 500 μl de una solución salina estéril previamente atemperada (Suero Fisiológico Braun, NaCl 0,9%) por vía intraperitoneal. En los del grupo de endotoxemia los ratones recibieron 125 μg de lipopolisacárido (LPS) de *E. Coli* (serotipo O55:B5, Fluka) disuelto en un volumen total de 500 μl de solución salina atemperada. Esta dosis no letal es capaz de producir lesión pulmonar en 24h, caracterizada por un incremento en la elastancia pulmonar de 1,5 veces (Menezes y col., 2005; Leite-Junior y col., 2008). Tras veinticuatro horas los animales fueron anestesiados con una combinación de Ketamina (Ketolar®, Parke-Davis Grupo Pfizer) y Xylacina (Rompun®, Bayer) por vía intraperitoneal, tras lo cual se les realizó una laparotomía y fueron sacrificados por exanguinación a través de la arteria renal. Para estudiar el efecto de MMP-8 sobre la supervivencia a endotoxemia, se les inyectó 250 μg de LPS disuelto en un volumen total de 500μl de solución salina estéril y se observó la supervivencia en un periodo de 108 horas.

Modelo de fibrosis pulmonar

Tras la anestesia de los ratones con sevofluorano se realizó una incisión transversal de 2 cm en el cuello, disecando la musculatura pretraqueal hasta exponer la tráquea. Posteriormente se inyectaron, mediante una aguja 28G, 50 μl de suero

salino isotónico o bleomicina (2 U/Kg, Sigma-Aldrich). Tras la sutura y la aplicación de un antiséptico todos los animales permanecieron en las mismas condiciones controladas descritas anteriormente. Las variables del estudio fueron el perfil genético (*Mmp8*$^{+/+}$ y *Mmp8*$^{-/-}$), el tratamiento recibido (bleomicina o suero salino) y el tiempo hasta el sacrificio (3 días, 3 semanas o 6 semanas).

Inhibición de MMP-8 in vivo y pan-inhibición de MMPs

La inhibición farmacológica de MMP-8 en ratones se llevó a cabo mediante la inyección a intervalos de 12 horas de cinco dosis intraperitoneales (40 mg/kg) de ácido (R)-1-(3'metilbifenil-4-sulfoamino)-metilpropil fosfónico, sal de ciclohexilamina con efecto inhibidor específico de MMP-8 y sin actividad frente a otras MMPs (Biasone y col., 2007). Como control se utilizaron ratones a los que se inyectó el mismo volumen de vehículo [200 µl de DMSO (dimetilsulfóxido) al 5% en PBS). La pan-inhibición de MMPs (**Artículo 5**) se llevó a cabo mediante la inyección intraperitoneal de una dosis de doxiciclina (50 mg/Kg).

Obtención de muestras

Una vez sacrificados los animales, se extrajo el bloque corazón-pulmones ligando posteriormente el bronquio derecho. Al pulmón izquierdo se le instiló formaldehído (3,7-4,0% pH 7, Panreac Química S.A) por vía intratraqueal mediante una catéter de 20G, conservándose 24 horas sumergido en el mismo fijador para el estudios histológicos posteriores. El pulmón derecho se congeló inmediatamente a -80°C para ser usado en posteriores estudios moleculares. En experimentos adicionales se realizó un lavado broncoalveolar a los animales inmediatamente antes de su sacrificio. Para ello se inyectó en el pulmón un volumen de 4 ml de salino en cuatro alícuotas de 1 ml a través la traqueotomía. Las poblaciones celulares presentes en el lavado broncoalveolar (BALF, *broncoalveolar lavage fluid*) se contaron e identificaron en 200 µl de volumen mediante una cámara de Neubauer y un hemocitómetro. El BALF

restante se centrifugó a 900 g y se congeló inmediatamente a -80°C para análisis posteriores. No se recogieron más muestras de estos animales.

Con el objetivo de identificar células mieloides supresoras (MDSCs, *Myeloid derived suppressor cells*) en los pulmones de los ratones sometidos al modelo de endotoxemia se sacrificaron animales de ambos genotipos, se les extrajo el pulmón izquierdo y se sumergió en 2 ml de PBS estéril. Inmediatamente después se realizaron cortes en el pulmón y con ayuda de unas pinzas se extrajo el infiltrado celular. Se centrifugó a 900g y el precipitado celular se resuspendió en un volumen de 100 μl de PBS y se incubaron durante 15 minutos con los anticuerpos anti CD11b, LY-6G APC, LY-6G PE y CD45 (Becton Dickinson). Tras tres lavados posteriores con PBS y una eliminación de eritrocitos mediante lisis osmótica, las muestras se analizaron en un citómetro Cytomics FC500 (Becton Coulter).

Muestras humanas

Para la realización de esta tesis se utilizaron muestras de hipocampo extraídas en autopsias de pacientes sometidos a ventilación mecánica y de pacientes control no ventilados tratados en la unidad de cuidados intensivos del Hospital Universitario Central de Asturias (HUCA) , cedidas por el Banco de Cerebros del mismo hospital.

Para los ensayos de cierre de heridas se utilizaron muestras de lavados broncoalveolares (BALF) de pacientes que cumplían los criterios de SDRA y que habían sido sometidos a ventilación mecánica durante al menos cinco días. Previamente a su utilización, los lavados fueron filtrados a través de una gasa estéril, centrifugados a 900 g durante 15 min y vueltos a filtrar a través de membranas de 0,2 μm (Acrodisc filter, Pall Life Sciences). En todos los casos, las muestras humanas fueron obtenidas tras consentimiento informado de los familiares de los pacientes.

Estudios histológicos

Determinación del daño pulmonar

Tras la fijación en formaldehido del pulmón izquierdo, se incluyó en parafina para realizar los cortes histológicos. Se tomaron tres secciones pulmonares de 4 μm de grosor, separadas por 200 μm, que fueron teñidas con hematoxilina-eosina para su análisis al microscopio óptico. Dos patólogos, que desconocían las condiciones experimentales de la muestra, evaluaron los cortes histológicos. Cada sección se analizó siguiendo una escala de 0 a 5:

Grado	Severidad
0	Pulmones normales.
1	Congestión del septo.
2	Aumento del grosor del tabique alveolar a expensas de pneumocitos tipo II.
3	Presencia de infiltrado inflamatorio.
4	Hemorragia alveolar y/o formación de membranas hialinas.
5	Aparición de zonas sólidas con pérdida del patrón arquitectural y colapso del espacio alveolar.

Edema pulmonar

Para medir la afectación de la permeabilidad de la barrera alveolocapilar se pesó el lóbulo superior derecho del pulmón de algunos animales, antes y después del secado durante 48 horas en una estufa a 50°C. Se calculó la relación peso húmedo-peso seco como marcador del grado de edema pulmonar. También se utilizó como marcador de permeabilidad la presencia de proteínas en el lavado broncoalveolar medidas mediante la técnica del ácido bicinconínico (BCA, Pierce).

Cuantificación de la fibrosis y bronquiolización

Para cuantificar el grado de fibrosis pulmonar se analizaron tres secciones pulmonares de 4 μm de grosor, separadas por 200 μm que fueron teñidas con

tricrómico de Masson. La fibrosis pulmonar se puntuó de 0 (sin fibrosis) a 8 (fibrosis masiva en todos los campos) utilizando la escala Ashcroft (Ashcroft y col., 1988). El fenómeno de bronquiolización (presencia de células bronquiales en los alveolos) fue cuantificado utilizando la escala Jensen-Taubman (Jensen-Taubman y col., 1998). Ambas evaluaciones se realizaron por un patólogo que desconocía las condiciones experimentales.

Análisis inmunohistoquímicos (IHC)

Los análisis inmunohistoquímicos se realizaron en muestras parafinadas en colaboración con las doctoras Aurora Astudillo y María Soledad Fernández en el laboratorio de Anatomía Patológica Animal del IUOPA. El procesado de las muestras se llevo a cabo en el inmunoteñidor automático (Discovery XT System, Ventana) con un software específico, el cual establece los reactivos y el orden en el que estos se suministran.

Los bloques de parafina se cortaron en secciones de 4 µm, las cuales se desparafinaron tras un paso sucesivo por alcoholes de menor graduación hasta llegar al agua (STP 120, Microm). Seguidamente, se llevó a cabo el desenmascaramiento antigénico con una solución recuperadora de antígenos a pH 6 a 95 ºC durante 20 min. Posteriormente, las secciones se incubaron con una solución de bloqueo de la peroxidasa endógena contenida en la muestra con el fin de reducir la tinción de fondo no específica. Tras el bloqueo, las muestras se incubaron con el anticuerpo primario previamente diluido durante 1 h a temperatura ambiente. Tras lavar las preparaciones, se procedió a la incubación con el anticuerpo secundario unido a peroxidasa (Omnimap) durante 30 min. Tras lavar, se reveló con el sistema de sustrato incluido en el kit, compuesto por una solución de 3,3'-diaminobenzidina (DAB) concentrada y una solución en la que se debe diluir la DAB. La peroxidasa cataliza la peroxidación de la DAB, la cual vira a un color marrón en los lugares de unión antígeno-anticuerpo. El contrateñido con hematoxilina se llevó a cabo en un aparato Discovery (Ventana, ROCHE), la cual tiñe de color azul el núcleo de las células. Finalmente, se procedió al montaje de las muestras mediante el medio Entellan (Dako), tras haber sido

previamente sometidas a deshidratación y aclaramiento con xilol. Cuando fue posible, el número de células positivas se calculó promediando el resultado del contaje en tres campos de gran aumento elegidos aleatoriamente en el corte histológico.

Análisis inmunofluorescentes

Las muestras previamente incluidas en parafina, se desparafinaron como se ha descrito en el apartado anterior. El desenmascaramiento antigénico se llevo a cabo hirviendo las secciones en una solución de citrato 0,1 M a pH 6.0 durante 20 min. Posteriormente se trataron con 0,1% Triton X-100 en PBS durante 15 min a temperatura ambiente para permeabilizar y con glicina 1 M en PBS durante 30 min para disminuir la autofluorescencia causada por la fijación con formaldehído. El bloqueo se llevo a cabo en una solución al 5% de suero de cabra y 0,3% Triton X-100 en PBS durante 30 min a temperatura ambiente. La incubación con el anticuerpo primario se llevó a cabo durante la noche en una cámara húmeda a 4°C en una solución al 1% de albúmina de suero bovino (BSA), 0,3% Triton X-100 en PBS. Tras lavar las preparaciones, se procedió a la incubación con el anticuerpo secundario unido a fluoróforo (Alexa Fluor 488, Life Technologies) durante 1 h a temperatura ambiente y en oscuridad. Finalmente los núcleos se contratiñeron con 4',6-diamidino-2-fenilindol (DAPI) incluido en la solución de montaje Vectashield (Vector laboratorios, CA).

Técnicas de biología celular

Cultivos celulares

Las líneas celulares A549 y MLE-12 se adquirieron en la colección *American Type Culture Collection* (ATCC). La línea de neumocitos humanos A549 se cultivó en medio DMEM suplementado con 10% de suero fetal bovino (FBS) y 1% de penicilina/estreptomicina/glutamina. La línea de neumocitos murinos MLE-12 se

cultivó en medio DMEM/HAM's F-12 suplementado con 2% de FBS, insulina (0,005 mg/ml), transferrina (0,01 mg/ml), selenito de sodio (30 nM), hidrocortisona (10 nM), β-estradiol (10 nM), HEPES (10 mM) y un 1% de penicilina/estreptomicina/glutamina.

Cultivo primario de fibroblastos para ensayos de actividad de IL-10

Los fibroblastos se extrajeron de explantes pulmonares tanto de ratones control como de ratones deficientes en MMP-8. Los pulmones se lavaron en PBS (*Dulbecco's Phosphate buffered Saline*, Gibco) y se trituraron con cuchillas. Se permitió a los explantes adherirse al fondo de la placa de cultivo antes de cubrirlos con medio de cultivo DMEM suplementado con 1% de penicilina/estreptomicina/gentamicina, FBS 10%, aminoácidos no esenciales 0,1 mM, piruvato sódico 1 mM, HEPES 2 mM (ácido N-2-hidroxietilpiperacina-N'-2'-etanesulfónico). Tras dos semanas a 37°C y 5% de CO_2, la mayoría de las células de tipo no fibroblástico habían muerto mientras que los fibroblastos se establecieron como el tipo celular predominante. Los cultivos se trataron con tripsina, se filtraron para eliminar restos celulares y finalmente se lavaron con PBS. Se sembraron fibroblastos en placas de 12 pocillos con DMEM sin FBS en las siguientes condiciones: Basal, bleomicina 100 nM, bleomicina 100 nM más un anticuerpo de bloqueo para IL-10, y bleomicina más una inmunoglobulina inespecífica (IgG, Abcam, UK). Tras 12 horas se recogieron los sobrenadantes y extractos celulares y se congelaron a -80°C para su análisis.

Ensayo de cierre de heridas

Se cultivaron por separado las líneas celulares A549 y MLE-12 en sus respectivos medios en placas de 24 pocillos. Una vez alcanzada la confluencia se realizó una "herida" denudando la monocapa celular con una punta de pipeta. Se llevaron a cabo tres lavados con PBS y se añadió medio sin FBS suplementado en el caso de las MLE-12 con un 10% de BALF procedente de ratones sometidos a ventilación mecánica y en el caso de las A549 con un 10% de BALF obtenido de pacientes que cumplían los criterios del SDRA y habían sido sometidos al menos a 5

días de ventilación mecánica. Se utilizaron medios de cultivo sin BALF como controles. Todas las condiciones se estudiaron por triplicado. Para estudiar el efecto de IL-4, MIP-2, MMP-2 y TNFα en el cierre de la herida se añadieron anticuerpos bloqueantes de estos mediadores en experimentos paralelos y se estudió el efecto de pan-inhibición de MMPs mediante la adición de doxiciclina (25 μM). Los cultivos se fotografiaron inmediatamente tras realizarse la herida y tras 3, 6, 9 y 12 horas en el caso de las MLE-12 y cada 24 horas durante 4 días en el caso de las A549. Se utilizó un microscopio *Olympus BH-2* acoplado a una cámara *Olympus C-5060*. Las imágenes se estudiaron utilizando el programa *ImageJ*, calculándose el porcentaje del área denudada inicial cubierta por las células en los distintos periodos de tiempo.

Técnicas de biología molecular

Materiales

Anticuerpos: Los anticuerpos utilizados fueron los siguientes: anti-p100/p52, anti-caspasa-7, anti-caspasa 9, anti-AKT, anti-fosfo AKT ser473, anti-GSK3β, anti-fosfo GSK3β ser9, anti-PTEN, anti-PTEN fosforilado ser380, anti-PARP, anti-PARP procesado y anti-RabbitIgG HRP-linked de Cell Signaling; anti-LC3 de Nanotools; anti-fosfo P65 ser536, anti-IL10, anti-IL10RA, anti-MMP-8, anti-MIP1α, anti-TIMP-1 y anti-MMP-2 de Abcam; anti-P62 de Abnova; anti-Disbindina de Millipore; anti-MIP2 de AbD Serotec; anti-βActina y anti-MMP-9 de Santa Cruz biotechnology; anti-S100A6, anti-S100A8, anti-S100A9, anti-GoatIgG HRP-linked y anti-MouseIgG HRP-linked de R&D Systems; anti-MPO de Thermo Fisher Scientific; anti-STAT y anti-fosfo STAT Tyr705 de Signalway Antibody Co; anti-LIX de Peprotech; anti-TNFα y anti-IL4 de Ebioscience.

Otros materiales: Los marcadores de peso molecular para proteínas (*Precision plus protein strandards Dual color Prestained Standards*) procedían de BioRad. Los reactivos empleados para la electroforesis de proteínas (acrilamida/N,N'-

metilenbisacrilamida, β-mercaptoetanol, glicina, N,N,N',N'-tetrametiletilendiamina y persulfato amónico, entre otros) se adquirieron indistintamente en Sigma, Fluka y BioRad. Los productos utilizados para el cultivo celular fueron adquiridos en Gibco y PAA Laboratories, excepto los soportes de plástico desechable que procedían de LabClinics y Falcon. El uso de otros materiales específicos para cada ensayo se detalla en los siguientes apartados.

Extracción de ARN

El ARN se extrajo tanto de las líneas celulares como de las muestras de tejido empleando el reactivo TRIzol (Invitrogen Life Technologies) siguiendo las indicaciones facilitadas por el fabricante. El ARN se resuspendió en agua MilliQ previamente tratada con dietilpirocarbonato (DEPC, *diethylpyrocarbonate*). La cantidad de ARN se cuantificó por análisis espectrofotométrico a 260 nm de longitud de onda y se determinó su calidad mediante la relación OD 260/280 nm por espectrofotometría. Las muestras de ARN se conservaron a -80ºC.

Transcripción reversa de ARN acoplada a PCR (RT-PCR)

La obtención de ADN complementario (ADNc) se llevó a cabo mediante el kit *SuperscriptTM II (*Invitrogen Life Technologies) o el *Enhanced Avian HS RE-PCR* (Sigma, Poole, UK), partiendo de 1 µg de ARN total y siguiendo las instrucciones de la casa comercial. Se emplearon hexámeros aleatorios como oligonucleótidos para la síntesis.

Los análisis de expresión por RT-PCR se llevaron a cabo por triplicado para cada muestra utilizando 10 o 20 ng de ADNc y siempre en presencia de un control negativo que incluía agua en lugar de ADNc. Se utilizaron ensayos de expresión génica TaqMan para la determinación de la expresión relativa de los genes *S100a8* (Mm00496696_g1), *S100a9* (Mm00656925_m1), *Il10* (Mm01288386), *Dtnbp1* (Mm00458743_m1) y *Dtnbp1C* (4331348ctg) con su respectiva *Taqman Universal PCR master mix* (Applied Biosystems, San Francisco, CA, USA). Se utilizaron cebadores específicos para

determinar la expresión relativa de los genes *Th* (Fw 5'-ACTGCTGCCACGAGCTGCT-3' / Rv 5'-TCAGGGACGCCGTGCACCTA-3') y *Hif1α* (Fw 5'-CATGATGGCTCCCTTTTTCA-3' / Rv 5'-GTCACCTGGTTGCTGCAATA-3') y *2x SYBR Green PCR Master Mix,* (Applied Biosystems). Las reacciones tuvieron lugar en el equipos de PCR cuantitativa a tiempo real *7300 Real Time PCR System* mediante el sistema de detección *ABI Prism 7700* siguiendo las instrucciones del fabricante y se analizaron empleando el *Software SDS 1.4 y 2.1* de Applied Biosystems. La expresión relativa de los genes se determinó mediante empleo del método de $2^{-\Delta\Delta Ct}$ (Livak and Schmittgen, 2001), normalizando en cada caso los datos respecto al gen de expresión constitutiva *Gapdh* (gliceraldehído-3-fosfato deshidrogenasa) o *Actb* (β-actina).

Extracción de proteínas

Las muestras se homogeneizaron en un buffer RIPA [199mM Tris-hidroximetil-aminometano (Tris) pH 7,4, 150mM NaCl, 1 mM ácido etilendiaminotetraacético (EDTA), 1% Acido deoxicólico, 1% Triton x-100, 0,25% SDS, 1 mM Ortovanadato] con un coctel de inhibidores de proteasas (*Complete Mini EDTA-free*, Roche) usando un sistema de homogeneización mecánico (Polytron). En aquellos casos en los que se estudió la fosforilación de proteínas se incluyó un añadido de inhibidores de fosfatasas (5 mM β-glycerofosfato, 50 mM NaF). Posteriormente las muestras se centrifugaron a 16200 g y 4°C durante 15 min. Los sobrenadantes se guardaron a -80°C para su posterior análisis.

La concentración de proteína en el homogeneizado pulmonar se cuantificó mediante un kit comercial (*Kit BCA protein assay*, Pierce) basado en la reacción entre el ácido bicincronínico y cationes de cobre reducidos al quelarse en medio alcalino con las proteínas de la muestra. Se añadieron 2 μl de muestra + 18 μl de agua + 80 μl de solución. Como patrón de estándares se utilizó la albúmina sérica bovina. Tras incubación a 37°C durante 40 minutos, se midió la absorbancia a 562 nm y se calculó la concentración de la proteína correspondiente a cada muestra.

Análisis *western blot*

Geles de Tris-HCl: Las muestras a analizar se mezclaron con tampón de disociación (pH 6,8, 62,5 mM Tris-HCl, 2% SDS, 10% glicerol, 0,62% 2-βmercaptoetanol y 0,0005% azul de bromofenol) y se desnaturalizaron a 100°C durante 10 min antes de cargarlas en geles de poliacrilamida con dodecil sulfato de sodio (SDS-PAGE, *sodium dodecyl sulfate polyacrylamide gel electrophoresis*), con una concentración de poliacrilamida adecuada al tamaño de las proteínas analizadas que oscilaba entre el 5 y el 15%. La electroforesis se realizó a un voltaje constante de 150 V en tampón de electroforesis (24,8 mM Tris-HCl, 192 mM glicina, 0,1% SDS, pH 8,8). Posteriormente se procedió a la transferencia de las proteínas a membranas de nitrocelulosa (*Trans-Blot blotting Media*, Bio-Rad) o de difluoro polivinilideno (PVDF, *Immobilon-P Transfer Membrane*, Millipore) preactivadas en metanol. La transferencia se realizó en un tampón de transferencia (24,8 mM Tris, 192 mM Glicina, 20% metanol) durante 60 min a voltaje constante de 50 V en un soporte *Miniprotean II* (Bio-Rad). Las membranas se bloquearon en una solución de Tris a pH 7,6 con Tween-20 al 0,1% (TBS-T) y leche desnatada en polvo (Biorad) o seroalbúmina bovina (Sigma) al 5% durante 1 h en agitación a temperatura ambiente para evitar posibles uniones inespecíficas. Posteriormente, se incubó con un anticuerpo primario toda la noche a 4°C. Tras lavarse durante 30 min con TBS-T, se incubaron durante 1 h con el anticuerpo secundario correspondiente conjugado a peroxidasa (HRP, *horseradish peroxidase*) y diluido en TBS-T con leche desnatada en polvo o BSA. Tras lavar de nuevo con TBS-T, se llevó a cabo la detección de los complejos antígeno-anticuerpo mediante generación de quimio-luminiscencia con un sustrato comercial (Millipore) en un equipo *LAS3000 mini*, de FUJI. La densidad de las bandas se cuantificó utilizando el programa *Image J* (National Institutes of Health, USA).

Geles de Tris-Tricina: Las muestras a analizar se mezclaron con 10 mM ditiotreitol y se calentaron a 100°C durante 5 min (las muestras procedentes del análisis DIGE se dejaron a temperatura ambiente con 10 mM ditiotreitol durante 15 minutos). Posteriormente se les añadió 10 mM acrilamida, se mezclaron con un tampón (pH 6,8, 62,5 mM Tris-HCl, 2% SDS, 10% glicerol y 0,01% azul de bromofenol) y fueron cargadas en geles de Tris-Tricina al 16,5%. Se sometieron a electroforesis con

un voltaje constante de 90 V en tampón Tris-Tricina (0,1M Tris, 0,1M Tricina, 0,1% SDS). A continuación, se lavaron los geles en tampón de transferencia (24,8 mM Tris, 192 mM Glicina, 25% metanol) y se procedió a la transferencia de las proteínas a membranas de PVDF preactivadas en metanol, en el mismo tampón durante 90 min a voltaje constante de 50 V en un soporte *Miniprotean II* (Bio-Rad). Posteriormente las membranas fueron hidratadas en agua Milli-Q. A partir de este paso se siguió lo especificado para los geles de Tris-HCl.

DIGE, digestión con tripsina y análisis MALDI-ToF

A dos ratones adicionales de cada genotipo se les inyectó 125μg de LPS como ha sido descrito anteriormente y, tras su muerte por exanguinación, se les realizó una toracotomía con el fin de exponer el bloqué corazón-pulmón. Seguidamente se eliminó la sangre de la circulación pulmonar perfundiendo a través del ventrículo izquierdo 2 ml de una solución de lavado TAM [10 mM TRIS pH 8,5 (HCl), 5 mM acetato de magnesio]. Posteriormente se extrajo el pulmón izquierdo, se aclaró en tampón TAM y se homogenizó manualmente en tampón TUCT [7M urea, 2M tiourea , 4% CHAPS (3-[(3-cholamidopropyl) dimethylammonio]-1-propanesulfonate), 30 mM TRIS pH 8.5 (HCl)].

Por cada 50 μg de proteína procedentes de estas muestras, se usaron para el marcaje en oscuridad 400 pmol de fluorocromos (GE Healthcare) CyDye3 (muestra silvestre), CyDye5 (muestra mutante), y una mezcla de ambos extractos se marcó con CyDye2 con el fin de servir de estándar interno en el posterior análisis informático.

Para separar las muestras por su punto isoeléctrico mediante la aplicación de voltaje no constante durante 18 h a 20°C (primera dimensión), mezclamos los extractos marcados y añadimos el mismo volumen de tampón UCDA [8 M urea, 4% CHAPS 130 mM Ditiotreitol (DTT), 2% tampón IEF], completando hasta 450 μL con tampón UCda (8 M urea, 4% CHAPS, 13 mM DTT, 1% tampón IEF). La mezcla de muestras marcadas con los tampones UCDA y UCda se cargó dentro del sarcófago de cerámica y se extendió por toda su superficie. Sobre ella, se colocó una tira de 24 cm

pH 3-11, no lineal (IPG strip; GE Healthcare) y se cubrió con aceite mineral antes de colocar la tapa de plástico para evitar la deshidratación de la muestra durante el isoelectroenfoque.

Tras la primera dimensión, las tiras de pH fueron equilibradas en SES-DTT por 15 minutos [6M urea ,30% glicerol,2% SDS, 75 mM TRIS pH 6,8 (HCl), 0.5% DTT y azul de bromofenol] y otros 15 minutos en SES-IA [6M urea ,30% glicerol,2% SDS, 75 mM TRIS pH 6,8 (HCl), 4.5% iodoacetamida y azul de bromofenol] para facilitar el paso de las proteínas, de la tira al gel de poliacrilamida-SDS al 13%, que las separó a voltaje constante y a 18°C durante toda la noche por su masa molecular (segunda dimensión).

Al concluir esta última separación, los geles se escanearon (*Typhoon 9400*; GE Healthcare) siguiendo las especificaciones que recomienda el fabricante para cada fluorocromo. Las imágenes digitalizadas se analizaron con *Progenesis SameSpots* (Nonlinear Dynamics), lo que permitió visualizar las diferencias entre extractos silvestre y mutante. Tras teñir los geles con *SyproRuby* (Molecular Probes), los puntos diferenciales fueron recortados, desteñidos y posteriormente digeridos con tripsina (12 ng/µL, Promega) durante 1 h a 60°C de forma individual. Los péptidos trípticos generados en cada muestra, se purificaron a 18ºC con Zip-Tip C18 (Millipore) y se eluyeron con CHCA 10 mg/mL (ácido α-ciano-4-hidroxicinnámico) en acetonitrilo / TFA 0,1% (50/50 v/v) sobre una placa de teflón para MALDI-ToF (Applied Biosystems) donde se las dejó secar toda la noche.

Posteriormente se utilizó un espectrómetro de masas (*MALDI-ToF Voyager-DE STR Biospectrometry Workstation*) para obtener las huellas peptídicas que se analizaron con el programa bioinformático *Aldente*.

Ensayo de mieloperoxidasa (MPO)

La cuantificación de los niveles de mieloperoxidasa en los tejidos sirve como marcador de infiltración de neutrófilos. Se incubó lavado broncoalveolar (50 µl) o tejido pulmonar previamente homogeneizado en tampón fosfato y bromuro de cetiltrimetilamonio (CTAB) al 5% con O-dianisidina (0,167 mg/ml) y H_2O_2 (0,0005%) en

tampón fosfato 50 mM a pH 6 durante 15 min, posteriormente se midió su absorbancia a 460 nm y se calculó la concentración de MPO utilizando una curva de calibrado construida con el estándar suministrado por el fabricante.

Cuantificación de Colágeno

La cuantificación de colágeno pulmonar se llevo a cabo utilizando el ensayo Sircol (Biocolor LTD, UK) de acuerdo con las instrucciones del fabricante. Cincuenta microlitros del homogeneizado pulmonar (0,1 mg/ml) se incubó en pepsina ácida (0,1 mg/ml) en ácido acético 0,5M a 4°C toda la noche. Se añadió Rojo Sirius y se mantuvo en agitación durante 30 min. El complejo colágeno-colorante se centrifugó a 16000 g durante 5 min y se disolvió en NaOH 0,5M. Finalmente se midió la absorbancia de las muestras a 540 nm y se calculó su concentración utilizando una a curva estándar construida con concentraciones de 5, 15, 30, 50 y 100 μg del estándar de referencia (Biocolor).

Zimografía de gelatina

La actividad de las metaloproteasas 2 y 9 (Gelatinasa A y B respectivamente) se midió mediante zimografías de gelatina (gelatinogramas). Al contrario que las tradicionales electroforesis de proteínas que utilizan condiciones desnaturalizantes como la SDS-PAGE, esta técnica electroforética se realiza en condiciones no reductoras con el fin de evitar la pérdida de actividad en las enzimas estudiadas y en geles con una concentración predeterminada de gelatina. La degradación de la gelatina indica la ubicación de gelatinasas y la intensidad la actividad proteolítica. Esta degradación se revela tiñendo el gel con colorantes que tengan afinidad por proteínas, observándose una zona blanca donde hubo lisis. Todos los homogeneizados pulmonares o BALF se resolvieron en geles de poliacrilamida al 8% con un 0,2% de gelatina. La electroforesis se llevó a cabo en el tampón SDS-PAGE (24,8 mM Tris base; 192 mM glicina; 2 mM EDTA; 0,1% SDS), a una intensidad de corriente constante de 20 mA por gel. Tras incubarse en una disolución de Triton X-100 al 2,5% durante 30 minutos a temperatura

ambiente para retirar el SDS, se lavaron en agua destilada hasta eliminar completamente el Triton X-100 y se dejaron durante la noche a 37°C en un tampón de digestión (20 mM Tris pH 7,4 , 5 mM Cl_2Ca). A la mañana siguiente fueron teñidos con Comassie (45% metanol, 10 % ácido acético glacial, 0,25% azul Comassie) 20 minutos a 55°C y posteriormente desteñidos (10% metanol, 7,5% ácido acético). Se escanearon con el programa *SilverFast V3.1.1 (*LaserSoft Imaging AG, Alemania) y la densidad de las bandas gelatinolíticas se cuantificó utilizando el programa *ImageJ* (National Institutes of Health, USA).

Ensayos de medición de citoquinas y quimiocinas

Utilizamos inmunoensayos comerciales (ELISA, *enzyme linked immunoassay*) fabricados por BD eBioscience o R&D Systems para la determinación de IL-1β, IFN-γ, MIP-2, LIX, IL-4, IL-10, TGFβ y TNF-α. Cuando las placas no venían pretratadas con el anticuerpo de unión específico, se cubrieron con 100 µl del anticuerpo de unión específico diluido en tampón de revestimiento y se incubaron a 4°C durante la noche. A la mañana siguiente se bloquearon durante una hora a temperatura ambiente con BSA al 5% diluida en tampón de bloqueo, se añadieron las muestras por triplicado y se incubaron durante 24 horas a 20°C. Posteriormente se añadió el anticuerpo de detección (conjugado con peroxidasa) y se incubó durante 2-3 horas en agitación. Finalmente, se añadió una solución de detección cromogénica, que se dejó durante 30 min. La reacción se detuvo mediante adición de ácido sulfúrico y se determinaron las concentraciones midiendo la absorbancia especificada en cada ensayo en un espectrofotómetro e interpolándola con una curva de calibración realizada con concentraciones conocidas de las moléculas en cuestión.

En uno de los estudios también se llevó a cabo la medición de IFN-γ, MIP-2, LIX, IL-4 e IL-10 en homogeneizados pulmonares mediante un ensayo multiplexado (Milliplex Kit, Millipore) siguiendo las instrucciones del fabricante. Para ello se utilizó un sistema de análisis *Luminex 100* (Bio-Rad Life Science, USA), capaz de detectar una

amplia variedad de sustratos por muestra en un solo micropocillo utilizando volúmenes de 50 µl de homogeneizado.

Ensayo de actividad colagenolítica

La actividad colagenolítica total se cuantificó en homogeneizados pulmonares utilizando un kit comercial (EnzChek collagenase assay, Invitrogen, USA). El colágeno conjugado con fluoresceína (*DQ collagen*, Invigrogen, USA) a una concentración de 100 µg/ml se incubó en un tampón de reacción con 100 µg de homogeneizado pulmonar a 37°C y en condiciones de oscuridad. El incremento de la fluorescencia se midió a las 0,5, 1, 3 y 5 horas en un espectrofluorímetro LS 50-B (Perkin-Elmer) a una longitud de onda de excitación de 495 nm y de emisión fluorescente de 515 nm.

Ensayo de enzimático de MMP-8

La actividad enzimática de la MMP-8 sobre la citoquina IL-10 tanto humana como murina se evaluó mediante un ensayo enzimático. Previamente a su uso, se preactivó MMP-8 en 1 mM APMA (acetato de 4-animofenilmerurio) a temperatura ambiente durante 30 min. Posteriormente se incubó MMP-8 (240 ng/µl) junto con IL-10 (100 µg/ml) a 37°C en un tampón de incubación (150 mM NaCl, 5 mM $CaCl_2$, 50 mM Tris-HCl, pH 7,6) durante toda la noche. Se llevaron en paralelo experimentos sin MMP-8 y con TIMP-1 (7,36 µM) como controles negativos. Las muestras se concentraron en una *Speed-Vac* y se resuspendieron en 20 µL de solución SDS-PAGE para su análisis mediante *western blot*.

Análisis estadísticos

Los resultados se expresan como la media ± error estándar de la media (SEM) excepto en el **Artículo 1** que están expresados como la media ± la desviación estándar (SD). La distribución normal de los datos se comprobó mediante el test Kolgomorov-

Smirnov. Las diferencias entre los grupos se comprobaron mediante un análisis univariante de la varianza (ANOVA). Cuando se encontraron diferencias significativas en alguno de los factores del ANOVA, se realizaron comparaciones *post-hoc* por pares, usando la corrección de Bonferroni para comparaciones múltiples o la corrección Dunnet. Cuando sólo hubo que comparar diferencias entre dos variables se utilizó la prueba T. Las diferencias en supervivencia se analizaron usando curvas de Kaplan-Meier y el test Log-rank. Los resultados de los ensayos del cierre de heridas se compararon utilizando un ANOVA para medidas repetidas. La existencia de correlación se evaluó mediante el coeficiente de Spearman (ρ). Se consideró significativa una $p<0,05$. Todos los cálculos se llevaron a cabo utilizando el programa *SPSS 15.0* o versiones superiores del mismo (SPSS Inc., Chicago, IL).

RESULTADOS

I. Estudio el papel de la metaloproteasa MMP-8 en un modelo de daño pulmonar agudo inducido por ventilación mecánica.

Las metaloproteasas de matriz extracelular o MMPs han demostrado ser capaces de llevar a cabo una variedad de funciones que van más allá del procesamiento de los elementos estructurales de la matriz extracelular, modulando aspectos concretos de la respuesta inflamatoria mediante su interacción con distintas cito- y quimiocinas. Basándonos en un trabajo previo realizado en nuestro laboratorio que determinó el papel protector de la MMP-9 en un modelo de lesión pulmonar aguda inducida por ventilación mecánica (VILI) (Albaiceta y col., 2008), decidimos llevar a cabo el estudio del papel de la MMP-8 en este mismo modelo. La ausencia de esta metaloproteasa disminuyó significativamente el daño tisular y mejoró la función pulmonar tras dos horas de ventilación con presiones elevadas. Este efecto no se asoció a alteraciones en la capacidad colagenolítica. Sin embargo, estos ratones mostraron un perfil antiinflamatorio significativo, marcado por una elevación de citoquinas antiinflamatorias y un menor infiltrado inflamatorio pulmonar. La inhibición farmacológica de MMP-8 confirmó estos resultados y apuntó a un posible papel regulador de MMP-8 sobre IL-10 *in vivo*. Los resultados obtenidos muestran el papel proinflamatorio de MMP-8 durante las primeras horas del VILI.

Artículo 1: Guillermo M. Albaiceta, Ana Gutiérrez-Fernández, Emilio García-Prieto, Xose S. Puente, Diego Parra, Aurora Astudillo, Cristina Campestre, Sandra Cabrera, **Adrián González-López,** Antonio Fueyo, Francisco Taboada, and Carlos López-Otín. "Absence or inhibition of matrix metalloproteinase-8 decreases ventilator-induced lung injury".

American Journal of Respiratory Cell and Molecular Biology. 2010 Nov;43(5):555-63. I.F 2010: 4.42

Aportación personal al trabajo.

Me incorporé a este proyecto a mi llegada al laboratorio. Mi contribución personal a este trabajo se centró en la determinación y estudio de los niveles de cito- y quimicionas, así como el descarte de los posibles mecanismos de compensación mediante gelatinogramas. Además colaboré en la elaboración del manuscrito así como las figuras que lo acompañan.

Absence or Inhibition of Matrix Metalloproteinase–8 Decreases Ventilator-Induced Lung Injury

Guillermo M. Albaiceta[1,5], Ana Gutierrez-Fernández[2], Emilio García-Prieto[5], Xose S. Puente[2], Diego Parra[5], Aurora Astudillo[3], Cristina Campestre[4], Sandra Cabrera[2], Adrian Gonzalez-Lopez[1], Antonio Fueyo[1], Francisco Taboada[5,6], and Carlos López-Otin[2]

[1]Departments of Biología Funcional, [2]Bioquímica y Biología Molecular, and [3]Cirugía y Especialidades Médico-Quirurgicas, Universidad de Oviedo, Instituto Universitario de Oncología del Principado de Asturias, Oviedo, Spain; [4]Dipartimento di Scienze del Farmaco, Università "G. d'Annunzio," Chieti, Italy; [5]Intensive Care Unit, Hospital Universitario Central de Asturias, Oviedo, Spain; and [6]Department of Medicina, Universidad de Oviedo, Instituto Universitario de Oncología del Principado de Asturias, Oviedo, Spain

Mechanical ventilation is a life-saving therapy that can also damage the lungs. Ventilator-induced lung injury (VILI) promotes inflammation and up-regulates matrix metalloproteinases (MMPs). Among these enzymes, MMP-8 is involved in the onset of inflammation by processing different immune mediators. To clarify the role of MMP-8 in a model of VILI and their relevance as a therapeutic target, we ventilated wild-type and MMP-8–deficient mice with low or high pressures for 2 hours. There were no significant differences after low-pressure ventilation between wild-type and knockout animals. However, lack of MMP-8 results in better gas exchange, decreased lung edema and permeability, and diminished histological injury after high-pressure ventilation. *Mmp8*$^{-/-}$ mice had a different immune response to injurious ventilation, with decreased neutrophilic infiltration, lower levels of IFN-γ and chemokines (LPS-induced CXC chemokine, macrophage inflammatory protein–2), and significant increases in anti-inflammatory cytokines (IL-4, IL-10) in lung tissue and bronchoalveolar lavage fluid. There were no differences in MMP-2, MMP-9, or tissue inhibitor of metalloproteinase–1 between wild-type and knockout mice. These results were confirmed by showing a similar protective effect in wild-type mice treated with a selective MMP-8 inhibitor. We conclude that MMP-8 promotes acute inflammation after ventilation with high pressures, and its short-term inhibition could be a therapeutic goal to limit VILI.

Keywords: ventilator-induced lung injury; mechanical ventilation; matrix metalloproteinases

The application of high pressures or large volumes to lungs during mechanical ventilation can induce a severe injury type, known as ventilator-induced lung injury (VILI) (1). There are different mechanisms by which a physical stimulus can lead to an inflammatory response within the respiratory system and in distal organs (2). Several of these pathways result in the synthesis, release, and activation of matrix metalloproteinases (MMPs) (3, 4). MMPs are a family of metalloenzymes with a wide range of biological substrates, from virtually all the components of the extracellular matrix to different cyto- and chemokines. Accordingly, MMPs are currently viewed as key modulators of different cellular processes (5). Increased levels of MMPs have been documented in ventilated patients (6–8), as well as in experimental models of VILI (4), implicating MMPs in the pathophysiology of VILI (9, 10). Moreover, MMPs regulate critical processes associated with VILI, including inflammation, matrix turnover, and apoptosis (11).

CLINICAL RELEVANCE

Matrix metalloproteinase (MMP)–8 promotes acute lung inflammation. Genetic ablation or pharmacologic inhibition of this enzyme leads to an attenuated inflammatory response that ameliorates ventilator-induced lung injury. Our results point to MMP-8 inhibition as a therapeutic target to avoid acute inflammation after high-pressure ventilation.

Individual MMPs may have opposite effects. Nonselective inhibition of MMPs results in decreased lung injury after high-pressure ventilation due to a reduction in the inflammatory response (4, 12). However, these results preclude any conclusion about the precise enzymes involved in this beneficial effect. Moreover, different MMPs may have opposite effects. We have previously shown that absence of MMP-9 worsens VILI (9), and other authors have shown a similar protective role of MMP-9 in different models of lung injury (9, 13–16). These data suggest that other metalloproteinases should be responsible for the benefits of MMP inhibition in lung injury. MMP-8 (also known as collagenase-2 or neutrophil collagenase) deserves special attention, as this enzyme is synthesized by neutrophils, stored in secretory granules, and released during the inflammatory response. MMP-8 can cleave native collagen, and is essential for *in vivo* chemokine processing (17, 18). Critically, in a model of acute liver injury (19), mice lacking MMP-8 have decreased neutrophil infiltration, resulting in reduced tissue damage.

Accordingly, in this study, we examined whether MMP-8 is a mediator of VILI, and, consist with this, whether its absence correlates to a reduction of inflammation and lung injury after high-pressure ventilation. To test this hypothesis, we compared the effects of different ventilatory strategies in genetically modified mice lacking MMP-8 and their wild-type counterparts, studying the differences in gas exchange, lung edema, histological injury, and inflammatory response. Finally, the effects of a selective MMP-8 inhibitor were studied to explore a putative clinical application of our findings.

Some of these results have been previously reported in the form of an abstract (20).

MATERIALS AND METHODS

All the experiments were performed according to the guidelines of the Committee on Animal Experimentation of the Universidad de Oviedo (Oviedo, Spain).

(*Received in original form January 22, 2009 and in final form December 4, 2009*)

This work was supported by Instituto de Salud Carlos III grant FIS PI-07/0597, Ministerio de Educación y Ciencia, Fundación M. Botín, and Fundación Lilly. The Instituto Universitario de Oncología is supported by Obra Social Cajastur and Acción Transversal del Cáncer–Red tematica de Investigacion Cooperativa en Cancer. S.C. is the recipient of a grant from Consejo Nacional de Ciencia y Tecnologia de Mexico. A.G.L. is the recipient of a grant from Fundacion para la investigacion cientifica y tecnologia del Prinipado de Asturias.

Correspondence and requests for reprints should be addressed to Guillermo M. Albaiceta, M.D., Ph.D., Intensive Care Unit, Hospital Universitario Central de Asturias, St. Celestino Villamil s/n. 33006-Oviedo, Spain. E-mail: guillermo.muniz@sespa.princast.es

This article has an online supplement, which is accessible from this issue's table of contents at www.atsjournals.org

Am J Respir Cell Mol Biol Vol 43. pp 555–563, 2010
Originally Published in Press as DOI: 10.1165/rcmb.2009-0034OC on December 7, 2009
Internet address: www.atsjournals.org

Animals

Mice used were 10- to 12-week-old males lacking MMP-8 (*Mmp8*$^{-/-}$), of a mixed C57BL/6J/129 background (17), and wild-type littermates, and were kept in specific pathogen–free conditions.

These mice have no baseline differences in lung collagen content, MMP-2, MMP-9, or in any of the cytokines studied (*see* the online supplement).

Experimental Protocol

Wild-type and knockout mice were anesthetized (ketamin and xylazin, intraperitoneally), and a tracheostomy performed. Briefly, a 20-gauge catheter was inserted in the trachea and tightened to avoid air leaks, and the animals were then ventilated (Evita 2 Dura with Neoflow; Dräger, Lübeck, Germany) in pressure-controlled mode. Mice were randomly assigned to one of two ventilatory strategies: low pressure (peak inspiratory pressure [PIP], 15 cm H_2O [PIP 15]; positive end-expiratory pressure [PEEP], 2 cm H_2O; respiratory rate, 100 breaths/min) or high-pressure ventilation (PIP, 25 cm H_2O [PIP 25]; PEEP, 0 cm H_2O; respiratory rate, 50 breaths/min). These pressure settings result in tidal volumes around 10 and 25 ml/kg at the start of the experiment, and respiratory rates were selected to achieve normocapnia, both based on preliminary experiments. Inspiratory-to-expiratory ratio was set at 1:1. Inspiratory and expiratory pauses were done after the onset of ventilation to exclude leaks or air trapping. Different experimental models of VILI lead to different responses in gas exchange, lung permeability, and tissue injury (12, 21, 22), depending on the ventilatory settings, time, and mouse strain (23). Our model results in a highly reproducible injury after 2 hours of ventilation (9, 24), with the main characteristics of lung dysfunction, including impairment in oxygenation, an increase in lung permeability, and structural damage.

After 2 hours of ventilation, a laparotomy was performed, and the aorta punctured to draw an arterial blood sample for gases measurement (NPT7; Radiometer Medical, Brønshøj, Denmark). The animal was then killed by exsanguination, the chest open, and the heart–lung block dissected and removed. The right lower lobe was weighed, dried in an oven (50°C for 48 h), and weighed again to calculate the wet-to-dry weight ratio. The remaining right lung was homogenized in a lysis buffer containing 20 mM Tris, 300 mM sucrose, 1% Triton X-100, and a protease inhibitor cocktail without EDTA (Complete; Roche, Berlin, Germany) and stored at −80°C.

Bronchoalveolar Lavage

Animals of both genotypes were subjected to the ventilatory strategies described previously here. A bronchoalveolar lavage (BAL) was performed at the end of the ventilatory period, before animals were killed. Four aliquots (1 ml) of saline were injected through the tracheostomy tube and recovered to isolate BAL fluid (BALF). Cell count and populations were measured through the use of a Neubauer chamber and in a hemocytometer. The remaining BALF was immediately frozen at −80°C. No other samples were collected from these animals. The protein content of the lysates and BALF was quantified (BCA protein assay; Pierce, Thermo Scientific, Rockford, IL).

Histological Study

The left lung was fixed with intratracheal formaldehyde at 20 cm H_2O and immersed in the same fixative for 24 hours. After fixation, the left lung was embedded in paraffin and processed for a standard hematoxylin and eosin staining. Three slices, with a minimum separating distance of 1 mm, were scored by a pathologist blinded to the genotype and experimental conditions. A semiquantitative scale was used, scoring congestion and edema, hemorrhage, inflammatory cells, and septal thickening (scored from 0 to 4 each) (25).

Western Blot

Levels of MMP-8 in lung homogenates and BALF were determined by Western blotting. Samples containing 50 μg of protein or 12 μl of BALF were loaded in an 8% SDS–polyacrylamide gel. Gels were run and proteins transferred to a nitrocellulose membrane. These membranes were blocked with 3% nonfat milk, and incubated with a polyclonal antibody against murine MMP-8 raised in rabbits. A secondary peroxidase-linked antibody (Anti-Rabbit IgG; Cell Signaling, Danvers, MA) was added and bands of MMP-8 were detected by chemiluminiscence (Immobilon; Millipore, Billerica, MA). Membranes were scanned in a LAS-3000 mini camera (Fujifilm, Barcelona, Spain) and intensity of bands measured (in arbitrary density units) using ImageJ software (National Institutes of Health, Bethesda, MD). Purified murine MMP-8 from bone marrow cell culture supernatant was used as positive control. Tissue inhibitor of metalloproteinase (TIMP)–1 in lung tissue was measured by Western blotting following the same protocol, but using 15% SDS-polyacrylamide gels and a polyclonal antibody purchased from Abcam (Cambridge, UK). Recombinant TIMP-1 was used as positive control.

Gelatin Zymography

MMP-9 is stored in neutrophils together with MMP-8. Previous studies in models of chronic inflammation have shown that MMP-8$^{-/-}$ mice have a compensatory increase in MMP-9 (26, 27). To address this issue, we measured the activity of MMP-2 and MMP-9 in lung tissue or BALF using gelatin zymography. The method is described in detail in the online supplement. Briefly, the volume of lung homogenate corresponding to 95 μg of protein or 12 μl of BALF were loaded in an 8% SDS-polyacrylamide gel containing 0.2% gelatin, electrophoresed, and incubated overnight in a buffer. After staining with Coomassie blue and destaining, gelatinolytic activity appears as white bands in a blue background. The gels were then scanned, and the intensity of the bands quantified with ImageJ software (National Institutes of Health).

ELISAs

IL-1β, IFN-γ, macrophage inflammatory protein (MIP)–2, LPS-induced CXC chemokine (LIX), IL-4, and IL-10 were quantified in lung homogenates (with a volume corresponding to 50 μg of protein) and BALF (8 μl) with standard ELISA kits purchased from BD Biosciences (IL-4, IL-10; Madrid, Spain) or R&D Systems (the remaining molecules; Minneapolis, MN).

Myeloperoxidase Assay

Myeloperoxidase was quantified as a marker of neutrophil infiltration in BALF. BALF (50 μl) were incubated with O-dianisidine and H_2O_2 in phosphate buffer, as previously described (28), and light absorbance at 460 nm was measured.

Collagen Quantification

Total lung collagen was measured in homogenized lungs with the Sircol assay (Biocolor, Carrickfergus, UK), following the manufacturer's instructions. Briefly, lung tissue homogenates were mixed with the Sircol dye and centrifuged at 12,000 rpm for 15 minutes. The pellet was resuspended in NaOH, and the optical density at 540 nm was measured.

In Vivo MMP-8 Inhibition

Wild-type mice were treated with five intraperitoneal doses of 40 mg/kg of the cyclohexylamine salt of (R)-1-(3′methylbiphenyl-4-sulfonylamino)-methylpropyl phosphonic acid, a specific MMP-8 inhibitor with no activity against other MMPs or a disintegrin and a metalloproteinase (ADAM)s (29), with 12-hour intervals between doses. Wild-type littermates were treated with the same volume of vehicle (200 μl of 5% DMSO in PBS). At 1 hour after the last dose, mice were anesthetized and ventilated with the high-pressure protocol. After 2 hours of ventilation, an arterial blood sample was drawn here to measure blood gases, and lung was harvested and processed as previously described here to measure wet-to-dry weight ratio, histological injury, MMP-2 and -9 activity, and IL-4, IL-10 and IFN-γ levels.

Statistical Analysis

Data are expressed as means (±SD). Normal distribution of the data was assessed with a Kolgomorov-Smirnov test. The effects of genotype and ventilatory strategy were compared with a two-way ANOVA. *Post hoc* tests were done, when appropriate, using the Bonferroni correction. The differences between vehicle- and inhibitor-treated mice were compared with a *t* test. A *P* value of less than 0.05 was considered

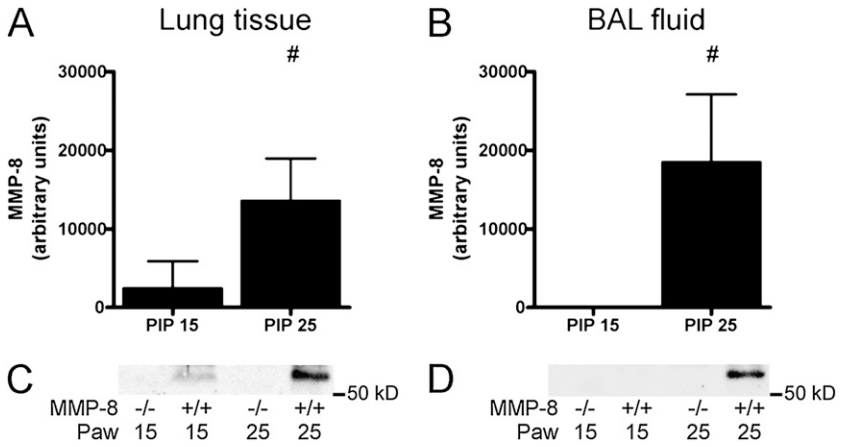

Figure 1. Matrix metalloproteinase (MMP)–8 increases in lung tissue homogenates (*A*) (n = 10/group) and bronchoalveolar lavage fluid (BALF) (*B*) (n = 5/group) after high-pressure ventilation. Representative Western blots are presented of (*C*) lung tissue and (*D*) BALF, showing no detectable MMP-8 in knockout mice. $^{\#}P <$ 0.05 versus peak inspiratory pressure (PIP) 15 in *post hoc* tests.

significant. All calculations were done with SPSS 15.0 software (SPSS Inc., Chicago, IL).

RESULTS

A total of 76 animals were included in the study, with 10 wild-type and 10 knockout mice assigned to each ventilatory group in the main experiment. BAL was performed in five additional animals from each genotype and ventilatory group. Finally, eight wild-type mice were treated with either the specific MMP-8 inhibitor or vehicle, and ventilated with high pressures to assess the efficacy of MMP-8 inhibition in the prevention of VILI. All of the animals survived the ventilatory protocol.

Injurious Mechanical Ventilation Induces the Release of MMP-8

After low-pressure ventilation, the levels of MMP-8 in wild-type animals were low in lung tissue and undetectable in BALF (Figure 1). However, ventilation with high pressures resulted in a significant increase in MMP-8 in both lung parenchyma and BALF (Figures 1A and 1B). As expected, no MMP-8 was detected in *Mmp8*$^{-/-}$ animals (Figures 1C and 1D).

Loss of MMP-8 Protects against VILI

To investigate whether the increase in MMP-8 produced after high-pressure ventilation could contribute to VILI, mice lacking MMP-8 were ventilated simultaneously to their wild-type counterparts to compare the effects of mechanical ventilation between genotypes. No differences in gas exchange, histological lung injury, or wet-to-dry weight ratio between wild-type and knockout mice were observed after low-pressure ventilation (Table 1). Conversely, after high-pressure ventilation, there was a significant impairment in arterial oxygenation in *Mmp8*$^{+/+}$ mice, with no changes in arterial carbon dioxide pressure (Pa_{CO_2}) or arterial pH. This alteration observed in wild-type mice was related to an increase in the histological score of lung injury and in lung edema, quantified using the wet-to-dry weight ratio. Lungs from these animals showed an increase in septal edema, a prominent inflammatory infiltrate, and perivascular hemorrhages (Figure 2C). However, mice lacking MMP-8 developed only moderate lung injury after high-pressure ventilation, with no significant changes in arterial oxygen pressure:fraction of inspired oxygen ratio, in the histological scores or in lung edema quantification (P = 0.16, 0.13, and 0.08 in *post hoc* tests, respectively; Table 1). A mild septal edema and a reduced inflammatory infiltrate were the only findings in the histological study of these animals (Figure 2D), indicating a role of MMP-8 in VILI.

Parallel studies revealed the absence of significant differences between *Mmp8*$^{+/+}$ and *Mmp8*$^{-/-}$ mice in BALF protein content or cell count after low-pressure ventilation (Figures 3A and 3B), although myeloperoxidase activity was significantly lower in knockout mice (Figure 3C). After ventilation at high pressures, wild-type animals showed a significant increase in BALF protein content, cell count, and myeloperoxidase activity, suggesting increased alveolocapillary permeability and polymorphonuclear infiltration. In contrast, *Mmp8*$^{-/-}$ mice ventilated at high pressures showed smaller amounts of protein and no significant changes in cell count or myeloperoxidase activity (Figure 3). In spite of the differences in absolute cell counts, there were no differences between wild-type and knockout mice in percentages of neutrophils in peripheral blood (wild-type, 9 ± 5.75%; knockout, 14 ± 6.6%; n = 4; P = 0.28) or BALF (wild-type, 28.6 ± 13.2%; knockout, 33.6 ± 14.6%; P = 0.72), suggesting

TABLE 1. GAS EXCHANGE, pH, HCO_3, LUNG EDEMA (MEASURED AS WET-TO-DRY WEIGHT RATIO), AND HISTOLOGICAL INJURY SCORE IN EACH EXPERIMENTAL GROUP

	PIP 15		PIP 25	
	Mmp8$^{+/+}$	Mmp8$^{-/-}$	Mmp8$^{+/+}$	Mmp8$^{-/-}$
Pa_{O_2}/FI_{O_2}, mm Hg	408 ± 59	386 ± 46	290 ± 49$^{\#}$	345 ± 60*
Pa_{CO_2}, mm Hg	52 ± 13	47 ± 14	40 ± 5	42 ± 15
pH	7.31 ± 0.09	7.34 ± 0.10	7.31 ± 0.25	7.39 ± 0.14
HCO_3, mEq/L	24.6 ± 1.9	23.3 ± 2.8	20.1 ± 8.1	23.9 ± 4.3
Wet-to dry weight ratio	4.10 ± 0.75	4.48 ± 0.24	6.00 ± 0.69$^{\#}$	5.12 ± 0.96*
Histological score	0.67 ± 0.82	0.75 ± 0.53	3.1 ± 1.24$^{\#}$	1.44 ± 0.73*

Definition of abbreviations: FI_{O_2}, fraction of inspired oxygen; MMP, matrix metalloproteinase; Pa_{CO_2}, arterial carbon dioxide pressure; Pa_{O_2}, arterial oxygen pressure; PIP, peak inspiratory pressure.

In each experimental group, n = 10.

* $P <$ 005 versus wild-type in *post hoc* tests.

$^{\#}$ $P <$ 005 versus PIP 15 in *post hoc* tests.

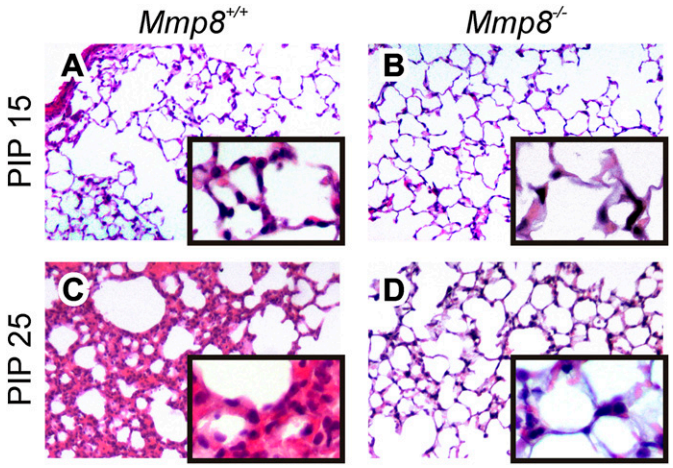

Figure 2. Representative slides stained with hematoxylin-eosin from wild-type and knockout mice after ventilation with low (PIP 15) or high (PIP 25) pressures. Note the mild septal thickening in knockout mice after injurious ventilation compared with the increased injury in wild-type mice.

that the relative composition of the cellular infiltrates is not influenced by MMP-8.

Injurious Ventilation Increases Lung Collagen Content

To determine if the effect of MMP-8 on VILI was related to its collagenolytic activity, total collagen was measured in homogenized lungs from animals subjected to both ventilator strategies. This analysis showed that ventilation using high pressures increased total lung collagen, although no differences were found between wild-type (26.6 ± 4.7 versus 31.2 ± 3.6 μg/mg protein for PIP 15 and PIP 25, respectively; $P < 0.05$) and knockout mice (23.7 ± 3.4 versus 33.6 ± 3.9 μg/mg protein for PIP 15 and PIP 25, respectively; $P < 0.05$), suggesting that the effect of MMP-8 on VILI is not dependent on its collagenolytic activity.

MMP-8 Deficiency Modifies the Immune Response to Ventilation

MMP-8 has been shown to process different cytokines and chemokines *in vivo*, affecting the inflammatory response. On this basis, we investigated whether the different response to ventilation between wild-type and *Mmp8*-deficient mice could be due to changes in the immune response. For this purpose, we determined the concentration of T helper (Th) 1 (IL-1β and IFN-γ) and Th2 (IL-4 and IL-10) cytokines, as well as two CXC chemokines (MIP-2 and LIX) in lung homogenates and BALF (Figure 4). The inflammatory response caused by high-pressure ventilation resulted in a significant up-regulation of these six mediators in lung tissue when compared with low-pressure ventilation, and all except IL-4 and MIP-2 were also up-regulated in BALF. Mmp-8–deficient mice showed a blunted response in the increases of MIP-2 in lung tissue and LIX in BALF. These mutant animals also showed significantly lower levels of IFN-γ in lung tissue and BALF, irrespective of the ventilatory strategy used. Moreover, high-pressure ventilation resulted in higher levels of Th2 cytokines (IL-4 and IL-10) only in $Mmp8^{-/-}$ mice subjected to injurious ventilation.

Mice Lacking MMP-8 Have No Compensatory Changes in MMP-2, MMP-9, or TIMP-1

To investigate whether the absence of MMP-8 could be compensated by other MMPs present in the lung, we measured the activities of MMP-2 and MMP-9 in lung homogenates and

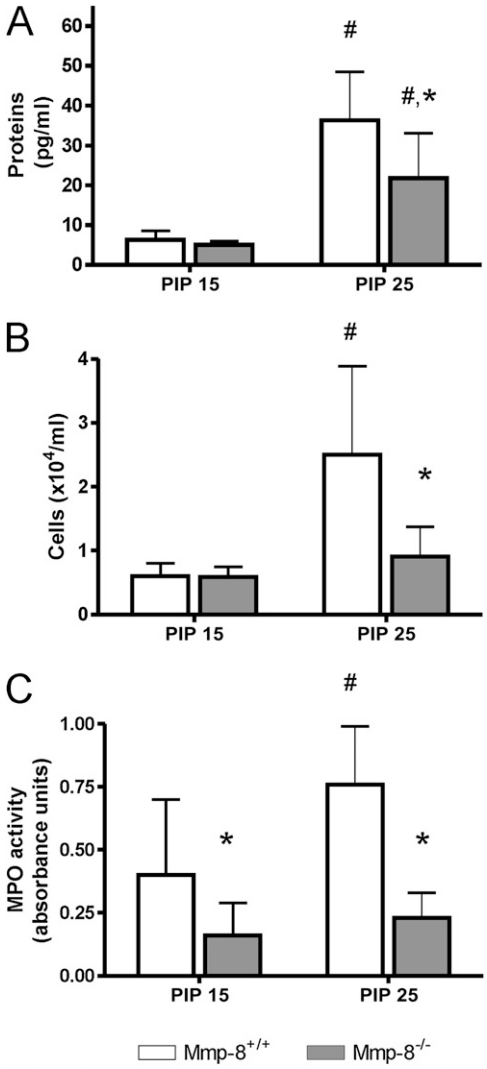

Figure 3. Markers of lung injury in BALF ($n = 5$/group). Differences in protein content (*A*), cell count (*B*), and myeloperoxidase activity (*C*) between wild-type and MMP-$8^{-/-}$ mice show a decreased protein and cell influx in the airspace in the latter. *$P < 0.05$ versus wild-type in *post hoc* tests; #$P < 0.05$ versus PIP 15 in *post hoc* tests.

BALF by gelatin zymography. After high-pressure ventilation, there was an increase in MMP-9 activity in lung homogenates and BALF, whereas MMP-2 increased only in the latter (Figures 5A–5D). However, there were no differences between the genotypes in the activities of MMP-2 or MMP-9. There were no significant differences in TIMP-1 between ventilatory strategies or genotypes (Figure 5E). Figure 5F shows representative zymography and Western blots of these measurements. Together, these results indicate that neither gelatinases (MMP-2 and MMP-9) nor TIMP-1 compensate for the loss of MMP-8 in mice.

Selective Inhibition of MMP-8 Prevents VILI in Wild-Type Mice

The data presented in this study suggest that MMP-8 activity contributes to the tissue damage caused by injurious ventilation. Therefore, to test the clinical relevance of the findings obtained with $Mmp8^{-/-}$ mice, we evaluated the effect of an MMP-8–selective inhibitor in VILI. Accordingly, wild-type mice were treated either with the cyclohexylamine salt of (R)-1-(3′methylbiphenyl-4-sulfonylamino)-methylpropyl phosphonic

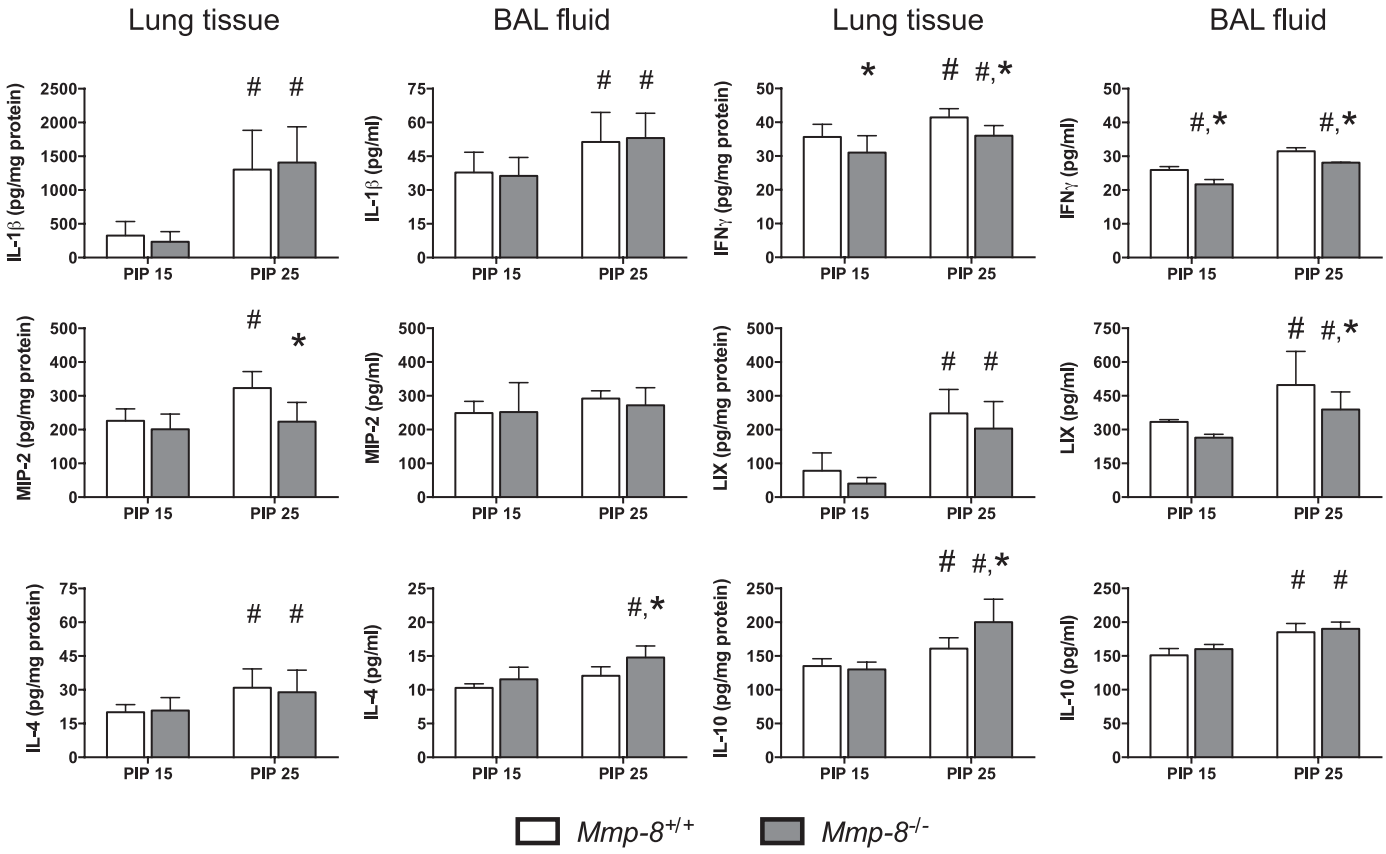

Figure 4. Cytokine (IL-1β, IFN-γ, IL-4, IL-10) and chemokine (macrophage inflammatory protein [MIP]–2, LPS-induced CXC chemokine [LIX]) levels in lung homogenate (n = 10/group) and BALF (n = 5/group) for each experimental group (*see* main text for details). *$P < 0.05$ versus wild-type in *post hoc* tests; #$P < 0.05$ versus PIP 15 in *post hoc* tests.

acid or with vehicle (DMSO). No mice showed any sign of toxicity caused by the drug or the vehicle, and all survived the ventilatory period. Mice treated with the inhibitor showed a better arterial oxygenation than vehicle-treated mice after 2 hours of high-pressure ventilation (Figure 6A). In agreement with these findings, we observed that animals treated with the MMP-8–specific inhibitor had lower wet-to-dry weight ratios and histological scores of lung injury (Figures 6B–6E). In addition, there was a trend toward an increase in Pa_{CO_2} in vehicle-treated mice (60.3 ± 25.2 versus 40.6 ± 14.1 mm Hg; $P = 0.10$), with no significant differences in pH (7.20 ± 0.12 versus 7.30 ± 0.15; $P = 0.16$). No signs of atelectasis were documented in the lungs of these animals, although the increase in Pa_{CO_2} could suggest the existence of areas of hypoventilation or increased alveolar dead space in these extensively injured lungs.

The effects of inhibitory therapy on selected cytokines and MMPs were studied (Figure 7). Treatment with the inhibitor was associated with an increase in IL-10 in lung tissue homogenates, with no differences in IL-4 or IFN-γ. To eliminate the possibility of compensatory changes in MMP-2 and/or MMP-9, gelatin zymography was performed. There were no differences in the activity of these enzymes between inhibitor- or vehicle-treated mice. Collectively, these results demonstrate that selective pharmacological inhibition of MMP-8 has a positive effect on VILI in this experimental model.

DISCUSSION

Our results demonstrate that MMP-8 plays a key role in VILI by promoting a proinflammatory response within the lung, but not by contributing to changing the collagen content of the extracellular matrix. Results from *Mmp-8* knockout mice show that the absence of this enzyme shifts the inflammatory response to an anti-inflammatory one, decreasing tissue damage and improving lung function. The relevance of our findings is reinforced by the demonstration of decreased VILI after treatment with an MMP-8–selective inhibitor. Importantly, these results suggest that MMP-8 inhibition could be an effective therapeutic approach to treating this type of lung injury.

Role of MMP-8 in Inflammation and VILI

MMP-8 is stored in neutrophils and released at the sites of inflammation (26). Its substrates are native collagen, as well as a number of immune mediators, including several cyto- and chemokines. It can inactivate IL-10, and splenocytes from *Mmp8*$^{-/-}$ mice release more IL-4 and IL-10 after a stimulus (27). Other studies have also emphasized the relevance of the proteolytic activity of MMP-8 over CXC chemokines. Processing of LIX (a murine ortholog of IL-8) by MMP-8 increases its chemotactic activity (30), whereas *Mmp8*-null mice have a delayed peak in MIP-2 after injury (26). By these mechanisms, MMP-8 modulates the onset and the clearance of inflammation. Thus, mice lacking this enzyme have a delayed neutrophilic infiltration after an inflammatory stimulus, but also a slower clearance of it (17, 26, 30). These features make these mutant mice more resistant to acute liver injury (19) or autoimmune encephalomyelitis (27).

MMP-8 increases in patients with both acute and chronic lung injuries, such as the acute respiratory distress syndrome (8), chronic obstructive pulmonary disease (31), and pulmonary fibrosis (32). Furthermore, our data show a highly significant

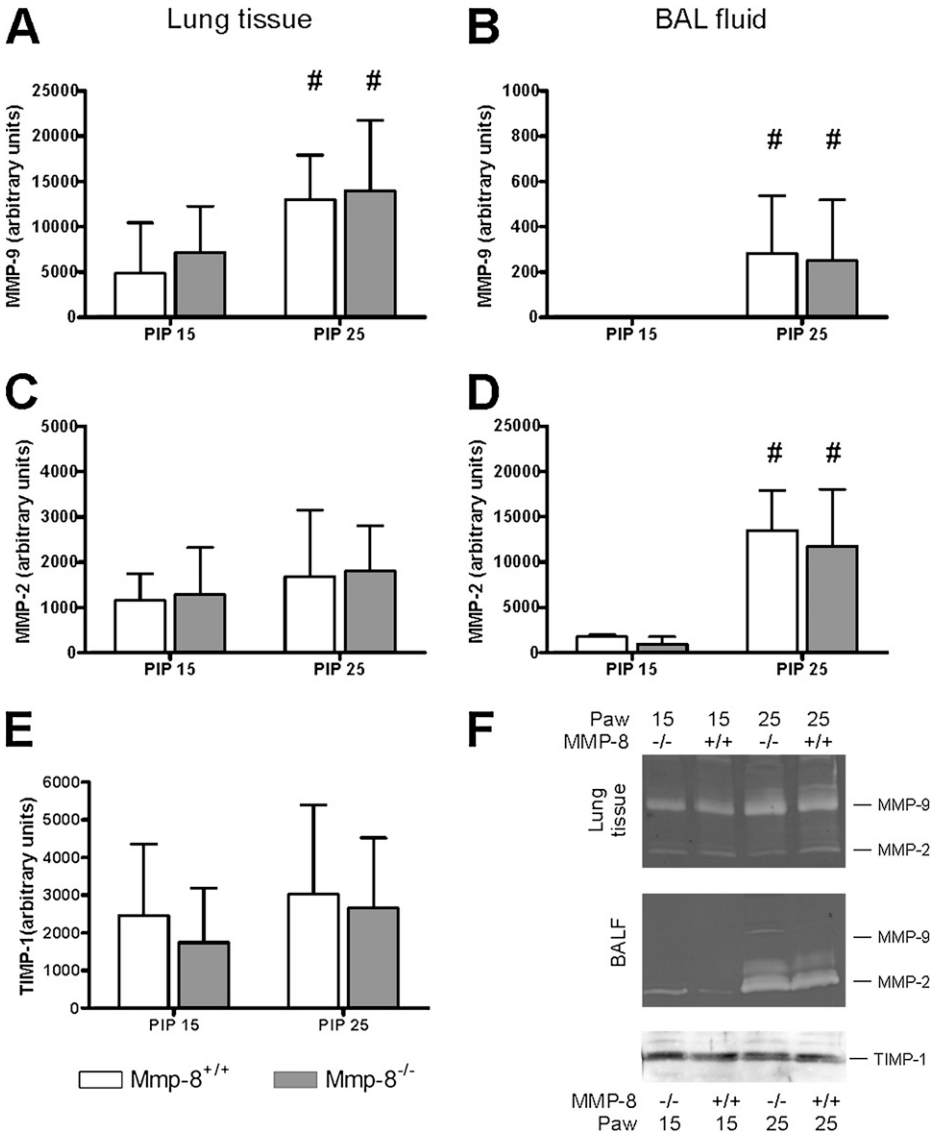

Figure 5. Absence of MMP-8 does not trigger a compensatory gelatinolytic increment. Gelatinase activity ([*A* and *B*] MMP-9; [*C* and *D*] MMP-2) was measured in lung homogenates (n = 10/group) and BALF (n = 5/group). In the same sense, there were no differences in tissue inhibitor of metalloproteinase (TIMP)–1 in lung tissue (*E*). Representative zymographs and Western blotting (*F*) are shown. $^{\#}P < 0.05$ versus PIP 15 in *post hoc* tests.

increase of this MMP after injurious ventilation, consistent with recent studies on MMP-8 (33) and the increases observed for other MMPs (4, 10, 34). More interesting is the finding of decreased VILI in MMP-8–deficient animals after 2 hours of ventilation. These benefits were not related to changes in collagen content of the lung. The small but statistically significant increase in collagen content of the lungs is consistent with the results of other groups, which found an increase in procollagen gene expression after VILI (35). Of note, no signs of fibrosis were found in the histological study; there were no differences between genotypes in this result. It is possible that collagen turnover is regulated by overlapping mechanisms, with MMP-13 being the main collagenolytic enzyme in mice.

However, we did find significant differences in the inflammatory response; specifically, a decrease in CXC chemokines (MIP-2 and LIX) and an increase in anti-inflammatory cytokines (IL-4 and IL-10) in mutant mice. Importantly, treatment with a specific MMP-8 inhibitor increased IL-10 levels. These results suggest that MMP-8 could be an important regulator of IL-10 function *in vivo*. Similar benefits of an anti-inflammatory response mediated by IL-10 during VILI have been previously shown (24, 36–38). Finally, we have observed lower levels of IFN-γ in mutant animals, irrespective of the ventilatory strategy, reinforcing the idea of a modified inflammatory response in *Mmp8*$^{-/-}$ mice. However, this cytokine did not change with inhibitor therapy, so its pathogenetic relevance is less clear.

Our results differ from those recently reported by Dolinay and colleagues (33). They have found that *Mmp8*$^{-/-}$ mice develop more alveolar permeability than their wild-type counterparts after 8 hours of mechanical ventilation with moderate tidal volumes (10 ml/kg) and PEEP of 2 cm H_2O, with no differences in lung edema or cell/neutrophil count in BALF. The comparison with our work suggests that inflammation and permeability in VILI could be independent phenomena with different time patterns, and with MMP-8 acting as a modulator of both processes. For instance, lack of MMP-8 is associated with a slower clearance of the inflammatory infiltrate in a model of skin wounds, causing an impaired healing (26). Similarly, such a persistent inflammation within the lungs could result in chronic damage. These results highlight that the benefits of MMP-8 inhibition should be viewed with caution in regard to long-term therapy. In contrast, long-term MMP-8 inhibition improved outcome in a model of autoimmune encephalomyelitis (27).

Study Limitations

In addition to the uncertainties related to long-term inhibition discussed previously here, our methodology has some limitations that should be discussed:

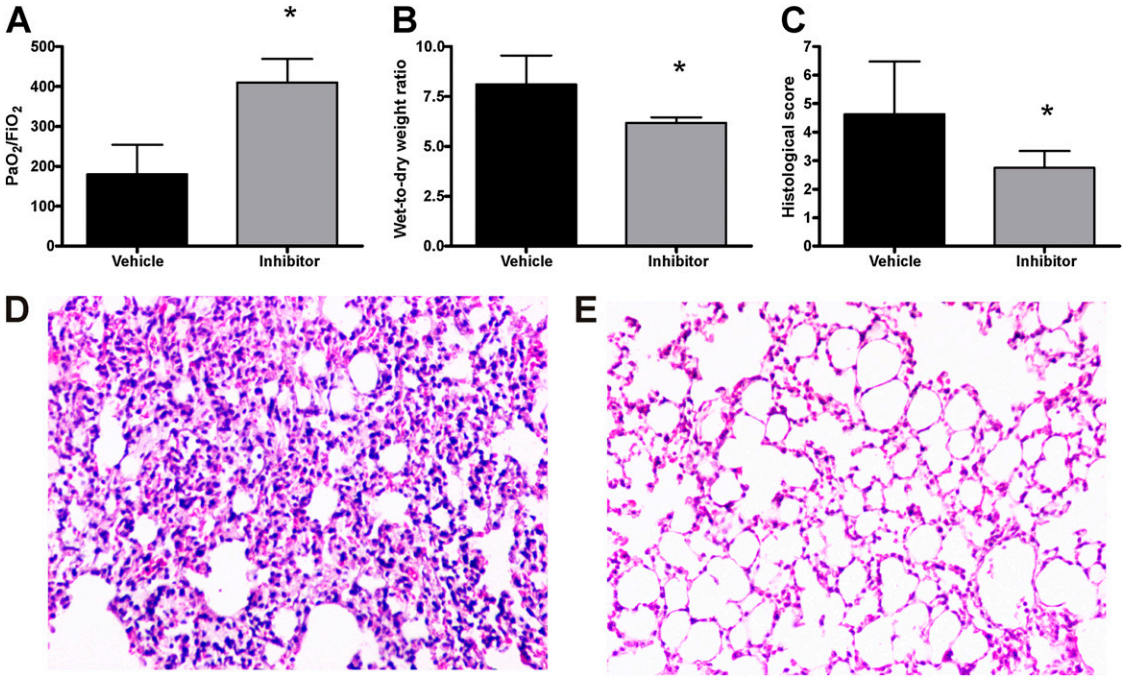

Figure 6. Effects of MMP-8 inhibition in wild-type mice. Oxygenation (A), lung wet-to-dry weight ratio (*B*), and histologic injury (*C*) were measured in wild-type mice treated with an MMP-8–specific inhibitor ($n = 8$) or only with vehicle ($n = 8$), showing the benefits of MMP-8 inhibition in ventilator-induced lung injury. Representative slides (hematoxylin and eosin staining) of vehicle (*D*) and inhibitor-treated (*E*) mice are shown. *$P < 0.05$ versus vehicle-treated mice.

1. Animal model: the injurious ventilatory strategy tested has no clinical counterpart. However, findings from other studies using similar strategies have shown similarities to those in patients under high-volume ventilation in regard to inflammatory response (39).
2. Hemodynamic factors: the role of vascular injury in VILI has been widely studied, and hemodynamic factors could be relevant. These were not measured in our study, and, therefore, a role of MMP-8 in these mechanisms of VILI cannot be discarded. However, the absence of metabolic acidosis at the end of the experiment allows us to discard a severe systemic hypoperfusion.
3. Inhibitor therapy: dosages and timing of the phosphonate were empirically chosen based on published results with other inhibitors. The impact of other doses or administration schedules has not been determined. Moreover, lung injury in DMSO-treated mice was increased when compared with nontreated, wild-type mice. It has been described that DMSO can aggravate lung injury (40, 41), but the solvent was unavoidable due to the lipophilic nature of the substance. This does not invalidate our results, as both vehicle- and inhibitor-treated mice received equal amounts of DMSO.

Clinical Implications

Avoidance of lung injury during mechanical ventilation is an important goal in both patients with and those without lung injury. However, there are patients at risk of ventilator-

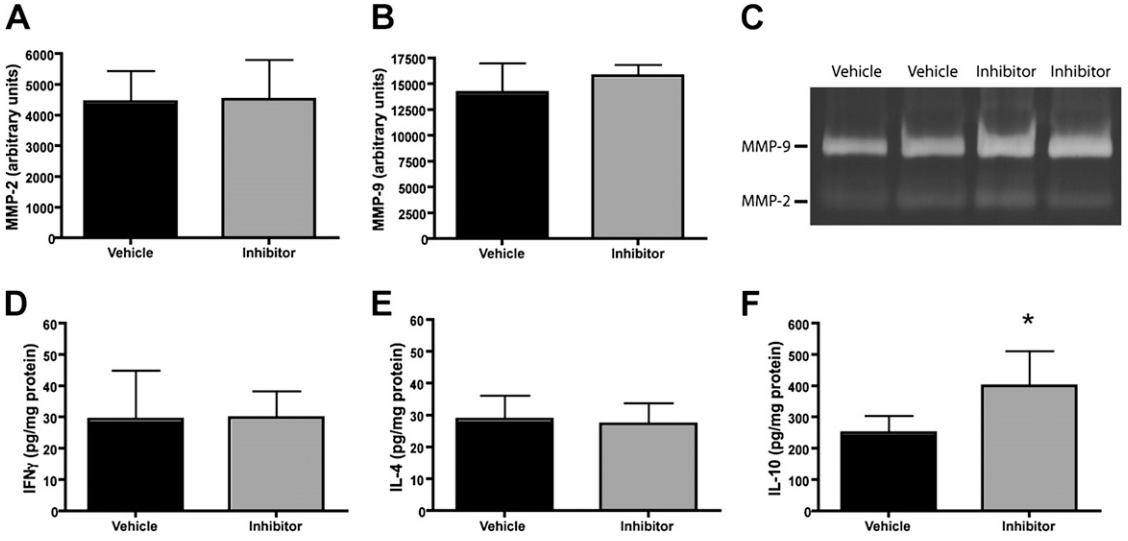

Figure 7. Treatment with the specific MMP-8 inhibitor does not modify MMP-2 or MMP-9 activities (*A*–*C*), IFN-γ (*D*), or IL-4 (*E*) in lung tissue, but significantly increases the anti-inflammatory cytokine, IL-10 (*F*) ($n = 8$/group). *$P < 0.05$ versus vehicle-treated mice.

associated lung injury even during protective ventilation (42). Moreover, limitation of one mechanism of VILI, such as alveolar instability with high PEEP values, can lead to alveolar overstretching (43), complicating the determination of an optimal equilibrium when setting the ventilator. For these reasons, the combination of a protective ventilatory strategy and a drug aimed to limit VILI could be a promising therapeutic strategy. Previous groups (4, 12) have demonstrated a decrease in VILI with broad-spectrum MMP inhibitors (with activity against MMP-1, -2, -9, and other enzymes, such as inducible nitric oxide synthase or cyclooxygenase-2 [44]). However, data from models using knockout mice suggest that some MMPs could play a protective role. Specifically, the absence of MMP-9 is related to a more severe injury after high-pressure ventilation (9), abdominal sepsis (13), ozone exposure (14), or in bronchopulmonary dysplasia (15). Hence, the search for specific MMPs related to tissue injury is warranted to develop specific inhibitors that could have a clinical application. Unfortunately, although some drugs have shown beneficial effects in experimental models, none has been tested in clinical trials.

The results observed in mice deficient for MMP-8 activity, rendered by both genetic manipulation and chemical inhibition, illustrate the potential of this enzyme as a therapeutic target in acute VILI. According to our observations, targeting MMP-8 could be useful during periods of high-pressure ventilation, such as recruitment maneuvers or in patients with the most severe disease. However, the benefits seen in our study, and the concerns over the safety of MMP-8 inhibition at later time points found by other researchers, suggest that this strategy should be viewed with caution. Therefore, more complex experiments, using two-hit models, for example, should be assessed before any clinical recommendation can be provided.

Conclusions

Our results show that MMP-8 plays a key role in triggering a proinflammatory response in the lungs after injurious ventilation. Furthermore, we show that absence or inhibition of this enzyme results in decreased lung injury, probably by enhancing the anti-inflammatory response. Therefore, MMP-8 inhibition could be a useful strategy to prevent VILI. However, slower clearance of the inflammatory infiltrates seen in other models of injury using *Mmp8*$^{-/-}$ animals warrants more studies aimed at clarifying the safety of prolonged therapy against MMP-8.

Author Disclosure: None of the authors has a financial relationship with a commercial entity that has an interest in the subject of this manuscript.

Acknowledgments: The authors thank M.S. Pitiot, A.R. Folgueras, C. Garabaya, and A. Lopez for their help with the histological and biochemical work, and A. Ramsay for his careful review of the manuscript.

References

1. Slutsky AS. Ventilator-induced lung injury: from barotrauma to biotrauma. *Respir Care* 2005;50:646–659.
2. Gattinoni L, Carlesso E, Cadringher P, Valenza F, Vagginelli F, Chiumello D. Physical and biological triggers of ventilator-induced lung injury and its prevention. *Eur Respir J Suppl* 2003;47:15s–25s.
3. Kheradmand F, Werner E, Tremble P, Symons M, Werb Z. Role of rac1 and oxygen radicals in collagenase-1 expression induced by cell shape change. *Science* 1998;280:898–902.
4. Foda HD, Rollo EE, Drews M, Conner C, Appelt K, Shalinsky DR, Zucker S. Ventilator-induced lung injury upregulates and activates gelatinases and emmprin: attenuation by the synthetic matrix metalloproteinase inhibitor, prinomastat (ag3340). *Am J Respir Cell Mol Biol* 2001;25:717–724.
5. Nagase H, Visse R, Murphy G. Structure and function of matrix metalloproteinases and TIMPs. *Cardiovasc Res* 2006;69:562–573.
6. Demoule A, Decailliot F, Jonson B, Christov C, Maitre B, Touqui L, Brochard L, Delclaux C. Relationship between pressure–volume curve and markers for collagen turn-over in early acute respiratory distress syndrome. *Intensive Care Med* 2006;32:413–420.
7. Ricou B, Nicod L, Lacraz S, Welgus HG, Suter PM, Dayer JM. Matrix metalloproteinases and TIMP in acute respiratory distress syndrome. *Am J Respir Crit Care Med* 1996;154:346–352.
8. Fligiel SE, Standiford T, Fligiel HM, Tashkin D, Strieter RM, Warner RL, Johnson KJ, Varani J. Matrix metalloproteinases and matrix metalloproteinase inhibitors in acute lung injury. *Hum Pathol* 2006; 37:422–430.
9. Albaiceta GM, Gutierrez-Fernandez A, Parra D, Astudillo A, Garcia-Prieto E, Taboada F, Fueyo A. Lack of matrix metalloproteinasec9 worsens ventilator-induced lung injury. *Am J Physiol Lung Cell Mol Physiol* 2008;294:L535–L543.
10. Haseneen NA, Vaday GG, Zucker S, Foda HD. Mechanical stretch induces MMP-2 release and activation in lung endothelium: role of emmprin. *Am J Physiol Lung Cell Mol Physiol* 2003;284:L541–L547.
11. Greenlee KJ, Werb Z, Kheradmand F. Matrix metalloproteinases in lung: multiple, multifarious, and multifaceted. *Physiol Rev* 2007;87: 69–98.
12. Kim JH, Suk MH, Yoon DW, Lee SH, Hur GY, Jung KH, Jeong HC, Lee SY, Suh IB, Shin C, *et al.* Inhibition of matrix metalloproteinasec9 prevents neutrophilic inflammation in ventilator-induced lung injury. *Am J Physiol Lung Cell Mol Physiol* 2006;291:L580–L587.
13. Renckens R, Roelofs JJ, Florquin S, de Vos AF, Lijnen HR, van't Veer C, van der Poll T. Matrix metalloproteinasec9 deficiency impairs host defense against abdominal sepsis. *J Immunol* 2006;176:3735–3741.
14. Yoon HK, Cho HY, Kleeberger SR. Protective role of matrix metalloproteinasec9 in ozone-induced airway inflammation. *Environ Health Perspect* 2007;115:1557–1563.
15. Lukkarinen H, Hogmalm A, Lappalainen U, Bry K. Matrix metalloproteinasec9 deficiency worsens lung injury in a model of bronchopulmonary dysplasia. *Am J Respir Cell Mol Biol* 2009;41:59–68.
16. Cabrera S, Gaxiola M, Arreola JL, Ramirez R, Jara P, D'Armiento J, Richards T, Selman M, Pardo A. Overexpression of MMP9 in macrophages attenuates pulmonary fibrosis induced by bleomycin. *Int J Biochem Cell Biol* 2007;39:2324–2338.
17. Balbin M, Fueyo A, Tester AM, Pendas AM, Pitiot AS, Astudillo A, Overall CM, Shapiro SD, Lopez-Otin C. Loss of collagenase-2 confers increased skin tumor susceptibility to male mice. *Nat Genet* 2003;35: 252–257.
18. Van Lint P, Libert C. Matrix metalloproteinase–8: cleavage can be decisive. *Cytokine Growth Factor Rev* 2006;17:217–223.
19. Van Lint P, Wielockx B, Puimege L, Noel A, Lopez-Otin C, Libert C. Resistance of collagenase-2 (matrix metalloproteinase–8)–deficient mice to TNF-induced lethal hepatitis. *J Immunol* 2005;175:7642–7649.
20. Albaiceta GM, Parra D, Garcia-Prieto E, Astudillo A, Fueyo A, Puente XS, Taboada F, Lopez-Otin C. Decreased ventilator-induced lung injury in matrix metalloproteinase–8 deficient mice. *Intensive Care Med* 2008;34:S96.
21. Kaynar AM, Houghton AM, Lum EH, Pitt BR, Shapiro SD. Neutrophil elastase is needed for neutrophil emigration into lungs in ventilator-induced lung injury. *Am J Respir Cell Mol Biol* 2008;39:53–60.
22. Wilson MR, Choudhury S, Takata M. Pulmonary inflammation induced by high-stretch ventilation is mediated by tumor necrosis factor signaling in mice. *Am J Physiol Lung Cell Mol Physiol* 2005;288: L599–L607.
23. Eckle T, Fullbier L, Grenz A, Eltzschig HK. Usefulness of pressure-controlled ventilation at high inspiratory pressures to induce acute lung injury in mice. *Am J Physiol Lung Cell Mol Physiol* 2008;295: L718–L724.
24. Pedreira PR, Garcia-Prieto E, Parra D, Astudillo A, Diaz E, Taboada F, Albaiceta GM. Effects of melatonin in an experimental model of ventilator-induced lung injury. *Am J Physiol Lung Cell Mol Physiol* 2008;295:L820–L827.
25. Belperio JA, Keane MP, Burdick MD, Londhe V, Xue YY, Li K, Phillips RJ, Strieter RM. Critical role for CXCR2 and CXCR2 ligands during the pathogenesis of ventilator-induced lung injury. *J Clin Invest* 2002;110:1703–1716.
26. Gutierrez-Fernandez A, Inada M, Balbin M, Fueyo A, Pitiot AS, Astudillo A, Hirose K, Hirata M, Shapiro SD, Noel A, *et al.* Increased inflammation delays wound healing in mice deficient in collagenase-2 (MMP-8). *FASEB J* 2007;21:2580–2591.
27. Folgueras AR, Fueyo A, Garcia-Suarez O, Cox J, Astudillo A, Tortorella P, Campestre C, Gutierrez-Fernandez A, Fanjul-Fernandez M, Pennington CJ, *et al.* Collagenase-2 deficiency or inhibition impairs

experimental autoimmune encephalomyelitis in mice. *J Biol Chem* 2008;283:9465–9474.
28. Bradley PP, Priebat DA, Christensen RD, Rothstein G. Measurement of cutaneous inflammation: estimation of neutrophil content with an enzyme marker. *J Invest Dermatol* 1982;78:206–209.
29. Biasone A, Tortorella P, Campestre C, Agamennone M, Preziuso S, Chiappini M, Nuti E, Carelli P, Rossello A, Mazza F, *et al.* Alpha-biphenylsulfonylamino 2-methylpropyl phosphonates: enantioselective synthesis and selective inhibition of MMPs. *Bioorg Med Chem* 2007;15:791–799.
30. Tester AM, Cox JH, Connor AR, Starr AE, Dean RA, Puente XS, Lopez-Otin C, Overall CM. LPS responsiveness and neutrophil chemotaxis *in vivo* require PMN MMP-8 activity. *PLoS One* 2007;2: e312.
31. Vernooy JH, Lindeman JH, Jacobs JA, Hanemaaijer R, Wouters EF. Increased activity of matrix metalloproteinase–8 and matrix metalloproteinase–9 in induced sputum from patients with COPD. *Chest* 2004;126:1802–1810.
32. Manoury B, Nenan S, Guenon I, Lagente V, Boichot E. Influence of early neutrophil depletion on MMPs/TIMP-1 balance in bleomycin-induced lung fibrosis. *Int Immunopharmacol* 2007;7:900–911.
33. Dolinay T, Wu W, Kaminski N, Ifedigbo E, Kaynar AM, Szilasi M, Watkins SC, Ryter SW, Hoetzel A, Choi AM. Mitogen-activated protein kinases regulate susceptibility to ventilator-induced lung injury. *PLoS One* 2008;3:e1601.
34. Hasaneen NA, Zucker S, Cao J, Chiarelli C, Panettieri RA, Foda HD. Cyclic mechanical strain-induced proliferation and migration of human airway smooth muscle cells: role of emmprin and MMPs. *FASEB J* 2005;19:1507–1509.
35. de Carvalho ME, Dolhnikoff M, Meireles SI, Reis LF, Martins MA, Deheinzelin D. Effects of overinflation on procollagen type III expression in experimental acute lung injury. *Crit Care* 2007;11:R23.
36. Donnelly SC, Strieter RM, Reid PT, Kunkel SL, Burdick MD, Armstrong I, Mackenzie A, Haslett C. The association between mortality rates and decreased concentrations of interleukin-10 and interleukin-1 receptor antagonist in the lung fluids of patients with the adult respiratory distress syndrome. *Ann Intern Med* 1996;125:191–196.
37. Lee HS, Wang Y, Maciejewski BS, Esho K, Fulton C, Sharma S, Sanchez-Esteban J. Interleukin-10 protects cultured fetal rat type II epithelial cells from injury induced by mechanical stretch. *Am J Physiol Lung Cell Mol Physiol* 2008;294:L225–L232.
38. Hoegl S, Boost KA, Czerwonka H, Dolfen A, Scheiermann P, Muhl H, Zwissler B, Hofstetter C. Inhaled IL-10 reduces biotrauma and mortality in a model of ventilator-induced lung injury. *Respir Med* 2009;103:463–470.
39. Ranieri VM, Suter PM, Tortorella C, De Tullio R, Dayer JM, Brienza A, Bruno F, Slutsky AS. Effect of mechanical ventilation on inflammatory mediators in patients with acute respiratory distress syndrome: a randomized controlled trial. *JAMA* 1999;282:54–61.
40. Haschek WM, Baer KE, Rutherford JE. Effects of dimethyl sulfoxide (DMSO) on pulmonary fibrosis in rats and mice. *Toxicology* 1989;54: 197–205.
41. Santos NC, Figueira-Coelho J, Martins-Silva J, Saldanha C. Multidisciplinary utilization of dimethyl sulfoxide: pharmacological, cellular, and molecular aspects. *Biochem Pharmacol* 2003;65:1035–1041.
42. Terragni PP, Rosboch G, Tealdi A, Corno E, Menaldo E, Davini O, Gandini G, Herrmann P, Mascia L, Quintel M, *et al.* Tidal hyperinflation during low tidal volume ventilation in acute respiratory distress syndrome. *Am J Respir Crit Care Med* 2007;175:160–166.
43. Albaiceta GM, Luyando LH, Parra D, Menendez R, Calvo J, Pedreira PR, Taboada F. Inspiratory vs. expiratory pressure–volume curves to set end-expiratory pressure in acute lung injury. *Intensive Care Med* 2005;31:1370–1378.
44. Steinberg J, Halter J, Schiller H, Gatto L, Carney D, Lee HM, Golub L, Nieman G. Chemically modified tetracycline prevents the development of septic shock and acute respiratory distress syndrome in a clinically applicable porcine model. *Shock* 2005;24:348–356.

ONLINE DATA SUPPLEMENT

Mice lacking MMP-8 and their wildtype counterparts have no fenotypic differences in baseline conditions. These animals have a normal lifespan, and the majority of differences appear only after an stimulus like the induction of an inflammatory response. To doccument the absence of differences in baseline conditions in any of the parameters measured in this study, we quantified lung collagen, MMP-2, MMP-9, cyto-and chemokines in intact wildtype and knockout mice.

Methods.

Intact wildtype and Mmp-8 knocout mice of 8 weeks were anesthesized using ketamin and xylazin. A laparotomy was performed and the animals sacrified by exanguination. After this, the chest wall was opened and the lung removed and frozen inmediately. These lungs were homogenized in a buffer (20 mM TRIS, 300 mM sucrose, 1% Triton X-100 and a protease inhibitor cocktail without EDTA (Complete, Roche, Germany)). The protein content of the homogenates was measured using the BCA protein assay (Pierce, USA).

Collagen content. Total lung collagen was measured in homogenized lungs using the Sircol assay (Biocolor, UK), following manufacturer's instructions. Lung tissue homogenates were mixed with the Sircol dye, incubated at room temperature for 30 minutes and centrifugated at 12000 rpm for 15 minutes. This procedure precipitates the collagen in the sample. The pellet was resuspended in NaOH and the optical density at 540 nm measured. Collagen content was normalized by the total protein content.

Gelatin Zymography. MMP-2 and MMP-9 were measured in homogenates using gelatin zymography. The volume of lung homogenate corresponding to 95μg of protein or 12μL of BAL fluid were loaded in an 8% SDS-polyacrylamide gel containing 0.2% gelatin. The protein samples were electrophoresised before the gel was washed three times in 2.5% Triton X-100 and incubated overnight at 37ºC in a buffer containing 20 mM Tris/HCl, 5 mM $CaCl_2$, pH 7.4 Gels were stained using Coomassie Blue and destained with a mixture of acetic acid and methanol, then scanned and the intensity of the bands quantified using ImageJ software (National Institutes of Health, USA).

Cytokine/Chemokine assay. Concentrations of IL-1β, IFNγ, IL-4, IL-10, MIP-2 and LIX in lung tissue homogenates were measured by multiplex immunoassay (Luminex 100) using a mouse Milliplex kit (Millipore, US) according to manufacturer's instructions. The results were normalized by protein content in the homogenate.

Statistical analysis. Data are expressed as mean±standard deviation. Values from wildtype and Mmp8-/-mice were compared using a T-test. A p value lower than 0.05 was considered significant.

Additional Results.

There were no differences between intact wildtype and knocout mice in any of the parameters studied. Baseline lung collagen was similar in both genotypes (p=0.74), with values close to those found after low-pressure ventilation in the main experiment (Figure E1). In the same sense, baseline levels of MMP-2 and MMP-9 were similar (Figure E2).

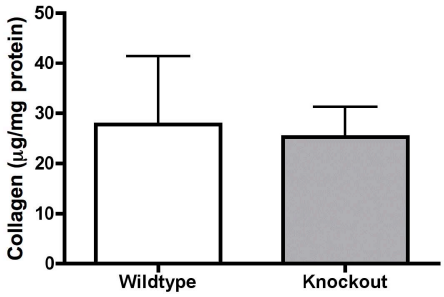

Figure E1. Collagen content of the lungs of intact wildtype (white bars) and knocout mice (gray bars).

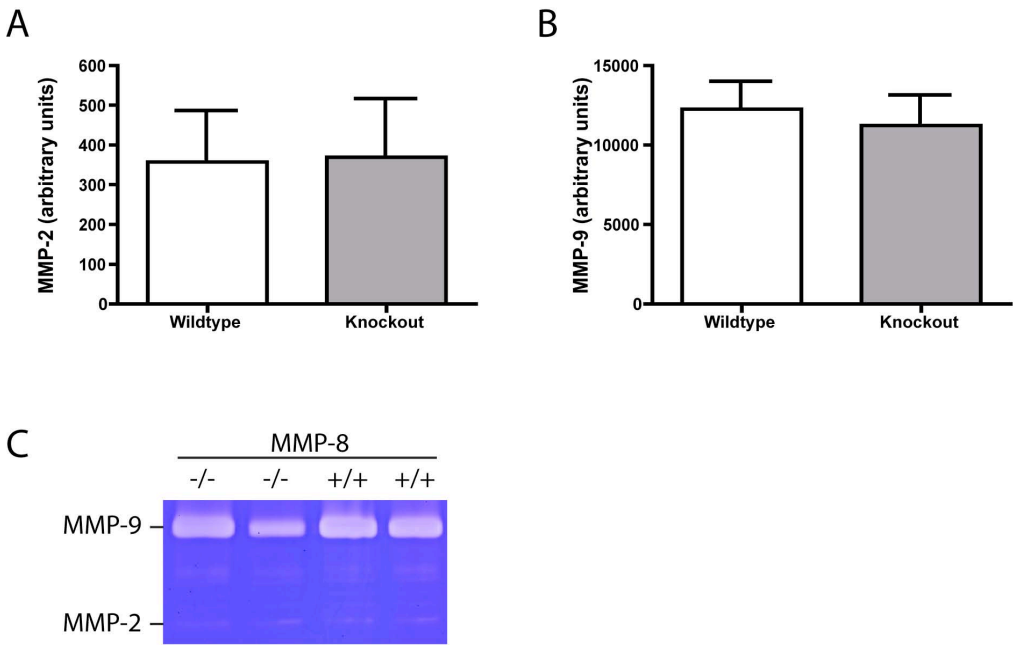

Figure E2. Intact mice of both genotypes does not differ in MMP-2 (p=0.91, A) or MMP-9 (p=0.21, B) levels measured by zymography. A representative gelatin zymography is shown (C).

Finally, baseline levels of immune mediators were measured. There were no differences in any of the molecules measured (Figure E3). These results are similar to those found by other authors who have demonstrated the absence of differences in the baseline levels of IL-4 (E1), LIX (E1) or MIP-2 (E2) in these mice. Collectively, these results show that *Mmp8*$^{-/-}$ mice do not show relevant differences when compared to their wildtype counterparts in baseline conditions, and that differences emerge only when these mutant animals are exposed to an stimulus.

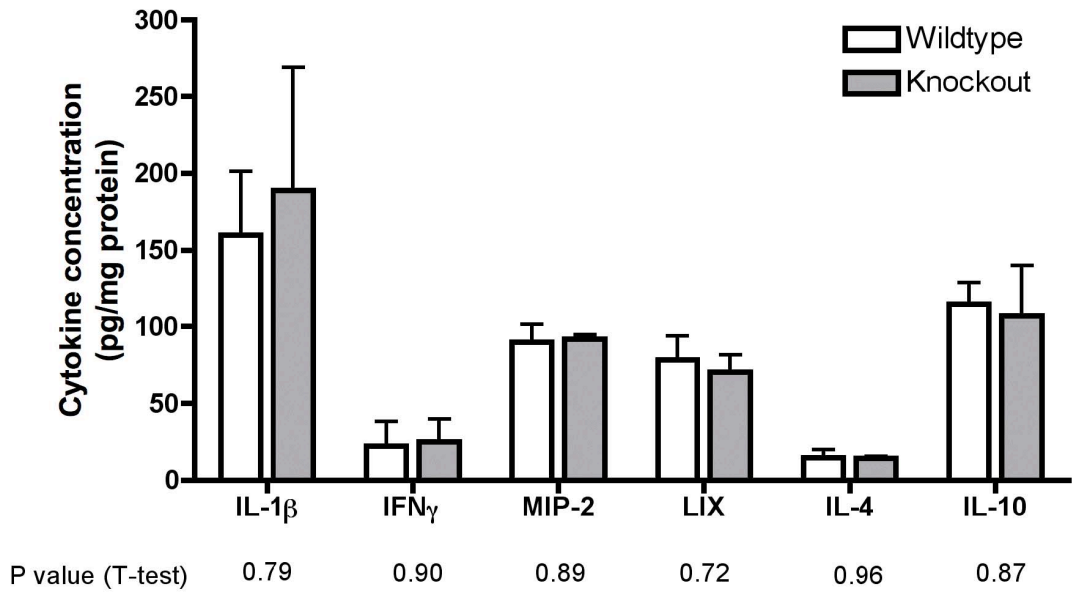

Figure E3. Immune mediators concentration in lung tissue homogenates of intact wildtype (n=4) and Mmp8 knockout mice (n=4). There were no differences in baseline levels in any of the cytokines/chemokines studied. IL-1β: Interleukin 1β. IFNγ: Interferon gamma. MIP-2: Macrophage inflammatory protein-2. LIX: Lipopolysaccharide-induced CXC chemokine. IL-4: Interleukin 4. IL-10: Interleukin

10.

References.

E1. Gueders MM, Balbin M, Rocks N, Foidart JM, Gosset P, Louis R, Shapiro S, Lopez-Otin C, Noel A, Cataldo DD. Matrix metalloproteinase-8 deficiency promotes granulocytic allergen-induced airway inflammation. *J Immunol* 2005;175(4):2589-2597. E2. Gutierrez-Fernandez A, Inada M, Balbin M, Fueyo A, Pitiot AS, Astudillo A, Hirose K, Hirata M, Shapiro SD, Noel A, et al. Increased inflammation delays wound healing in mice deficient in collagenase-2 (mmp-8). *FASEB J* 20021(10):2580-2591.

II. La ausencia de MMP-8 incrementa los niveles de los ligandos de TLR/RAGE, S100A8 y S100A9 exacerbando la inflamación pulmonar durante la endotoxemia.

La presencia en el pulmón de una elevada cantidad de receptores tipo TLR (del inglés *Toll-like receptors*) y RAGE (del inglés *Receptor of advanced glicosilation end-products*), hace que este órgano sea especialmente vulnerable a la endotoxemia. Dada la importancia de MMP-8 en la modulación de la respuesta inflamatoria local, nos planteamos la hipótesis de que esta metaloproteasa también podría regular la respuesta inflamatoria a distancia. Veinticuatro horas tras la administración de LPS, la ausencia de MMP-8 se tradujo en un mayor aumento del infiltrado inflamatorio y el daño histológico en estos ratones. Además de un aumento en los niveles de MIP-1α, el análisis proteómico mostró a las alarminas S100A8 y S100A9 como posibles participes de este efecto. La habilidad quimiotáctica de estas proteínas y su capacidad para activar la vía de NFκB refuerzan el papel central de MMP-8 en la regulación del reclutamiento de neutrófilos a los pulmones durante la sepsis.

Artículo 2: González-López A, Aguirre A, López-Alonso I, Amado L, Astudillo A, Fernández-García MS, Suárez MF, Batalla-Solís E, Colado E, Albaiceta GM. "MMP-8 deficiency increases TLR/RAGE ligands S100A8 and S100A9 and exacerbates lung inflammation during endotoxemia".

PLoS One. 2012;7(6). I.F 2011: 4.09

Aportación personal al trabajo.

Para este proyecto colaboré desde su inicio en el diseño experimental, llevé a cabo el modelo de endotoxemia en los animales, contribuí a los estudios histológicos, así como las determinaciones *western blot*, PCR cuantitativas y su posterior análisis estadístico. Así mismo colaboré en la escritura del artículo y en la elaboración de sus figuras.

OPEN ACCESS Freely available online

PLoS one

MMP-8 Deficiency Increases TLR/RAGE Ligands S100A8 and S100A9 and Exacerbates Lung Inflammation during Endotoxemia

Adrián González-López[1], Alina Aguirre[1], Inés López-Alonso[1], Laura Amado[2], Aurora Astudillo[3], María Soledad Fernández-García[3], María F. Suárez[4], Estefanía Batalla-Solís[1,2], Enrique Colado[5], Guillermo M. Albaiceta[1,2,6]*

1 Departamento de Biología Funcional, Instituto Universitario de Oncología del Principado de Asturias, Universidad de Oviedo, Oviedo, Spain, **2** Servicio de Medicina Intensiva, Hospital Universitario Central de Asturias, Oviedo, Spain, **3** Servicio de Anatomía Patológica, Hospital Universitario Central de Asturias, Oviedo, Spain, **4** Departamento de Bioquímica y Biología Molecular, Instituto Universitario de Oncología del Principado de Asturias, Universidad de Oviedo, Oviedo, Spain, **5** Servicio de Hematología y Hemoterapia, Hospital Universitario Central de Asturias, Oviedo, Spain, **6** CIBER-Enfermedades Respiratorias, Instituto de Salud Carlos III, Madrid, Spain

Abstract

Matrix metalloproteinase-8, released mainly from neutrophils, is a critical regulator of the inflammatory response by its ability to cleave multiple mediators. Herein, we report the results of a model of endotoxemia after intraperitoneal LPS injection in mice lacking MMP-8 and their wildtype counterparts. Control, saline-treated animals showed no differences between genotypes. However, there was an increased lung inflammatory response, with a prominent neutrophilic infiltration in mutant animals after LPS treatment. Using a proteomic approach, we identify alarmins S100A8 and S100A9 as two of the main differences between genotypes. Mice lacking MMP-8 showed a significant increase in these two molecules in lung homogenates, but not in spleen and serum. Mice lacking MMP-8 also showed an increase in MIP-1α levels and a marked activation of the non-canonical NF-κB pathway, with no differences in CXC-chemokines such as MIP-2 or LIX. These results show that MMP-8 can modulate the levels of S100A8 and S100A9 and its absence promotes the lung inflammatory response during endotoxemia.

Citation: González-López A, Aguirre A, López-Alonso I, Amado L, Astudillo A, et al. (2012) MMP-8 Deficiency Increases TLR/RAGE Ligands S100A8 and S100A9 and Exacerbates Lung Inflammation during Endotoxemia. PLoS ONE 7(6): e39940. doi:10.1371/journal.pone.0039940

Editor: Tim D. Oury, University of Pittsburgh, United States of America

Received April 6, 2012; **Accepted** May 29, 2012; **Published** June 29, 2012

Funding: Supported by Instituto de Salud Carlos III (FIS PI 07-0597). AGL is the recipient of a grant from Universidad de Oviedo (UNOV-09-pf). A. Aguirre is the recipient of a grant from Instituto Universitario de Oncología del Principado de Asturias. EBS is the recipient of a grant from Fundación para el Fomento en Asturias de la Investigación Científica Aplicada y la Tecnología (FICYT, COF-11-40). GMA is the recipient of a grant from Instituto de Salud Carlos III (Intensificación de la Actividad Investigadora-INT 11/14). The funders had no role in study design, data collection and analysis, decision to publish, or preparation of the manuscript.

Competing Interests: The authors have declared that no competing interests exist.

* E-mail: Guillermo.muniz@sespa.princast.es

Introduction

The inflammatory response consists not only in local inflammation. In severe cases, this response spreads from the site of onset and evolves into a systemic injury [1]. In this setting, the lungs are amongst the most commonly involved organs. Neutrophils are recruited from the circulation [2], and a full-blown immune response takes place in both the interstitium and the alveolar spaces. This syndrome has been termed acute lung injury and may result in a severe lung dysfunction by altering gas exchange and respiratory mechanics. In patients with the systemic inflammatory response syndrome, lung injury is related to a high mortality rate [3].

The regulatory mechanisms responsible for the switch from a local to a systemic response are only partially known. There is increasing evidence that matrix metalloproteinases, a family of enzymes with a great variety of substrates, may modulate the inflammatory response by cleaving immune mediators and regulating cell migration [4]. Matrix metalloproteinase-8, also known as collagenase-2 or neutrophil collagenase, plays different roles in the regulation of the inflammatory response [5]. Mice lacking this enzyme show a delayed onset and also a slow clearance of the local inflammatory infiltrates [6,7]. Several immune mediators, such as MIP-1α [8], IL-10 [9] or LIX [10], have been involved in this characteristic pattern and shown to be substrates of MMP-8.

We hypothesized that MMP-8 plays also a role in the lung response to endotoxemia. To test this hypothesis we used an experimental model of inflammation by intraperitoneal injection of lipopolysaccharide in wildtype and MMP-8 deficient mice. After documentation of increased neutrophil recruitment in the lungs from knockout mice compared to wildtype animals, we used a proteomic approach to identify the molecules involved in the observed differences in mice from both genotypes. These studies revealed the alarmins S100A8 and S100A9, which are significantly increased in mice lacking MMP-8, as two of the candidates to be responsible for the increased inflammatory response in mutant mice.

Methods

Animals

Mice deficient in MMP-8 were generated as previously described [6] and backcrossed to obtain a pure C57BL6 background. Normal mice with the same C57BL6 background were used as wildtype counterparts. Seventy-two animals were used in the study. Genotypes were confirmed by PCR in all animals. Animals were kept in SPF conditions, with 12:12 hours light/dark cycles and free access to water and food. All the experimental protocols were reviewed and approved by the University of Oviedo Animal Research Ethics committee.

Experimental Model

A dose of 5 mg/Kg of lipopolysaccharide (serotype O55:B5, Sigma-Aldrich) was intraperitoneally injected to wildtype and knockout mice. This dose induces lung inflammation with a peak 24 hours after injection [11]. Control animals from both genotypes were injected only with vehicle (sterile saline). After 24 hours, mice were anesthetized with a mixture of ketamine and xylazine, a laparotomy was performed and the animals were sacrificed by exsanguination. The lungs and the spleen were then removed. The right lung and the spleen were frozen at $-80^{\circ}C$ for further analysis. The left lung was fixated by intratracheal administration of 4% formaldehyde and immersed in the same fixative. In additional animals, a blood sample was obtained by cardiac puncture.

Histological Study

Paraffin embedded sections were stained using a standard hematoxylin-eosin technique. Three sections per mouse were evaluated by two independent pathologists (AA, MSFG), blinded to the experimental conditions. Each section was scored from 0 to 3 based on the septal thickening (grade 1), areas of alveolar flooding (grade 2) and loss of normal alveolar structure (grade 3). Lung neutrophil recruitment was evaluated by immunohistochemical staining against myeloperoxidase (MPO) using an anti-MPO antibody (Thermo Scientific). The number of MPO positive cells in three randomly chosen high-power fields was counted and averaged for each animal.

Bronchoalveolar Lavage

Four animals of each genotype were treated with LPS as described. After 24 hours, mice were anesthetized and a tracheostomy performed. Lungs were lavaged with three aliquots (700 microliters) of sterile saline. Neutrophils in the recovered bronchoalveolar lavage fluid (BALF) were counted in a hemocytometer.

Flow Cytometry

For quantification of cell populations, additional mice from both genotypes and treatments were studied. After sacrifice, the left lung was washed in sterile PBS immediately after removal, cut in sections and manually homogenized. The resulting extracts were centrifuged, resuspended in 100 microliters of PBS and incubated with fluorescence-labeled anti-CD45, antiCD11b, anti-Gr1 and anti-Ly6G antibodies (BD Biosciences). Cell populations were identified using a FACScanto flow cytometer (BD Biosciences).

DiGE Analysis

Lungs from WT and KO mice were perfused and then rinsed in TAM (10 mM TRIS-HCl pH 8.5, 5 mM magnesium acetate) and homogenized manually at room temperature in TUCT (7 M urea, 2 M tiourea, 4% CHAPS, 30 mM TRIS- HCl pH 8.5). 50 μg of each sample were covalently labeled with 400 pmol of a specific fluorophore (GE Healthcare): CyDye 3 (WT sample), CyDye 5 (KO sample) and CyDye 2 (pool of WT and KO sample 1:1). Labeled samples were combined and UCDA (8 M urea, 4% CHAPS, 130 mM DTT, 2% IEF buffer) was added in a 1:1 ratio. Samples were isoelectrofocused (voltage in gradient for 26 hours at $18^{\circ}C$) in 24 cm pH 3–11 NL strips following manufacturer's instructions (GE Healthcare). Once the IEF step finished, strips were equilibrated for 15 min in SES (6 M UREA, 30% glycerol, 2% SDS, 75 mM TRIS-HCl pH 6.8), 0.5% DTT and bromophenol blue, and for another 15 minutes in SES+4.5% iodoacetamide and bromophenol blue. Then, they were mounted on top of a 13% SDS–PAGE with stacking gel in a Hoefer S600 apparatus (Ettan DALT Six, GE Healthcare). Electrophoresis was performed at 80 V overnight in the dark at $18^{\circ}C$. After SDS–PAGE, cyanine dye-labeled proteins were visualized directly by scanning using a Typhoon 9400 imager (GE Healthcare). The scanned gels were then directly analyzed with Progenesis SameSpots software (Nonlinear dynamics) and stained with SYPRO Ruby (Molecular Probes).

Tryptic Digestion and MALDI-ToF Analysis

Differential spots were manually excised over a transilluminator. Gel pieces were washed twice with 180 μL of 25 mM ammonium bicarbonate/acetonitrile (70:30), dried for 15 min at $90^{\circ}C$, and incubated with 12 ng/μL trypsin (Promega) in 25 mM ammonium bicarbonate. The digestion was allowed to proceed for 1 h at $60^{\circ}C$. Peptides were purified with ZipTip C18 (Millipore) and eluted with 1 μL of CHCA (α-cyano-4-hydroxycinnamic acid) to be placed onto MALDI-ToFs plate. Once dried, they were analyzed by mass spectrometry on a time-of-flight mass spectrometer equipped with a nitrogen laser source (Voyager-DE STR, Applied Biosystems). Data from 200 laser shots were collected to produce a mass spectrum. Data explorer version 4.0.0.0 (Applied Biosystems) was the software used to analyze the spectra.

Western Blotting

Tissues were homogenated in a standard RIPA buffer (100 mM TRIS pH 7.4, 150 mM NaCl, 1 mM EDTA, 1% deoxycholic acid, 1% Triton X-100, 0,25% SDS, 1 mM ortovanadate and a protease inhibitor cocktail) and the protein content measured (BCA kit, Pierce, USA). Twelve micrograms of protein or 4 microlitres of serum were loaded in 12% SDS-PAGE or 16.5% Tris-tricine gels and electrophoresed. Then, proteins were transferred to PVDF membranes, blocked in non-fat milk or bovine albumin as needed, and incubated with antibodies against S100A6 (R&D Systems), S100A8 (R&D Systems), S100A9 (R&D Systems), MIP-2 (AbD serotec), LIX (Peprotech), MIP-1α (Abcam), IL-10 (Abcam), p65 (phosphorylated and total, Abcam), p52 (Cell signaling) and actin (Santa Cruz Biotechnology #SC1616). Proteins were then detected by chemoluminiscence (Millipore) using secondary peroxidase-linked antibodies. The resulting images were acquired with a LAS-3000 camera and analyzed using ImageJ software (NIH, USA).

Quantitative RT-PCR Analysis

RNA was extracted from frozen lung tissue using the Trizol reagent. One microgram of RNA was used to synthesize cDNA using superscript II reverse transcriptase following manufacturer's instructions. Then, a quantitative PCR was performed using 20 ng of cDNA and TaqMan Universal PCR master mix and the specific TaqMan probes for S100A8 (Mm00496696_g1) and S100A9 (Mm00656925_m1) genes (Applied Biosystems). These probes

span along two exons of the gene, thus avoiding the amplification of genomic DNA. Samples were studied in triplicate in an Applied Biosystems 7300 real-time PCR system. Beta-actin was used as control and the relative expression of the analyzed genes was calculated according to manufacturer's instructions.

Gelatin Zymography

Activity of matrix metalloproteinases −2 and −9 was measured by standard gelatin zymography as previously described [12]. Briefly, lung homogenates were loaded in a 8% SDS-PAGE gel containing 0.2% gelatin and electrophoresed. The gels were washed in 2.5% Triton X-100 and incubated in a buffer (20 mM TRIS, 5 mM CaCl2, pH 7.4). After staining with Commassie blue and destaining with a methanol/acetic acid mixture, gelatinolytic activity was identified as white bands over a blue background. Gels were scanned and quantified using ImageJ software.

Statistical Analysis

Data are expressed as mean±SEM. Differences among groups were evaluated using a two-way ANOVA, including genotype and treatment (LPS or saline) as factors. Post-hoc tests were done using the Bonferroni's correction. A p value lower than 0.05 was considered significant.

Results

Increased Lung Inflammatory Response in Mmp8$^{-/-}$ Mice

Seven LPS-treated and 7 saline-treated animals per genotype were studied. Treatment with LPS induced histological lung injury in both genotypes (Figure 1A–B), when compared to baseline ($p = 0.042$ and $p = 0.001$ for wildtype and knockout mice, respectively). However, the severity of injury in knockout mice doubled that from wildtype counterparts ($p = 0.004$ for the difference between genotypes in LPS-treated animals). There were no differences between genotypes in saline-treated animals.

Neutrophil infiltration within the lungs was measured by counting MPO-positive cells in immunohistochemical preparations (n = 7/group, Figure 1C–D). As expected, there were no differences in saline-treated animals. LPS administration induced a small but significant increase in lung neutrophils in *Mmp8*$^{+/+}$ animals ($p<0.05$ *vs* saline-treated wildtype mice), and a three-fold higher increase in *Mmp8*$^{-/-}$ mice ($p<0.001$ *vs* saline treated knockout mice, $p<0.001$ *vs* LPS-treated wildtype mice). There were no differences in leukocyte populations measured by flow cytometry or in the accumulation of myeloid-derived suppressor cells (defined as CD45+, Gr1+, Mac-1+, 28±2% vs 27,2±7% after LPS in wildtype and knockout mice, respectively; n = 5/group, $p = 0.92$). Neutrophil count in the BALF was also higher in *Mmp8*$^{-/-}$ animals than in their wildtype counterparts (Figure 1E). There were no differences in the number of macrophages (data not shown). In spite of the differences in lung injury and inflammation, there were no significant differences in survival between genotypes (Figure 1F).

Proteomic Analysis of Lung Tissue

To identify MMP-8 substrates responsible for the differences in leukocyte infiltration, lung tissue homogenates were analyzed using 2D-DIGE (n = 4/group). Interestingly, members from the S100 protein family, involved in the inflammatory response, were identified, so we focused on these molecules as putative mediators responsible for the differences. Figure 2 shows a representative 2D gel (A) together with the protein spots (B) and confirmatory western blots (C).

S100 Proteins are Increased in Lungs of MMP-8-deficient Mice

To confirm the results of the proteomic analysis, we performed western blot experiments using lung tissue homogenates (n = 7/group) and antibodies against S100A6, S100A8 and S100A9. There were no differences in S100A6 protein (Figure 3A, $p = 0.45$ in ANOVA). Regarding S100A8, we did not observe any difference between genotypes in saline-treated animals, but a significant increase after LPS injection (Figure 3B, $p<0.001$ and $p = 0.015$ for wildtype and knockout mice respectively). Moreover, S100A8 levels were significantly higher in knockout mice ($p = 0.004$ for the difference between genotypes). S100A9 showed a similar pattern (Figure 3C). Representative western blots are presented in Figure 3D. S100A8 and S100A9 protein levels were strongly correlated with the leukocyte count in histological sections (correlation coefficients of 0.80 and 0.78 for S100A8 and S100A9 respectively, $p<0.01$ in both cases).

S100a8 and *S100a9* gene expression was also studied by quantitative PCR (n = 6/group). Crossing thresholds were 21.779±1,048, 28.125±0.702 and 27.062±0.629 for *actin*, *S100a8* and *S100a9* respectively. The results for each genotype are shown in figure 3E. There were no differences between LPS-treated wildtype and knockout mice ($p = 0.531$ and $p = 0.776$ for S100A8 and S100A9 in the ANOVA, respectively).

Finally, we measured S100A8 and S100A9 levels in serum and spleen homogenates to check if the differences observed in lung tissue are a local phenomenon or the manifestation of a systemic difference in alarmin levels. There were no differences in these two molecules in serum or spleen (Figure 3F). These results suggest that the differences observed in protein abundance are not caused by a differential gene expression, but a different protein clearance in lung parenchyma.

MMP-2 or MMP-9 do not Compensate the Absence of MMP-8

As gelatinases MMP-2 and -9 have been involved in processing of S100A8 and S100A9, we studied their levels by gelatin zymography (n = 7/group, Figure 4). There was a non-significant trend to higher levels of MMP-9 in lung tissue after LPS treatment, with no differences between genotypes ($p = 0.791$ in ANOVA). There were no differences in MMP-2 in response to LPS injection in any of the genotypes. Figure 4C shows a representative zymography.

Absence of MMP-8 affects Multiple Immune Mediators

It has been reported that MMP-8 can process a number of immune mediators, including chemokines responsible for the leukocyte infiltration. To study these factors that were not identified by our proteomic approach, we measured the abundance of MIP-1α, MIP-2 and LIX in lung tissue homogenates (n = 7/group). MIP-1α increased in both genotypes after LPS injection. This increase was more pronounced in mice lacking MMP-8 (Figure 5A). In opposite, there were no differences between genotypes in MIP-2 levels (Figure 5B). Likewise, we did not observe changes in LIX abundance in any experimental group (Figure 5C).

Activation of Non-canonical NF-κB Pathway in Mmp8$^{-/-}$ Mice

The NF-κB pathway is one of the main intracellular triggers of the inflammatory response. Activation of this route was evaluated by western blotting against p65 and p52 (markers of canonical and non-canonical NF-κB pathway respectively). Seven mice per

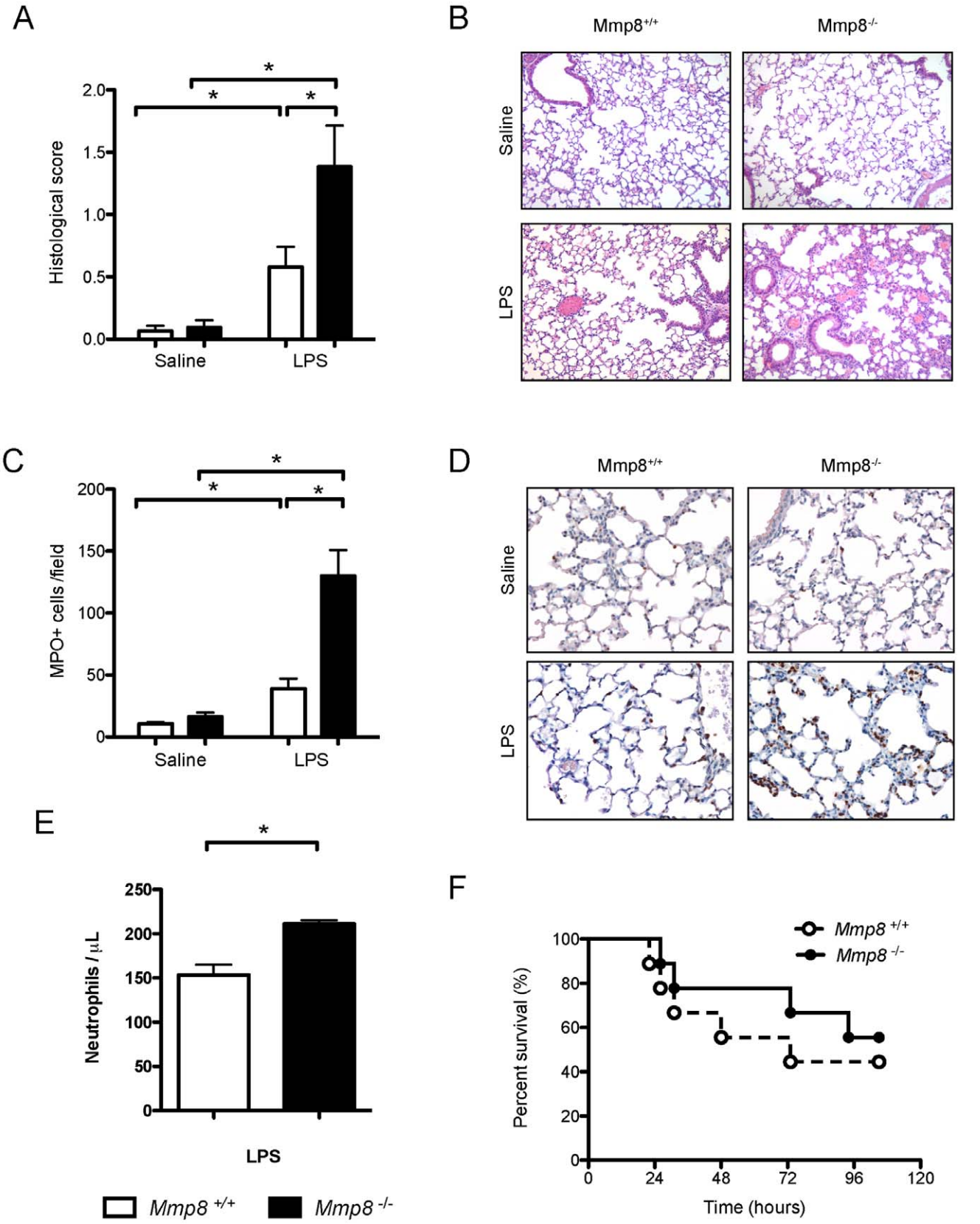

Figure 1. Lung inflammation during endotoxemia. N = 7/group. LPS injection increases histological damage (A-B) and neutrophilic infiltration (C-E). Mice lacking MMP-8 show a more severe injury with increased neutrophils within the lung tissue (C-D) and bronchalveolar lavage fluid (N = 4/group, E). However, there were no differences in survival (F, n = 9 per genotype, log rank test p = 0.52). *p<0.05 in post-hoc tests.
doi:10.1371/journal.pone.0039940.g001

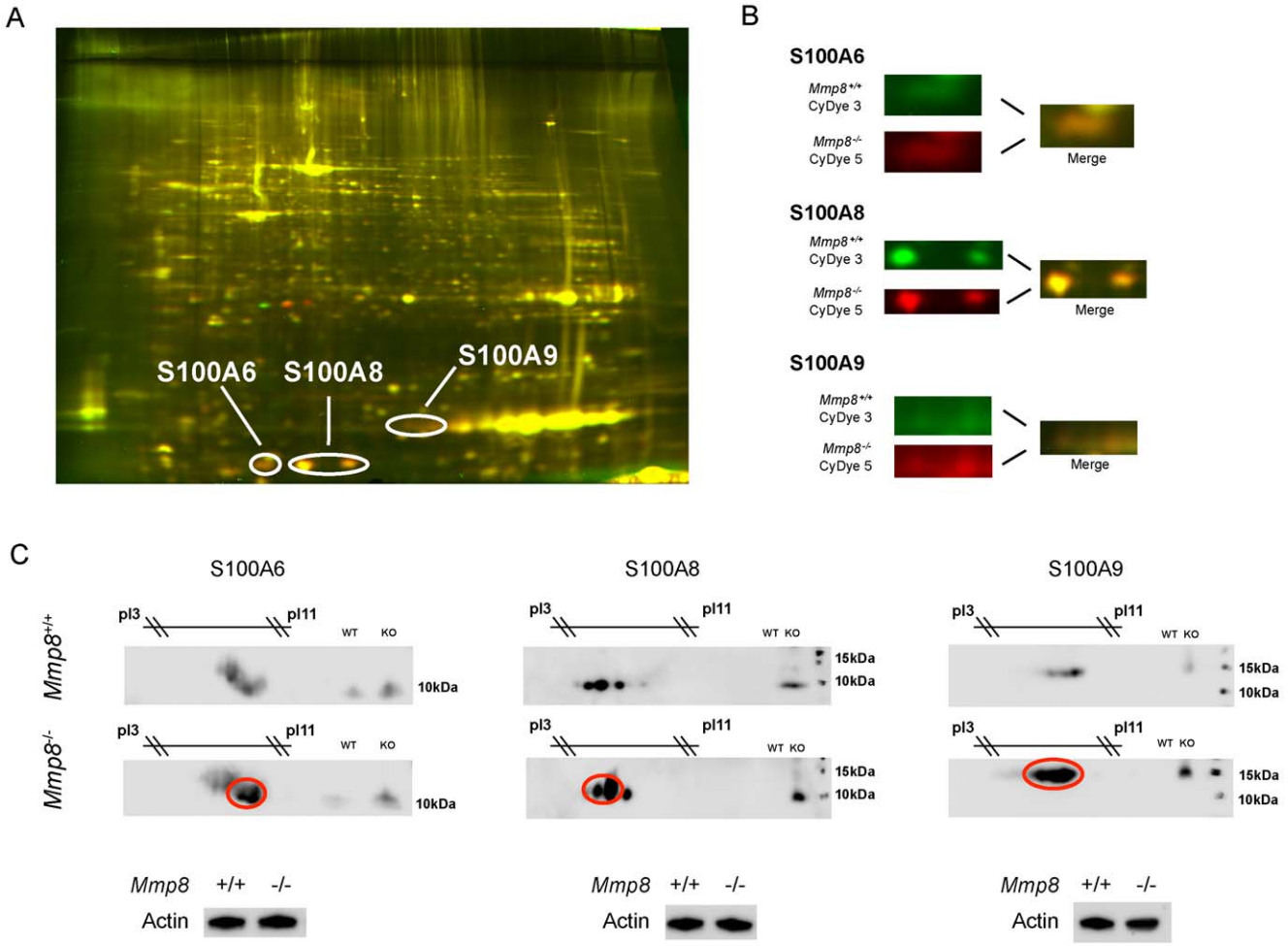

Figure 2. Proteomic identification of S100 proteins in lung from LPS treated animals. A 2D protein electrophoresis (DiGE) was performed with samples from both genotypes (A). Differential spots corresponding to S100A6, S100A8 and S100A9 were identified (B) and validated by western blotting (C). Red circles show the differential spots in 2D western blots.
doi:10.1371/journal.pone.0039940.g002

group were studied. There were no differences between genotypes in p65 phosphorylation (Figure 6A). However, there was a marked activation of the non-canonical NF-κB pathway, demonstrated by a 10-fold increase in p52 levels only in mice lacking MMP-8 (Figure 6B).

Discussion

Our results demonstrate that the absence of MMP-8 increases the neutrophilic lung infiltration after LPS injection. This effect could be explained by the accumulation of S100A8 and S100A9 proteins, in addition to other chemokines. These findings highlight the central role of MMP-8 during the regulation of inflammatory cell recruitment to the lungs by processing a variety of immune mediators.

Matrix metalloproteinases have a wide range of substrates that are responsible for their variety of effects. MMP-8, also known as collagenase-2, has emerged as one of the most important regulators of the inflammatory response [5]. Mutant mice lacking MMP-8 show a characteristic inflammatory response, with an initial delay in cell recruitment, but also with a later persistence of the neutrophilic infiltration [6,13–15]. Therefore, absence of this enzyme ameliorates hyperacute inflammation, but also worsens the response later on [7]. Noteworthy, blood cell counts and the migratory properties of neutrophils in knockout mice are normal [8], so the differences between genotypes rely on the regulation of the inflammatory response.

There are several molecular mechanisms that could be responsible for these opposite effects of MMP-8. First, inflammatory cells must degrade the extracellular matrix fibers in order to migrate, so the collagenolytic activity must be essential for neutrophils to reach the injured site [16]. Additionally, it has been reported that this protease can cleave different chemokines such as LIX [10,17] or MIP-1α [8]. By this proteolytic inactivation, MMP-8 exerts an anti-inflammatory role. Finally, MMP-8 also regulates neutrophil apoptosis, contributing to the persistence of the infiltrate [18].

The results of the present study show that, in absence of MMP-8, there is an accumulation of S100A8 and S100A9. These myeloid-related proteins, included in the alarmins family, are constitutively expressed in neutrophils, representing the 40–50% of the cytoplasmic content [19], and released at the sites of injury. By binding to RAGE and TLR4, they can trigger a proinflammatory response [20]. Both RAGE and TLR4 are widely expressed in the lung tissue, so this pathway is of major relevance during the alveolar inflammatory response after endotoxemia [21].

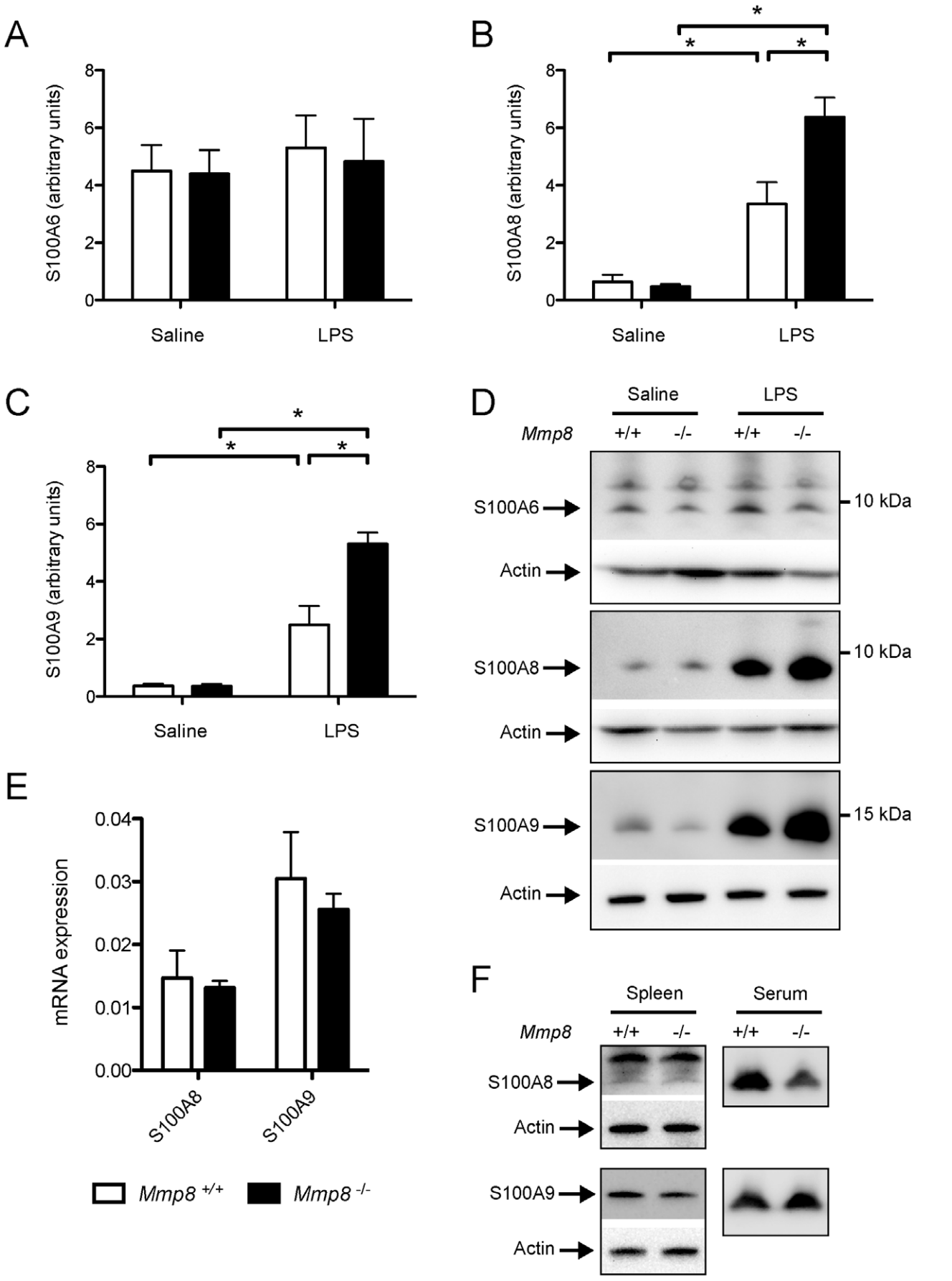
A
S100A6 (arbitrary units)
0
2
4
6
8
Saline
LPS
B
S100A8 (arbitrary units)
*
*
*
Saline
LPS
C
S100A9 (arbitrary units)
*
*
*
Saline
LPS
D
Saline
LPS
Mmp8
+/+
-/-
+/+
-/-
S100A6
Actin
10 kDa
S100A8
Actin
10 kDa
S100A9
Actin
15 kDa
E
mRNA expression
0.00
0.01
0.02
0.03
0.04
S100A8
S100A9
Mmp8 +/+
Mmp8 -/-
F
Spleen
Serum
Mmp8
+/+
-/-
+/+
-/-
S100A8
Actin
S100A9
Actin

Figure 3. Differential expression of S100 proteins between genotypes. N = 7/group. The differences in S100A6 levels were not confirmed (A, p = 0.45 in the ANOVA). However, S100A8 (B) and S100A9 (C) protein levels increased after LPS injection in both genotypes ($p<0.05$ in all post-hoc tests). Mice lacking MMP-8 showed significantly higher levels of these two proteins than their wildtype counterparts ($p<0.01$ and $p<0.001$ for the differences between genotypes in S100A8 and S100A9 respectively). Panel D shows representative western blots. However, S100A8 and S100A9 gene expression was not different between genotypes during endotoxemia (n = 6/group, E). To discard systemic differences in alarmins, levels of S100A8 and S100A9 were measured in spleen homogenates (n = 7/group) and serum (n = 4/group) from LPS-treated animals, with no significant differences between genotypes (F). *$p<0.05$ in post-hoc test.
doi:10.1371/journal.pone.0039940.g003

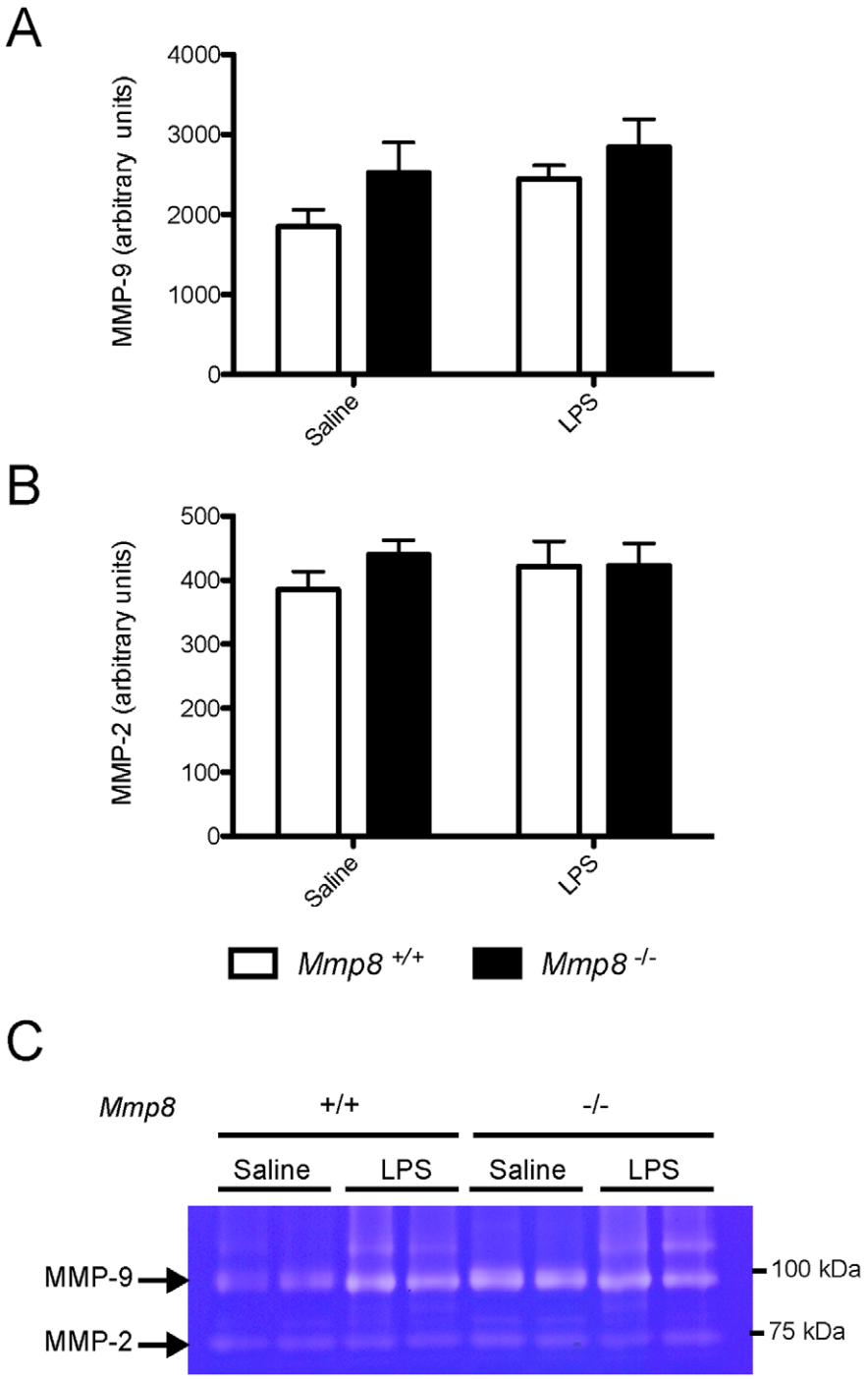

Figure 4. Absence of compensatory changes in MMP-9 (A) or MMP-2 (B) in mice lacking MMP-8 (n = 7/group). A representative zymography is shown in panel C.
doi:10.1371/journal.pone.0039940.g004

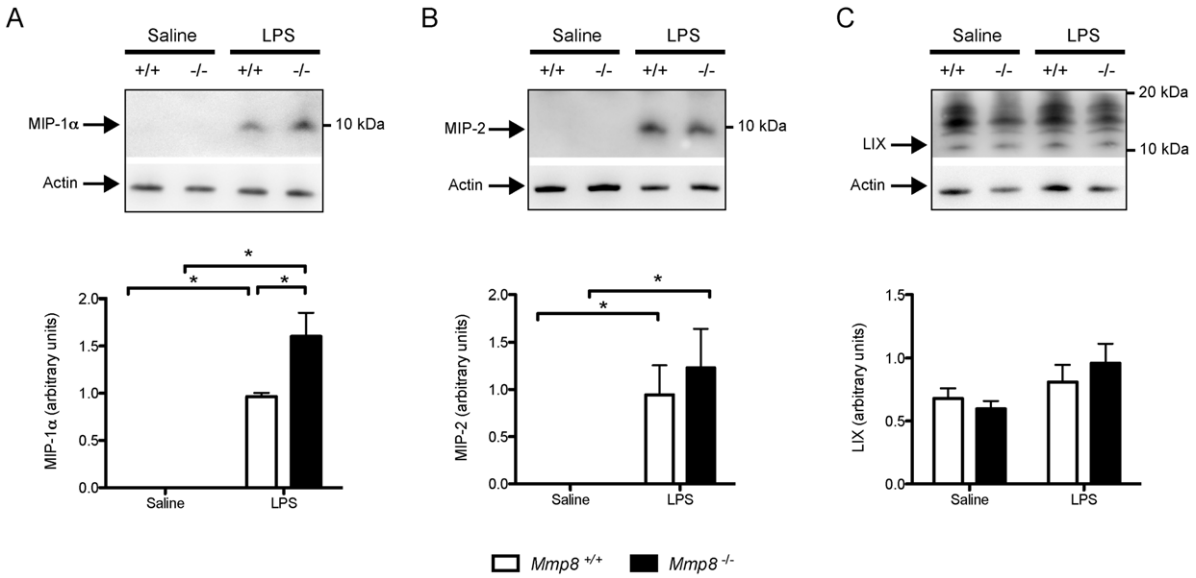

Figure 5. Chemokine levels in lung tissue. N = 7/group. LPS injection increased levels of MIP-1α (A, $p<0.001$ and $p<0.001$ for wildtype and knockout mice), and MIP-2 (B, $p<0.01$ and $p = 0.01$ for wildtype and knockout mice) but not LIX (C, $p = 0.56$ in the ANOVA). Moreover, MIP-1α was significantly higher in mice lacking MMP-8 ($p<0.01$ for the comparison between genotypes). *$p<0.05$ in post-hoc test.
doi:10.1371/journal.pone.0039940.g005

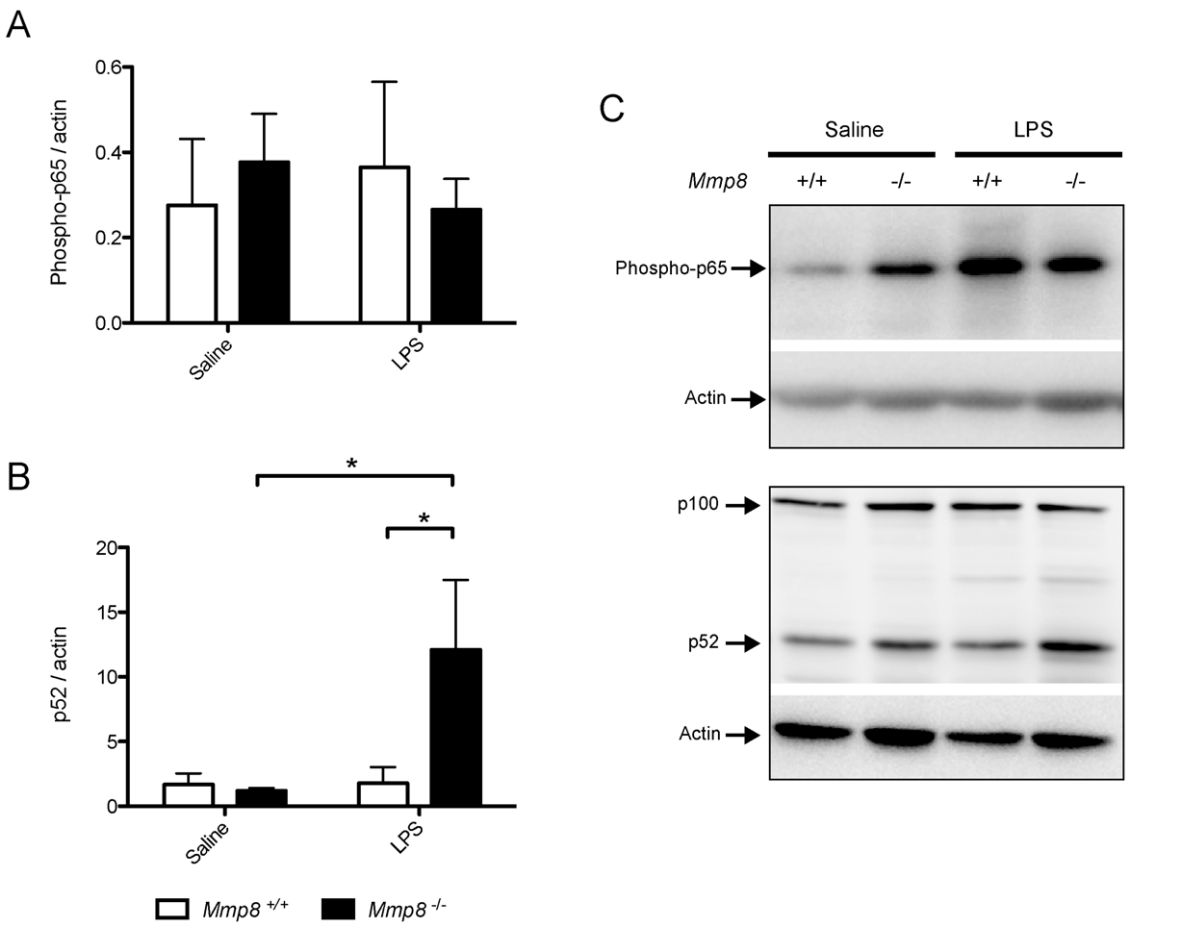

Figure 6. Non-canonical NF-κB activation in LPS-treated, *Mmp8*$^{-/-}$ mice. The lung levels of p52 increased significantly in knockout mice after LPS challenge (n = 7/group, $p = 0.01$ vs saline-treated knockout mice, $p<0.02$ vs LPS-treated wildtype animals). *$p<0.05$ in post-hoc test.
doi:10.1371/journal.pone.0039940.g006

Moreover, it has been demonstrated that both S100A8 and S100A9 have chemotactic properties that favor neutrophilic recruitment to the tissues [22]. Although S100A8 and S100A9 can also mediate the recruitment of myeloid-derived suppressor cells [23], with anti-inflammatory properties, we did not find the accumulation of these cells in the lung tissue in our model irrespective of the genotype.

There is increasing evidence that MMPs can regulate the alarmins/RAGE pathway by different mechanisms [24]. MMP-3 and -13 can release RAGE from alveolar epithelial cells [25]. The resulting soluble RAGE could act as a decoy receptor with anti-inflammatory properties. Although MMP-8 shares some structural and functional characteristics with MMP-13 (both are interstitial collagenases), the effects of the former on the release of RAGE have not been addressed. Other MMPs, namely MMP-2 and MMP-9 (gelatinases A and B respectively), can cleave and inactivate S100A8 and S100A9. This mechanism limits the inflammatory response in a model of lung allergic inflammation [26]. The absence of compensatory changes in MMP-2 or MMP-9 supports the role of MMP-8 in the observed differences between genotypes.

In this setting, MMP-8 appears as a central regulator of neutrophilic chemotaxis by its effects on MIP-1α and alarmins. Additionally, MMP-8 can modulate LIX activity and IL-10 levels, as shown in other experimental models [6,9,10]. All these signals may result in the activation of the NF-κB route. The chemotactic activity of another RAGE and TLR ligand, HMGB1, has been related to the activation of the non-canonical NF-κB pathway [27]. Our results showing increased levels of p52 in mice lacking MMP-8 resemble this finding. However, we cannot discard that other factors not identified in our study are the cause of the increase in NF-κB activity, as this is a final common pathway in the inflammatory response.

The multiple and opposite effects of MMPs, and MMP-8 in particular, can explain some contradictory results in the literature. Absence of MMP-8 has been related to pro- and anti-inflammatory responses. Regarding to MMP-8 and sepsis, all the experimental models using LPS, either intratracheal [8,17] or intraperitoneal (present study), report an increase in lung inflammation in knockout mice. Recently, Solan et al. [28] have shown the opposite effect (decreased neutrophilic infiltration and better outcome in $Mmp8^{-/-}$ mice) in a model of cecal ligation and puncture. The differences in the type and severity of injury (with a survival rate in wildtype mice of 40% in our study, but 0% in the peritonitis model), or the involvement of other mediators such as IL-10 (which is increased in knockout mice [9]) may explain these discrepancies. In human sepsis, MMP-8 correlates with severity, mortality and organ failures [28,29]. Therefore, targeting this enzyme could be an interesting therapeutic approach. However, a deeper knowledge of the pro- and anti-inflammatory effects of the enzyme is needed to make any firm recommendation.

In conclusion, the results described here reinforce the central role of MMP-8 in the regulation of neutrophil recruitment to the lungs during sepsis, adding the myeloid-related proteins S100A8 and S100A9 as one of the involved mediators. This anti-inflammatory role of MMP-8 must be considered before proposing anti-MMP strategies in sepsis.

Acknowledgments

The authors thank Carlos López-Otin for his support during the realization of this project.

Author Contributions

Conceived and designed the experiments: AGL GMA. Performed the experiments: AGL A. Aguirre ILA LA EBS. Analyzed the data: AGL GMA. Wrote the paper: AGL GMA. Proteomic analysis: MFS. Histological studies: A. Astudillo MSFG. Flow cytometry: EC.

References

1. Gustot T (2011) Multiple organ failure in sepsis: prognosis and role of systemic inflammatory response. Curr Opin Crit Care 17: 153–159.
2. Brown KA, Brain SD, Pearson JD, Edgeworth JD, Lewis SM, et al. (2006) Neutrophils in development of multiple organ failure in sepsis. Lancet 368: 157–169.
3. Ferguson ND, Frutos-Vivar F, Esteban A, Gordo F, Honrubia T, et al. (2007) Clinical risk conditions for acute lung injury in the intensive care unit and hospital ward: a prospective observational study. Crit Care 11: R96.
4. Fanjul-Fernandez M, Folgueras AR, Cabrera S, Lopez-Otin C (2010) Matrix metalloproteinases: evolution, gene regulation and functional analysis in mouse models. Biochim Biophys Acta 1803: 3–19.
5. Dejonckheere E, Vandenbroucke RE, Libert C (2011) Matrix metalloproteinase8 has a central role in inflammatory disorders and cancer progression. Cytokine Growth Factor Rev 22: 73–81.
6. Balbin M, Fueyo A, Tester AM, Pendas AM, Pitiot AS, et al. (2003) Loss of collagenase-2 confers increased skin tumor susceptibility to male mice. Nat Genet 35: 252–257.
7. Gutierrez-Fernandez A, Inada M, Balbin M, Fueyo A, Pitiot AS, et al. (2007) Increased inflammation delays wound healing in mice deficient in collagenase-2 (MMP-8). FASEB J 21: 2580–2591.
8. Quintero PA, Knolle MD, Cala LF, Zhuang Y, Owen CA (2010) Matrix metalloproteinase-8 inactivates macrophage inflammatory protein-1 alpha to reduce acute lung inflammation and injury in mice. J Immunol 184: 1575–1588.
9. Garcia-Prieto E, Gonzalez-Lopez A, Cabrera S, Astudillo A, Gutierrez-Fernandez A, et al. (2010) Resistance to bleomycin-induced lung fibrosis in MMP-8 deficient mice is mediated by interleukin-10. PLoS One 5: e13242.
10. Tester AM, Cox JH, Connor AR, Starr AE, Dean RA, et al. (2007) LPS responsiveness and neutrophil chemotaxis in vivo require PMN MMP-8 activity. PLoS ONE 2: e312.
11. Menezes SL, Bozza PT, Neto HC, Laranjeira AP, Negri EM, et al. (2005) Pulmonary and extrapulmonary acute lung injury: inflammatory and ultrastructural analyses. J Appl Physiol 98: 1777–1783.
12. Albaiceta GM, Gutierrez-Fernandez A, Parra D, Astudillo A, Garcia-Prieto E, et al. (2008) Lack of matrix metalloproteinase-9 worsens ventilator-induced lung injury. Am J Physiol Lung Cell Mol Physiol 294: L535–543.
13. Van Lint P, Wielockx B, Puimege L, Noel A, Lopez-Otin C, et al. (2005) Resistance of collagenase-2 (matrix metalloproteinase-8)-deficient mice to TNF-induced lethal hepatitis. J Immunol 175: 7642–7649.
14. Albaiceta GM, Gutierrez-Fernandez A, Garcia-Prieto E, Puente XS, Parra D, et al. (2010) Absence or inhibition of matrix metalloproteinase-8 decreases ventilator-induced lung injury. Am J Respir Cell Mol Biol 43: 555–563.
15. Folgueras AR, Fueyo A, Garcia-Suarez O, Cox J, Astudillo A, et al. (2008) Collagenase-2 deficiency or inhibition impairs experimental autoimmune encephalomyelitis in mice. J Biol Chem 283: 9465–9474.
16. Khatwa UA, Kleibrink BE, Shapiro SD, Subramaniam M (2010) MMP-8 promotes polymorphonuclear cell migration through collagen barriers in obliterative bronchiolitis. J Leukoc Biol 87: 69–77.
17. Balbin M, Fueyo A, Knauper V, Pendas AM, Lopez JM, et al. (1998) Collagenase 2 (MMP-8) expression in murine tissue-remodeling processes. Analysis of its potential role in postpartum involution of the uterus. J Biol Chem 273: 23959–23968.
18. Gueders MM, Balbin M, Rocks N, Foidart JM, Gosset P, et al. (2005) Matrix metalloproteinase-8 deficiency promotes granulocytic allergen-induced airway inflammation. J Immunol 175: 2589–2597.
19. Hessian PA, Edgeworth J, Hogg N (1993) MRP-8 and MRP-14, two abundant Ca(2+)-binding proteins of neutrophils and monocytes. J Leukoc Biol 53: 197–204.
20. Bianchi ME (2007) DAMPs, PAMPs and alarmins: all we need to know about danger. J Leukoc Biol 81: 1–5.
21. Raquil MA, Anceriz N, Rouleau P, Tessier PA (2008) Blockade of antimicrobial proteins S100A8 and S100A9 inhibits phagocyte migration to the alveoli in streptococcal pneumonia. J Immunol 180: 3366–3374.
22. Ryckman C, Vandal K, Rouleau P, Talbot M, Tessier PA (2003) Proinflammatory activities of S100: proteins S100A8, S100A9, and S100A8/A9 induce neutrophil chemotaxis and adhesion. J Immunol 170: 3233–3242.
23. Sinha P, Okoro C, Foell D, Freeze HH, Ostrand-Rosenberg S, et al. (2008) Proinflammatory S100 proteins regulate the accumulation of myeloid-derived suppressor cells. J Immunol 181: 4666–4675.

24. Hergrueter AH, Nguyen K, Owen CA (2011) Matrix metalloproteinases: all the RAGE in the acute respiratory distress syndrome. Am J Physiol Lung Cell Mol Physiol 300: L512–515.
25. Yamakawa N, Uchida T, Matthay MA, Makita K (2011) Proteolytic release of the receptor for advanced glycation end products from in vitro and in situ alveolar epithelial cells. Am J Physiol Lung Cell Mol Physiol 300: L516–525.
26. Greenlee KJ, Corry DB, Engler DA, Matsunami RK, Tessier P, et al. (2006) Proteomic identification of in vivo substrates for matrix metalloproteinases 2 and 9 reveals a mechanism for resolution of inflammation. J Immunol 177: 7312–7321.
27. Penzo M, Molteni R, Suda T, Samaniego S, Raucci A, et al. (2010) Inhibitor of NF-kappa B kinases alpha and beta are both essential for high mobility group box 1-mediated chemotaxis. J Immunol 184: 4497–4509.
28. Solan PD, Dunsmore KE, Denenberg AG, Odoms K, Zingarelli B, et al. (2012) A novel role for matrix metalloproteinase-8 in sepsis. Crit Care Med 40: 379–387.
29. Lauhio A, Hastbacka J, Pettila V, Tervahartiala T, Karlsson S, et al. (2011) Serum MMP-8, -9 and TIMP-1 in sepsis: high serum levels of MMP-8 and TIMP-1 are associated with fatal outcome in a multicentre, prospective cohort study. Hypothetical impact of tetracyclines. Pharmacol Res 64: 590–594.

III. La resistencia a la fibrosis inducida por bleomicina en ratones deficientes en MMP-8 esta mediada por la IL-10.

Los estudios previos nos animaron a estudiar el papel de la MMP-8 en un proceso patológico crónico como es la fibrosis pulmonar, en la que un exceso de remodelado tisular y acumulación de matriz extracelular provocan una pérdida de función pulmonar. En este contexto las MMP-8 nos pareció un candidato idóneo para el estudio de esta patología. Pudimos detectar que los ratones *Mmp8*$^{+/+}$ presentaban niveles elevados de MMP-8 tras la administración de bleomicina y que la falta de esta proteína disminuía la fibrosis provocada por este fármaco, disminuyendo tanto la síntesis de *novo* de colágeno como los niveles del mediador profibrótico TGF-β y aumentando los del antifibrótico IL-10. Ensayos *in vitro* de proteólisis y de actividad de IL-10 mostraron que MMP-8 procesa IL-10 e inactiva su capacidad antifibrótica. Del mismo modo la persistencia del infiltrado inflamatorio característica en estos ratones mutantes se tradujo en un aumento de los niveles de la metaloproteasa con actividad antifibrótica MMP-9.

Artículo 3: Emilio García-Prieto, **Adrián González-López,** Sandra Cabrera, Aurora Asturdillo, Ana Gutiérrez-Fernández, Miriam Fanjul-Fernández, Estefanía Batalla-Solís, Xose S. Puente, Antonio Fueyo, Carlos López Otín, Guillermo M. Albaiceta. "Resistance to bleomycin-induced lung fibrosis in MMP-8 deficient mice is mediated by interleukin-10".

PLoS One. 2010 Oct 7;5(10). I.F 2010: 4.41

Aportación personal al trabajo.

En lo referente a este proyecto colaboré en el protocolo *in vivo* de fibrosis, participando tanto en la cirugía como la obtención de muestras y su análisis *western blot*. Participé en los ensayos de actividad proteolítica y llevé a cabo los ensayos de actividad de IL-10 en cultivos celulares. Finalmente, participé en el análisis estadístico y la elaboración del manuscrito bajo la supervisión del Dr. Guillermo Muñiz Albaiceta.

OPEN ACCESS Freely available online

PLoS one

Resistance to Bleomycin-Induced Lung Fibrosis in MMP-8 Deficient Mice Is Mediated by Interleukin-10

Emilio García-Prieto[1,4], Adrián González-López[1], Sandra Cabrera[2], Aurora Astudillo[3], Ana Gutiérrez-Fernández[2], Miriam Fanjul-Fernandez[2], Estefanía Batalla-Solís[1], Xose S. Puente[2], Antonio Fueyo[1], Carlos López-Otín[2], Guillermo M. Albaiceta[1,4]*

1 Department of Biología Funcional, Universidad de Oviedo, Instituto Universitario de Oncología (IUOPA), Oviedo, Spain, **2** Department of Bioquímica y Biología Molecular, Universidad de Oviedo, Instituto Universitario de Oncología (IUOPA), Oviedo, Spain, **3** Department of Cirugía y Especialidades Médicoquirurgica, Universidad de Oviedo, Instituto Universitario de Oncología (IUOPA), Oviedo, Spain, **4** Unidad de Cuidados Intensivos, Hospital Universitario Central de Asturias, CIBER Enfermedades Respiratorias-Instituto de Salud Carlos III, Oviedo, Spain

Abstract

Background: Matrix metalloproteinases (MMPs) may have pro and antifibrotic roles within the lungs, due to its ability to modulate collagen turnover and immune mediators. MMP-8 is a collagenase that also cleaves a number of cytokines and chemokines.

Methodology and Principal Findings: To evaluate its relevance in lung fibrosis, wildtype and *Mmp8*$^{-/-}$ mice were treated with either intratracheal bleomycin or saline, and lungs were harvested at different time points. Fibrosis, collagen, collagenases, gelatinases, TGFβ and IL-10 were measured in lung tissue. *Mmp8*$^{-/-}$ mice developed less fibrosis than their wildtype counterparts. This was related to an increase in lung inflammatory cells, MMP-9 and IL-10 levels in these mutant animals. *In vitro* experiments showed that MMP-8 cleaves murine and human IL-10, and tissue from knockout animals showed decreased IL-10 processing. Additionally, lung fibroblasts from these mice were cultured in the presence of bleomycin and collagen, IL-10 and STAT3 activation (downstream signal in response to IL-10) measured by western blotting. In cell cultures, bleomycin increased collagen synthesis only in wildtype mice. Fibroblasts from knockout mice did not show increased collagen synthesis, but increased levels of unprocessed IL-10 and STAT3 phosphorylation. Blockade of IL-10 reverted this phenotype, increasing collagen in cultures.

Conclusions: According to these results, we conclude that the absence of MMP-8 has an antifibrotic effect by increasing IL-10 and propose that this metalloprotease could be a relevant modulator of IL-10 metabolism *in vivo*.

Citation: García-Prieto E, González-López A, Cabrera S, Astudillo A, Gutiérrez-Fernández A, et al. (2010) Resistance to Bleomycin-Induced Lung Fibrosis in MMP-8 Deficient Mice Is Mediated by Interleukin-10. PLoS ONE 5(10): e13242. doi:10.1371/journal.pone.0013242

Editor: Martin R. J. Kolb, McMaster University, Canada

Received April 19, 2010; **Accepted** September 13, 2010; **Published** October 7, 2010

Funding: Supported by grants from Fondo de Investigación Sanitaria (PI07/0597), Ministerio de Ciencia e Innovación, Fundación M. Botín and European Union (FP7 MicroEnviMet). AGL is the recipient of a grant from FICYT (COF-08-20) and Universidad de Oviedo (UNOV-09-BECDOC). EBS is the recipient of a grant from FICYT (COF-08-20). SC is the recipient of a grant from CONACYT. Instituto Universitario de Oncologia is supported by Obra Social Cajastur-Asturias, Spain. The funders had no role in study design, data collection and analysis, decision to publish or preparation of the manuscript.

Competing Interests: The authors have declared that no competing interests exist.

* E-mail: Guillermo.muniz@sespa.princast.es

Introduction

The accumulation of collagen fibers in the lung interstitium is a form of abnormal repair in some respiratory diseases. The primary forms of this syndrome are largely unknown and grouped under the term idiopathic pulmonary fibrosis [1]. Lung fibrosis can be also secondary to different types of injury, such as persistent acute respiratory distress syndrome, asbestos or silica exposure or treatment with drugs such as bleomycin [2]. Chronic inflammation is one of the mechanisms leading to these diseases. This is especially relevant in secondary fibrosis, but its involvement in the idiopathic forms is discussed [3]. The clinical course of this pathology shows a poor response to different therapies including steroids and other immuno-suppressors, and often evolves to irreversible respiratory failure [4].

Matrix metalloproteinases (MMPs) are a family of enzymes involved in different processes such as modulation of inflammation, tissue remodeling and collagen processing [5]. These enzymes play an important role in the pathogenesis of pulmonary fibrosis [6]. By targeting different substrates and being controlled by diverse regulatory mechanisms [7], MMPs establish a complex network in which different enzymes may play opposite roles. Likewise, specific family members may also play different roles in different time points of the disease. This is the case for MMP-8, also known as collagenase-2. This enzyme can digest native collagen, but its function in vivo seems to be more related to the control of the inflammatory response [8,9]. By the ability to cleave different cytokines and chemokines, MMP-8 promotes the initial onset and the later clearance of the neutrophilic inflammatory response. Mice lacking MMP-8 show a delayed wound healing due to a persistent inflammatory infiltrate [10]. Additionally, it has been observed a decreased collagen deposition in the wounds of these animals. This abnormal response could be of interest within the lungs challenged with a profibrotic stimulus. Therefore, we hypothesized that mice

lacking MMP-8 would develop less lung fibrosis than their respective wildtype counterparts. To test this hypothesis, we used a widely known model of lung fibrosis based on the administration of intratracheal bleomycin [11]. This drug induces an acute inflammatory response followed by the development of fibrosis, allowing to study the putative role of MMP-8 by assessing the differences between wildtype and *Mmp8* knockout mice after injury.

Results

Lung fibrosis is decreased in Mmp8$^{-/-}$ mice

Lung fibrosis was quantified using the Ashcroft scale in histological sections stained with Masson's trichrome (Figure 1A). No sign of fibrosis was detected in saline-treated mice of either genotype. Bleomycin injection induced a fibrotic response after 3 weeks. However, the degree of fibrosis was lower in MMP-8 deficient animals, as mutant mice scores were significantly lower than their wildtype counterparts ($p<0.05$ in post-hoc pairwise comparisons). After 6 weeks, fibrosis persisted in wildtype mice, but was partially solved in mutant animals. Consistent with this finding, there was a peak in recently synthesized collagen (Figure 1B) only in wildtype mice 3 weeks after bleomycin injection. Knockout mice showed a non-significant increase in this parameter (Figure 1B). Representative histological preparations are shown in Figure 2.

Bronchiolization appeared only after bleomycin administration, and not in saline-treated mice and increased progressively up to 6 weeks after injury. There were no differences between genotypes (data not shown).

Changes in collagenolytic and gelationlytic activities after bleomycin treatment

Collagenases and gelatinases act sequentially to degrade collagen. To study the implication of MMP-8 in the pathogenesis of bleomycin-induced fibrosis we measured its level in lung homogenates (Figure 3A). This enzyme increased 3 days after bleomycin instillation, to decrease later. Of note, saline-treated mice showed a modest increase in this enzyme, suggesting that the instillation procedure can induce a minor inflammatory response within the lungs. As expected, MMP-8 was not detected in knockout mice.

Then, we focused on differences in other collagenases and gelatinases to discard compensatory mechanisms in mutant mice. First, we assessed collagenolytic activity of lung homogenates (3 days and 3 weeks after bleomycin treatment). There were no differences in total collagenolytic activity between wildtype and knockout mice, thus discarding an overcompensatory increase of other collagenolytic enzymes in *Mmp8*$^{-/-}$ mice that could explain the decreased fibrosis (Figure 3B–C).

Regarding gelatinases, knockout mice showed a significant increase in MMP-9 in lung homogenates when studied 3 days after bleomycin instillation (Figure 3D). Values returned to baseline levels at the other time points of the study. In contrast, wildtype mice showed only a small increase that did not reach statistical significance. MMP-2 (Figure 3D) is another gelatinase involved in the pathogenesis of lung fibrosis [12]. We observed an increase in this enzyme in both wildtype and knockout mice 3 weeks after injury. There were no changes in any gelatinase in saline-treated animals. MMP-8 (Figure 3G) was expressed mainly in fibroblasts, whereas MMP-9 expression was restricted to inflammatory cells, mainly neutrophils, as shown by immunohistochemistry (Figure 3H).

Increased inflammatory infiltrate in Mmp8$^{-/-}$ mice

Bleomycin causes an acute inflammatory response within the lungs, which was measured by quantifying myeloperoxidase activity in tissue extracts. Myeloperoxidase (Figure 4A) increased

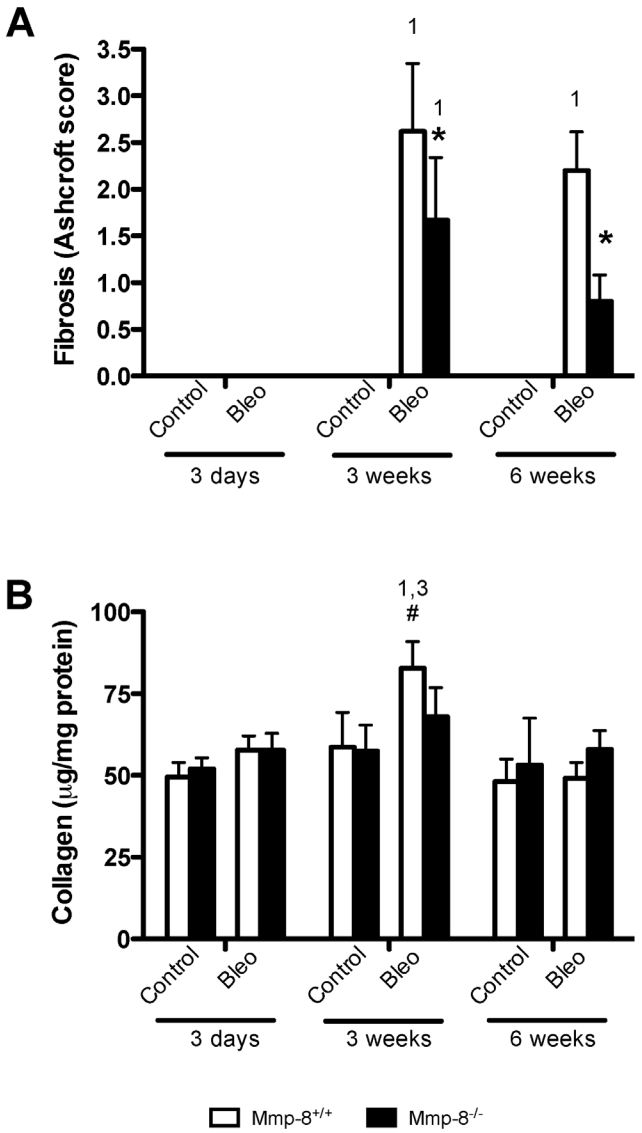

Figure 1. Decreased fibrosis in mice lacking MMP-8 challenged with intratracheal bleomycin. Fibrosis was quantified using the Ashcroft score (**A**) and recently synthesized collagen (**B**) measured in lung homogenates ($n\geq6$ per group). $^{1,2,3}P<0.05$ in post-hoc test when compared against 3 days (1), 3 weeks (2) or 6 weeks (3) within the same genotype and treatment; *$p<0.05$ when compared against wildtype within the same time and treatment; $^{\#}p<0.05$ when compared against saline within the same time and genotype.
doi:10.1371/journal.pone.0013242.g001

in both wildtype and knockout mice 3 days after bleomycin injection, but not after saline. Noteworthy, that increase was more pronounced in knockout mice, as demonstrated by immunohistochemical analysis showing higher counts of myeloperoxidase-positive cells (Figure 4B–D). In mutant animals, increased levels of myeloperoxidase persisted along the 6 weeks of the experiment, whereas returned to baseline levels in wildtype mice.

Th2 cytokines TGFβ and IL-10 are differentially regulated in Mmp8$^{-/-}$ mice

Th2 cytokines could play a relevant role in the development of fibrosis after bleomycin instillation. TGFβ is a profibrogenic factor that increased 3 and 6 weeks after bleomycin treatment only in

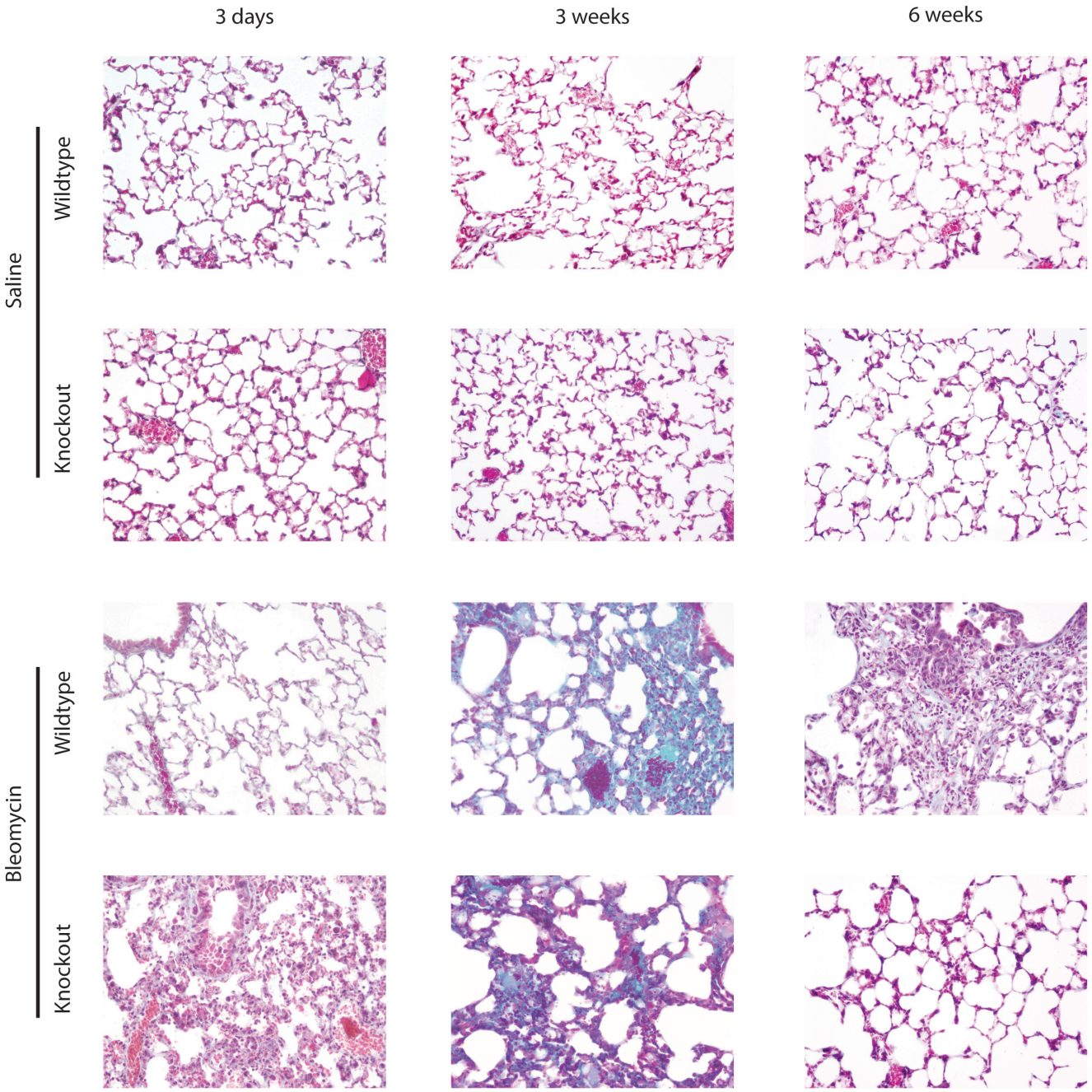

Figure 2. Representative histological sections (20×) from each experimental group. After staining with Masson's trichrome, fibrosis appears as green fibers, whereas epithelial and inflammatory cells are stained in red.
doi:10.1371/journal.pone.0013242.g002

wildtype mice. In contrast, *Mmp8*-deficient mice showed lower levels of this cytokine in the early phase (3 days) and values comparable to saline-treated mice at the other time points (Figure 5A).

IL-10 is another anti-inflammatory cytokine that can suppress TGFβ synthesis, thus exerting antifibrotic effects. There were no changes in this cytokine in saline-treated mice of both genotypes, or in bleomycin-treated wildtype animals. However, *Mmp8*$^{-/-}$ mice showed a 3-fold increase in IL-10 3 weeks after bleomycin treatment, and a smaller but still significant increase persisted 6 weeks after injury (Figure 5B). Immunohistochemical studies demonstrated IL-10 expression in epithelial cells and fibroblasts, whereas MMP-8 was expressed in fibroblasts (Figure 5C). When IL-10 gene expression was studied, mRNA levels of this cytokine in baseline conditions were undetectable. However, they were detected 3 days after bleomycin instillation with no differences between genotypes. Interestingly, IL-10 mRNA decreased significantly in knockout mice 3 weeks after bleomycin (Figure 5D). These findings open the possibility that IL-10 could be responsible for the benefits seen in terms of fibrosis in knockout mice and suggests that MMP-8 can be a relevant modulator of IL-10 function.

MMP-8 processes IL-10 *in vitro* and *in vivo*

To explore the possibility that IL-10 could be a substrate of MMP-8, recombinant murine IL-10 was incubated with this

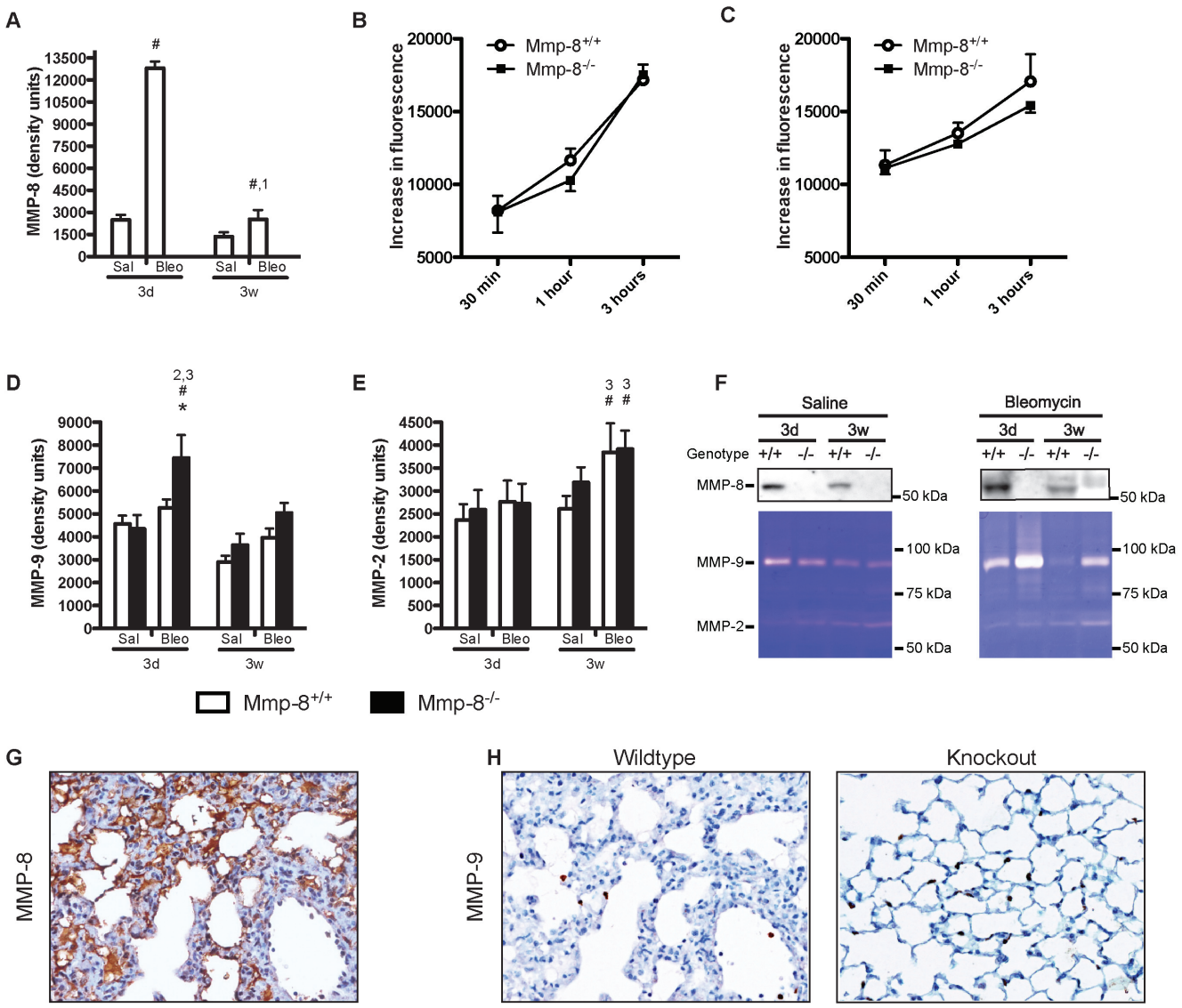

Figure 3. MMP activity in each experimental group. A: MMP-8 increased after bleomycin instillation. As expected, no MMP-8 was detected in knockout mice (n≥7 per group). **B–C**: Collagenolytic activity of lung tissue homogenates from wildtype and knockout mice 3 days (B) and 3 weeks (C) after bleomycin instillation (n = 3 per group). There are no significant differences between genotypes. **D**: MMP-9 has an acute increase after bleomycin instillation only in knockout mice (n≥7 per group). **E**: MMP-2 increases in both wildtype and knockout mice 3 weeks after injury (n≥7 per group). **F**: Representative western blotting and gelatin zymography used to quantify these MMPs. G–H: Immunohistochemical staining of MMP-8 (G) and MMP-9 (H) after bleomycin instillation. [1,2,3]p<0.05 in post-hoc test when compared against 3 days (1), 3 weeks (2), 6 weeks (3) within the same genotype and treatment; *p<0.05 when compared against wildtype within the same time and treatment; #p<0.05 when compared against saline within the same time and genotype.

doi:10.1371/journal.pone.0013242.g003

enzyme. After 18 hours of incubation, proteolytic processing of the cytokine was demonstrated by western blotting, showing that IL-10 (18 kDa) was converted to lower molecular mass species (~14 kDa). The appearance of these species was inhibited by TIMP-1 (Figure 6A). We repeated this experiment using recombinant human IL-10, showing the same result (Figure 6B).

In vivo processing of IL-10 by MMP-8 was studied in lung tissue homogenates by western blotting using a polyclonal antibody against mouse IL-10. Two IL-10 positive bands were detected at 18 and 14 kDa, corresponding to intact and processed IL-10 (Figure 6C). The percentage of intact IL-10 was higher in knockout mice three days and three weeks after bleomycin instillation (Figure 6D), demonstrating that absence of MMP-8 results in higher levels of unprocessed IL-10 and, therefore, that MMP-8 is an important regulator of IL-10 function in vivo.

Antifibrotic response in Mmp8$^{-/-}$ fibroblasts is IL-10 dependent

The relationship between IL-10 processing and lung fibrosis suggested by the above experiments was demonstrated in a culture model. Lung fibroblasts from wildtype and mutant mice were treated with bleomycin. After bleomycin challenge, there was an increase in IL-10 processing in wildtype fibroblasts, and intact IL-10 (18 kD) was significantly decreased. However, there was no change in IL-10 processing in cultures from knockout mice (Figure 7A–B). We also studied STAT3 phosphorylation as a marker of IL-10 activity. The ratio of phosphorylated to non-

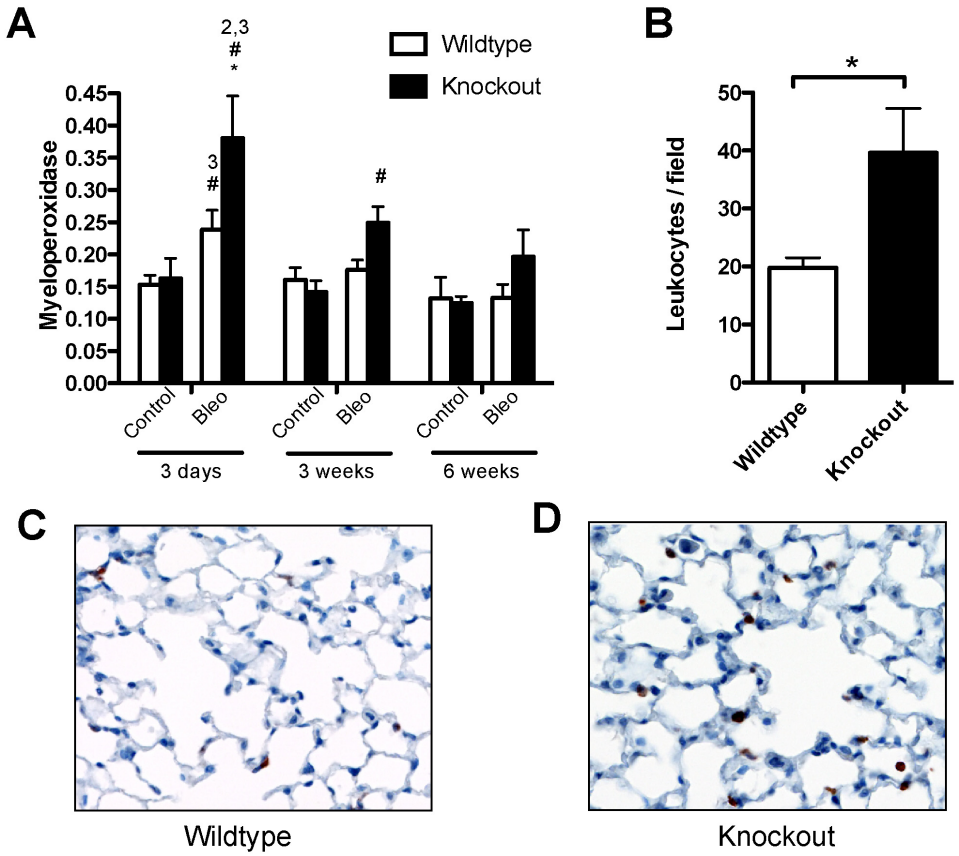

Figure 4. Increased inflammatory infiltrate activity in *Mmp8*$^{-/-}$ mice treated with bleomycin. A: Myeloperoxidase was considered a surrogate marker of neutrophilic infiltration of lung tissue (n≥7 per group). **B**: The number of myeloperoxidase-positive cells was higher in knockout mice. **C–D**: Representative immunohistochemistry for myeloperoxidase in wildtype (C) and knockout (D) animals. $^{1,2,3}P<0.05$ in post-hoc test when compared against 3 days (1), 3 weeks (2), 6 weeks (3) within the same genotype and treatment; *$p<0.05$ when compared against wildtype within the same time and treatment; $^{\#}p<0.05$ when compared against saline within the same time and genotype.
doi:10.1371/journal.pone.0013242.g004

phosphorylated STAT3 was markedly increased in cultures from knockout mice in the presence of bleomycin. This increase was significantly attenuated when a blocking anti-IL10 antibody was added to the medium, thus demonstrating that it was caused by an increase in bioactive IL-10 (Figure 7C) and therefore suggesting that the cleaved form of IL-10 has a decreased activity. In agreement with the results observed in mice, collagen increased after bleomycin treatment in cell cultures from *Mmp8*$^{+/+}$ mice but not from *Mmp8*$^{-/-}$ animals. The addition of an IL-10 blocking antibody increased collagen levels in cultures from *Mmp8*$^{-/-}$ mice up to those seen in their wildtype counterparts (Figure 7D). These results demonstrate that the decreased fibrosis seen in mutant mice is caused directly by the increase in IL-10. There were no differences in IL-10 receptor expression (Figure 7E). Representative western blots of these experiments are shown in Figure 7E.

Discussion

Our results demonstrate that absence of MMP-8 results in an anti-fibrotic effect after bleomycin administration. This effect is mediated by the absence of proteolytic cleavage and subsequent inactivation of endogenous IL-10. Collectively, these results demonstrate that MMP-8 is an important regulator of IL-10 in vivo and point this metalloprotease as a potential therapeutic target in lung fibrosis.

Matrix metalloproteinases have been involved in different phenomena that occur during inflammation and tissue repair, such as modulation of the immune response, extracellular matrix turnover or cell migration [13,14]. There is clear evidence that MMPs play a key role in lung fibrosis [6,15], although different enzymes may have opposite effects. For instance, it has been documented that mice lacking MMP-7 are protected from bleomycin-induced fibrosis [16]. In contrast, overexpression of MMP-9 protects against lung fibrosis [17] and absence of this gelatinase resulted in decreased bronchiolization but no differences in fibrosis [18]. This variety of effects highlights the need of specific inhibitors for a clinical application of the experimental findings [19].

The decreased collagen levels in mice lacking a collagenase suggested that the benefits seen in these animals were not related to the effects of MMP-8 on the extracellular matrix proteins. Moreover, our results show no overcompensatory increase in other collagenases, and even a slightly decreased collagenolytic activity in knockout mice. As the Sircol assay only measures newly synthesized collagen, and not covalent cross-linked fibers, the lower levels of collagen seen in mutant animals suggest a decreased rate of synthesis. This can also explain the absence of differences in soluble collagen seen after 6-weeks in spite of a marked difference in histological scores.

Therefore, we focused on mechanisms other than collagen degradation. MMP-8 has some interesting effects in acute and chronic inflammation. Animals lacking this enzyme have a delayed onset of the acute inflammatory response in different experimental

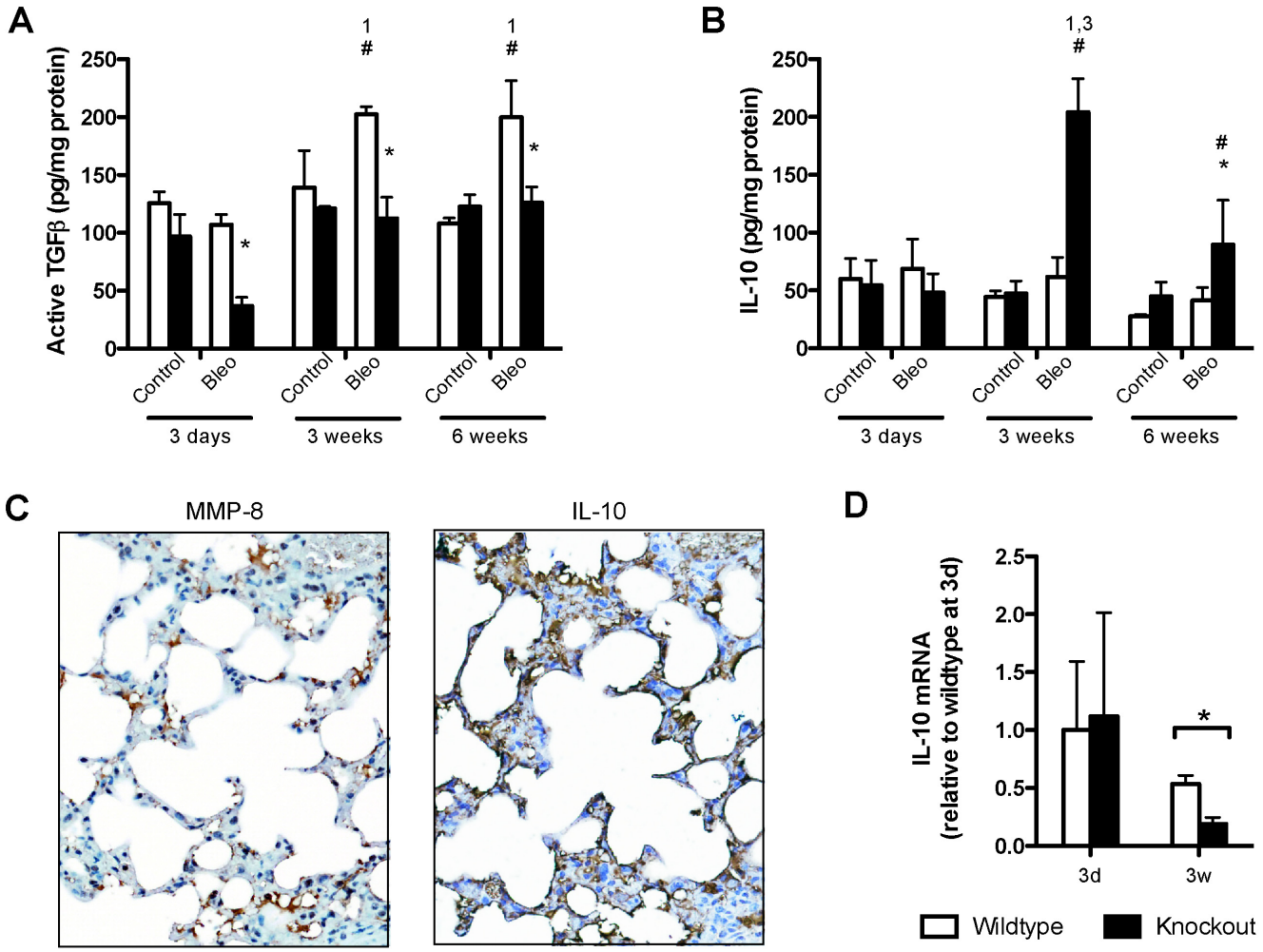

Figure 5. Cytokines in lung homogenates. A: TGFβ increases after bleomycin-induced lung injury only in wildtype mice, whereas knockout mice show lower level in all the stages of the experiment. **B**: IL-10 increases in knockout mice during the chronic phase. N≥5 per group. **C**: Immunohistochemistry for IL-10 and MMP-8 in lungs from wildtype mice after bleomycin instillation, showing IL-10 expression in epithelium and fibroblasts within the alveolar septa. MMP-8 was expressed in fibroblasts. D: IL-10 expression after bleomycin instillation shows no differences between genotypes after 3 days, and a significant decrease in IL-10 mRNA in knockout mice 3 weeks after instillation. $^{1,2,3}P<0.05$ in post-hoc test when compared against 3 days (1), 3 weeks (2), 6 weeks (3) within the same genotype and treatment; *$p<0.05$ when compared against wildtype within the same time and treatment; $^{\#}p<0.05$ when compared against saline within the same time and genotype.
doi:10.1371/journal.pone.0013242.g005

models [8,10,20]. However, once established, the inflammatory infiltrate persists for longer times than in controls. Moreover, MMP-8 may also regulate lung permeability [21], which is an important determinant of outcome in pulmonary fibrosis [22], and apoptosis of inflammatory cells [23]. It has been proposed that MMP-8 is a master regulator of neutrophil chemotaxis by cleavage of chemokines such as MIP-1α [24] or LIX [9], the murine ortologue of human IL-8. This increased inflammation after bleomycin instillation has been recently described in detail [24]. Based on these results, the decreased fibrosis seen in or mice cannot be explained by lower levels of acute damage, as lung injury at 7 days after bleomycin instillation is even higher in mutant animals.

A collateral effect of this delayed clearance of inflammation in a model of skin wounds was a decreased collagen deposition and therefore a delayed healing [10]. Our results follow the same pattern, but in this case the decreased fibrosis is beneficial rather than a side effect. In contrast to the findings in MMP-9 deficient mice [18], we did not observe differences in bronchiolization.

Many of the results seen in disease models using mice lacking MMPs are due to differences in cytokine and chemokine processing. Cleavage of these immune mediators by MMPs can modulate their activity [25]. Different cytokines are involved in the pathogenesis of pulmonary fibrosis. TGFβ is the most important profibrotic mediator [26]. This cytokine has also an anti-inflammatory effect. Of note, the pattern of increased inflammation and decreased fibrosis after bleomycin instillation has been observed in mice lacking the integrin $\alpha_v\beta_6$, which is an activator of latent TGFβ [27].

Another cytokine involved in the regulation of the inflammatory response, fibrosis and TGFβ regulation is IL-10. We found an increase in this cytokine in mice lacking MMP-8 submitted to ventilator-induced lung injury [28]. Moreover, it has been published that interleukin-10 can exert antifibrotic effects after bleomycin instillation. Arai and coworkers [29] demonstrated that overexpression of IL-10 reduced fibrosis in vivo. Similar results were found by Nakagome et al [30], who showed in bleomycin-injected mice that IL-10 decreased TGFβ expression in the lung,

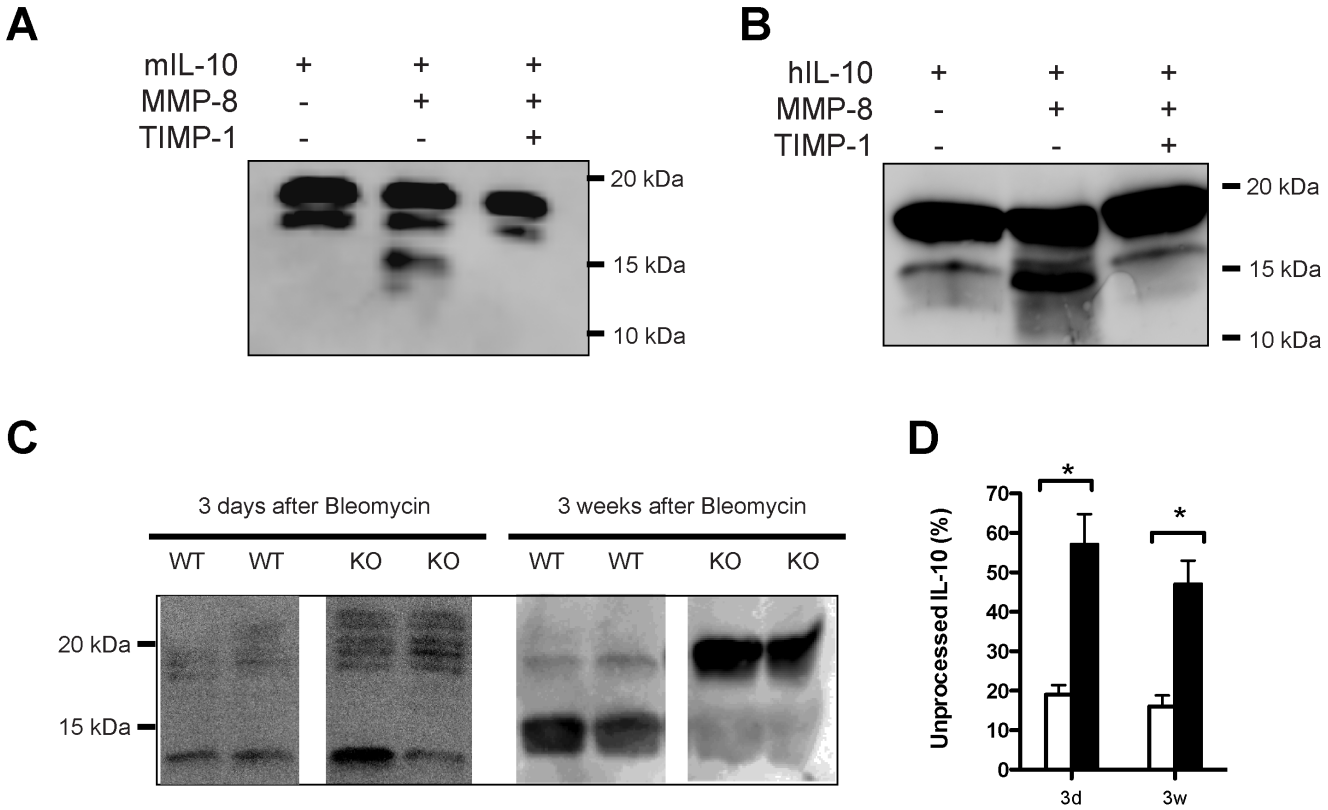

Figure 6. *In vitro* cleavage of IL-10. MMP-8 processing of murine (**A**) and human (**B**) IL-10 in vitro. Cleavage results in a 14 kDa fragment in addition to intact IL-10 (18 kDa). In vivo cleavage (**C**) also occurs. Although there is a 14 kDa fragment in both genotypes, indicating overlapping of other proteases, the percentage of intact IL-10 is significantly higher (*$p<0.05$) in knockout mice (**D**), demonstrating the relevance of MMP-8 in IL-10 metabolism in vivo.
doi:10.1371/journal.pone.0013242.g006

especially in macrophages. Part of the inhibitory effect of IL-10 on TGFβ is caused by a decreased expression of integrin $\alpha_v\beta_6$. However, this cannot be the only mechanism responsible for decreased TGF in knockout mice, as these animals show lower levels even before the increase in IL-10 (i.e. 3 days after bleomycin). Although it has been reported that *Mmp8*$^{-/-}$ mice have a defective TGFβ signaling pathway, the underlying mechanisms are not completely elucidated [10].

Similar results were found using a model of fibrosis associated with chronically inhaled endotoxin [31]. However, there are also reports of a profibrotic role of IL-10 in lung fibrosis induced by silica [32]. Differences in injury model could have been responsible for the discrepancies.

We have shown here that IL-10 is inactivated by MMP-8. This result is reinforced by the absence of differences in IL-10 expression, and even by the decrease in IL-10 expression coinciding with the peak of protein levels. It has been published that IL-10 exerts a paracrine negative feedback involving its own receptors [33]. Moreover, the culture model suggests that the antifibrotic effect seen in our mutant mice is IL-10-dependent. Using IL-10 deficient animals, Kradin and coworkers have not found a difference in lung fibrosis [34]. This is in agreement with our findings, as one can expect that released IL-10 in wildtype mice is inactivated by MMP-8. Collectively, our results are consistent with a model in which absence of MMP-8 results in increased inflammation, but also increased levels of IL-10. Recruited neutrophils release MMP-9, which has a protective role in bleomycin-induced fibrosis [17] through cleavage of potential profibrotic mediators such as insulin-like growth factor binding protein-3 (IGFBP3). Simultaneously, intact IL-10, either directly or by decreasing TGFβ [30], ameliorates the fibrotic process, therefore leading to the beneficial effects seen in knockout mice. This mechanism is depicted in figure 8.

Based on these findings, MMP-8 could be a therapeutic target in lung fibrosis. For this strategy to be effective, selective inhibitors should be used to avoid interference with other MMPs with antifibrotic properties. However, this therapeutic approach should be viewed with caution by different reasons: First, the increased inflammatory response seen in absence of MMP-8 could be detrimental and promote additional injury. Although there was no increased lung damage in *Mmp8*$^{-/-}$ mice, and the role of inflammation in idiopathic fibrosis is discussed, this could be a relevant side effect. Second, the bleomycin model is not fully representative of the human disease, neither idiopathic nor secondary [11].

Another implication of our results is that MMP-8 is an important regulator if IL-10 activity in vivo. This anti-inflammatory cytokine has been proposed as a therapeutic agent in inflammatory and autoimmune diseases [35]. In these cases, the possibility of targeting MMP-8 to increase the levels of active IL-10 could be considered.

In conclusion, we have demonstrated that absence of MMP-8 has an antifibrotic effect mainly driven by an increase in IL-10. Therefore, selective inhibition of this enzyme could be a therapeutic approach in pulmonary fibrosis. Our findings illustrate how this MMP plays a key role in the regulation of the inflammatory response and the subsequent repair. Moreover, they open the possibility to modulate IL-10 metabolism by MMP-8 targeting in a variety of diseases.

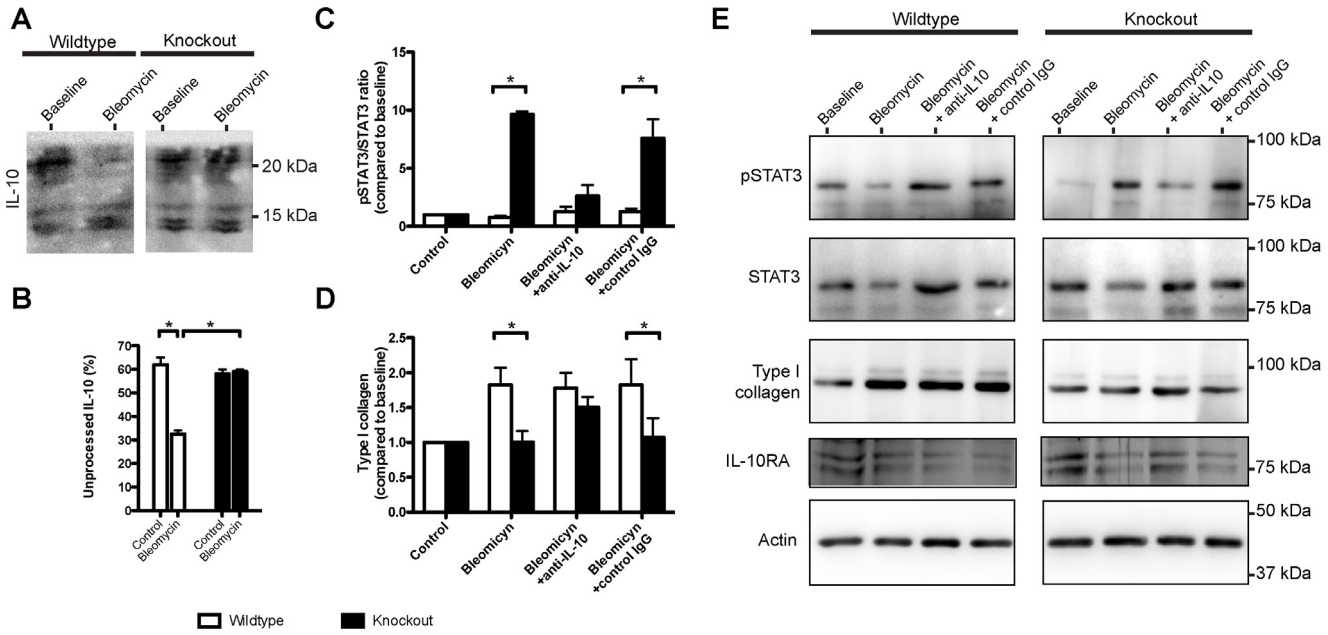

Figure 7. Biological activity of IL-10. The effects of MMP-8 on IL-10 activity were studied in cultured lung fibroblasts from wildtype and knockout mice (n = 4 per group). Intact IL-10 decreased in wildtype cells cultured in presence of bleomycin (Representative western blot: **A**; quantification: **B**). This was related to a decrease in phosphorylated STAT3 (**C**), demonstrating a decrease in the activity of IL-10 signaling pathway, and an increase in Type I collagen (**D**). In contrast, fibroblasts from knockout mice showed no IL-10 cleavage (**A–B**), an increase in STAT3 phosphorylation (**C**) and decreased collagen synthesis (**D**). Addition of a neutralizing antibody against IL-10 decreased STAT3 activation and increased collagen. Addition of a control IgG had no effects. Panel **E** shows representative western blots of these experiments. *$p<0.05$ compared against wildtype under the same culture conditions.
doi:10.1371/journal.pone.0013242.g007

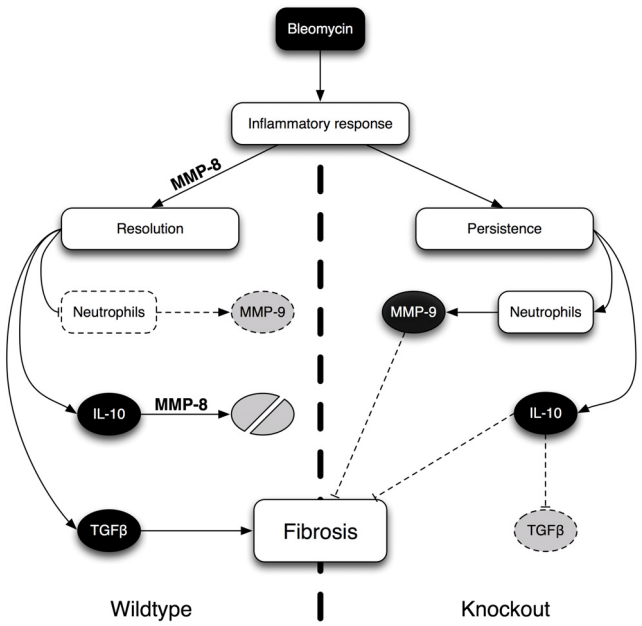

Figure 8. Schematic representation of the mechanisms by which absence of MMP-8 ameliorates lung fibrosis. In normal mice (left), presence of MMP-8 facilitates the resolution of inflammation, thus decreasing MMP-9 (by the clearance of neutrophils) and IL-10 (by cleavage). The increased TGFβ promotes fibrosis. In absence of MMP-8 (right), there are increased levels of MMP-9 and IL-10, both of them with antifibrotic properties. IL-10 can also inhibit TGFβ synthesis. For further details, see text.
doi:10.1371/journal.pone.0013242.g008

Methods

Animals

Eight-week-old male wildtype and *Mmp8*$^{-/-}$ mice generated in a mixed C57/Sv129 background [8] were used. Genotypes were confirmed by PCR. The Animal Research Committee of the Universidad de Oviedo authorized the experimental protocol.

Experimental design

Mice of both genotypes were randomly assigned to bleomycin or saline administration. Under anesthesia using vaporized fluorane, a midline neck incision was done and the trachea exposed. Either bleomycin (2 units/Kg) or isotonic saline were administered intratracheally using a 28G needle. After this, the skin was sutured and the animals left to recover. Four mice (1 saline-treated *Mmp8*$^{-/-}$, 1 bleomycin-treated *Mmp8*$^{-/-}$ and 2 bleomycin-treated *Mmp8*$^{+/+}$) died within the first 5 days after instillation and were replaced. There were no deaths after this time point. Mice were sacrificed 3 days, 3 weeks or 6 weeks after the intratracheal instillation. This results in 12 different groups, depending on the genotype, treatment and time course after the injury. We included 8-10 animals per group (total 106 mice).

Histological analysis

The left lung was fixated using formaldehyde. Three lung slices, stained with Masson's trichrome, were studied. Lung fibrosis was scored from 0 (no fibrosis) to 8 (massive fibrosis in all fields) using the Ashcroft scale [36]. Bronchiolozation (presence of bronchial-like cells in the alveoli) was quantified using the Jensen-Taubman scale [37]. A pathologist (AA), blinded to genotypes and experimental conditions, made all the evaluations.

To evaluate the inflammatory infiltrate within the lungs, immunohistochemical analysis was done in sections from bleomycin-treated mice of both genotypes using an anti-myeloperoxidase antibody (Thermo Fisher Scientific, USA). The number of positive cells in three microscopic fields (×20) was counted and averaged. Immunostaining in lung sections was done using antibodies against MMP-8 and IL-10 (Abcam, UK) and MMP-9 (Santa Cruz Biotechnologies, USA).

Collagen content

Soluble lung collagen was measured in lung homogenates using the Sircol assay (Biocolor, UK), following manufacturer's instructions. Briefly, lung tissue homogenates were mixed with the Sircol dye and centrifugated. The pellet was resuspended in NaOH and the optical density at 540 nm measured. The obtained absorbance is proportional to the abundance of recently synthesized collagen.

Quantification of MMP-8 by western blot

The levels of MMP-8 in lung tissue were measured by western blotting. Lung homogenates were resolved in a 8% SDS-polyacrilamide gel, transferred to a nitrocellulose membrane and incubated with a polyclonal antibody raised in rabbits against murine MMP-8. A secondary peroxidase-linked anti-rabbit antibody was used to detect MMP-8 by chemoluminescence, as previously described. Membranes were scanned in a LAS-3000 camera (Fujifilm, Germany), and intensity of the bands measured using the ImageJ software.

Collagenolytic activity

Total collagenolytic activity was quantified in lung homogenates using the EnzChek collagenase assay kit (Invitrogen, USA). Briefly, fluorescein-conjugate collagen (DQ collagen, Invitrogen, USA) and tissue homogenates (100 micrograms of total protein) were incubated at 37°C in a reaction buffer. The increase in fluorescence, measured at 0.5, 1, 3 and 5 hours, is proportional to collagenolytic activity of the tissue.

Gelatin zymography

MMP-2 and MMP-9 were measured in lung homogenates using gelatin zymography. Protein content was adjusted to 20 micrograms in all samples, and loaded in a SDS-polyacrylamide gel containing gelatin, electrophoresed and incubated overnight in an buffer (150mM NaCl, 5mM CaCl2, 50mM Tris-HCl, pH 7.6). After staining with Coomassie Blue, gelatinolytic activity appears as white bands in a blue background. The gels were scanned and quantified using ImageJ software (National Institutes of Health, USA).

Myeloperoxidase assay

Myeloperoxidase activity was measured as a marker of neutrophil infiltration. A lung fragment was homogenated in phosphate buffer containing CTAB. Tissue homogenates were incubated with O-dianisidine and H_2O_2 and light absorbance at 460 nm was measured as a marker of myeloperoxidase content.

Cytokine measurements

Total IL-10 and active TGFβ were measured in lung homogenates using commercial ELISA kits (eBioscience, UK), following manufacturers' instructions. Additionally, IL-10 expression was measured by quantitative PCR. Total lung RNA was extracted from mouse lungs using TRIzol reagent (Invitrogen Life Technologies,USA) and reversed transcribed into cDNA (Advantage RT-for-PCR Kit; Clontech, USA). Quantitative reverse transcription-PCR was carried out in duplicate for each sample using 20 ng of cDNA, TaqMan Universal PCR master mix and 1 μL of the specific TaqMan custom gene expression assay for IL10 (Mm01288386_m1, Applied Biosystems, USA). To quantify gene expression, PCR was performed at 95°C for 10 min, followed by 40 cycles at 95°C for 15 s, 60°C for 30 s, and 72°C for 30 s using an ABI Prism 7700 sequence detector system. Gene expression was normalized to β-actin as control. Relative expression of the analyzed genes was calculated according to manufacturer's instructions.

IL-10 digestion

To assess enzymatic processing of IL-10 by MMP-8, murine or human IL-10 were incubated with MMP-8 pre-activated with APMA, at 37°C in a buffer containing 150 mM NaCl, 5 mM CaCl2, 50 mM Tris-HCl (pH 7.6). Experiments without MMP-8 or adding TIMP-1 to the incubation buffer were conducted in parallel. After incubation, the samples were resolved by 15% SDS-PAGE. The proteins were transferred to a nitrocellulose membrane and detected by western blotting as described before, using polyclonal anti-mouse or anti-human IL-10 antibodies (purchased from Abcam, UK and R&D Systems, USA, respectively). To clarify the *in vivo* relevance of the cleavage of IL-10 by MMP-8, we detected the cytokine in lung tissue homogenates from wildtype and knockout mice 3 weeks after bleomycin administration. IL-10 was detected by western blotting using the same polyclonal antibody after 15% SDS-PAGE. Bands of different molecular weight were detected, the intensity of each one was quantified using ImageJ software. The percentage of unprocessed IL-10 with respect to the total amount was computed for each sample.

IL-10 activity assay in cell cultures

Fibroblast cultures were initiated from lung explants from WT and MMP8 deficient mice as described [38]. Lungs were washed with PBS, and triturated with razor blades. The disrupted explants were allowed to adhere to the bottom of the culture plates before covering them with DMEM cell culture medium supplemented with penicillin/streptomycin/gentamicin, 10% FBS, nonessential amino acids (0.1 mM), sodium pyruvate (1 mM), L-glutamine (2 mM) and N-2-hydroxyethylpiperazine-N′-2-ethanesulfonic acid (HEPES) (10 mM). Cultures were maintained at 37°C and 5% CO_2. After the first 2 weeks of culture, most nonfibroblast cells died while the fibroblasts established as the predominant cell type. Then, cultured cells were trypsinized, filtered, and washed. Fibroblasts were seeded in 12-well plates with DMEM without FBS under the following conditions: Baseline, bleomycin (bleomycin 100 nM), bleomycin plus IL-10 blockade (bleomycin 100 nM and anti-IL10 blocking antibody purchased from Peprotech Inc) and bleomycin plus unspecific IgG (Abcam, UK). After 12 hours, supernatants were removed and cell extracts obtained using a RIPA buffer (100 mM TRIS pH 7.4, 150 mM NaCl, 10 mM EDTA, 1% deoxycolic acid, 1% Triton X-100, 0.1% SDS, 50 mM NaF, 1 mM orthovanadate and protease inhibitor cocktail) and stored at −80°C. In these extracts, western blots were done to measure type I collagen (using an antibody purchased from Calbiochem, Merck, UK), IL-10 and IL-10 receptor (IL-10RA antibody, Abcam, UK). To measure IL-10 activity, we quantified the phosphorylation balance of the transcription factor STAT-3 by western blot using antibodies against phosphorylated and non-phosphorylated forms of STAT3 (Signalway Antibody Co, USA). As loading control we used a polyclonal anti-actin antibody purchased from Santa Cruz

Biotechnology Inc (USA). Detection and quantification of the bands was done as previously described.

Statistical analysis

Results are expressed as mean±SEM. Variables were compared using an ANOVA, including genotype, treatment and time of study as factors. When appropriate, post-hoc tests were done using Bonferroni's correction. Comparisons between two variables were done using a T test. A p value lower than 0.05 was considered significant.

Acknowledgments

The authors thank Cecilia Garabaya and Maria Fernández their help with the experimental work, and Marta S Pitiot and Laura Suarez Fernandez for processing histological samples.

Author Contributions

Conceived and designed the experiments: EGP AGL SC AGF XSP AF CLO GMA. Performed the experiments: EGP AGL SC AA AGF MFF EBS XSP GMA. Analyzed the data: EGP AGL AF CLO GMA. Contributed reagents/materials/analysis tools: AA CLO. Wrote the paper: AGL SC AF CLO GMA.

References

1. Maher TM, Wells AU, Laurent GJ (2007) Idiopathic pulmonary fibrosis: multiple causes and multiple mechanisms? Eur Respir J 30: 835–839.
2. Strieter RM (2008) What differentiates normal lung repair and fibrosis? Inflammation, resolution of repair, and fibrosis. Proc Am Thorac Soc 5: 305–310.
3. Selman M, King TE, Pardo A (2001) Idiopathic pulmonary fibrosis: prevailing and evolving hypotheses about its pathogenesis and implications for therapy. Ann Intern Med 134: 136–151.
4. Walter N, Collard HR, King TE, Jr. (2006) Current perspectives on the treatment of idiopathic pulmonary fibrosis. Proc Am Thorac Soc 3: 330–338.
5. Greenlee KJ, Werb Z, Kheradmand F (2007) Matrix metalloproteinases in lung: multiple, multifarious, and multifaceted. Physiol Rev 87: 69–98.
6. Pardo A, Selman M (2006) Matrix metalloproteases in aberrant fibrotic tissue remodeling. Proc Am Thorac Soc 3: 383–388.
7. Fanjul-Fernandez M, Folgueras AR, Cabrera S, Lopez-Otin C (2009) Matrix metalloproteinases: Evolution, gene regulation and functional analysis in mouse models. Biochim Biophys Acta 1803: 3–19.
8. Balbin M, Fueyo A, Tester AM, Pendas AM, Pitiot AS, et al. (2003) Loss of collagenase-2 confers increased skin tumor susceptibility to male mice. Nat Genet 35: 252–257.
9. Tester AM, Cox JH, Connor AR, Starr AE, Dean RA, et al. (2007) LPS responsiveness and neutrophil chemotaxis in vivo require PMN MMP-8 activity. PLoS ONE 2: e312.
10. Gutierrez-Fernandez A, Inada M, Balbin M, Fueyo A, Pitiot AS, et al. (2007) Increased inflammation delays wound healing in mice deficient in collagenase-2 (MMP-8). FASEB J 21: 2580–2591.
11. Moore BB, Hogaboam CM (2008) Murine models of pulmonary fibrosis. Am J Physiol Lung Cell Mol Physiol 294: L152–160.
12. Kunugi S, Fukuda Y, Ishizaki M, Yamanaka N (2001) Role of MMP-2 in alveolar epithelial cell repair after bleomycin administration in rabbits. Lab Invest 81: 1309–1318.
13. Nagase H, Visse R, Murphy G (2006) Structure and function of matrix metalloproteinases and TIMPs. Cardiovasc Res 69: 562–573.
14. O'Reilly PJ, Gaggar A, Blalock JE (2008) Interfering with extracellular matrix degradation to blunt inflammation. Curr Opin Pharmacol 8: 242–248.
15. Rosas IO, Richards TJ, Konishi K, Zhang Y, Gibson K, et al. (2008) MMP1 and MMP7 as potential peripheral blood biomarkers in idiopathic pulmonary fibrosis. PLoS Med 5: e93.
16. Zuo F, Kaminski N, Eugui E, Allard J, Yakhini Z, et al. (2002) Gene expression analysis reveals matrilysin as a key regulator of pulmonary fibrosis in mice and humans. Proc Natl Acad Sci U S A 99: 6292–6297.
17. Cabrera S, Gaxiola M, Arreola JL, Ramirez R, Jara P, et al. (2007) Overexpression of MMP9 in macrophages attenuates pulmonary fibrosis induced by bleomycin. Int J Biochem Cell Biol 39: 2324–2338.
18. Betsuyaku T, Fukuda Y, Parks WC, Shipley JM, Senior RM (2000) Gelatinase B is required for alveolar bronchiolization after intratracheal bleomycin. Am J Pathol 157: 525–535.
19. Overall CM, Lopez-Otin C (2002) Strategies for MMP inhibition in cancer: innovations for the post-trial era. Nat Rev Cancer 2: 657–672.
20. Van Lint P, Wielockx B, Puimege L, Noel A, Lopez-Otin C, et al. (2005) Resistance of collagenase-2 (matrix metalloproteinase-8)-deficient mice to TNF-induced lethal hepatitis. J Immunol 175: 7642–7649.
21. Dolinay T, Wu W, Kaminski N, Ifedigbo E, Kaynar AM, et al. (2008) Mitogen-activated protein kinases regulate susceptibility to ventilator-induced lung injury. PLoS ONE 3: e1601.
22. McKeown S, Richter AG, O'Kane C, McAuley DF, Thickett DR (2009) MMP expression and abnormal lung permeability are important determinants of outcome in IPF. Eur Respir J 33: 77–84.
23. Gueders MM, Balbin M, Rocks N, Foidart JM, Gosset P, et al. (2005) Matrix metalloproteinase-8 deficiency promotes granulocytic allergen-induced airway inflammation. J Immunol 175: 2589–2597.
24. Quintero PA, Knolle MD, Cala LF, Zhuang Y, Owen CA (2009) Matrix Metalloproteinase-8 Inactivates Macrophage Inflammatory Protein-1{alpha} To Reduce Acute Lung Inflammation and Injury in Mice. J Immunol 184: 1575–1588.
25. Van Lint P, Libert C (2007) Chemokine and cytokine processing by matrix metalloproteinases and its effect on leukocyte migration and inflammation. J Leukoc Biol 82: 1375–1381.
26. Krein PM, Winston BW (2002) Roles for insulin-like growth factor I and transforming growth factor-beta in fibrotic lung disease. Chest 122: 289S–293S.
27. Munger JS, Huang X, Kawakatsu H, Griffiths MJ, Dalton SL, et al. (1999) The integrin alpha v beta 6 binds and activates latent TGF beta 1: a mechanism for regulating pulmonary inflammation and fibrosis. Cell 96: 319–328.
28. Albaiceta GM, Gutierrez-Fernandez A, Garcia-Prieto E, Puente XS, Parra D, et al. (2009) Absence or Inhibition of Matrix Metalloproteinase-8 Decreases Ventilator-induced Lung Injury. Am J Respir Cell Mol Biol;(e-pub ahead of print).
29. Arai T, Abe K, Matsuoka H, Yoshida M, Mori M, et al. (2000) Introduction of the interleukin-10 gene into mice inhibited bleomycin-induced lung injury in vivo. Am J Physiol Lung Cell Mol Physiol 278: L914–922.
30. Nakagome K, Dohi M, Okunishi K, Tanaka R, Miyazaki J, et al. (2006) In vivo IL-10 gene delivery attenuates bleomycin induced pulmonary fibrosis by inhibiting the production and activation of TGF-beta in the lung. Thorax 61: 886–894.
31. Garantziotis S, Brass DM, Savov J, Hollingsworth JW, McElvania-TeKippe E, et al. (2006) Leukocyte-derived IL-10 reduces subepithelial fibrosis associated with chronically inhaled endotoxin. Am J Respir Cell Mol Biol 35: 662–667.
32. Barbarin V, Xing Z, Delos M, Lison D, Huaux F (2005) Pulmonary overexpression of IL-10 augments lung fibrosis and Th2 responses induced by silica particles. Am J Physiol Lung Cell Mol Physiol 288: L841–848.
33. Giambartolomei GH, Dennis VA, Lasater BL, Murthy PK, Philipp MT (2002) Autocrine and exocrine regulation of interleukin-10 production in THP-1 cells stimulated with Borrelia burgdorferi lipoproteins. Infect Immun 70: 1881–1888.
34. Kradin RL, Sakamoto H, Jain F, Zhao LH, Hymowitz G, et al. (2004) IL-10 inhibits inflammation but does not affect fibrosis in the pulmonary response to bleomycin. Exp Mol Pathol 76: 205–211.
35. Zhou X, Schmidtke P, Zepp F, Meyer CU (2005) Boosting interleukin-10 production: therapeutic effects and mechanisms. Curr Drug Targets Immune Endocr Metabol Disord 5: 465–475.
36. Ashcroft T, Simpson JM, Timbrell V (1988) Simple method of estimating severity of pulmonary fibrosis on a numerical scale. J Clin Pathol 41: 467–470.
37. Jensen-Taubman SM, Steinberg SM, Linnoila RI (1998) Bronchiolization of the alveoli in lung cancer: pathology, patterns of differentiation and oncogene expression. Int J Cancer 75: 489–496.
38. Baglole CJ, Reddy SY, Pollock SJ, Feldon SE, Sime PJ, et al. (2005) Isolation and phenotypic characterization of lung fibroblasts. Methods Mol Med 117: 115–127.

IV. Revisión sobre la reparación tras la lesión pulmonar aguda: mecanismos moleculares y oportunidades terapéuticas.

La actividad científica en el campo del daño pulmonar se ha centrado clásicamente en estudiar posibles modos de eliminar o al menos reducir la lesión pulmonar inicial. Aun cuando el uso de diferentes aproximaciones terapéuticas han dado buenos resultados en modelos experimentales animales, el traslado de estas prácticas a la clínica no han demostrado los mismos resultados beneficiosos. La causa de esta disparidad en los resultados podría estar debida, en parte, al papel del sistema inflamatorio en la reparación posterior del tejido lesionado. De ahí que en los últimos años hayan aparecido cada vez más trabajos enfocados en el estudio de posibles terapias para mejorar el proceso de reparación. En este contexto nos pareció adecuado llevar a cabo una revisión bibliográfica sobre el tema con el objetivo de afianzar los conocimientos necesarios para poder desarrollar nuevas aportaciones.

Artículo 4: González-López A, Albaiceta GM. "Repair after acute lung injury: molecular mechanisms and therapeutic opportunities".

Crit Care. 2012 Dec 12;16(2):209. I.F: 4.61

Aportación personal al trabajo.

En este trabajo compartí, junto con el Dr. Muñiz Albaiceta, la tarea de elaborar un manuscrito que proporcionase una visión actual sobre el conocimiento de los mecanismos y posibilidades terapéuticas de la reparación tras la lesión pulmonar. Para ello participe en la búsqueda bibliográfica, su organización y la posterior escritura del manuscrito.

CRITICAL CARE

REVIEW

Repair after acute lung injury: molecular mechanisms and therapeutic opportunities

Adrián González-López and Guillermo M Albaiceta*

This article is one of eleven reviews selected from the *Annual Update in Intensive Care and Emergency Medicine* 2012 (Springer Verlag, DOI: 10.1007/978-3-642-25716-2) and co-published as a series in *Critical Care*. Other articles in the series can be found online at http://ccforum.com/series/annualupdate2012. Further information about the *Annual Update in Intensive Care and Emergency Medicine* is available from http://www.springer.com/series/8901.

Introduction

Acute lung injury (ALI) is a clinical syndrome characterized by impairment in gas exchange and/or lung mechanics that leads to hypoxemia and increased work of breathing (WOB). When respiratory failure occurs, most patients require mechanical ventilation. This clinical scenario is related to high morbidity and mortality rates.

There have been large amounts of research on the pathogenetic mechanisms of lung injury, which include changes in alveolocapillary permeability, the inflammatory response, extracellular matrix remodeling and abnormal alveolar micromechanics. In spite of this knowledge, no effective therapy, other than treating the initial cause of injury and providing supportive treatment, has been shown to have a significant clinical benefit. Fortunately, the cause of ALI is known in most cases, so specific therapy can be initiated (e.g., antibiotics in sepsis, surgery when appropriate). In other cases, the cause is time-limited, such as in aspiration pneumonitis or polytrauma. However, even in these cases, ALI may persist beyond the initial insult. In this setting, restoration of normal lung structure and function is of paramount importance for survival.

There is increasing evidence of the lung's capacity to repair itself. This process involves an interplay between various cellular and molecular mechanisms, including resolution of edema and inflammation, cell proliferation and tissue remodeling. Moreover, it is possible that some of these mechanisms, activated early in the response to injury, are essential for normal repair later on. With this in mind, timing of a therapeutic intervention becomes a critical issue, as blockade of one mediator may prevent injury when administered early, but also impair the repair phase. Moreover, strategies aimed at promoting repair could represent a new alternative for patients with ALI.

Knowledge of the repair mechanisms could, therefore, be the next step to understanding the lung response to injury. In this review, we will summarize some of these mechanisms and discuss their relevance as potential therapeutic targets in ALI.

An overview of the repair process

The lung response to an injurious stimulus involves transduction of the danger signal into a biochemical response. Depending on the cause, there are many pathways that can be activated. For instance, bacterial antigens may trigger an inflammatory response by activating any of the Toll-like receptors (TLR). Chemical agents induce cell membrane damage and, in some cases, oxidative stress, leading to the activation of a number of intracellular kinases. Mechanical stress, such as positive pressure ventilation, can also precipitate a biological response after a mechanotransduction process [1].

In addition to exogenous causes, an endogenous system detects tissue and cell damage and triggers the physiological response. Alarmins, a subgroup of molecules of a larger set called DAMPs (damage-associated molecular patterns), lead to this system. Structurally different, these endogenous molecules are released in response to tissue damage by dead cells and local inflammatory cells (alveolar macrophages in the case of lung), activating and recruiting immune cells through binding to different receptors, such as TLR, interleukin-1 receptor (IL-1R) and RAGE (receptor of advanced glycation end-products) [2], thereby activating the pro-inflammatory pathway. Irrespective of the cause, these signals converge in a group of transcription factors (e.g., nuclear factor-kappa B [NF-κB], activator protein [AP]-1), which induce the synthesis of new molecules that ultimately mediate the

*Correspondence: guillermo.muniz@sespa.princast.es
Department of Functional Biology, Physiology Area, Faculty of Medicine, University of Oviedo, Julian Claveria s/n, 33006 Oviedo, Spain

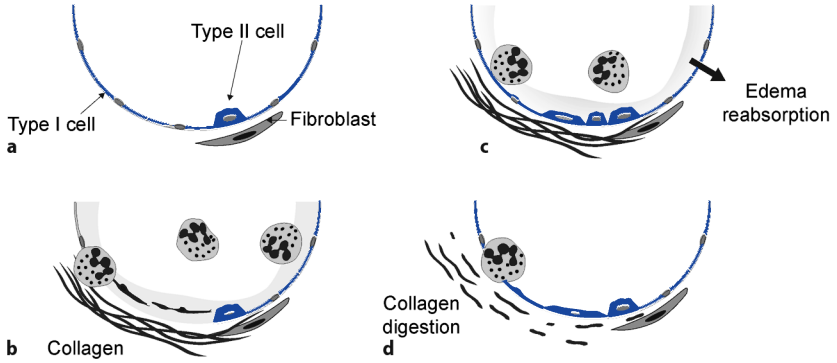

Figure 1. Overview of the injury and repair mechanisms in an alveolus. (a) The normal alveolus is formed by type I and type II alveolar cells. The former cover the majority of the alveolar area, and the latter are reduced in number. **(b)** After acute lung injury, the inflammatory response results in the recruitment of neutrophils from the circulation, the development of alveolar edema and the deposition of collagen fibers. The necrotic alveolar cells are detached from the basement membrane. **(c)** During the repair phase, the alveolar fluid is reabsorbed, the inflammatory response attenuated, and type II alveolar cells (among others) proliferate and differentiate into type I pneumocytes. In this phase, collagen fibers may facilitate cellular migration. **(d)** Finally, digestion of the collagen scar is needed for complete normalization of lung functions.

inflammatory response to the aggression. Hallmarks of this response are the increased alveolocapillary permeability, which causes a protein-rich edema, the neutrophil infiltrate (recruited from the circulation in response to chemokines), and the release of a wide variety of mediators, such as cyto- and chemokines, proteases, eicosanoids and growth factors, into the extracellular space. Figure 1 summarizes this process. During this stage, pneumocyte death due to apoptosis (in response to released mediators) and/or necrosis (caused by toxins, proteases...) results in exposure of the basement membrane of the alveolar epithelium.

One of the key steps in the tissue response is the deposition of collagen fibers at the sites of injury. Similarly to what happens in skin wounds, lung fibroblasts release procollagen peptides into the extracellular space, in order to create a scar. This is probably an attempt to keep the lung structure as intact as possible. So collagen deposition must not be viewed as a late response to abnormal healing, but as an early phenomenon. Some experimental studies corroborate this early onset of collagen deposition [3]. Moreover, patients show an increase in procollagen levels in the first 48 hours after meeting ALI criteria [4].

Tissue repair involves a variety of mechanisms including edema reabsorption, resolution of inflammation and cell proliferation in order to repopulate the alveolar epithelium (Figure 1c). Lung edema clearance is a crucial step. It has been documented that mild alveolar injury results in increased alveolar fluid reabsorption. However, in severe cases, the injured pneumocytes cannot sustain the active transport of ions and water across the epithelium. Therefore, cell integrity is essential for edema clearance. The molecular mechanisms of ion and water transport in lung exceed the scope of this article, and have been reviewed elsewhere [5]. Regulation of the inflammatory response is a complex mechanism that requires interplay between several immune mediators [6]. Some anti-inflammatory cytokines, IL-10 being the most studied, are released even during a pro-inflammatory response as a negative feedback mechanism. When the pro-inflammatory pathways are downregulated (i.e., after cessation of the stimulus), these anti-inflammatory mediators decrease cytokine expression. Apoptosis of inflammatory cells (mainly neutrophils) has also been documented when pro-survival signals, such as granulocyte-colony stimulating factor (G-CSF), disappear. Alveolar macrophages also play a role in this phase engulfing death cells.

Finally, the regeneration of the alveolar structure requires the proliferation and differentiation of some progenitors into type I pneumocytes (Figure 2). Different growth factors (e.g. epidermic [EGF], keratinocyte [KGF] or hepatic growth factor [HGF]), acting through tyrosin-kinase receptors, promote cell proliferation. The cell lines implicated in this step are a matter of research, stimulated by the growing interest in stem cells and regenerative medicine [7]. Endogenous progenitor cells include both resident stem cells and bone marrow-derived cells. Regarding the first, type II pneumocytes proliferate after injury and can originate type I cells. This has been demonstrated after pneumonectomy, hyperoxia or repeated bleomycin instillation in mice. Moreover, bone marrow-derived stem cells could also participate in alveolar repair, although data on the engraftment and differentiation of these cells are more focused on their therapeutic use than to clarify their role in the normal repair process. In addition, other cell types may also play

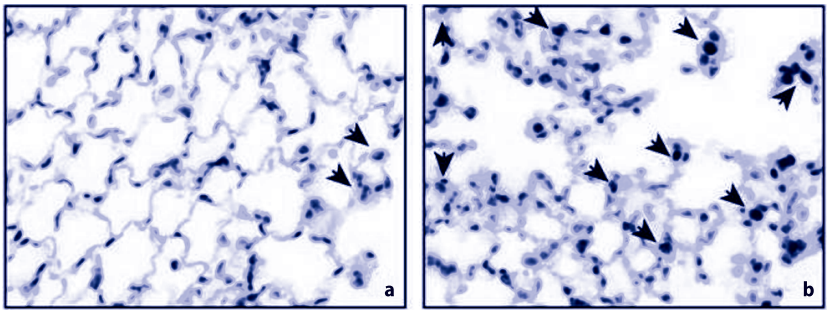

Figure 2. Cell proliferation in control mice (a) and during the repair phase after ventilator-induced lung injury (b). Some cells (arrows) show positive staining for Ki-67, a marker of cell proliferation.

a role in alveolar regeneration. Lung mesenchymal cells are activated after ALI and, in addition to collagen synthesis, they may secrete growth factors and even modulate the immune response by secreting anti-inflammatory cytokines [8].

The previously formed collagen scar can facilitate cell attachment to keep the alveolar structure. Again, collagen synthesis should be viewed as part of the normal healing process. However, excessive collagen deposition may impair gas exchange and lung mechanics. So, in order to restore normal respiratory function, the previously formed scar must be processed and removed (Figure 1d). This can be carried out by matrix metalloproteinases (MMPs), a family of enzymes that can digest virtually all types of extracellular fibers [9]. One of the most important sources of MMPs is inflammatory cells (neutrophils and macrophages contain significant amounts of MMP-8 and MMP-9). Therefore, it can be hypothesized that the inflammatory response is important for adequate lung repair, and that MMPs are one of the links between these two phenomena. The underlying mechanisms that regulate this step in ALI are unknown, but knowledge of these mechanisms could help clarify why some patients develop a severe fibrotic response, which can cause long-term disabilities.

The special case of repair after ventilator-induced lung injury

Ventilation with high tidal volumes or transpulmonary pressures may cause severe injury to the lungs. In experimental models, there is a clear causality relationship between ventilatory settings and so-called ventilator-induced lung injury (VILI). Although this relationship is less clear in patients, especially those with previous ALI, the development of ventilatory strategies aimed to avoid further lung injury has been shown to decrease mortality. Therefore, although experimental models of VILI cannot be directly extrapolated to critically ill patients, they highlight the mechanisms of injury and repair involved.

A few studies have focused on repair after VILI, giving some insights into this process. The first was published by Nin et al. in 2008 [10]. These authors submitted Sprague-Dawley rats to injurious ventilation for one hour, reestablishing spontaneous breathing and letting them recover. Histological studies showed a significant reduction in capillary congestion, interstitial edema, type-I pneumocyte necrosis and hyaline membrane formation after 24 hours of recovery, reaching normality after 72 hours. Inflammatory markers showed a similar pattern. Aortic vascular and pulmonary microvessel responses to acetylcholine and norepinephrine were impaired and returned to normal at 168 and 72 hours respectively. This study demonstrated that VILI can revert rapidly after spontaneous breathing is reestablished.

In another study, Gonzalez-Lopez et al. [11] submitted CD1 mice to a combination of two ventilator strategies. One group was ventilated for 90 minutes with high pressures and another group was ventilated with the same strategy followed by up to 4 hours of protective ventilation. Histological score, pulmonary edema, alveolar permeability and tumor necrosis factor (TNF)-α increased during injury and returned to baseline values during repair. Later comparisons of the repair phase showed that survivors had higher pneumocyte proliferation and leukocyte infiltration and lower alveolar permeability and collagen content than non-survivors. MMP-2 levels were also increased in survivors. This MMP improves wound healing in *ex vivo* models using mice and human alveolar epithelial cell lines. Taken together, these studies suggest that an appropriate inflammatory response and tissue remodeling are key events during repair.

The role of inflammation in tissue damage and repair

Inflammation is necessary for the development of a proper response to the insult, but it can damage the tissue where it takes place. Inflammation leads initially to an alteration in homeostasis, during which tissue partially

sacrifices cellular and extracellular matrix integrity and tissue functionality for the benefit of a quick response. A good example of this compromise is the early recruitment of immune cells to the site of injury. The first cells arriving are neutrophils [12]. Representing 70% of total circulating leukocytes, these cells are rapid responders to chemokines, appearing in the lungs a few minutes after initial injury. But this recruitment has a price for lung integrity; after migrating through endothelial cells and before arriving in the alveolar space, leukocytes find the basement membrane, a highly organized extracellular matrix mainly composed of four families of glycoproteins (laminin, collagen type IV isoforms, nidogen and heparan sulfate proteoglycans). The basement membrane is actively involved in leukocyte recruitment by its potential to bind and release cytokines and chemotactic factors. The only way neutrophils can cross this barrier is by proteolytic degradation [13], contributing to further damage of lung structure. Once in the lung, the release of a variety of alarmins, free oxygen radicals, leukotrienes, proteases and other pro-inflammatory molecules maintain the inflammatory state, thereby contributing to the ALI phase.

The role of proteases, especially of MMPs, in the pathogenesis of ALI has been controversial. Extracellular matrix processing releases some bioactive molecules. For example, type I collagen degradation generates an acetylated tripeptide with similar chemotactic activity to IL-8 [14]; moreover, MMPs process many immune mediators, like pro- and anti-inflammatory cytokines and chemokines, altering their activity (e.g., IL-1β, transforming growth factor [TGF]β and lipopolysaccharide-induced CXC chemokine [LIX] activation and macrophage inflammatory protein [MIP]-1α inactivation) and bioavailability (TNF-α and TGFβ release from cell surface and extracellular matrix, respectively) [15]. Their ability to regulate the inflammatory mediators and degrade collagen fibers also makes MMPs key elements in the later stages of inflammation, when resolution and repair of the injured tissue are of paramount importance. In a model of liver injury, it has been demonstrated that neutropenic animals develop more severe fibrosis, probably due to the lack of MMPs (released by neutrophils) in the repair phase [16]. A similar dependence between inflammation and collagenolysis in the lung has not been demonstrated, but these findings warrant more research.

Research on models of lung injury using knock-out mice for single MMPs, such as MMP-2, MMP-3, MMP-7, MMP-8 and MMP-9, has shed some light on this issue. MMP-2 [11], MMP-7 [17] and MMP-9 [18] have been shown to be involved in alveolar epithelial repair in experimental models of wound healing. Furthermore, a model of VILI [19] demonstrated that MMP-9 function is worth preserving, given that mice deficient in this protease had increased levels of lung injury. On the other hand, MMP-3 may be detrimental, as mice lacking this MMP were protected against lung injury caused by administration of nonspecific IgG [20] or bleomycin [21]. Regarding MMP-8, this protease has shown different effects depending on the experimental model. It has a detrimental role in models of VILI [22] and lung fibrosis, due to IL-10 cleavage [23]. However, this enzyme may be beneficial after lipopolysaccharide (LPS) or hyperoxia exposition [24]. Moreover, it may have a role in resolution stages of ALI, as it seems to be involved in neutrophil apoptosis through modulation of IL-4 levels [25].

Therefore, this complex family serves not only to regulate the influx and clearance of leukocytes and the inflammatory process itself, but also the removal of excess deposits of collagen fibers released by fibroblasts during ALI. It is becoming clearer that pharmacotherapy should be aimed at blocking specific MMPs during the early stages of ALI, in order to avoid destruction of the basement membrane and extracellular matrix caused by their proteolytic action. Although this could have an initial benefit it may turn detrimental to the repair process if treatment is continued.

Signs of tissue repair in patients

The assessment of lung repair in patients could be of great interest because of its prognostic relevance in ALI patients. However, measurement of any mediator involved in tissue repair has one fundamental limitation: If a patient shows high levels of a given marker, it could be due to ongoing repair and, therefore, associated with a good prognosis. However, the same high levels could also be due to massive injury triggering a full-blown response. In this case, the outcome may not be so good.

Collagen levels illustrate this two-sided interpretation of biomarkers. As mentioned before, collagen deposition is an early event during ALI. Increased levels of procollagen in pulmonary edema fluid may have a prognostic significance in patients with ALI. For instance, Chesnutt et al. [26] reported that a procollagen concentration above 1.75 U/ml had a positive predictive value for death of 0.75. However, a recent article by Quesnel et al. [27] showed that patients with ALI/acute respiratory distress syndrome (ARDS) with fibroblasts in their alveolar fluid had increased levels of type I procollagen, a decreased pro-inflammatory response (lower neutrophil count, decreased IL-8 levels), and improved prognosis, suggesting a switch from inflammation and tissue destruction to alveolar repair.

Research on the prognostic value of MMP-9 has yielded similar conflicting results. Abundance of this protease in bronchoalveolar lavage (BAL) fluid has been related to a worse outcome. However, MMP-9 has shown a protective role in experimental models of lung injury

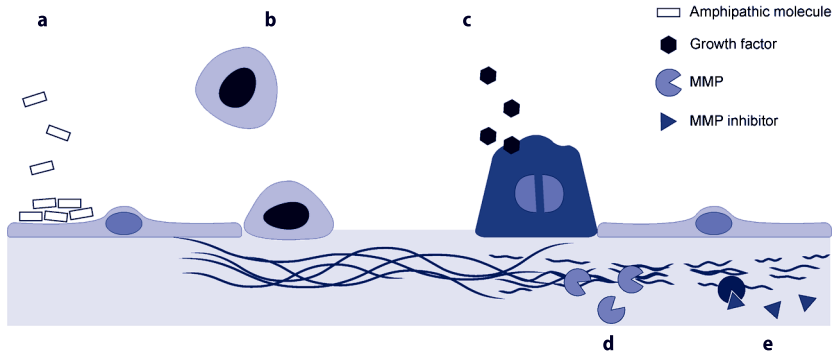

Figure 3. Therapeutic approaches to promote lung repair. (a) Direct repair of the plasma membrane could be achieved using amphipathic compounds that seal injured membranes. **(b)** Exogenous stem cells to repair the denuded areas. **(c)** Administration of growth factors to stimulate the proliferation of endogenous stem cells. **(d)** Stimulation or **(e)** selective blockade of different matrix metalloproteinases (MMPs) to promote collagen processing or avoid the adverse effects of these enzymes.

[19,28], and a clinical study demonstrated that this enzyme could have therapeutic value (see below). Finally, the prognostic value of growth factors in ALI was addressed years ago by Verghese et al. [29]. Lower levels of HGF and KGF were found in survivors. Although these mediators promote cell proliferation, differentiation and, ultimately, alveolar repair, their presence reflects a worse outcome. But, as the authors of the article discussed, the increased levels in non-survivors may be a marker of more severe injury.

Collectively, published results suggest that measurement of a single biomarker in patients can be misleading, as it can reflect both the severity of the injury and the subsequent healing process. An accurate prediction may require complex reasoning that takes into account the initial conditions but also the host's biological response. Therefore, an approach based on multiple markers could offer an alternative to monitor the course of this disease in patients.

Therapeutic strategies aimed at lung repair

Since identification of the pathways involved in lung injury, most literature has been focused on the use of therapies aimed at reducing ALI by truncating the inflammatory response. Unfortunately, none of these strategies has been successfully applied in the clinical practice. Recently, a significant number of studies have centered their efforts on enhancing the repair process using different approaches, ranging from the use of biocompatible materials or cells to the therapeutic use of mediators aimed at promoting cell proliferation, migration and differentiation. Figure 3 summarizes the different therapeutic targets aimed at favoring lung repair.

In many cases, these studies are still at the *in vitro* stages, such as the use of vimentin to improve wound repair [30], or just suggest a possible beneficial role (e.g., connexins [31], adrenomedullin [32] or a possible modulation of the transcription factors, FoxM1 and Runx3 [33,34]) and need further research to prove their viability *in vivo.* Improvement of plasma membrane repair is a possible direct treatment. A recent study in an *ex vivo* model using an amphiphilic macromolecule (Poloxamer 188) with sealing properties showed signs of membrane repair in alveolar resident cells and an improvement in conventional measures of lung injury [35].

Enhancement of the epithelial repopulation is a promising therapeutic target that could be achieved in different ways. In recent years, therapy using stem cells is gaining considerable interest. It has been demonstrated that these cells are active players in lung repair [36]. In spite of doubts about their safety and the best administration route to improve their engraftment, use of stem cells in animal models has been demonstrated to attenuate damage and fibrosis in lungs challenged with endotoxin [37]. In a recent study, Curley et al. [38] submitted a group of rats to VILI followed by an intravenous injection of mesenchymal stem cells; these animals showed less lung injury and increased levels of the anti-inflammatory and anti-fibrotic cytokine, IL-10, than did rats who did not receive the stem cells. The specific mechanisms by which stem cells perform their functions in tissue repair are still under study, but the release of several growth factors and the suppression of pro-inflammatory cytokines seem to be involved.

An alternative approach is the therapeutic use of exogenous growth factors to induce the proliferation of endogenous stem cells. Among these factors, EGF, KGF and HGF have been the most studied. All of them are mitogens in type II pneumocytes, and act synergistically to mediate their maturation and increase surfactant synthesis [8]. EGF had beneficial effects in an animal model of ALI [39], and inhibition of EGF receptor had a

detrimental effect during airway epithelium repair [40]. KGF has been linked to upregulation of anti-inflammatory cytokines and modulation of epithelial cell migration [41]. In the same way, HGF attenuates inflammation and showed antifibrotic effects in a murine model of bleomycin-induced fibrosis [42]. Vascular endothelial growth factor (VEGF) could also have a therapeutic effect by its ability to repair damaged endothelium, therefore helping in clearance of lung edema, but animal models have shown disappointing results [43].

Finally, manipulation of tissue remodeling could improve the outcome of ALI patients by favoring re-epithelization or avoiding fibrosis. The use of steroids in ALI has yielded conflicting results, depending on the time of application. These discrepancies can be explained if one takes into account the beneficial effects of inflammation during the repair phase discussed earlier. However, no study has specifically addressed the effects of steroids during lung repair.

MMPs are alternative targets to promote repair. Non-selective MMP inhibitors are available, but the lack of specificity could limit their benefits and none of them has been tested in ALI. Selective blockade or stimulation (depending on the role of the MMP and timing) could be a more promising approach. One of the first examples that has arrived in human trials is the use of beta-2 adrenergic receptor agonists. Intravenous administration of salbutamol decreased the duration and severity of lung injury by reducing lung edema in patients with ARDS [44]. This finding was associated with an upregulation of MMP-9 [18] and, therefore, with better alveolar epithelial repair [45]. Nevertheless, the route of administration could be relevant, as a recent trial has concluded that patients with ALI treated with inhaled salbutamol show no significant improvement in clinical outcomes [46]. On the other hand, blockade of MMP-8 has shown beneficial effects in experimental models of lung injury [22], including decreased lung fibrosis after bleomycin administration [23]. However, no clinical study aimed at modulating this protease has yet been proposed.

Conclusion

The lungs have a substantial potential for recovery after ALI. Of note, the mechanisms that can cause tissue disruption in the early phase also contribute to its repair later on, inflammation and matrix remodeling being paradigmatic examples. Therefore, therapies that disrupt these pathways, such as MMP inhibition, may have a prophylactic value, but their application at a later phase could be detrimental. Knowledge of the mediators involved in tissue repair could lead to new therapeutic strategies being applied after the initial insult has been controlled. Growth factors, exogenous stem cells (including type II pneumocytes) or drugs that promote matrix remodeling could be new alternatives to improve the prognosis of patients with ALI.

Abbreviations

ALI, acute lung injury; AP, activator protein; ARDS, acute respiratory distress syndrome; BAL, bronchoalveolar lavage; DAMPs, damage-associated molecular patterns; EGF, epidermic growth factor; G-CSF, granulocyte-colony stimulating factor; HGF, hepatic growth factor; IL-1R, interleukin-1 receptor; KGF, keratinocyte growth factor; LIX, lipopolysaccharide-induced CXC chemokine; LPS, lipopolysaccharide; MIP, macrophage inflammatory protein; MMPs, matrix metalloproteinases; NF-κB, nuclear factor-kappa B; RAGE, receptor of advanced glycation end-products; TGF, transforming growth factor; TLR, Toll-like receptors; TNF, tumor necrosis factor; VEGF, vascular endothelial growth factor; VILI, ventilator induced lung injury; WOB, work of breathing.

Competing interests

The authors declare that there are no competing interests.

Acknowledgement

Supported by Instituto de Salud Carlos III (Fondo de Investigación Sanitaria PI 10/00606) and Universidad de Oviedo (UNOV-09-BECDOC), Spain.

Published: 20 March 2012

References

1. Ventrice EA, Marti-Sistac O, Gonzalvo R, Villagra A, Lopez-Aguilar J, Blanch L: **[Molecular and biophysical mechanisms and modulation of ventilator-induced lung injury].** *Med Intensiva* 2007, **31:**73–82.
2. Bianchi ME: **DAMPs, PAMPs and alarmins: all we need to know about danger.** *J Leukoc Biol* 2007, **81:**1–5.
3. de Carvalho ME, Dolhnikoff M, Meireles SI, Reis LF, Martins MA, Deheinzelin D. **Effects of overinflation on procollagen type III expression in experimental acute lung injury.** *Crit Care* 2007, **11:**R23.
4. Armstrong L, Thickett DR, Mansell JP, *et al.*: **Changes in collagen turnover in early acute respiratory distress syndrome.** *Am J Respir Crit Care Med* 1999, **160:**1910–1915.
5. Berthiaume Y, Matthay MA: **Alveolar edema fluid clearance and acute lung injury.** *Respir Physiol Neurobiol* 2007, **159:**350–359.
6. Bhatia M, Moochhala S: **Role of inflammatory mediators in the pathophysiology of acute respiratory distress syndrome.** *J Pathol* 2004, **202:**145–156.
7. Kubo H: **Molecular basis of lung tissue regeneration.** *Gen Thorac Cardiovasc Surg* 2011, **59:**231–244.
8. Lindsay CD: **Novel therapeutic strategies for acute lung injury induced by lung damaging agents: the potential role of growth factors as treatment options.** *Hum Exp Toxicol* 2011, **30:**701–724.
9. Davey A, McAuley DF, O'Kane CM: **Matrix metalloproteinases in acute lung injury: mediators of injury and drivers of repair.** *Eur Respir J* 2011, **38:**959–970.
10. Nin N, Lorente JA, de Paula M, *et al.*: **Rats surviving injurious mechanical ventilation show reversible pulmonary, vascular and inflammatory changes.** *Intensive Care Med* 2008, **34:**948–956.
11. Gonzalez-Lopez A, Astudillo A, Garcia-Prieto E, *et al.*: **Inflammation and matrix remodeling during repair of ventilator-induced lung injury.** *Am J Physiol Lung Cell Mol Physiol* 2011, **301:**L500–L509.
12. Abraham E: **Neutrophils and acute lung injury.** *Crit Care Med* 2003, **31:**S195–S199.
13. Korpos E, Wu C, Sorokin L: **Multiple roles of the extracellular matrix in inflammation.** *Curr Pharm Des* 2009, **15:**1349–1357.
14. Lin M, Jackson P, Tester AM, *et al.*: **Matrix metalloproteinase-8 facilitates neutrophil migration through the corneal stromal matrix by collagen degradation and production of the chemotactic peptide Pro-Gly-Pro.** *Am J Pathol* 2008, **173:**144–153.
15. Van Lint P, Libert C: **Chemokine and cytokine processing by matrix metalloproteinases and its effect on leukocyte migration and inflammation.** *J Leukoc Biol* 2007, **82:**1375–1381.
16. Harty MW, Muratore CS, Papa EF, *et al.*: **Neutrophil depletion blocks early collagen degradation in repairing cholestatic rat livers.** *Am J Pathol* 2010, **176:**1271–1281.
17. Parks WC: **Matrix metalloproteinases in lung repair.** *Eur Respir J* 2003,

22(Suppl 44):36s-38s.
18. O'Kane CM, McKeown SW, Perkins GD, *et al.*: **Salbutamol up-regulates matrix metalloproteinase-9 in the alveolar space in the acute respiratory distress syndrome.** *Crit Care Med* 2009, **37:**2242–2249.
19. Albaiceta GM, Gutierrez-Fernandez A, Parra D, *et al.*: **Lack of matrix metalloproteinase-9 worsens ventilator-induced lung injury.** *Am J Physiol Lung Cell Mol Physiol* 2008, **294:**L535–L543.
20. Nerusu KC, Warner RL, Bhagavathula N, McClintock SD, Johnson KJ, Varani J: **Matrix metalloproteinase-3 (stromelysin-1) in acute inflammatory tissue injury.** *Exp Mol Pathol* 2007, **83:**169–176.
21. Yamashita CM, Dolgonos L, Zemans RL, *et al.*: **Matrix metalloproteinase 3 is a mediator of pulmonary fibrosis.** *Am J Pathol* 2011, **179:**1733–1745.
22. Albaiceta GM, Gutierrez-Fernandez A, Garcia-Prieto E, *et al.*: **Absence or inhibition of matrix metalloproteinase-8 decreases ventilator-induced lung injury.** *Am J Respir Cell Mol Biol* 2010, **43:**555–563.
23. Garcia-Prieto E, Gonzalez-Lopez A, Cabrera S, *et al.*: **Resistance to bleomycin-induced lung fibrosis in MMP-8 deficient mice is mediated by interleukin-10.** *PLoS One* 2010, **5:**e13242.
24. Quintero PA, Knolle MD, Cala LF, Zhuang Y, Owen CA: **Matrix metalloproteinase-8 inactivates macrophage inflammatory protein-1 alpha to reduce acute lung inflammation and injury in mice.** *J Immunol* 2010, **184:**1575–1588.
25. Gueders MM, Balbin M, Rocks N, *et al.*: **Matrix metalloproteinase-8 deficiency promotes granulocytic allergen-induced airway inflammation.** *J Immunol* 2005, **175:**2589–2597.
26. Chesnutt AN, Matthay MA, Tibayan FA, Clark JG: **Early detection of type III procollagen peptide in acute lung injury. Pathogenetic and prognostic significance.** *Am J Respir Crit Care Med* 1997, **156:**840–845.
27. Quesnel C, Nardelli L, Piednoir P, *et al.*: **Alveolar fibroblasts in acute lung injury: biological behaviour and clinical relevance.** *Eur Respir J* 2010, **35:**1312–1321.
28. Yoon HK, Cho HY, Kleeberger SR: **Protective role of matrix metalloproteinase-9 in ozone-induced airway inflammation.** *Environ Health Perspect* 2007, **115:**1557–1563.
29. Verghese GM, McCormick-Shannon K, Mason RJ, Matthay MA: **Hepatocyte growth factor and keratinocyte growth factor in the pulmonary edema fluid of patients with acute lung injury. Biologic and clinical significance.** *Am J Respir Crit Care Med* 1998, **158:**386–394.
30. Rogel MR, Soni PN, Troken JR, Sitikov A, Trejo HE, Ridge KM: **Vimentin is sufficient and required for wound repair and remodeling in alveolar epithelial cells.** *FASEB J*, in press.
31. Losa D, Chanson M, Crespin S: **Connexins as therapeutic targets in lung disease.** *Expert Opin Ther Targets* 2011, **15:**989–1002.
32. Vadivel A, Abozaid S, van Haaften T, *et al.*: **Adrenomedullin promotes lung angiogenesis, alveolar development, and repair.** *Am J Respir Cell Mol Biol* 2010, **43:**152–160.
33. Liu Y, Sadikot RT, Adami GR, *et al.*: **FoxM1 mediates the progenitor function of type II epithelial cells in repairing alveolar injury induced by Pseudomonas aeruginosa.** *J Exp Med* 2011, **208:**1473–1484.
34. Lee JM, Kwon HJ, Bae SC, Jung HS: **Lung tissue regeneration after induced injury in Runx3 KO mice.** *Cell Tissue Res* 2010, **341:**465–470.
35. Plataki M, Lee YD, Rasmussen DL, Hubmayr RD: **Poloxamer 188 facilitates the repair of alveolus resident cells in ventilator injured lungs.** *Am J Respir Crit Care Med* 2011, **184:**939–947.
36. Giangreco A, Arwert EN, Rosewell IR, Snyder J, Watt FM, Stripp BR: **Stem cells are dispensable for lung homeostasis but restore airways after injury.** *Proc Natl Acad Sci USA* 2009, 106:9286–9291.
37. Yang KY, Shih HC, How CK, *et al.*: **IV delivery of induced pluripotent stem cells attenuates endotoxin-induced acute lung injury in mice.** *Chest* 2011, **140:**1243–1253.
38. Curley GF, Contreras M, Higgins BD, O'Toole DP, Laffey JG: **The role of mesenchymal stem cells during repair from ventilator induced lung injury.** *J Respir Crit Care Med*, in press.
39. Plopper CG, St George JA, Read LC, *et al.*: **Acceleration of alveolar type II cell differentiation in fetal rhesus monkey lung by administration of EGF.** *Am J Physiol* 1992, **262:**L313–L321.
40. Harada C, Kawaguchi T, Ogata-Suetsugu S, *et al.*: **EGFR tyrosine kinase inhibition worsens acute lung injury in mice with repairing airway epithelium.** *Am J Respir Crit Care Med* 2011, **183:**743–751.
41. Panoskaltsis-Mortari A, Ingbar DH, Jung P, *et al.*: **KGF pretreatment decreases B7 and granzyme B expression and hastens repair in lungs of mice after allogeneic BMT.** *Am J Physiol Lung Cell Mol Physiol* 2000, **278:**L988–L999.
42. Dohi M, Hasegawa T, Yamamoto K, Marshall BC: **Hepatocyte growth factor attenuates collagen accumulation in a murine model of pulmonary fibrosis.** *Am J Respir Crit Care Med* 2000, **162:**2302–2307.
43. Medford AR, Millar AB: **Vascular endothelial growth factor (VEGF) in acute lung injury (ALI) and acute respiratory distress syndrome (ARDS): paradox or paradigm?** *Thorax* 2006, **61:**621–626.
44. Perkins GD, McAuley DF, Thickett DR, Gao F: **The beta-agonist lung injury trial (BALTI): a randomized placebo-controlled clinical trial.** *Am J Respir Crit Care Med* 2006, **173:**281–287.
45. Perkins GD, Gao F, Thickett DR: **In vivo and in vitro effects of salbutamol on alveolar epithelial repair in acute lung injury.** *Thorax* 2008, **63:**215–220.
46. Matthay MA, Brower RG, Carson S, *et al.*: **Randomized, placebo-controlled clinical trial of an aerosolized beta-2 agonist for treatment of acute lung injury.** *Am J Respir Crit Care Med* 2011, **184:**561–568.

doi:10.1186/cc11224
Cite this article as: González-López A, Albaiceta GM: **Repair after acute lung injury: molecular mechanisms and therapeutic opportunities.** *Critical Care* 2012, **16:**209.

V. Inflamación y remodelado de matriz durante la reparación de la lesión pulmonar inducida por ventilación mecánica.

Aunque en los últimos años han ido apareciendo estudios centrados en la reparación del tejido pulmonar, el caso concreto del daño pulmonar asociado a la ventilación mecánica ha permanecido prácticamente sin explorar. Mediante un modelo de lesión con altas presiones seguido de una ventilación protectora nos propusimos estudiar los mecanismos subyacentes al proceso de reparación. Este modelo nos mostró que la lesión pulmonar es parcialmente reversible en un corto periodo de tiempo, dando lugar a un menor daño histológico, una menor permeabilidad alveolar y la normalización de las concentraciones de citoquinas proinflamatorias. Los animales supervivientes ofrecían signos claros de proliferación celular, mayor infiltrado inflamatorio y niveles elevados de MIP-2, MMP-2 y MMP-9 sugiriendo que una adecuada respuesta inflamatoria y remodelado de la matriz extracelular son procesos clave para la correcta recuperación. Los ensayos *in vitro* de cierre de heridas apuntaron a MMP-2 como posible participe en el proceso de reepitelización tanto en las líneas murinas como en las humanas tratadas con BALF de pacientes con SRDA.

Artículo 5: González-López A, Astudillo A, García-Prieto E, Fernández-García MS, López-Vázquez A, Batalla-Solís E, Taboada F, Fueyo A, Albaiceta GM. "Inflammation and matrix remodeling during repair of ventilator-induced lung injury".

Am J Physiol Lung Cell Mol Physiol. 2011 Oct;301(4):L500-9. I.F: 3.66

Aportación personal al trabajo.

En este trabajo corrió a mi cargo la mayor parte de la labor experimental tanto en el modelo animal como en los ensayos de cierre de heridas *in vitro*. También contribuí a los estudios histológicos, participé en el posterior análisis estadístico y la elaboración del manuscrito.

Am J Physiol Lung Cell Mol Physiol 301: L500–L509, 2011.
First published July 8, 2011; doi:10.1152/ajplung.00010.2011.

Inflammation and matrix remodeling during repair of ventilator-induced lung injury

Adrián González-López,[1] Aurora Astudillo,[2,5] Emilio García-Prieto,[4] María Soledad Fernández-García,[2,5] Antonio López-Vázquez,[6] Estefanía Batalla-Solís,[1] Francisco Taboada,[3,4] Antonio Fueyo,[1] and Guillermo M. Albaiceta[1,4,7]

Departments of [1]Biología Funcional, [2]Cirugía y Especialidades Médico-quirúrgicas, and [3]Medicina, Universidad de Oviedo, Instituto Universitario Oncologico del Principado de Asturias, Departments of [4]Medicina Intensiva, [5]Anatomía Patológica, and [6]Immunología, Hospital Universitario Central de Asturias, and [7]CIBER-Enfermedades Respiratorias, Oviedo, Spain

Submitted 13 January 2011; accepted in final form 30 June 2011

González-López A, Astudillo A, García-Prieto E, Fernández-García MS, López-Vázquez A, Batalla-Solís E, Taboada F, Fueyo A, Albaiceta GM. Inflammation and matrix remodeling during repair of ventilator-induced lung injury. *Am J Physiol Lung Cell Mol Physiol* 301: L500–L509, 2011. First published July 8, 2011; doi:10.1152/ajplung.00010.2011.—High-pressure ventilation triggers different inflammatory and matrix remodeling responses within the lung. Although some of them may cause injury, the involvement of these mediators in repair is largely unknown. To identify mechanisms of repair after ventilator-induced lung injury (VILI), mice were randomly assigned to baseline conditions (no ventilation), injury [90 min of high-pressure ventilation without positive end-expiratory pressure (PEEP)], repair (injury followed by 4 h of low-pressure ventilation with PEEP), and ventilated controls (low-pressure ventilation with PEEP for 90 and 330 min). Histological injury and lung permeability increased during injury, but were partially reverted in the repair group. This was accompanied by a proinflammatory response, together with increases in TNF-α and IFN-γ, which returned to baseline during repair, and a decrease in IL-10. However, macrophage inflammatory protein-2 (MIP-2) and matrix metalloproteinases (MMP)-2 and -9 increased after injury and persisted in being elevated during repair. Mortality in the repair phase was 50%. Survivors showed increased cell proliferation, lower levels of collagen, and higher levels of MIP-2 and MMP-2. Pan-MMP or specific MMP-2 inhibition (but not MIP-2, TNF-α, or IL-4 inhibition) delayed epithelial repair in an in vitro wound model using murine or human alveolar cells cultured in the presence of bronchoalveolar lavage fluid from mice during the repair phase or from patients with acute respiratory distress syndrome, respectively. Similarly, MMP inhibition with doxycycline impaired lung repair after VILI in vivo. In conclusion, VILI can be reverted by normalizing ventilation pressures. An adequate inflammatory response and extracellular matrix remodeling are essential for recovery. MMP-2 could play a key role in epithelial repair after VILI and acute respiratory distress syndrome.

mechanical ventilation; lung repair; matrix metalloproteinases; inflammatory response; wound healing

THE OUTCOME OF PATIENTS WITH the acute respiratory distress syndrome (ARDS) is related to the reduction of ventilator-associated lung injury. Research on its experimental counterpart, called ventilator-induced lung injury (VILI), has identified a variety of mechanisms of lung damage. The initial insult to the lungs is physical in nature (12); thus the main therapeutic strategy is the optimization of mechanical ventilation. This approach has been shown to be effective in reducing mortality (5). However, no single ventilatory settings exist that can minimize all of the pathogenetic mechanisms of injury [i.e., increasing positive end-expiratory pressure (PEEP) can decrease cyclic changes in aeration, but increases the risk of alveolar overstretching (4)]. The mechanical stimulus induces a secondary biochemical response in which inflammation (37) and extracellular matrix remodeling (32) are key processes. Although different pharmacological approaches have demonstrated a reduction in VILI (2, 20, 29, 31), they have not been translated into the clinical practice and also pose a risk of adverse events. For example, modulation of the immune response can lead to an increased incidence of infection.

The relevance of lung repair in this scenario is largely unknown (11). Pioneering work by Nin et al. (28) has demonstrated that VILI can be reverted after reestablishing spontaneous breathing. Furthermore, some of the mediators released during lung injury, such as IL-1 (33) and matrix metalloproteinase (MMP)-9 (30), promote epithelial repair and may have prognostic and therapeutic implications in ARDS patients. Interference with these molecules can further increase lung damage (3). Conversely, therapies aimed to promote lung repair may be an alternative in patients submitted to mechanical ventilation.

The objective of this study is to describe a model of repair after VILI, focusing on inflammatory mediators and extracellular matrix remodeling. Additionally, assessment of the effects of these mediators on lung epithelial wound closure could help to identify those involved in lung repair.

MATERIALS AND METHODS

Animals. Eight- to twelve-week-old CD1 mice were used in all experiments. Mice were kept under specific pathogen-free conditions, with free access to food and water, and exposed to 12:12-h light-dark cycles. The protocol was approved by the Committee on Animal Experimentation of the Universidad de Oviedo, Spain. The use of human samples was authorized by the Regional Ethics Committee, and informed consent was obtained from patients' next of kin.

Experimental protocol. Mice were anesthetized with a mixture of ketamin and xylazin administered intraperitoneally and placed on a heating pad. A tracheostomy was performed; a 20G catheter was inserted in the trachea and tightened to avoid air leaks. The animals were then ventilated (Evita 2 Dura with Neoflow, Drager, Germany). A 0.2-ml bolus of Ringer lactate was injected intraperitoneally at the onset of ventilation and repeated every 2 h. Anesthesia was maintained by administration of ketamin and xylazin, as needed.

Animals were ventilated in pressure-controlled mode using one of two ventilatory settings: high-pressure ventilation, peak inspiratory

Address for reprint requests and other correspondence: G. M. Albaiceta, Departamento de Biología Funcional, Area de Fisiología, Universidad de Oviedo, Facultad de Medicina, Julian Clavería, s/n 33006 Oviedo, Spain (e-mail: Guillermo.muniz@sespa.princast.es).

pressure (PIP) 25 cmH_2O, PEEP 0 cmH_2O, respiratory rate 50 breaths/min; and low-pressure ventilation, PIP 15 cmH_2O, PEEP 2 cmH_2O, respiratory rate 100 breaths/min. Fraction of inspired O_2 was 50%, and inspiratory-expiratory ratio was 1:1. The combination of these two ventilatory strategies with different ventilatory times led to the creation of five experimental groups (Table 1). Specifically, the group ventilated with high pressures for 90 min, followed by 240 min of low-pressure ventilation, was aimed to study repair after VILI. The mortality in this group was 50%, and all of the animals, irrespective of the time of ventilation, were included in the subsequent cellular, biochemical, and histological analysis. Animals were randomly assigned to each experimental group. The main objective was to obtain at least 16 mice surviving the repair phase, and mice were added in pairs to the "repair" and another group (randomly chosen) in parallel until reaching that objective, resulting in different sample sizes (Table 1). Additional mice ($n = 12$) were ventilated using high pressures until death. This group was used only for the survival analysis.

After ventilation or immediately after death, a laparotomy was performed, and mice were killed by exsanguination, the chest was opened, the heart-lung block was removed, and the right bronchus was ligated. The right upper lobe was weighed, dried in an oven (50°C for 72 h), and weighted again to calculate the wet-to-dry weight ratio. The remaining right lung was homogenized in a lysis buffer containing 20 mM Tris, 300 mM sucrose, 1% Triton X-100, and a protease inhibitor cocktail without EDTA (Complete, Roche, Germany), centrifuged (13,000 rpm for 15 min), and stored at −80°C for further studies. The protein content of the homogenate was quantified (BCA protein assay, Pierce, Rockford, IL).

Histological study. The left lung was fixed intratracheally with 300 μl of formaldehyde, tied, and immersed in the same fixative for at least 24 h. After fixation, the left lung was embedded in paraffin and processed for a standard hematoxylin-eosin staining. One pathologist blinded to the experimental conditions scored three slides of the left lung according to the following scale: 0, normal lung; 1, septal congestion; 2, epithelial thickening; 3, septal inflammatory infiltrates; 4, alveolar hemorrhage and/or hyaline membranes; 5, massive disruption of lung architecture. To study cell proliferation during the repair phase, the number of nuclei in the alveolar walls was counted in three randomly chosen high-power fields (×400). Additional lungs from animals during the injury and repair phases were processed for electron microscopy studies. Lung tissues were fixed in 3% glutaraldehyde and osmium tetroxyde, and semithin sections were stained with toluidine blue. After selection of regions of interest, ultrathin sections were collected, stained with uranyl acetate and lead citrate, and observed in a JEOL 1011 transmission electron microscope.

Immunohistochemistry studies were done in paraffin-embedded sections using antibodies against myeloperoxidase (MPO, Thermo Scientific), MMP-2 (Abcam), MMP-9 (Santa Cruz Biotechnology SC-6840), and Ki-67 (Abcam). The number of MPO-positive cells was counted in three randomly chosen ×200 fields and averaged. The percentage of Ki-67 positive nuclei was computed as an index of cell proliferation.

Bronchoalveolar lavage. In additional mice, submitted to the same ventilatory strategies described above, a lavage was performed via the tracheal catheter using three aliquots (0.7 ml) of saline. Two hundred microliters of the recovered bronchoalveolar lavage fluid (BALF) were used to measure cell count and population in a hemocytometer; the remaining volume was centrifugated (2,000 rpm for 15 min) and stored at −80°C for further analysis. The protein content of BALF fluids was quantified (BCA protein assay, Pierce). No other samples were harvested from these animals.

Cytokine/chemokine quantification. IFN-γ, IL-10, IL-4, MIP-2, and LPS-induced CXC chemokine (LIX) were measured in lung homogenates using a multiplexed assay (Milliplex kit, Millipore), according to the manufacturer's instructions and a Luminex 100 system. TNF-α was quantified using a commercial ELISA kit (mouse TNF-α ELISA kit, eBioscience).

Collagen measurement. Soluble lung collagen was measured in lung homogenates using the Sircol assay (Biocolor), following the manufacturer's instructions.

Quantification of MMP-2 and MMP-9. MMP-2 and MMP-9 activity was measured in lung homogenates and BALF by gelatin zymography. The volume of lung homogenate corresponding to 15 μg of protein or 6 μl of BALF was loaded in an 8% SDS-polyacrylamide gel containing 0.2% gelatine and electrophoresed. Afterwards, gels were washed twice in 2.5% Triton X-100 for 15 min, then washed again with deionized water until the complete removal of Triton X-100, and incubated overnight at 37°C in a buffer containing 20 mM Tris·HCl, 5 mM $CaCl_2$, pH = 7.4. Then gels were stained using Commassie blue, destained with a mixture of acetic acid and methanol, and scanned. Intensity of the gelatinolytic bands was quantified (in arbitrary density units) using ImageJ software (National Institutes of Health). All gels contained at least one sample of each experimental group to overcome differences among gels.

Wound healing in cultured alveolar cells. The effect of different mediators on epithelial repair was studied using cell cultures. Murine alveolar epithelial cells (MLE-12, ATCC) were cultured in 24-well plates in DMEM/Ham's F-12 supplemented with 2% fetal bovine serum and glutamine. After confluence, cells were wounded with a pipette tip and washed with PBS. Cells were then cultured using DMEM/Ham's F-12 medium supplemented with 10% BALF from ventilated mice after injury or repair (filtered using an Acrodisc 0.2-μm filter, Pall Life Sciences). Cells cultured in medium without BALF were used as controls. To assess the effect of mediators on wound healing, blocking antibodies against TNF-α (eBioscience), IL-4 (eBioscience), MIP-2 (AbD Serotec), and MMP-2 (Abcam) were added to the medium in parallel experiments. Additionally, cells were cultured in the presence of doxycycline (25 μM) to test the effects of nonspecific pan-MMP inhibition (16). Cultures were photographed using an Olympus BH-2 microscope and an Olympus C-5060 camera. Images were obtained immediately after wounding and 3, 6, 9, and 12 h later. The area not covered by cells was measured using the ImageJ software, and the percentage of the initial wound area covered by cells over time was computed.

To study the contribution of MMP-2 to wound closure in patients with ARDS, a similar assay was performed using human alveolar cells (A549). First, BALF from patients meeting ARDS criteria and who had had less than 5 days of mechanical ventilation, who also underwent a diagnostic bronchoscopy, was filtered through a sterile gauze and centrifuged at 3,000 rpm for 15 min; the supernatant was stored at −80°C. Four samples were finally collected. Informed consent for the use of these BALF samples was obtained from each patient's next of kin. A549 cells were cultured in DMEM supplemented with 10% FBS until confluence, wounded as previously described, washed and cultured using DMEM with 10% BALF from the patients meeting the described criteria, and filtered (Acrodisc 0.2-μm filter, Pall Life Sciences). Again, cells grown in medium without BALF were used as controls. In duplicate cultures, an anti-MMP-2 blocking antibody was added to the medium. As doubling time is longer in A549 cells under these conditions, cultures were photographed every 24 h for 4 days. Wound area was measured as previously described.

Table 1. *Composition of the experimental groups*

Group	*N* (Tissue/BALF)	Time of Ventilation, min	
		High pressure	Low pressure
Baseline	10/11	0	0
Injury	12/15	90	0
Repair	17/15	90	240
Control 90 min	11/9	0	90
Control 330 min	7/10	0	330

BALF, bronchoalveolar lavage fluid.

Effects of MMP inhibition on lung repair in vivo. The effects of MMP inhibition in vivo were studied using additional mice. Due to the lack of specific MMP-2 inhibitor available for in vivo use, doxycycline was administered as a pan-MMP blocker. The animals were submitted to 90 min of injurious ventilation. Then a dose of 50 mg/kg of doxycycline or vehicle was administered intraperitoneally, and the ventilatory settings were switched to low pressures to allow the lungs to repair. Vehicle-treated mice were studied after the same ventilatory time than doxycycline-treated animals. The lungs were harvested, and histological sections scored as previously described.

Statistical analysis. Data are expressed as means ± SE. Results were compared using a one-way ANOVA. Post hoc tests were done when appropriate using the Dunnett test to compare against baseline or injury groups. Survival was studied using Kaplan-Meier curves and the log-rank test. Differences between the animals that did or did not survive through the repair phase, or between doxycycline- and vehicle-treated mice, were compared using a *T*-test. Results from wound healing assays were compared using a repeated-measurements ANOVA. A P value <0.05 was considered significant. All the calculations were done using SPSS 17.0 software (SPSS).

RESULTS

One hundred twenty-nine animals were included in the study. The composition of each experimental group is presented in Table 1.

Reversibility of lung injury. VILI results in structural damage of lung parenchyma and increased lung edema and permeability. After 90 min of high-pressure ventilation, mice showed a 6-fold increase in the injury score (Fig. 1*A*), a 62% increase in the wet-to-dry weight ratio (Fig. 1*B*), and a 10-fold increase in BALF protein concentration (Fig. 1*C*) compared with baseline ($P < 0.001$ in all post hoc tests). All of these changes were partially reverted during repair, with significant decreases in the histological score, the wet-to-dry weight ratio, and the BALF protein concentration. Representative optical and electronic microscopy images are presented in Fig. 1, *D* and *E*. Increases in epithelial cell size, septal thickness, and deposition of interstitial fibers were observed during injury and decreased during the repair phase.

In addition, results from mice ventilated with low pressures for 330 min showed that prolonged ventilation with lower pressures can also induce a mild lung injury.

Collectively, these results demonstrate that lung injury caused by high-pressure ventilation can be partially reversed after 4 h of ventilation with low pressures and PEEP.

Proinflammatory response to high-pressure ventilation can be rapidly reverted. The inflammatory response to mechanical ventilation was studied by quantification of cells in BALF and immune mediators in lung tissue. There were no significant differences in leukocyte counts in BALF ($P = 0.2$ in the ANOVA test, Fig. 2*A*). However, a change in cell populations was observed (Fig. 2*B*). The number of macrophages decreased

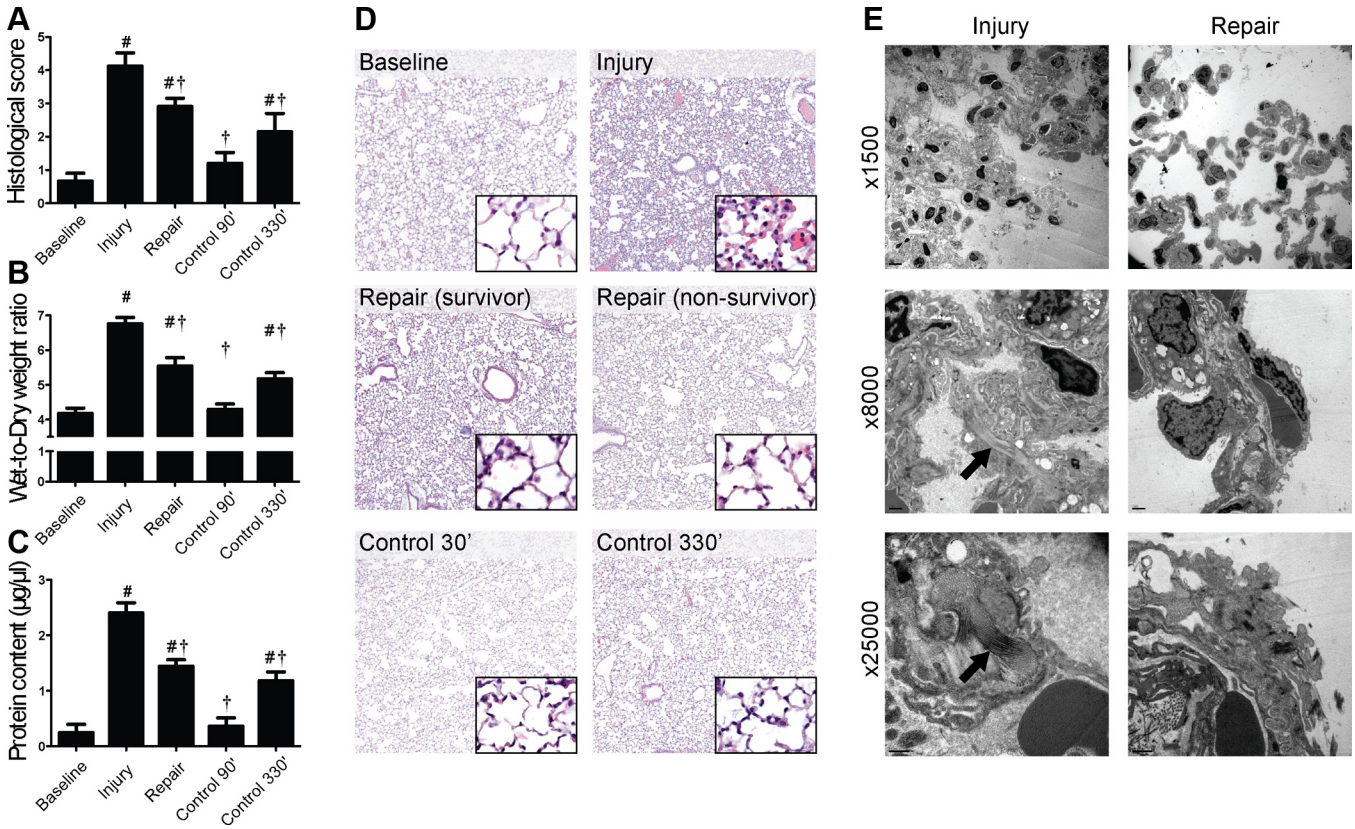

Fig. 1. Lung injury in the different experimental groups. Structural injury (*A*), lung edema (*B*), and permeability [as protein content of the bronchoalveolar lavage fluid (BALF); *C*] were measured. There were significant improvements in tissue damage, edema, and BALF protein content during the repair phase. Values are means ± SE. *D*: representative histological sections at low (×40) and high (×400) magnification. *E*: different ultrastructural details of injury and repair. Note the restoration of the normal alveolar structure (×1,500), the decrease in alveolar wall thickness (×8,000), and the intense deposition of extracellular matrix fibers (arrows at ×8,000 and ×25,000), which is not seen during repair. #$P < 0.05$ in post hoc test compared with baseline. †$P < 0.05$ in post hoc test compared with injury.

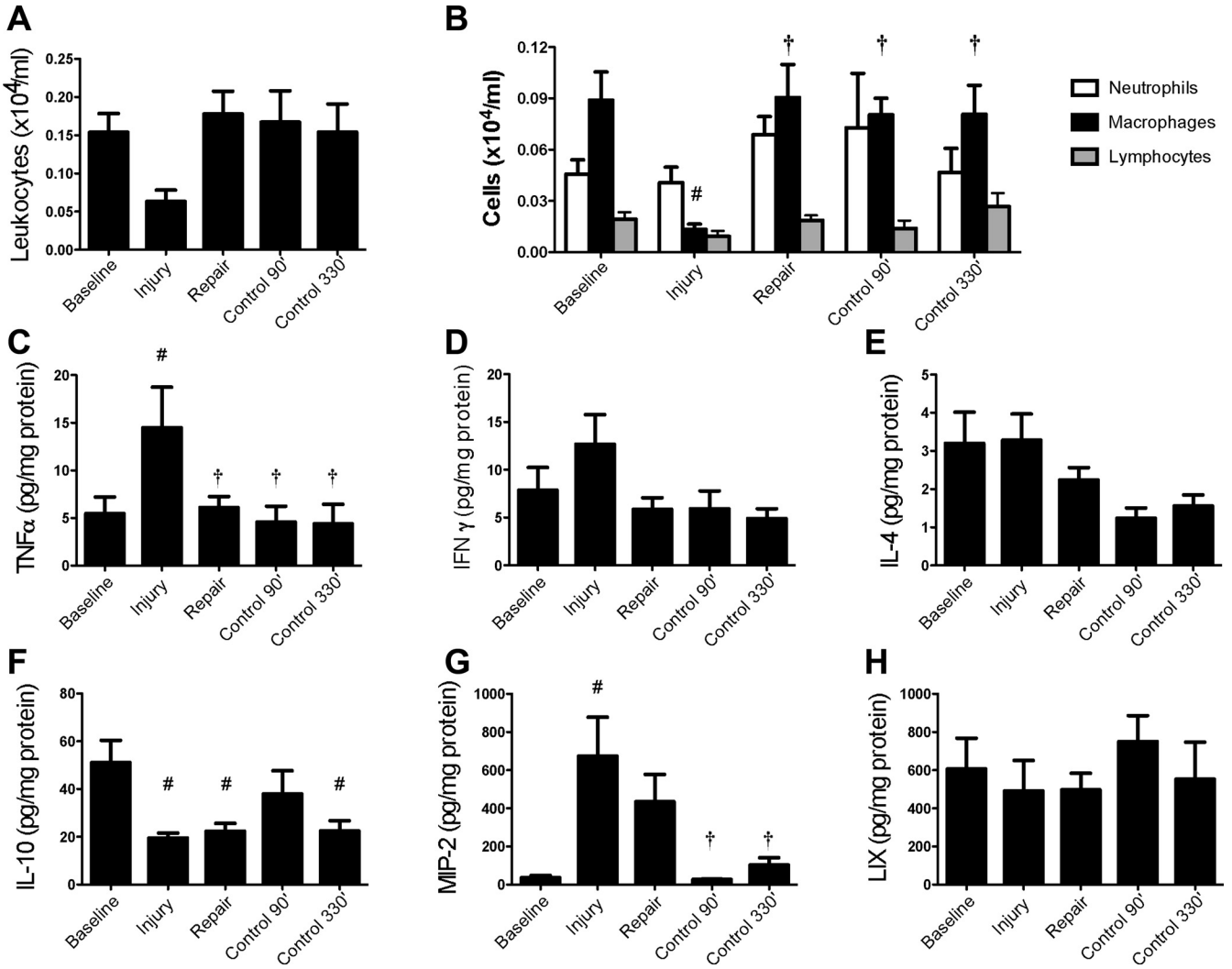

Fig. 2. Inflammatory response to ventilation. There were no significant differences in total cell count (*A*), but cell types differed among the different groups (*B*). Additionally, different mediators were measured in lung tissue homogenates. There were increases in proinflammatory cytokines, such as TNF-α (*C*) and IFN-γ ($P = 0.098$; *D*), and a decrease in the anti-inflammatory cytokine IL-10 (*F*). *G*: there was also a marked increase in the chemokine macrophage inflammatory protein-2 (MIP-2) that persisted throughout the repair phase. No significant differences in IL-4 (*E*) and LPS-induced CXC chemokine (LIX; *H*) were observed. Values are means ± SE. #$P < 0.05$ in post hoc test compared with baseline. †$P < 0.05$ in post hoc test compared with injury.

significantly after 90 min of injurious ventilation ($P < 0.01$ in all post hoc tests) and was similar to baseline values in all of the other groups. There were no significant changes in the absolute count of neutrophils or lymphocytes in BALF. However, immunohistochemical studies (Fig. 4) showed an increase in neutrophils, from 30 ± 2 cells/high power field at baseline to 88 ± 8 cells/high power field after injury and 88 ± 9 cells/high power field during repair, suggesting that these cells were firmly attached to the epithelium and were not recovered in BALF.

To characterize the humoral inflammatory response in the different ventilatory groups, we determined the concentration of Th1 cytokines (TNF-α, IFN-γ), Th2 cytokines (IL-4, IL-10), and chemokines (MIP-2 and LIX) in lung homogenates (Fig. 2, *C–H*). Injurious ventilation significantly increased levels of TNF-α compared with other groups (Fig. 2*C*, $P < 0.05$ in ANOVA and all post hoc tests). Mice submitted to further ventilation with low pressures for 4 h (repair) showed TNF-α levels similar to those of nonventilated controls ($P = 0.998$ in post hoc test). There were no significant differences between mice in baseline conditions (nonventilated) and after low-pressure ventilation. We observed also a trend toward higher levels of IFN-γ in mice ventilated with high pressures (Fig. 2*D*, $P = 0.098$ in ANOVA). Again, values during the repair phase were similar to baseline.

Regarding Th2 cytokines, there were no significant changes in IL-4 (Fig. 2*E*, $P = 0.2$ in ANOVA). However, IL-10 (Fig. 2*F*) decreased in mice submitted to high-pressure ventilation ($P < 0.05$ in ANOVA, $P = 0.001$ in post hoc test compared with baseline). This decrease was also significant in the repair phase ($P = 0.001$) and after prolonged low-pressure ventilation ($P = 0.008$).

The increase in neutrophils suggested that chemokines may play a relevant role in this kind of injury. MIP-2 significantly increased after 90 min of high-pressure ventilation (Fig. 2*G*, $P = 0.004$ in ANOVA, $P < 0.03$ in post hoc tests against baseline and ventilated control groups). Contrary to what we observed with cytokines, the decrease present during repair

was not significant ($P = 0.46$ in post hoc test against injury). There were no differences among groups in LIX levels (Fig. 2*H*).

Collectively, these differences show that high-pressure ventilation induces the release of proinflammatory cytokines and a decrease in anti-inflammatory cytokines; also, chemokine increase is more prolonged.

MMPs-2 and -9 increase during tissue repair. The extracellular matrix plays a key role in lung injury and repair. We evaluated collagen and MMPs-2 and -9 in lung homogenates. There were no differences in collagen content among groups ($P = 0.259$ in ANOVA, data not shown).

There were significant changes in MMP-9 and MMP-2 (Fig. 3, $P < 0.01$ in ANOVA in both cases). MMP-9 increased in lung tissue from all ventilated groups ($P < 0.01$ in post hoc tests when compared against baseline), and in BALF from animals during the injury and repair phase, as well as after prolonged low-pressure ventilation. MMP-2 followed a similar pattern. MMP-2 and -9 were detected by immunohistochemistry in parafin-embedded sections. MMP-2 was expressed mainly in epithelial and interstitial cells, although some intra-alveolar inflammatory cells were also positive. However, MMP-9 expression was restricted to inflammatory cells. Figure 4 shows representative sections (×200) of baseline, injury, and repair groups (survivors and nonsurvivors). The difference in MMP-2 expression between survivors and nonsurvivors was also confirmed in this immunohistochemical study.

The increased levels of MMPs during repair, despite a decrease in lung damage indexes, suggest that these molecules may have a role in tissue repair.

Survival. All of the mice subjected to low-pressure ventilation survived the 330 min of the experiment. In contrast, ventilation with high pressures for >90 min led to 100% mortality. Animals assigned to the repair group had a mortality of 50% (8 animals assigned to tissue sampling and 8 assigned to BALF survived). Survival curves are shown in Fig. 5*A*. The difference between curves was significant, as assessed by the log-rank test.

To further investigate the mechanisms responsible for survival in our model, we compared the data from the animals that did not survive the repair phase with those that did (Fig. 5). As sampling times were different between survivors and nonsurvivors, we first split the nonsurvivor group using the median ventilation time. There were no differences in any of the measured molecules between these two subgroups, thus discarding an influence of the temporal difference of sample collection (data not shown).

Regarding indexes of lung injury, survivors showed a more severe degree of histological injury (Fig. 5*B*, $P = 0.05$). The total number of pneumocytes and the percentage of Ki-67-positive nuclei were also significantly higher in survivors (Fig. 5, *C* and *D*, $P = 0.02$ and $P = 0.03$, respectively). Despite the absence of differences in the wet-to-dry ratio (Fig. 5*G*, $P = 0.32$), survivors showed a decreased protein content in BALF (Fig. 5*H*, $P = 0.05$). The leukocyte counts in BALF were

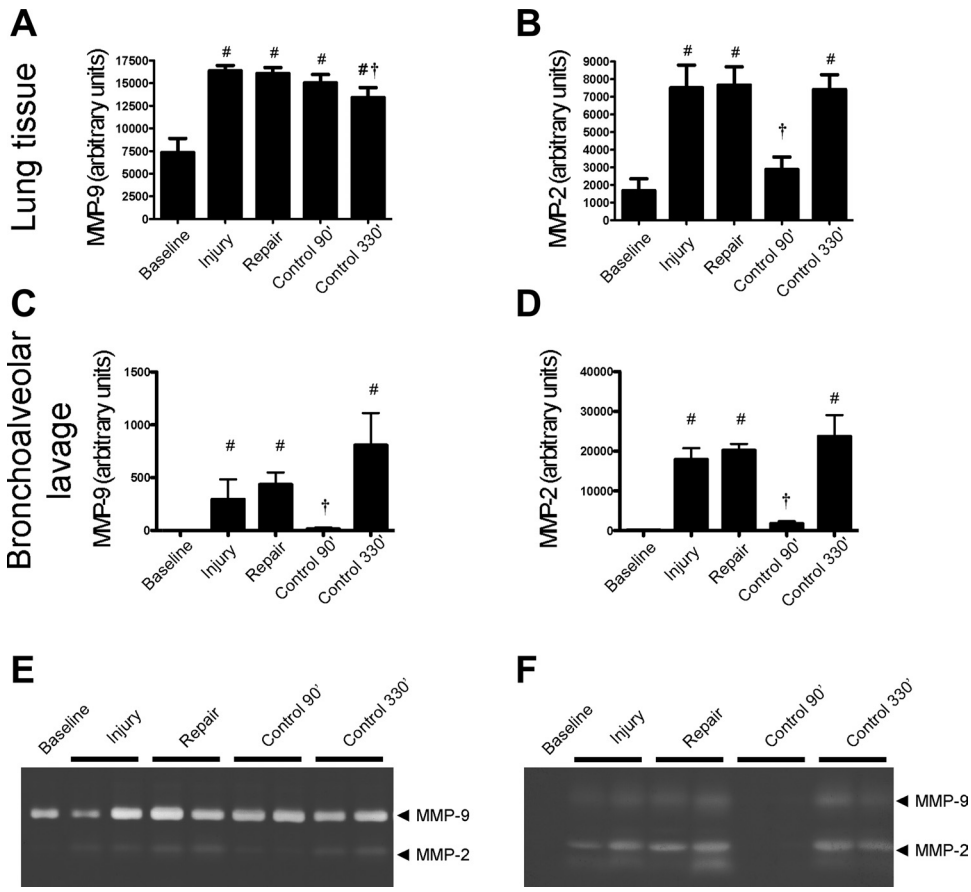

Fig. 3. Gelatinases during injury and repair. Matrix metalloproteinases (MMP)-9 (*A* and *C*) and -2 (*B* and *D*) were measured in lung tissue and BALF. Mechanical ventilation induced significant increases in both enzymes, which kept elevated levels during repair. Values are means ± SE. *E* and *F*: representative gelatin zymographies (lung tissue and BALF, respectively). #$P < 0.05$ in post hoc test compared with baseline. †$P < 0.05$ in post hoc test compared with injury.

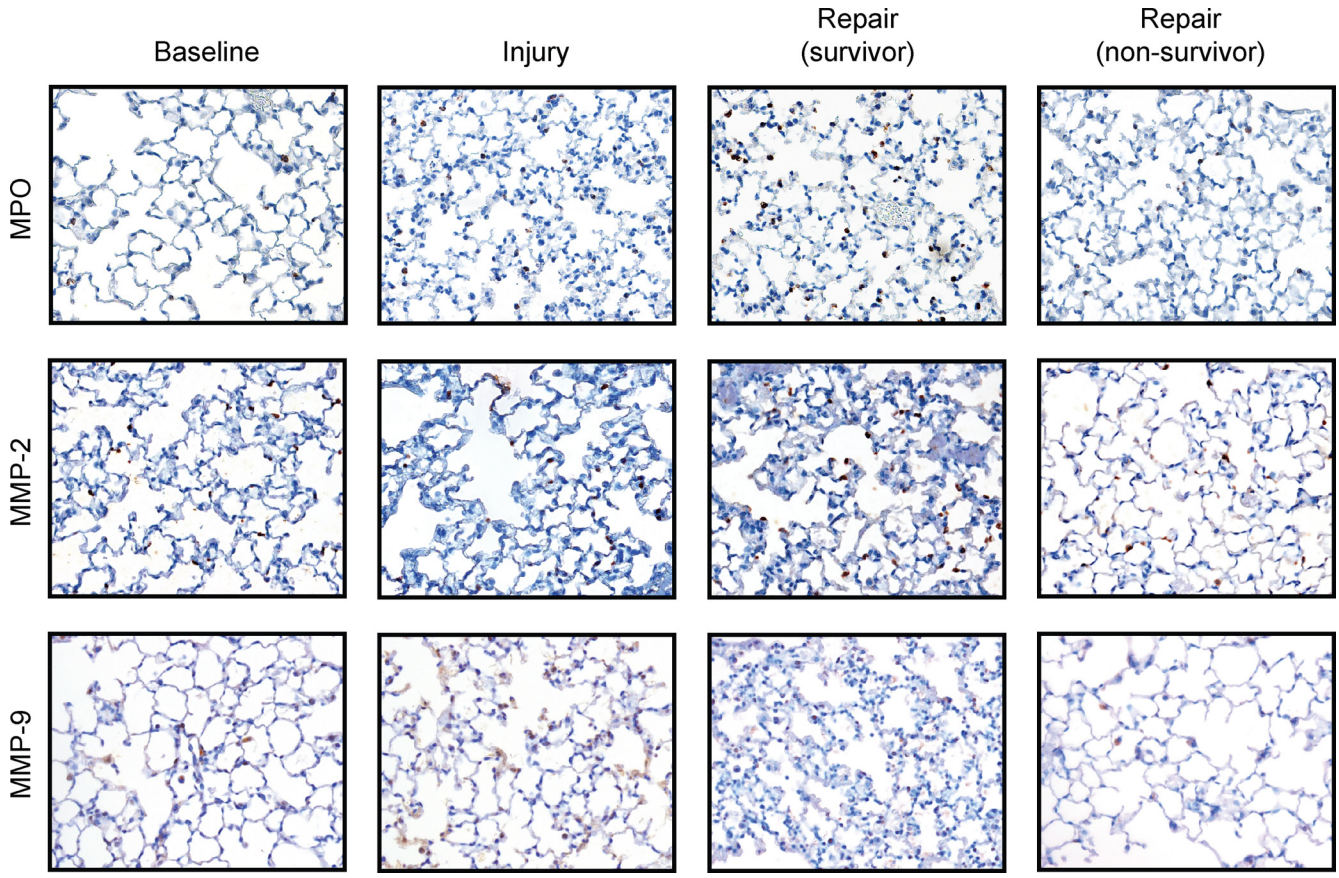

Fig. 4. Immunolocalization of myeloperoxidase (MPO), MMP-2, and MMP-9 in the different experimental groups. MPO is a marker of neutrophils. Whereas MMP-9 expression is restricted to inflammatory cells, MMP-2 is also expressed in epithelial and interstitial cells.

higher in survivors (2.3 ± 0.3 vs. 0.8 ± 0.2 × 10^3 cells/ml, $P = 0.01$), with higher neutrophil and macrophage counts (Fig. 5*I*, $P = 0.04$ and $P = 0.02$, respectively). The number of MPO-positive cells was also higher in survivors (Figs. 4 and 5*J*). The differences in immune mediators are presented in Table 2. There were no differences in TNF-α, IFN-γ or LIX; however, lower IL-4 levels and a trend toward higher IL-10 levels were observed in survivors. Nevertheless, the most striking difference was the eightfold increase of MIP-2 levels in survivors. Finally, extracellular matrix proteins were compared (Fig. 5, *K–M*). Lower collagen levels were found in survivors ($P = 0.05$). MMP-2 doubled its activity in the surviving mice ($P < 0.05$), with no significant differences in MMP-9 ($P = 0.531$). These results suggest that an adequate inflammatory response and tissue remodeling are both important phenomena in lung repair.

MMP-2 promotes alveolar wound healing in murine and human cells. The in vivo experiments revealed some mediators that could be responsible for the direct induction of injury or repair. Then we tested the effects of these molecules on wound healing using cell culture models. Control cultures (without BALF) showed a slower closure rate than those cultured with BALF, suggesting that cell growth is promoted by factors present in BALFs and not secreted by cultured cells. TNF-α, IL-4, or MIP-2 inhibition had no effect on the wound closure rate (data not shown). However, MMP-2 inhibition in cultures supplemented with BALF from mice during repair delayed wound closure after 12 h (Fig. 6*A*, $P = 0.04$ in a repeated-measurements ANOVA). Likewise, MMP-2 inhibition in a similar model using human alveolar A549 cells and BALF from ARDS patients impaired wound healing (Fig. 6*B*, $P = 0.007$). Pan-MMP inhibition with doxycycline further impaired wound healing in both murine and human culture models, but also induced changes in cell morphology and adhesion, rendering closure measurements unreliable. These results illustrate the relevance of MMPs in the healing process and, specifically, confirm that MMP-2 promotes epithelial cell migration and suggests that it contributes to alveolar repair after VILI or ARDS.

MMP inhibition impairs lung repair. The effects of MMPs on lung repair were studied using an in vivo model. The mortality of doxycycline-treated mice during the repair phase was 75%. Compared with vehicle-treated mice with the same ventilatory time, MMP inhibition results in higher histological scores of lung injury (Fig. 7). These results confirm that MMPs may be beneficial during lung repair after VILI.

DISCUSSION

Our results demonstrate that, in the present experimental models, repair after VILI can be rapidly achieved. Additionally, this study demonstrates the key role of extracellular matrix processing during lung repair, as lower levels of lung collagen and higher levels of MMP-2 were found in mice surviving lung injury. Finally, we have shown that MMP-2 promotes epithelial repair after VILI and in patients with early

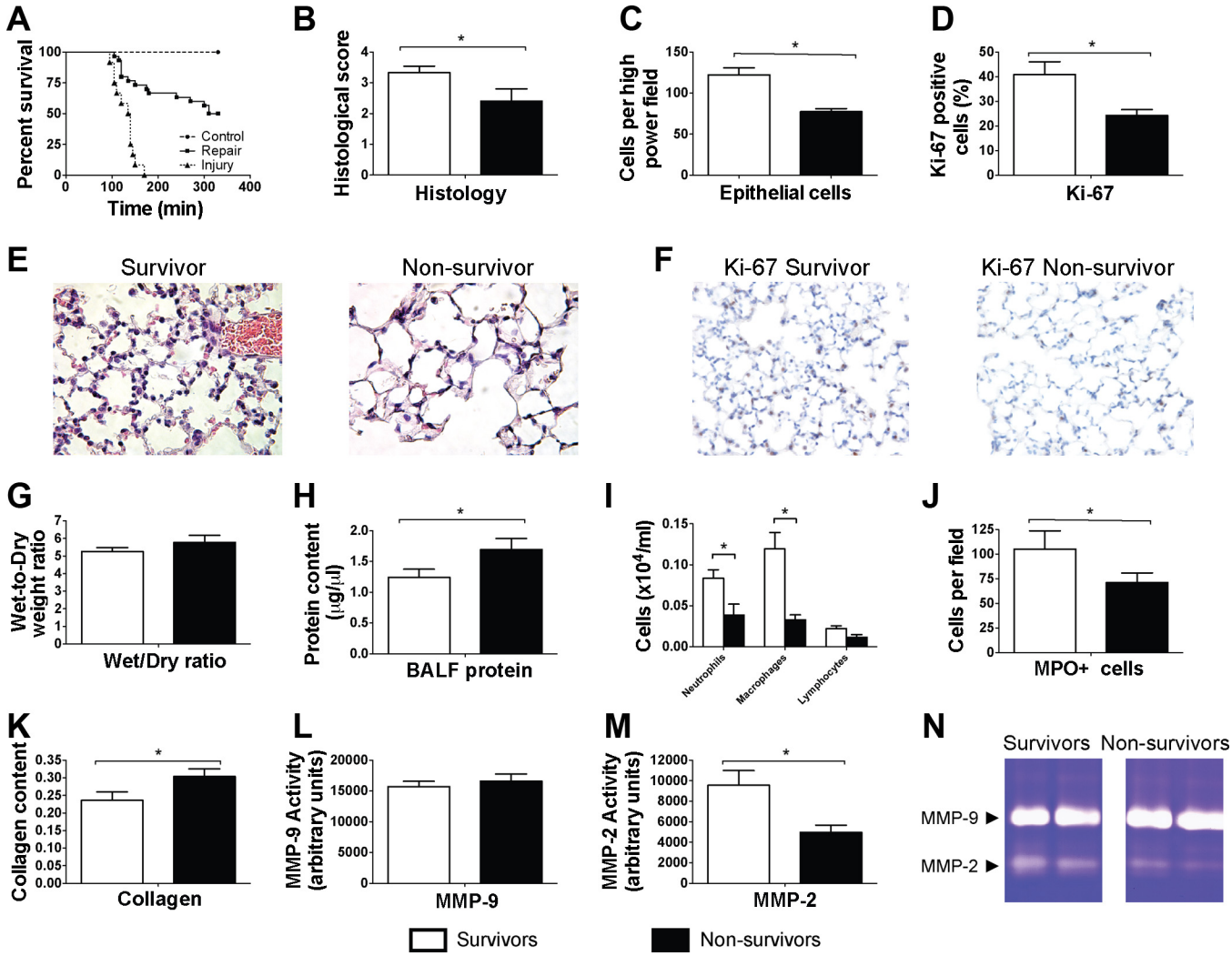

Fig. 5. Differences between surviving (open bars) and nonsurviving (solid bars) subjects after the repair phase. *A*: survival curves for ventilated animals. High-pressure ventilation led to a 100% mortality, and low-pressure ventilation to a 100% survival. The injury and repair group showed a 50% mortality after 330 min of ventilation. Survivors showed higher levels of histological scores (*B*) and an increase in pneumocyte counts (*C*) and a higher percentage of Ki-67-positive nuclei (*D*) in histological preparations. *E* and *F*: representative slides from a survivor and a nonsurvivor to illustrate these differences. There were no differences in lung edema (*G*), but nonsurvivors exhibited higher protein abundance in BALF (*H*). Survivors had higher counts of neutrophils and macrophages in BALF (*I*) and also in MPO-positive cells in lung tissue (*J*). Regarding extracellular matrix remodeling, survivors had lower levels of collagen (*K*), no differences in MMP-9 (*L*), and higher levels of MMP-2 (*M*) in lung tissue. *N*: gelatin zymography illustrating the difference in MMP-2 between survivors and nonsurvivors. Values are means ± SE. *$P < 0.05$ for the difference between groups.

ARDS. Although all of these mechanisms have been described in other forms of injury and repair, this work shows that inflammation, matrix remodeling, and cell migration act in an orchestrated fashion to repair the injured lung.

Table 2. *Differences in immune mediators in lung tissue between survivors and nonsurvivors to the repair phase of the experiment*

	Survivors	Nonsurvivors	*P*
TNF-α	4.92 ± 1.29	7.08 ± 1.86	0.370
IFN-γ	6.84 ± 1.86	4.44 ± 1.32	0.359
IL-4	1.59 ± 0.18	3.12 ± 0.51	0.011
IL-10	26.43 ± 5.07	16.62 ± 1.05	0.105
MIP-2	721.41 ± 196.5	135.56 ± 13.44	0.024
LIX	432.51 ± 96.1	587.79 ± 161.37	0.400

Values are means ± SE in pg/mg protein. MIP-2, macrophage inflammatory protein-2; LIX, LPS-induced CXC chemokine.

Inflammation and lung repair. Nin et al. (28) demonstrated that, after high-volume ventilation, lung injury could be reverted with restoration of spontaneous breathing. Our results confirm these findings, showing a partial repair after 4 h of noninjurious ventilation. The onset of this repair phase is characterized by the reversal of different pathogenetic mechanisms of VILI, namely lung edema, inflammatory response, and tissue remodeling. One of the most striking changes was the normalization of the alveolocapillary permeability, demonstrated by the rapid decrease in the protein content of the BALF. The reabsorption of lung edema and the normalization of fluid and protein filtration are key steps in recovering from ARDS (39).

Regarding inflammation, high-pressure ventilation triggers a mechanotransduction process (26) that leads to change in cell populations and immune mediators. The trend to lower absolute cell counts during injury has been explained by the dilution

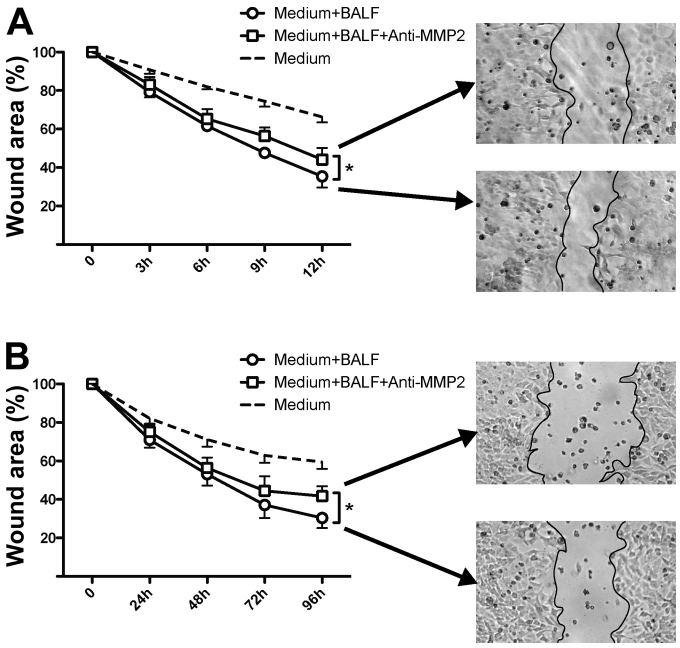

Fig. 6. Effects of MMP inhibition in wound closure. Murine (MLE-12; *A*) and human (A549; *B*) alveolar cells were cultured and wounded. Specific MMP-2 inhibition was achieved using a neutralizing antibody. The denuded area was measured over time to gauge the closure rate. The difference between curves was significant ($*P < 0.05$), as assessed by repeated measurements ANOVA. Values are means ± SE. *Insets* show micrographs of cultured cells, with the wound edges drawn for clarity.

caused by the increase in edema and attachment of cells to the alveolar epithelium (22). The specific decrease in macrophages has also been described (15). Although it has been recently reported that lymphocytes have a role in lung repair (10), we did not find any significant differences in our model.

Both neutrophils (18) and macrophages (35) are involved in wound healing. In skin wounds, the extracellular matrix builds a scar that replaces normal epithelium. However, this repair mechanism within the lungs results in fibrosis and impairs gas exchange and respiratory mechanics. In this setting, reepithelization and collagen degradation are essential, as shown in other models of tissue repair (18). Inflammatory cells can modulate both extracellular matrix degradation and epithelial cell migration through different mechanisms (24): release of proteases that cleave collagen, gelatin, and elastin; modulation of inflammation toward an anti-inflammatory response; and by directly releasing defensins and other growth factors that directly stimulate epithelial cell migration and proliferation (27). Our study supports the existence of some of these phenomena during the repair phase after VILI, including the release of proteases (MMP-2), a decrease of collagen levels, and the restoration of IL-10, an anti-inflammatory cytokine with beneficial effects in VILI (2, 20).

The elevation of proinflammatory cytokines, such as TNF-α or IFN-γ, and a decrease in anti-inflammatory mediators (IL-10) is in keeping with previous results (31). Restoration of low pressures induced a rapid normalization of these cell populations and cytokines. We cannot discard that this decrease is part of the normal cytokine kinetics during the inflammatory response. However, other studies (21) with prolonged injurious ventilation found elevated levels of TNF-α at later time points (4 h). None of these mediators had a significant impact in the wound-healing model. Therefore, these molecules could be involved in the changes in permeability or in the systemic response to VILI (1), but not directly in epithelial repair.

The increased cell counts seen during repair can be driven by the release of chemokines, such as MIP-2. This is especially evident in mice surviving the repair phase, which show higher levels of MIP-2 and inflammatory cells. This inflammatory infiltrate is, in part responsible for the higher histological scores seen in this group. Previous results have demonstrated that both MIP-2 (6) and inflammatory cell infiltration (15) can promote VILI. The findings presented here suggest that this response also drives lung repair. These dual effects of inflammation during VILI could explain the good responses seen with anti-inflammatory drugs, such as steroids, in experimental models of VILI (29) and the lack of benefits seen in the clinical practice (38).

MMP-2 in lung repair. Our laboratory has shown that MMP-2 plays a relevant role in lung repair after VILI. This gelatinase is constitutively secreted from a great variety of cells, including the lung epithelium, and in response to stretch (19). There is abundant evidence that MMP-2 is essential for cell migration, in both normal and cancer cells, and that it can also promote the cleavage of interstitial proteins (24). This is in agreement with our data, which show decreased levels of collagen and increased MMP-2 in survivors after lung injury, and is also consistent with the impairment of epithelial cell migration after MMP-2 inhibition. The involvement of this enzyme in other models of lung injury and repair has been described previously (7). Furthermore, MMP-2 can also facilitate the resolution of inflammation by cleavage of immune mediators (17), although the relevance of this mechanism has not been studied in the context of acute lung injury or VILI.

We have also described a role of MMP-2 in human ARDS. An increase in different proteases in the BALF from patients with this syndrome has been described (36). Our results show

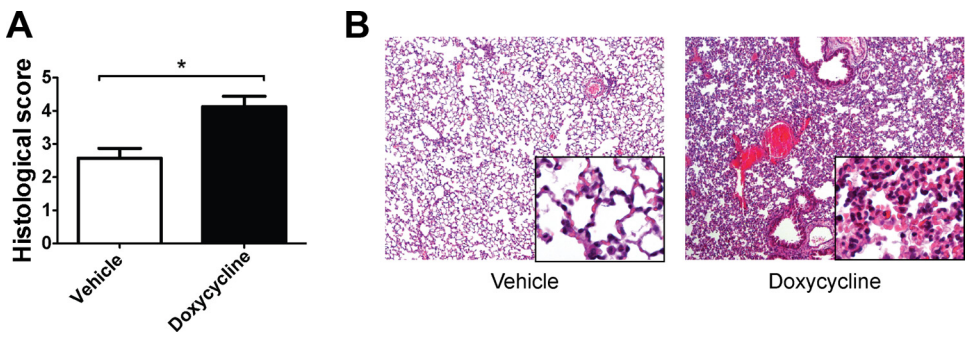

Fig. 7. Effects of MMP inhibition in lung repair. Mice were ventilated sequentially with high pressures to induce ventilator-induced lung injury and later with low pressures to facilitate repair. *A*: animals treated with doxycycline (a nonselective MMP inhibitor) administered at the end of the injury period showed higher lung damage scores after the repair phase than their counterparts. Values are means ± SE. $*P < 0.05$. *B*: two representative histological sections.

that human alveolar cells cultured in the presence of this BALF show a delay in wound closure when MMP-2 is inhibited, supporting the role of this protease in repair. O'Kane et al. have shown similar results involving MMP-9 in ARDS patients (30), which also resembles the results from a VILI model using *Mmp9* knockout mice (3). As both are gelatinases, it is probable overlapping effects take place. Furthermore, nonspecific MMP inhibition resulted in further impairment of in vitro wound healing. Although these findings are limited by the lack of data using cell stretch models, they suggest that different MMPs, including gelatinases, induce alveolar repair by promoting epithelial migration. Moreover, the results showing impaired repair after VILI in doxycycline-treated mice confirm this result. Therefore, preventive MMP inhibition can protect against VILI (14), but blocking these enzymes during the repair phase may be detrimental. These opposite effects illustrate the relationships between tissue remodeling, initial damage, and subsequent repair, and highlight the critical importance of timing when targeting these processes.

According to our results, overexpression of these enzymes could be of interest in the context of lung injury and mechanical ventilation. There are different drugs that promote MMP expression. Salbutamol increases MMP-9 expression in neutrophils and facilitates lung edema reabsorption (30). MMP-2 can be secreted in response to transforming growth factor-β (25) [which is released during lung injury (34)] or nitric oxide (8), but their therapeutic use on lung repair is yet to be studied.

Finally, the decreased closure rate seen in cell cultures without BALF suggests that there are other factors that may promote healing, which have not been identified in this work. Knowledge of molecules involved in epithelial repair, which may include growth factors, could offer new therapeutic approaches to lung injury.

Conclusions. In summary, we have shown that VILI is potentially reversible, and that the repair process depends on both an adequate inflammatory response and extracellular matrix remodeling. Regarding the latter, we have found that MMPs, and specifically MMP-2, promote lung repair by facilitating epithelial cell migration. This repair mechanism is also relevant in human ARDS. The finding of molecules directly involved in tissue repair constitutes a new therapeutic opportunity for the treatment of lung injury.

ACKNOWLEDGMENTS

The authors thank Marta S. Pitiot and Laura Suárez Fernández for help with the histological studies, María Fernández for help with protein processing, and Marino Santirso for the language review of the manuscript.

GRANTS

This study was supported by grants from Instituto de Salud Carlos III (Fondo de Investigación Sanitaria PI-10/00606), Fundación para el Fomento en Asturias de la Investigación Científica Aplicada y la Tecnología (FICYT) (COF-08-20), Universidad de Oviedo (UNOV-09-BECDOC), and FICYT-OIB. Instituto Universitario Oncologico del Principado de Asturias is supported by Obra Social Cajastur. CIBER-Enfermedades Respiratorias is supported by Instituto de Salud Carlos III.

DISCLOSURES

No conflicts of interest, financial or otherwise, are declared by the author(s).

REFERENCES

1. **Albaiceta GM, Fernandez A, Parra D, Gonzalo JA, Garcia-Prieto E, Taboada F.** Mechanical ventilation causes monocyte deactivation in intact and endotoxin-treated mice. *J Trauma* 64: 470–476, 2008.
2. **Albaiceta GM, Gutierrez-Fernandez A, Garcia-Prieto E, Puente XS, Parra D, Astudillo A, Campestre C, Cabrera S, Gonzalez-Lopez A, Fueyo A, Taboada F, Lopez-Otin C.** Absence or inhibition of matrix metalloproteinase-8 decreases ventilator-induced lung injury. *Am J Respir Cell Mol Biol* 43: 555–563, 2010.
3. **Albaiceta GM, Gutierrez-Fernandez A, Parra D, Astudillo A, Garcia-Prieto E, Taboada F, Fueyo A.** Lack of matrix metalloproteinase-9 worsens ventilator-induced lung injury. *Am J Physiol Lung Cell Mol Physiol* 294: L535–L543, 2008.
4. **Albaiceta GM, Luyando LH, Parra D, Menendez R, Calvo J, Pedreira PR, Taboada F.** Inspiratory vs. expiratory pressure-volume curves to set end-expiratory pressure in acute lung injury. *Intensive Care Med* 31: 1370–1378, 2005.
5. **[Anon]**. Ventilation with lower tidal volumes compared with traditional tidal volumes for acute lung injury, and the acute respiratory distress syndrome. The Acute Respiratory Distress Syndrome Network. *N Engl J Med* 342: 1301–1308, 2000.
6. **Belperio JA, Keane MP, Burdick MD, Londhe V, Xue YY, Li K, Phillips RJ, Strieter RM.** Critical role for CXCR2 and CXCR2 ligands during the pathogenesis of ventilator-induced lung injury. *J Clin Invest* 110: 1703–1716, 2002.
7. **Buckley S, Driscoll B, Shi W, Anderson K, Warburton D.** Migration and gelatinases in cultured fetal, adult, and hyperoxic alveolar epithelial cells. *Am J Physiol Lung Cell Mol Physiol* 281: L427–L434, 2001.
8. **Chen JH, Lin HH, Chiang TA, Hsu JD, Ho HH, Lee YC, Wang CJ.** Gaseous nitrogen oxide promotes human lung cancer cell line A549 migration, invasion, and metastasis via iNOS-mediated MMP-2 production. *Toxicol Sci* 106: 364–375, 2008.
9. **Colletti LM, Green M, Burdick MD, Kunkel SL, Strieter RM.** Proliferative effects of CXC chemokines in rat hepatocytes in vitro and in vivo. *Shock* 10: 248–257, 1998.
10. **D'Alessio FR, Tsushima K, Aggarwal NR, West EE, Willett MH, Britos MF, Pipeling MR, Brower RG, Tuder RM, McDyer JF, King LS.** CD4+CD25+Foxp3+ Tregs resolve experimental lung injury in mice and are present in humans with acute lung injury. *J Clin Invest* 119: 2898–2913, 2009.
11. **Dos Santos CC.** Advances in mechanisms of repair and remodelling in acute lung injury. *Intensive Care Med* 34: 619–630, 2008.
12. **dos Santos CC, Slutsky AS.** The contribution of biophysical lung injury to the development of biotrauma. *Annu Rev Physiol* 68: 585–618, 2006.
13. **Driscoll KE, Hassenbein DG, Howard BW, Isfort RJ, Cody D, Tindal MH, Suchanek M, Carter JM.** Cloning, expression, and functional characterization of rat MIP-2: a neutrophil chemoattractant and epithelial cell mitogen. *J Leukoc Biol* 58: 359–364, 1995.
14. **Foda HD, Rollo EE, Drews M, Conner C, Appelt K, Shalinsky DR, Zucker S.** Ventilator-induced lung injury upregulates and activates gelatinases and EMMPRIN: attenuation by the synthetic matrix metalloproteinase inhibitor, Prinomastat (AG3340). *Am J Respir Cell Mol Biol* 25: 717–724, 2001.
15. **Frank JA, Wray CM, McAuley DF, Schwendener R, Matthay MA.** Alveolar macrophages contribute to alveolar barrier dysfunction in ventilator-induced lung injury. *Am J Physiol Lung Cell Mol Physiol* 291: L1191–L1198, 2006.
16. **Golub LM, Lee HM, Ryan ME, Giannobile WV, Payne J, Sorsa T.** Tetracyclines inhibit connective tissue breakdown by multiple non-antimicrobial mechanisms. *Adv Dent Res* 12: 12–26, 1998.
17. **Greenlee KJ, Corry DB, Engler DA, Matsunami RK, Tessier P, Cook RG, Werb Z, Kheradmand F.** Proteomic identification of in vivo substrates for matrix metalloproteinases 2 and 9 reveals a mechanism for resolution of inflammation. *J Immunol* 177: 7312–7321, 2006.
18. **Harty MW, Muratore CS, Papa EF, Gart MS, Ramm GA, Gregory SH, Tracy TF Jr.** Neutrophil depletion blocks early collagen degradation in repairing cholestatic rat livers. *Am J Pathol* 176: 1271–1281.
19. **Haseneen NA, Vaday GG, Zucker S, Foda HD.** Mechanical stretch induces MMP-2 release and activation in lung endothelium: role of EMMPRIN. *Am J Physiol Lung Cell Mol Physiol* 284: L541–L547, 2003.
20. **Hoegl S, Boost KA, Czerwonka H, Dolfen A, Scheiermann P, Muhl H, Zwissler B, Hofstetter C.** Inhaled IL-10 reduces biotrauma and mortality in a model of ventilator-induced lung injury. *Respir Med* 103: 463–470, 2009.
21. **Hong SB, Huang Y, Moreno-Vinasco L, Sammani S, Moitra J, Barnard JW, Ma SF, Mirzapoiazova T, Evenoski C, Reeves RR, Chiang ET, Lang GD, Husain AN, Dudek SM, Jacobson JR, Ye SQ, Lussier YA, Garcia JG.** Essential role of pre-B-cell colony enhancing factor in

ventilator-induced lung injury. *Am J Respir Crit Care Med* 178: 605–617, 2008.
22. **Imanaka H, Shimaoka M, Matsuura N, Nishimura M, Ohta N, Kiyono H.** Ventilator-induced lung injury is associated with neutrophil infiltration, macrophage activation, and TGF-beta 1 mRNA upregulation in rat lungs. *Anesth Analg* 92: 428–436, 2001.
23. **Kalehua AN, Nagel JE, Whelchel LM, Gides JJ, Pyle RS, Smith RJ, Kusiak JW, Taub DD.** Monocyte chemoattractant protein-1 and macrophage inflammatory protein-2 are involved in both excitotoxin-induced neurodegeneration and regeneration. *Exp Cell Res* 297: 197–211, 2004.
24. **Korpos E, Wu C, Sorokin L.** Multiple roles of the extracellular matrix in inflammation. *Curr Pharm Des* 15: 1349–1357, 2009.
25. **Lechapt-Zalcman E, Pruliere-Escabasse V, Advenier D, Galiacy S, Charriere-Bertrand C, Coste A, Harf A, d'Ortho MP, Escudier E.** Transforming growth factor-beta1 increases airway wound repair via MMP-2 upregulation: a new pathway for epithelial wound repair? *Am J Physiol Lung Cell Mol Physiol* 290: L1277–L1282, 2006.
26. **Lionetti V, Recchia FA, Ranieri VM.** Overview of ventilator-induced lung injury mechanisms. *Curr Opin Crit Care* 11: 82–86, 2005.
27. **Madri JA, Graesser D.** Cell migration in the immune system: the evolving inter-related roles of adhesion molecules and proteinases. *Dev Immunol* 7: 103–116, 2000.
28. **Nin N, Lorente JA, de Paula M, El Assar M, Vallejo S, Penuelas O, Fernandez-Segoviano P, Ferruelo A, Sanchez-Ferrer A, Esteban A.** Rats surviving injurious mechanical ventilation show reversible pulmonary, vascular and inflammatory changes. *Intensive Care Med* 34: 948–956, 2008.
29. **Nin N, Penuelas O, de Paula M, Lorente JA, Fernandez-Segoviano P, Esteban A.** Ventilation-induced lung injury in rats is associated with organ injury and systemic inflammation that is attenuated by dexamethasone. *Crit Care Med* 34: 1093–1098, 2006.
30. **O'Kane CM, McKeown SW, Perkins GD, Bassford CR, Gao F, Thickett DR, McAuley DF.** Salbutamol up-regulates matrix metalloproteinase-9 in the alveolar space in the acute respiratory distress syndrome. *Crit Care Med* 37: 2242–2249, 2009.
31. **Pedreira PR, Garcia-Prieto E, Parra D, Astudillo A, Diaz E, Taboada F, Albaiceta GM.** Effects of melatonin in an experimental model of ventilator-induced lung injury. *Am J Physiol Lung Cell Mol Physiol* 295: L820–L827, 2008.
32. **Pelosi P, Rocco PR.** Effects of mechanical ventilation on the extracellular matrix. *Intensive Care Med* 34: 631–639, 2008.
33. **Perkins GD, Gao F, Thickett DR.** In vivo and in vitro effects of salbutamol on alveolar epithelial repair in acute lung injury. *Thorax* 63: 215–220, 2008.
34. **Pittet JF, Griffiths MJ, Geiser T, Kaminski N, Dalton SL, Huang X, Brown LA, Gotwals PJ, Koteliansky VE, Matthay MA, Sheppard D.** TGF-beta is a critical mediator of acute lung injury. *J Clin Invest* 107: 1537–1544, 2001.
35. **Pull SL, Doherty JM, Mills JC, Gordon JI, Stappenbeck TS.** Activated macrophages are an adaptive element of the colonic epithelial progenitor niche necessary for regenerative responses to injury. *Proc Natl Acad Sci U S A* 102: 99–104, 2005.
36. **Ricou B, Nicod L, Lacraz S, Welgus HG, Suter PM, Dayer JM.** Matrix metalloproteinases and TIMP in acute respiratory distress syndrome. *Am J Respir Crit Care Med* 154: 346–352, 1996.
37. **Slutsky AS.** Ventilator-induced lung injury: from barotrauma to biotrauma. *Respir Care* 50: 646–659, 2005.
38. **Steinberg KP, Hudson LD, Goodman RB, Hough CL, Lanken PN, Hyzy R, Thompson BT, Ancukiewicz M.** Efficacy and safety of corticosteroids for persistent acute respiratory distress syndrome. *N Engl J Med* 354: 1671–1684, 2006.
39. **Ware LB, Matthay MA.** Alveolar fluid clearance is impaired in the majority of patients with acute lung injury and the acute respiratory distress syndrome. *Am J Respir Crit Care Med* 163: 1376–1383, 2001.

VI. Manuscrito: La ventilación mecánica desencadena un proceso de apoptosis en el hipocampo a través de vías dopaminérgicas y vagales.

Los mecanismos de lesión desencadenados durante la ventilación mecánica distan de focalizarse únicamente en el pulmón. Otras regiones del organismo se ven afectadas en lo que se engloba bajo el concepto de biotrauma. Una de estas regiones es el cerebro: los pacientes ingresados en las unidades de cuidados intensivos y sometidos a ventilación mecánica presentan niveles de disfunción cerebral en forma de delirio y desórdenes cognitivos en un porcentaje muy superior al de los pacientes no ventilados. Nos centramos en el hipocampo, dado su papel en los desórdenes del comportamiento. Observamos que la ventilación mecánica desencadenaba una respuesta proapoptótica neuronal dependiente de dopamina, afectando a la vía de Akt, y que el bloqueo tanto de las aferencias vagales como de los receptores de dopamina tipo 2 (DRD2) atenuaban este efecto perjudicial. A su vez observamos un incremento en los niveles de disbindina, proteína capaz de internalizar los DRD2, tanto en los ratones ventilados como en autopsias de pacientes que habían sido ventilados mecánicamente. Nuestros datos, unidos a la existencia de polimorfismos patológicos para estas proteínas asociados a estados de hiperdopaminergia, sugieren a su posible utilidad como marcadores de riesgo en el desarrollo de delirio o desorden cognitivo en los pacientes ingresados en la UCI.

Aportación personal al trabajo.

En este trabajo corrió a mi cargo la mayor parte del trabajo experimental. Llevé a cabo el modelo animal y la recogida de muestras, los ensayos *in vitro*, así como las determinaciones *western blot* y PCR cuantitativas. También contribuí a los estudios histológicos, participé en el posterior análisis estadístico y la elaboración del manuscrito.

Mechanical ventilation triggers hippocampal apoptosis by vagal and dopaminergic pathways

Adrián González-López[1], Inés López-Alonso[1], Alina Aguirre[1], Laura Amado-Rodriguez[2], Estefanía Batalla-Solís[2], Aurora Astudillo[3], Cristina Tomás-Zapico[1], Antonio Fueyo[1], Claudia C. dos Santos[4], Konrad Talbot[5], Guillermo M Albaiceta[1,2,6].

[1]Departamento de Biología Funcional. Área de Fisiología. IUOPA. Universidad de Oviedo. Oviedo, Spain. [2]Servicio de Medicina Intensiva. Hospital Universitario Central de Asturias. Oviedo, Spain. [3]Departamento de Cirugía y Especialidades Médico-Quirurgicas. IUOPA. Universidad de Oviedo. Oviedo, Spain. [4]Interdepartamental Division of Critical Care, The Keenan Research Centre of the Li Ka Shing Knowledge Institute of St. Michael's Hospital, Toronto, ON, Canada. [5]Department of Psychiatry, University of Pennsylvania, Philadelphia, Pennsylvania, USA. [6]CIBER-Enfermedades Respiratorias. Instituto de Salud Carlos III. Spain.

Abstract.

Critically ill patients frequently develop neuropsychological disturbances including acute delirium or memory impairment. The need for mechanical ventilation is as a risk factor for these adverse events, but the mechanisms that link lung stretch and brain injury have not been identified. We describe herein that mechanical ventilation triggers hippocampal apoptosis as a result of a hyperdopaminergic state in response to vagal signaling. Increased activation of type-2 dopamine receptors blocks the Akt/GSK3β prosurvival pathway and activates the apoptotic cascade. This mechanism may be ameliorated by vagotomy or the dopamine antagonist haloperidol. Moreover, there is a concomitant change in the expression of dysbindin-1C, a regulator of the membrane availability of dopamine receptors. These changes were confirmed in brain samples from ventilated patients. In conclusion, we have described a pathogenetic mechanism of lung stretch-induced hippocampal apoptosis that could explain the neurological changes in ventilated patients and may help to identify novel therapeutic approaches.

Introduction

Up to 50% of critically ill patients develop some degree of mental dysfunction, including acute delirium and long-term cognitive impairment(1). These symptoms probably represent the extreme cases of a syndrome that includes more subtle disturbances such as post-traumatic stress disorder and depression(2). The clinical impact is thought to be significant; in fact, per day of delirium, length of stay increases by 20% and mortality by 10%(3, 4).

The cause of mental dysfunction in critically ill patients is unknown, though it is believed to involve not only the illness itself but its interactions with the treatment given and the ICU environment. Patients with delirium show brain structural alterations at ICU discharge and several months later(5, 6). The biochemical events that lead to these abnormalities are controversial, and several hypotheses have been proposed. An imbalance in neurotransmitters, resulting in an increase in dopaminergic activity, is supported by the prophylactic and therapeutic effects of haloperidol(7), a known blocker of the type 2-dopamine receptor (DRD2). In this model, increased dopamine triggers neuronal apoptosis by activating DRD2 and inhibiting the pro-survival Akt/GSK3β pathway(8-12). This pathway is regulated by PTEN, an inhibitor of Akt phosphorylation(13), and dysbindin-1, a protein involved in recycling of DRD2(14, 15). Certain polymorphisms of the gene encoding dysbindin-1 (*DTNBP1*) have been associated with familial cases of Schizophrenia(16).

In epidemiological studies, among the variables, the need for mechanical ventilation has been implicated in the development of delirium(17). Intubation and positive-pressure ventilation increases the incidence of delirium by up to 80% compared to 50% in non-intubated patients(1). Mechanotransduction of cyclic stretch signals triggers biological responses in the lung including the activation of proinflammatory and lung matrix remodeling pathways(18). Extension of these responses beyond the lungs is thought to account for the development of multiple organ dysfunction and death in ventilated patients with acute lung injury. Recent reports demonstrate that the brain may represent an important distal organ target for ventilator-induced lung injury (VILI). In a model of positive pressure-induced lung injury, different brain areas are activated as a consequence of mechanical ventilation,(19) and inhibition of neural

signaling by vagotomy enhances lung damage(20). However, the specific nature of brain-lung crosstalk has not been fully elucidated. To test the hypothesis that mechanical ventilation *per se* might cause brain injury, we studied alterations in brain areas using an animal model of mechanical ventilation. Additionally, the pathways leading to brain damage and their pharmacological treatment were explored.

Methods.

Animals. Eight to twelve week-old C57BL6 mice (n=127) were used in all experiments. Animals were kept under specific pathogen-free conditions and exposed to 12 hours light/dark cycles with free access to water and food. All the experimental protocols were reviewed and approved by the Animal Research Ethics committee of the Universidad de Oviedo, Spain.

Experimental protocol. Mice were anesthetized with an intraperitoneal injection of ketamine (80 mg/kg) and xylazin (25 mg/kg). Tracheostomy was performed and the trachea was cannulated with a 20G catheter. Animals were randomized to different experimental groups (n=12 per group). The spontaneously breathing (sham) mice received the same sedation protocol as the other animal groups: low-pressure ventilation (peak inspiratory pressure –PIP- 12 cmH_2O, PEEP 2 cmH_2O, respiratory rate 100 breaths/min) or high-pressure ventilation (PIP 20 cmH_2O, PEEP 0 cmH_2O, respiratory rate 50 breaths/min) for 90 minutes. Long-term ventilation experiments were performed for 330 minutes as previously described(21). Mechanical ventilation was provided using an Evita 2 Dura ventilator (Drager, Germany). FiO_2 was 50%, and inspiratory-expiratory ratio was 1:1 in all ventilatory strategies. Mice were placed on a heating pad and kept at 37°C

A 0.2 ml bolus of Ringer's lactate was injected intraperitoneally at the onset of ventilation and repeated every two hours in the long-term protocol to avoid hypotension. Hypoxemia was not induced as indicated by the fact that all mice showed a SpO_2 above 95% throughout the ventilatory period.

Additional animals were randomly chosen for injection of haloperidol (0,5 mg/kg in 0.2 ml of saline, intraperitoneal) thirty minutes prior to injurious ventilation or surgical

bilateral cervical vagotomy just before high-pressure ventilation.

Sample collection. At the end of the procedure, mice were sacrificed by decapitation. The hippocampal formation (HF, hippocampal fields CA1-3 + dentate gyrus + subiculum) was rapidly dissected, snap-frozen in liquid nitrogen and stored at -80°C for molecular analysis. Whole brains were also collected, washed in ice-cold Ringer's lactate solution and sliced into 4µm coronal sections. Sections were immersed in 4.5% formaldehyde for 24 hours and embedded in paraffin for future sectioning and immunohistochemistry.

Immunohistochemistry and immunofluorescence. These procedures were performed using antibodies against dysbindin (Merck KGaA, Germany) and cleaved poly [ADP-ribose] polymerase 1 (PARP-1) (Cell Signaling, MA, USA) and the corresponding secondary antibodies (Invitrogen, UK). Slides were deparaffinizated in xylene, boiled for 20 minutes in 0.1M citrate buffer (pH 6.0) for antigen-retrieval and permeabilizated in 0.1% Triton X-100 in PBS for 15 minutes. Goat serum (10% in PBS) was used for blocking. In immunofluorescence studies, slides were incubated with 1M glycine in PBS for 30 min to quench the autofluorescence and nuclei were counterstained with DAPI (Vector laboratories, CA).

Immunoblot analysis. Tissue samples were homogenized in a standard RIPA buffer containing 100 mM TRIS pH 7.4, 150 mM NaCl, 1 mM EDTA, 1% deoxycholic acid, 1% Triton X-100, 0,25% SDS, complete protease inhibitor cocktail (Roche Applied Science, Mannheim, Germany) and phosphatase inhibitors (1 mM ortovanadate, 5 mM β-glycerophosphate, 50 mM NaF). Once homogenized, tissue extracts were centrifuged at 13000 rpm and 4°C, and supernatants were collected. Protein concentrations were quantified by bicinchoninic acid technique (BCA protein assay, Pierce, USA).
Twenty-five micrograms of protein from each sample were loaded in SDS-polyacrylamide gels. After electrophoresis at 120mV, gels were electro-transferred onto Immobilon-P polyvinylidene fluoride membranes (PVDF), blocked in non-fat milk (Bio-rad, Hercules, CA, USA) or bovine serum albumin (Sigma, Poole, UK) as needed and incubated overnight with primary antibodies in TBST (phosphate buffered saline

with 0.05% Tween 20). Proteins were then detected by chemiluminiscence (Luminata Forte, Millipore-Merck, France) using secondary peroxidase-linked antibodies. β-Actin was measured to confirm equal amounts of protein loading. Resulting images were acquired with a LAS-3000 camera and analyzed using ImageJ software (NIH, USA).

Primary antibodies were used to detect Akt pS473, total Akt, GSK3β pS9, total GSK3β, PTEN pS380, total PTEN, complete caspase 9, cleaved caspase 7, PARP-1 (Cell Signaling, Beverly, MA, USA), LC-3 (Nanotools, Germany), p62 (Abnova, TW), dysbindin (Merck KGaA, Germany) and β-Actin (Santa Cruz SC1616, USA).

Incubation and treatment of hippocampal slices. Additional mice were sacrificed under baseline conditions. The brain was rapidly removed and washed constantly in ice-cold dissecting artificial CSF (ACSF)(124 mM NaCl, 2.69 mM KCl, 1.25 mM KH2PO4, 10 mM D-Glucose, 26 mM NaHCO3, 2 mM MgCl2 and 2 mM CaCl2) during hippocampi dissection and slice preparation(22). Slices were separated in recording ACSF solution (124 mM NaCl, 2.69 mM KCl, 1.25 mM KH2PO4, 10 mM D-Glucose, 26 mM NaHCO3, 1.2 mM MgCl2 and 2.5 mM CaCl2) at 4°C and allowed to recover for 30 minutes in the same solution at 37°C to slice stabilization. Both ACSF solutions were aerated with 95% O_2 and 5% CO_2 at pH 7.4 prior to use.

After stabilization, slices were incubated with dopamine to a final concentration of 100 μM for 90 minutes. In parallel experiments, haloperidol (40 μM) or the DRD1 antagonist SCH-23390 (10 μM) were added to the recording ACSF solution 30 minutes before dopamine and maintained during the 90 minutes of incubation with dopamine.

Quantitative RT-PCR analysis. Total RNA was isolated from frozen hippocampus tissue using the Trizol reagent (Sigma, Poole, UK) and processed by isopropanol precipitation. One microgram of RNA was used to synthesize cDNA using the Enhanced Avian HS RT-PCR kit (Sigma, Poole, UK) following the manufacturer's instructions. Quantitative real time-PCR (qRT-PCR) was carried out in triplicate for each sample using 10 ng of cDNA. TaqMan Universal PCR master mix and 1 μl the specific TaqMan custom gene expression assays were used for *Dtnbp1* (Mm00458743_m1) and *Dtnbp1C* (4331348ctg) genes (Applied Biosystems, San Francisco, CA, USA). SYBR® Green PCR master mix and 100 nM of the specific primers were used for the genes encoding tyrosine hydroxylase, *Th* (Fw 5'-ACTGCTGCCACGAGCTGCT-3' / Rv 5'-

TCAGGGACGCCGTGCACCTA-3'), and hypoxia-inducable factor-1α, *Hif1α* (Fw 5'-CATGATGGCTCCCTTTTTCA-3' / Rv 5'-GTCACCTGGTTGCTGCAATA-3') genes (Applied Biosystems, San Francisco, CA, USA). To quantify gene expression, PCR was performed at 95°C for 10 min and at 50°C for 2 min, followed by 40 cycles of 95°C for 15 s and 60°C for 1 min, using an Applied Biosystems 7300 real-time PCR system. β-actin expression was used as internal control, so the relative expression of the analyzed genes was calculated as $2^{\Delta CT(\text{gene of interest})-\Delta CT(\beta\text{-actin})}$. Values were normalized to the expression in the sham or control group(23).

Patients. Brains from 9 patients who died in the ICU while receiving mechanical ventilation and from 5 non-ventilated ICU patients were obtained from the brain bank at the Hospital Universitario Central de Asturias (Oviedo, Spain). Clinical data from these patients (age, sex, comorbid conditions, cause of ICU admission, days of mechanical ventilation) were collected (see Supplementary Table 1). Use of these samples and data was authorized by the Local Research Ethics Committee. Sections of the patients' hippocampi embedded in paraffin were sectioned coronally at 4 μm and immunoreacted with antibodies against dysbindin-1 as previously described. Intensity of immunoreaction was quantified by a blinded pathologist (AA) using a semiquantitative score from 0 to 4.

Statistical analysis. Data are expressed as mean ± SEM. Results were compared using a t-test or a one-way analysis of variance (ANOVA). Post-hoc tests were done when appropriate using the Dunnett test to compare against control conditions. Correlations were evaluated using the Spearman's coefficient (ρ). A p value lower than 0.05 was considered significant. All the calculations were done using SPSS 17.0 software (SPSS inc, USA).

Results

Mechanical ventilation causes hippocampal neuronal apoptosis.

Cleavage of poly(ADP-ribose) polymerase 1 (PARP-1) by caspases is considered to be a hallmark of apoptosis. Mice ventilated with either a low or high tidal volume strategy showed significantly elevated immunoreactivity for cleaved PARP-1 in hippocampal area after 90 min compared to non-ventilated mice (Figure 1a). No other brain areas showed a positive staining for cleaved PARP-1.

Western blots using whole hippocampal tissue homogenates, demonstrate a reduction of pro-caspase-9 (Figure 1b), and an increase in cleaved caspase-7 (Figure 1c) and cleaved PARP-1 in ventilated (Figure 1d), compared to non-ventilated mice. There were no signals of increased autophagy in these samples, as assessed by immunoblotting against p62 and LC3 (Supplemental Figure S1). These results demonstrate that positive pressure ventilation activates the intrinsic apoptotic pathway in hippocampal neurons.

These results were not due to brain hypoxia. All ventilated animals were kept at oxygen saturation levels above 95% throughout the experiments, and none of the animal groups showed elevated hippocampal formation expression of *Hif1*α, a rapid response gene in cases of hypoxia,(24) (Supplemental Figure S2).

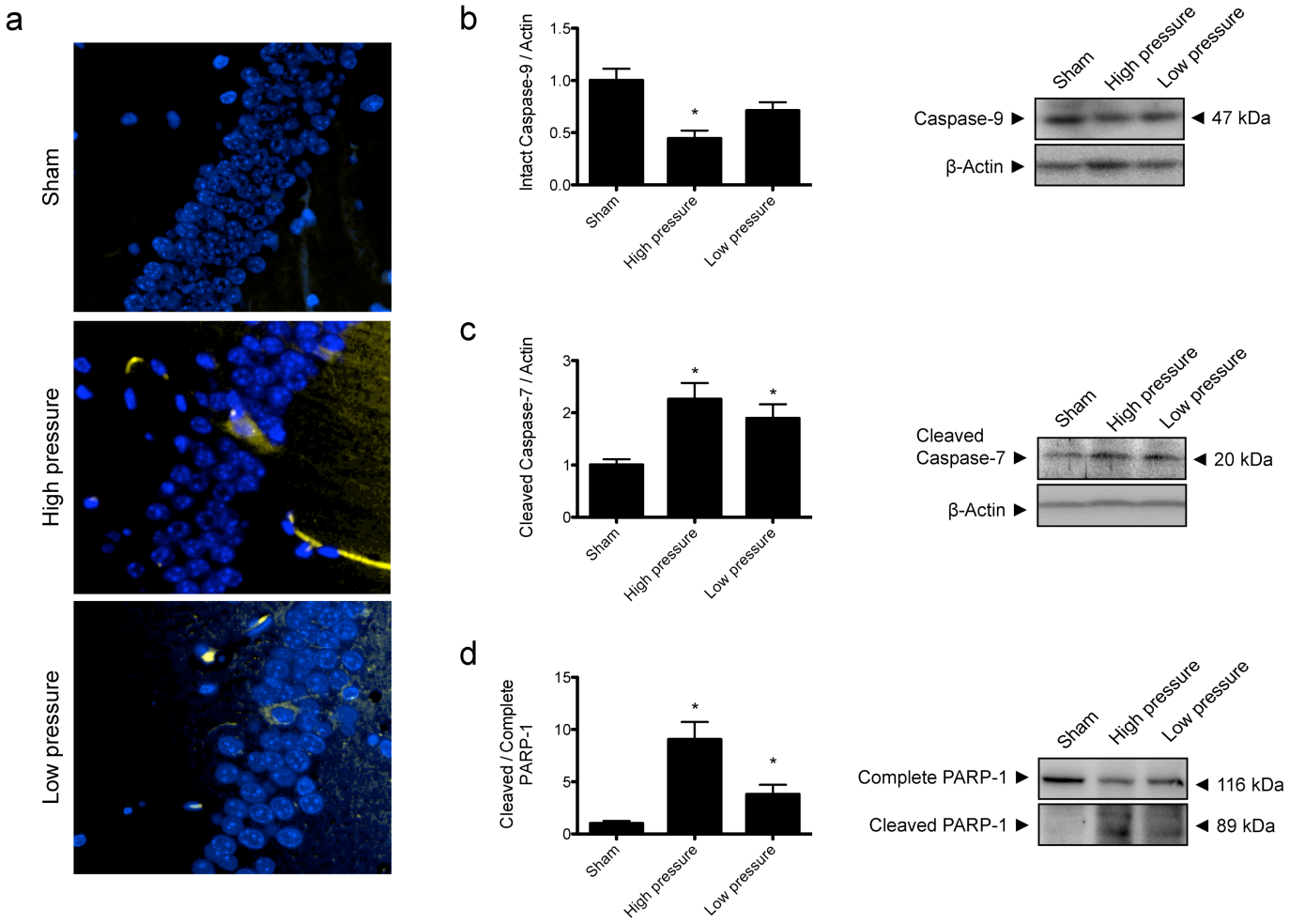

Figure 1. Mechanical ventilation results in hippocampal apoptosis. (a) Representative photomicrographs of immunoreactivity for cytosolic-cleaved PARP-1 (yellow) positive neurons after sham, low high pressure, or low pressure ventilation. Cleaved-PARP-1 positive neurons appear in mechanically ventilated animals, but not in the sham group. (b-d) The blue immunofluorescence is DAPI labeling of nuclei. Representative Western Blots and densitometry quantification showing activation of the intrinsic apoptosis pathway indicated by a decrease in intact caspase-9 (b), an increase in cleaved caspase-7 (c), and elevated cleaved PARP-1 (d) in hippocampus homogenates. *p<0.05 in post-hoc test vs the sham group, n=6 per group.

The Akt/ GSK3β *pathway is downregulated in hippocampal formation of ventilated animals.*

The Akt/glycogen synthase kinase-3 (GSK3) pathway plays an important role in the cell survival after a variety of cell death stimuli. Hippocampal formation homogenates from ventilated mice showed significantly decreased Akt pS473 (Figure 2a) and the corresponding decrease in GSK3β pS9 (Figure 2b) compared to sham mice. Phosphorylation of PTEN was also decreased in ventilated animals (Figure 2c).

Since hyperdopaminergia has been identified as a potential mechanism for inactivation of Akt/GSK3β pathway, we studied the effects of mechanical ventilation on *Th* gene expression, the rate-limiting enzyme in the synthesis of dopamine. Expresion of the *Th* gene was increased in the hippocampal formation of the ventilated animals (Figure 2d).

The inhibitory effect of dopamine over the Akt pathway is mediated by the DRD2. To confirm that this may also be the case in our model, brain slices obtained from mice under baseline conditions were cultured in presence of dopamine alone, dopamine plus haloperidol (a DRD2 blocker) or plus SCH-23390 (a DRD1 blocker). After 90 minutes of incubation, the slices were homogenized, and the phosphorylation status of Akt determined. Dopamine decreased Akt phosphorylation, which was partially reverted by haloperidol, but not by SCH-23390 (Figure 2e).

Collectively, our data strongly suggest that increased dopamine levels and activation of DRD2 secondary to VILI may result in both increased (intrinsic) cellular apoptosis and decreased survival pathways (Akt/GSK3β), thus resulting in neuronal apoptosis in the hippocampal formation.

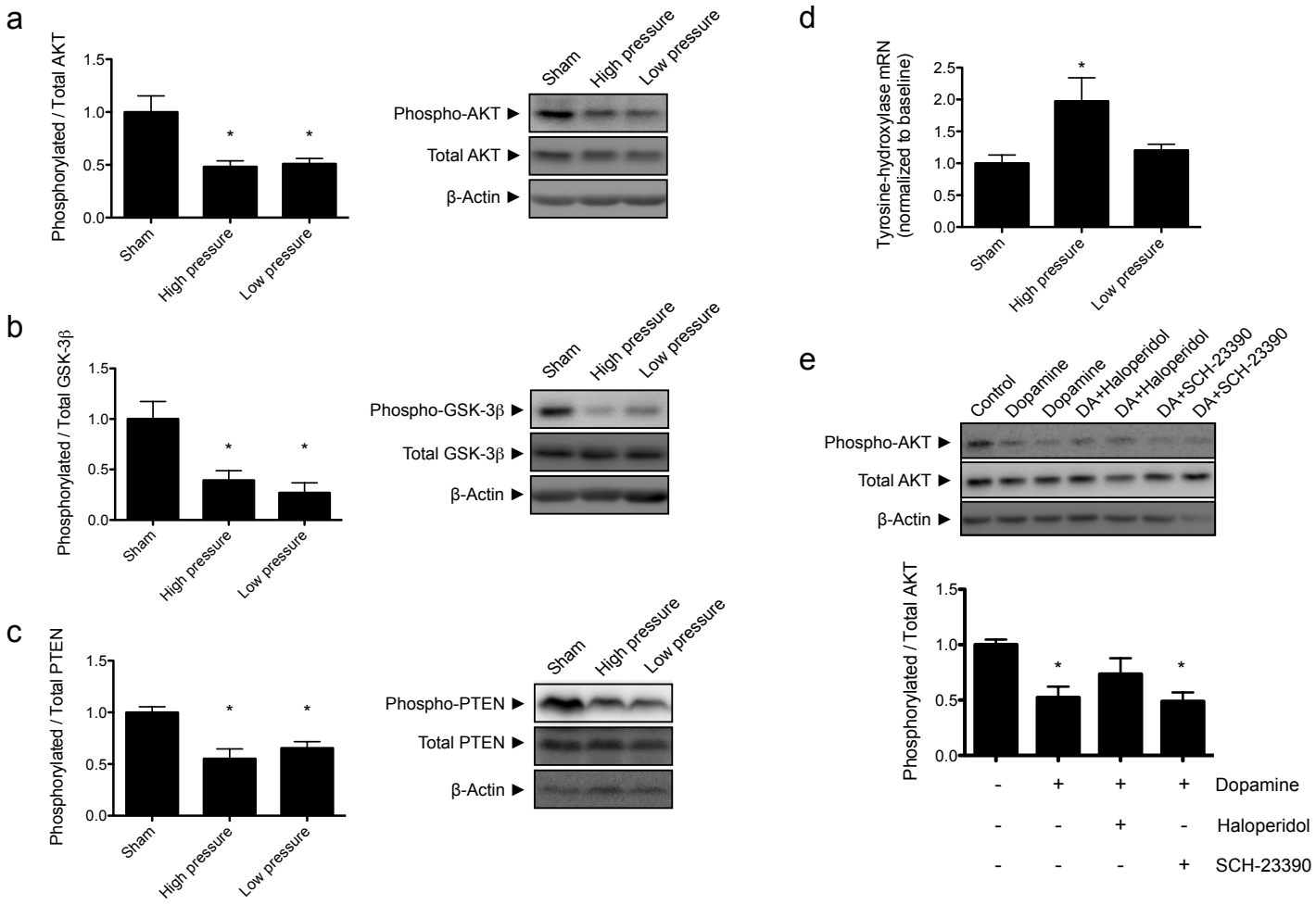

Figure 2. Mechanical ventilation, either with high or low pressures, interferes with the pro-survival Akt/GSK3β pathway. After mechanical ventilation (n=6 per group), there was a decrease in Akt pS473 (a), GSK3β pS9 (b) and PTEN pS380 (c). In these animals we observed an increase in the expression of the tyrosine hydroxylase gene (Th), a marker of dopaminergic activity (d). In brain slices (obtained under non-ventilated conditions, n=6-9 per group), dopamine caused a decrease in Akt pS473, which was mitigated by DRD2 receptor blockade with haloperidol. Treatment with a DRD1 receptor blocker (SCH-23390) did not result in attenuation of Akt phosphorylation (e). *p<0.05 in post-hoc test vs the sham group.

Mechanical ventilation causes hippocampal neural apoptosis by a vagal-dopaminergic axis.

To further identify the mechanisms responsible for ventilation-induced neuronal apoptosis in the HF, mice were randomized to high positive pressure ventilation alone, after pre-treatment with haloperidol or bilateral cervical vagotomy. Both haloperidol pre-treatment and vagotomy decreased the activation of the apoptotic cascade triggered by mechanical ventilation. This was evidenced by absence of changes in caspase-9, activated caspase-7 and cleaved PARP-1 in both the haloperidol and vagotomy treated animals (Figure 3a-c). Accordingly, no PARP-1-positive neurons were observed in hippocampal formation (HF) from treated mice (Figure 3d).

Both haloperidol and vagotomy restored the phosphorylation status of the PTEN/Akt/GSK3β pathway. Increase in the activity of this pro-survival pathway was moderate in mice treated with haloperidol, whereas vagotomized animals showed levels identical to those observed in the sham group (Figure 3e-g), suggesting afferent signals from the vagus nerve may play a fundamental role in brain “injury” during mechanical ventilation. Finally, vagotomy, but not haloperidol treatment, reversed the increase in Th expression induced by mechanical ventilation (Figure 3h).

Taken together these data suggest that stimulation of vagal afferents by mechanical ventilation may lead to increased dopamine levels which in turn activates DRD2 receptors mediating inactivation of the Akt/Gsk3 survival pathway.

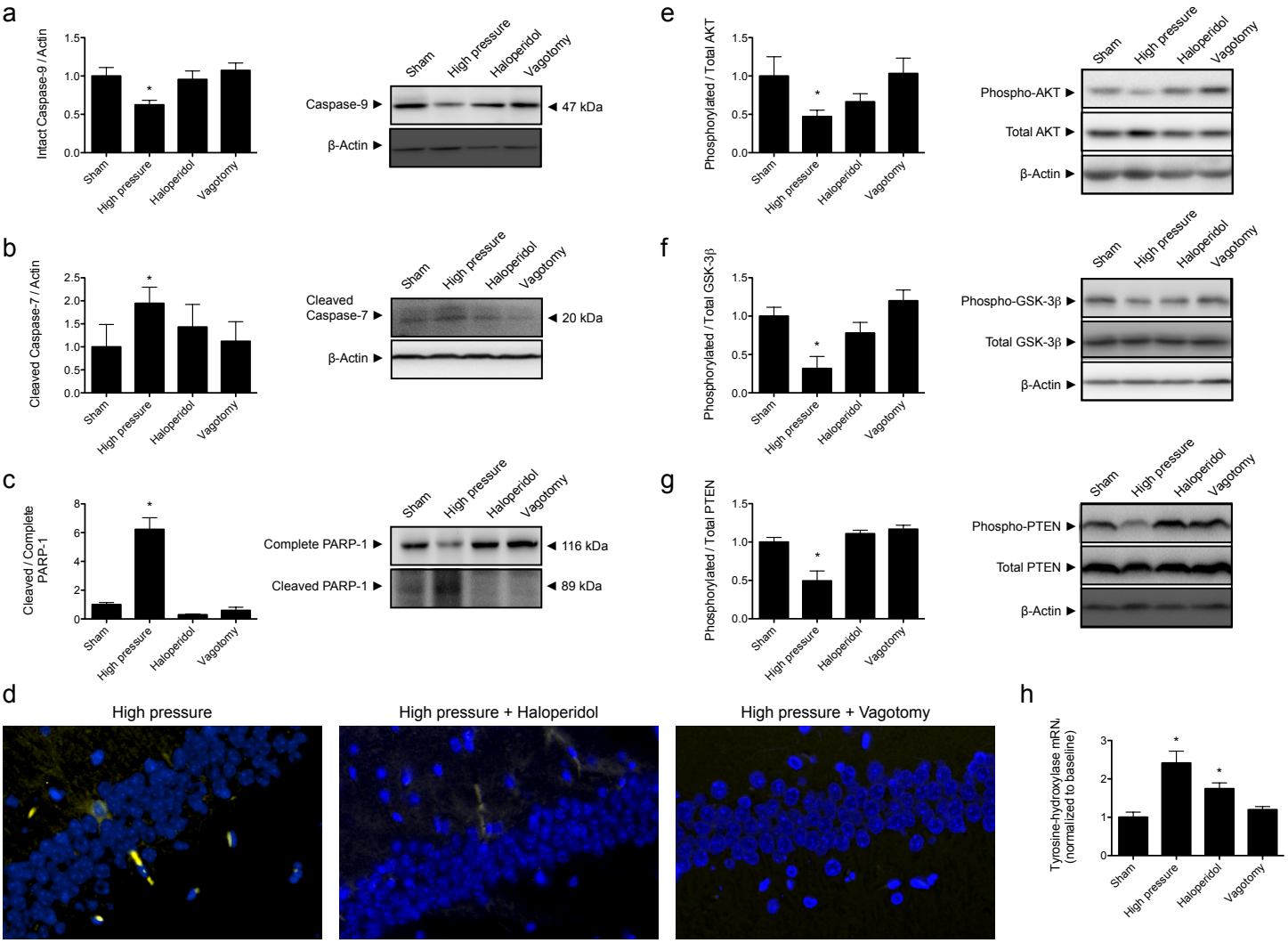

Figure 3. Hippocampal apoptosis is mediated by dopaminergic vagal afferent signaling. The changes in intact caspase-9 (a), cleaved caspase-7 (b) and cleaved PARP-1 (c) observed after high-pressure ventilation were prevented by treatment with haloperidol or vagotomy. No apoptotic neurons, detected by cleaved-PARP-1 immunoreactivity, were observed in ventilated mice after haloperidol treatment or bilateral vagotomy (d). Similarly, Akt pS473 (e), GSK3β pS9 (f) and PTEN pS308 (g) was attenuated in treated animals. Finally, vagotomy, but not haloperidol treatment, dampened Th gene expression (h). *p<0.05 in post-hoc test vs the sham group, n=6 per group.

Mechanical ventilation induces an increase in the hippocampal levels of dysbindin-1.

The protein dysbindin-1 is involved in the recycling of DRD2, and acts as a compensatory mechanism to reduce the effects of dopamine in hyperdopaminergic states[12,21-23]. To study the potential role of dysbindin-1 in apoptosis following activation of dopaminergic vagal afferents, we first measured the expression of the the gene encoding mouse dysbindin-1, *Dntbp1* in the HF. High-pressure mechanical ventilation did not affect total *Dntbp1* mRNA levels (Figure 4a), but induced an increase in the expression of the specific variant *1C* (Figure 4b). There was a slight increase in Dysbindin-1 protein after high-pressure ventilation. To further validate this finding, additional mice were ventilated for longer periods of time for 330 min. In this prolonged ventilation group, there was a significant increase in Dysbindin-1C, but not in the 1A variant (Figure 4c and supplemental Figure S3). Dysbindin-1B was not observed as it is not expressed in mice(25). These results were confirmed by immunohistochemistry studies showing prominent staining in hippocampal neurons for dysbindin-1 after longer ventilation time (Figure 4d).

To further characterize changes in dysbindin-1C levels in response to a hyperdopaminergic state, cultured brain slices were exposed to dopamine. In this model, dopamine treatment induced increased *Dntbp1C* gene expression, which was blocked by addition of haloperidol to the medium (Figure 4e). Moreover, in our *in vivo* model, blockade of DRD2 receptors or the afferent vagal signaling (with haloperidol or vagotomy respectively) inhibited dopamine-induced increases in *Dntbp1C* gene expression (Figure 4e) and decreased immunoreactivity for dysbindin-1 in HF sections (Figure 4g). These results indicate hyperdopaminergia triggers the expression of the dysbindin-1C gene.

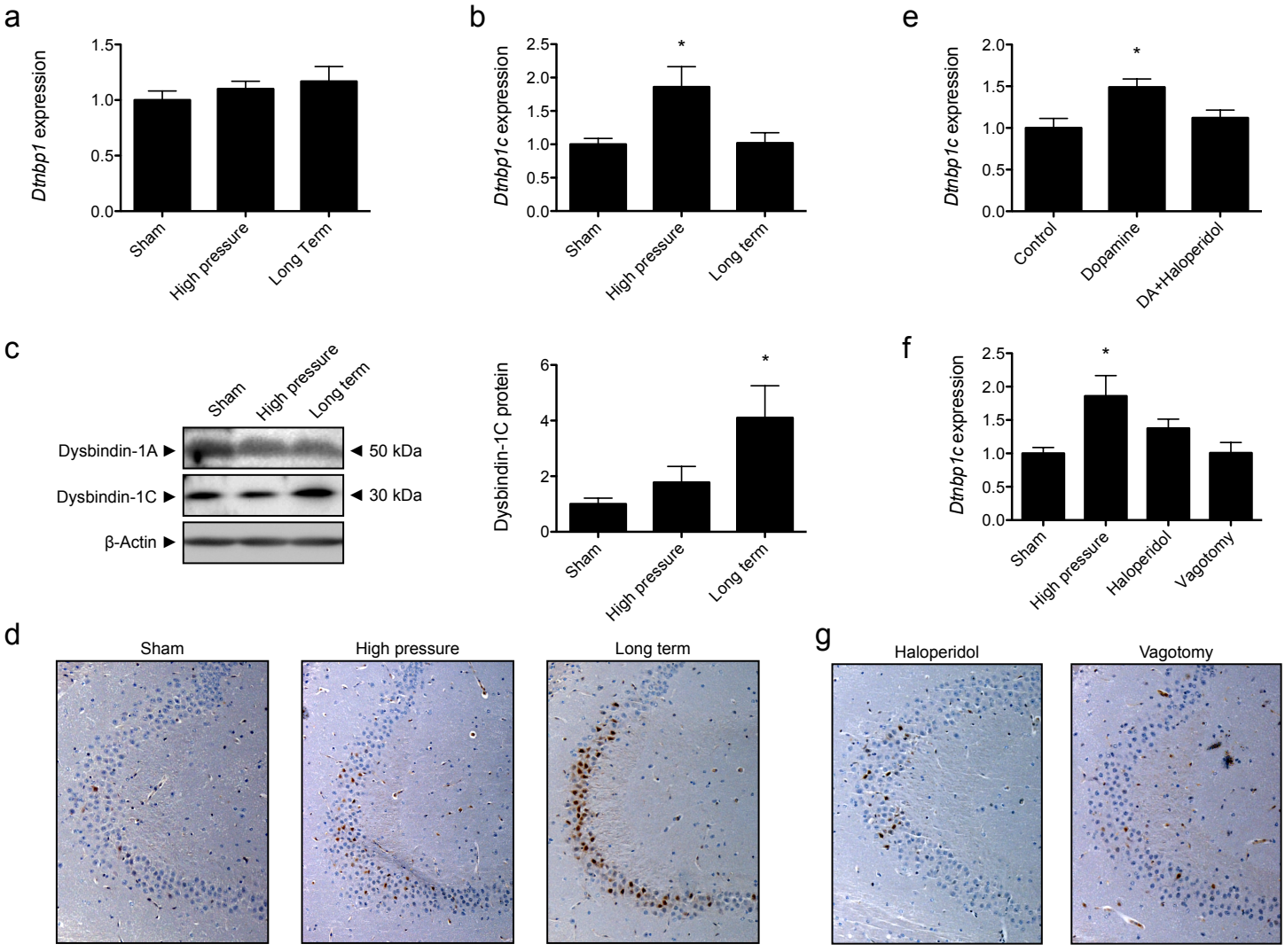

Figure 4. Changes in dysbindin-1 gene and protein expression in the hippocampal formation after mechanical ventilation. Although total expression of *Dtnbp1* gene did not change with mechanical ventilation (a, n=6 per group), there was a short-term increase in gene (though not protein) expression for dysbindin-1C (b), which later translated into an increased dysbindin-1C, but not dysbindin-1A protein (c). Immunohistochemistry for dysbindin-1 showed an increase in the expression of this protein in CA2/3 neurons (d). To demonstrate that this increase was triggered by dopamine, brain slices were cultured in the presence of dopamine, which resulted in increased Dntbp1C gene expression that could be inhibited by haloperidol (e, n≥6 per group). Similarly, haloperidol-treated or vagotomized mice did not show increased Dntbp1C gene expression (f, n≥5 per group) or elevated dysbindin-1 immunostaining in the CA2/3 (g). *p<0.05 in post-hoc test vs the sham/control group.

Dysbindin levels are increased in hippocampi of mechanically ventilated patients.

To extend the clinical validity of our findings, sections from the hippocampi from critically ill, mechanically ventilated (n=10) and non-ventilated patients (n=5) were reacted immunohistochemically for dysbindin-1, and the intensity of the signal quantified.

Clinical details of these patients are included in Supplemental Table 1. Brain samples from ventilated patients showed a statistically significant increase in levels of Dysbindin-1, mainly in CA2 and CA3 areas (Figure 5a) in contrast to the mild signal observed in non-ventilated patients (Figure 5b). Moreover, there was a moderate, but significant (ρ=0.633, p=0.015) correlation between intensity of the signal and duration of mechanical ventilation (Figure 5c) These data demonstrate that dysbindin-1 is overexpressed in brains from ventilated patients, which may reflect a compensatory mechanism to avoid the consequences of hyperdopaminergia.

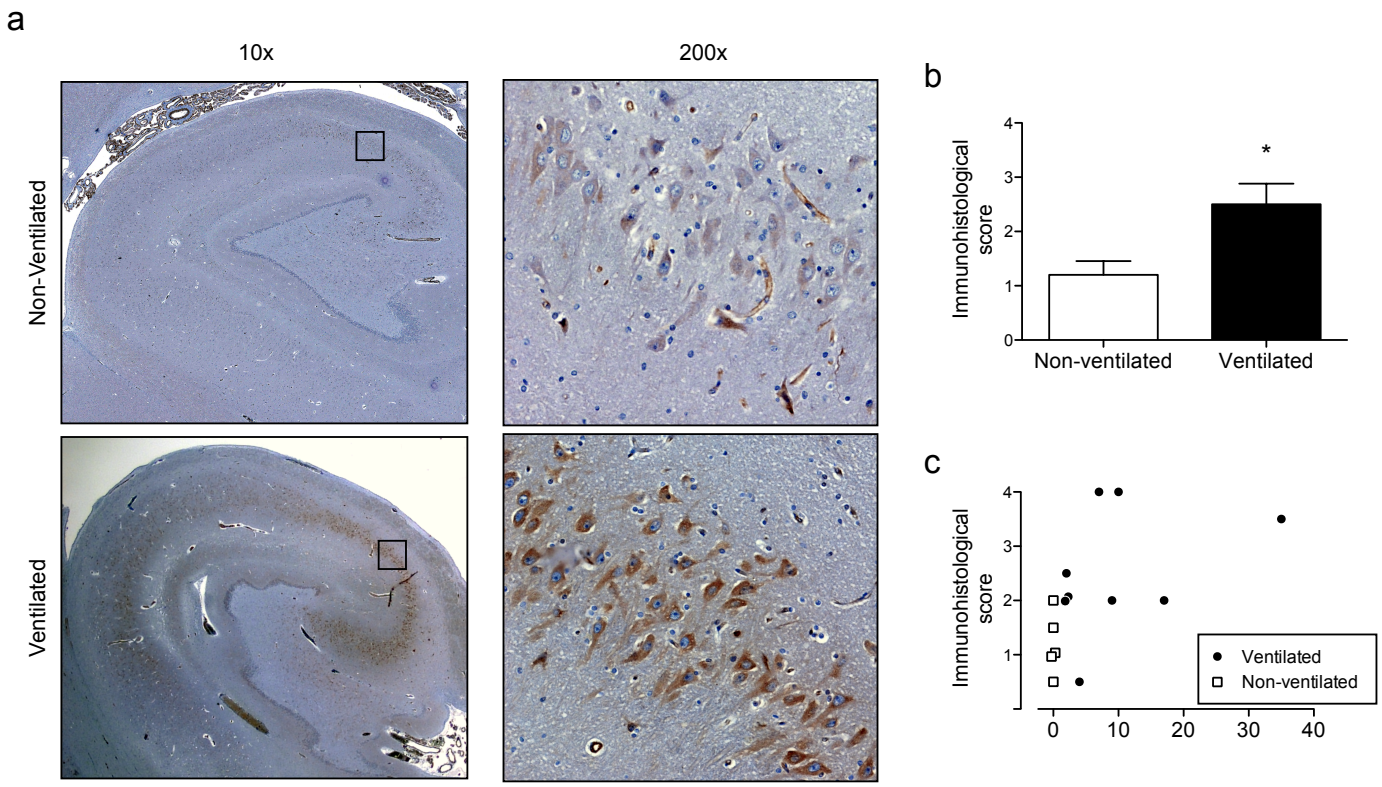

Figure 5. Dysbindin-1 immunohistochemistry of hippocampal formation sections from non-ventilated and mechanically-ventilated patients. Immunoreactivity in the ventilated patients was greater in neurons throughout the hippocampal formation (a, left panels), but was most apparent in CA2/3 (a, right panels). Squared areas in the left panels correspond to the high power fields. Intensity of immunoreaction was semiquantitatively analyzed, confirming that the difference was significant (b). *$p<0.05$ vs non-ventilated patients.

Discussion.

The results presented here demonstrate that mechanical ventilation selectively triggers hippocampal neuronal cell apoptosis. Based on our current findings, afferent vagus signals appear to be stimulated by positive pressure ventilation. The result is increased transcription of tyrosine hydroxylase, the rate-limiting enzyme in the synthesis of dopamine. Via activation of DRD2, ventilation-induced hyperdopaminergic state inhibits the Akt/ GSK3 cell survival pathway potentiating neuronal apoptosis. Concomitantly, mechanical ventilation also leads to increased expression of the transcripts for dysbindin-1C. Consequent increased in dysbindin-1 in hippocampal formation neurons presumably serves as a compensatory mechanism to counteract increased DRD2 receptor activation, because dysbindin-1 appears to depress recycling of DRD2(14, 15) and can thereby counteract its inhibitory effect on pro-survival pathways.

The development of neurobehavioral disorders in critically ill patients is an emerging concern in intensive care medicine. These patients show symptoms of brain dysfunction that range from delirium to long-term cognitive impairments(2). Moreover, the intensity of the former predicts the severity of the latter, suggesting that both syndromes could be related(6). Collectively, these neurological alterations pose a substantial burden among ICU survivors. However, the causes of these syndromes are unknown. Among different risk factors identified in observational studies, mechanical ventilation is one of the most relevant(26), but a causative relationship has not been identified. Here we demonstrate that positive-pressure ventilation causes hippocampal neuronal apoptosis.

In a recent study looking at brain autopsy samples from critically ill patients suffering from delirium, pathologic lesions normally attributed to hypoxia or ischemia were noted in the hippocampus, pons, and striatum. By far the most common neuropathologic site of injury associated with delirium is the hippocampus(27). Notably, most of the cases received mechanical ventilation. In a larger study, decreased hippocampal volumes were associated with a longer duration of delirium in similar populations(28). These results support the findings in septic animals, which show increased neuronal apoptosis in the hippocampal region correlated with a poor performance in behavior and memory tests(29). Since the HF integrates contextual

sensory information to consolidate memory, the observed neuronal apoptosis could be the basis for the behavioral disorders observed in ventilated patients.

The mechanisms that lead to cell death in our model include vagal afferent signaling, DRD2 activation, and inactivation of the Akt/ GSK3β pathway. Fibers from different organs, including the lungs, can reach the HF via the vagus nerve and its targets in the brainstem(30). The *nucleus tractus solitarius* is the main vagal target there, and lung stretch results in its activation(31). From here, fibers reach the HF by a multisynaptic pathway that includes catecholaminergic neurons(32). Moreover, the increased expression of tyrosine hydroxylase observed in our experiments, which is ameliorated by vagotomy but not by haloperidol, reinforces this result.

The release of dopamine within the hippocampus after vagal stimulation results in the activation of DRD2. Elevated dopaminergic activity has been invoked as the cause for a large number of neuropsychological and neuropsychiatric disturbances(33-35). In these hyperdopaminergic states, DRD2 signaling inactivates Akt in a cAMP-independent manner(8, 36). The decreased phosphorylation of PTEN results in the active form of this enzyme, thus inhibiting the PI3-kinase activity and blocking Akt phosphorylation. Deactivation of Akt results in a concomitant dephosphorylation/activation of GSK3β. Our results are in keeping with this overall hypothesis, which is also observed in other experimental and clinical studies dealing with dopamine-dependent behaviors like schizophrenia(9, 37, 38). Similarly, hippocampal cells exposed to dopamine show a decreased mitochondrial mobility in response to dopamine(39), which is mediated by GSK3β. The selective damage, the absence of changes in *Hif1α* (thus discarding hypoxia) and the effects of vagotomy and haloperidol reinforce the neural signaling as the main mechanism of brain injury in our study.

The resulting increased GSK3β activity may trigger apoptosis by direct mitochondrial injury(40). Similar apoptotic effects of dopamine have been observed in cortical neurons(41). Damaged mitochondria activate the caspase cascade, including activation of caspase-7, a major player of this pathway in the brain(42). This leads to the downstream cleavage of PARP-1 and the accumulation of the 89-kDa fragment in the cytoplasm, as observed in our immunohistochemical studies(43, 44). A schematic

representation of putative molecular mechanisms involved in ventilation-induced hippocampal neuronal cell apoptosis is presented in Figure 6.

Finally, we have observed an increase in gene and protein expression dysbindin-1. This protein participates in the recycling of postsynaptic DRD2 receptors(14), and its increase could be viewed as a compensatory mechanism aimed to ameliorate the detrimental effects of hyperdopaminergia. Increased dysbindin-1C expression in the hippocampi from ventilated patients suggests that this protein could play a role in the regulation of brain responses to critical illness and mechanical ventilation. Deficiencies in dysbindin-1C have been related to neurobehavioral diseases such as schizophrenia(45, 46).

Our results have some clinical implications. First, we have described a mechanism that explains the effects of mechanical ventilation on the brain, and could serve as a framework to study the neurocognitive disturbances in critically-ill, mechanically-ventilated patients and the effects of different treatments. In this sense, DRD2 blockers have been demonstrated as a useful strategy to decrease the incidence and severity of delirium(47). Additionally, the pathway identified may be genetically regulated. Different polymorphisms in *DRD2*(48), *Akt*(49) and *DTNBP1*(16) genes have been linked to hyperdopaminergic states. These could confer susceptibility to ICU-related delirium or cognitive impairment, and could help to identify patients amenable to prophylactic interventions, determine the proper antipsychotic treatment and predict its response.

In conclusion, we have identified a novel mechanism that triggers hippocampal apoptosis in response to lung stretch. In spite of the limitations of our experimental model, such as the short ventilatory time or the lack of a direct relationship between hippocampal cell apoptosis and functional impairment, our results propose a novel framework to explain the development of neurobehavioral disorders in patients exposed to mechanical ventilation. The data from autopsy material also support the translation of our results to patients. Ultimately, these findings could help to develop novel therapeutic strategies for improving the outcome of critically ill patients.

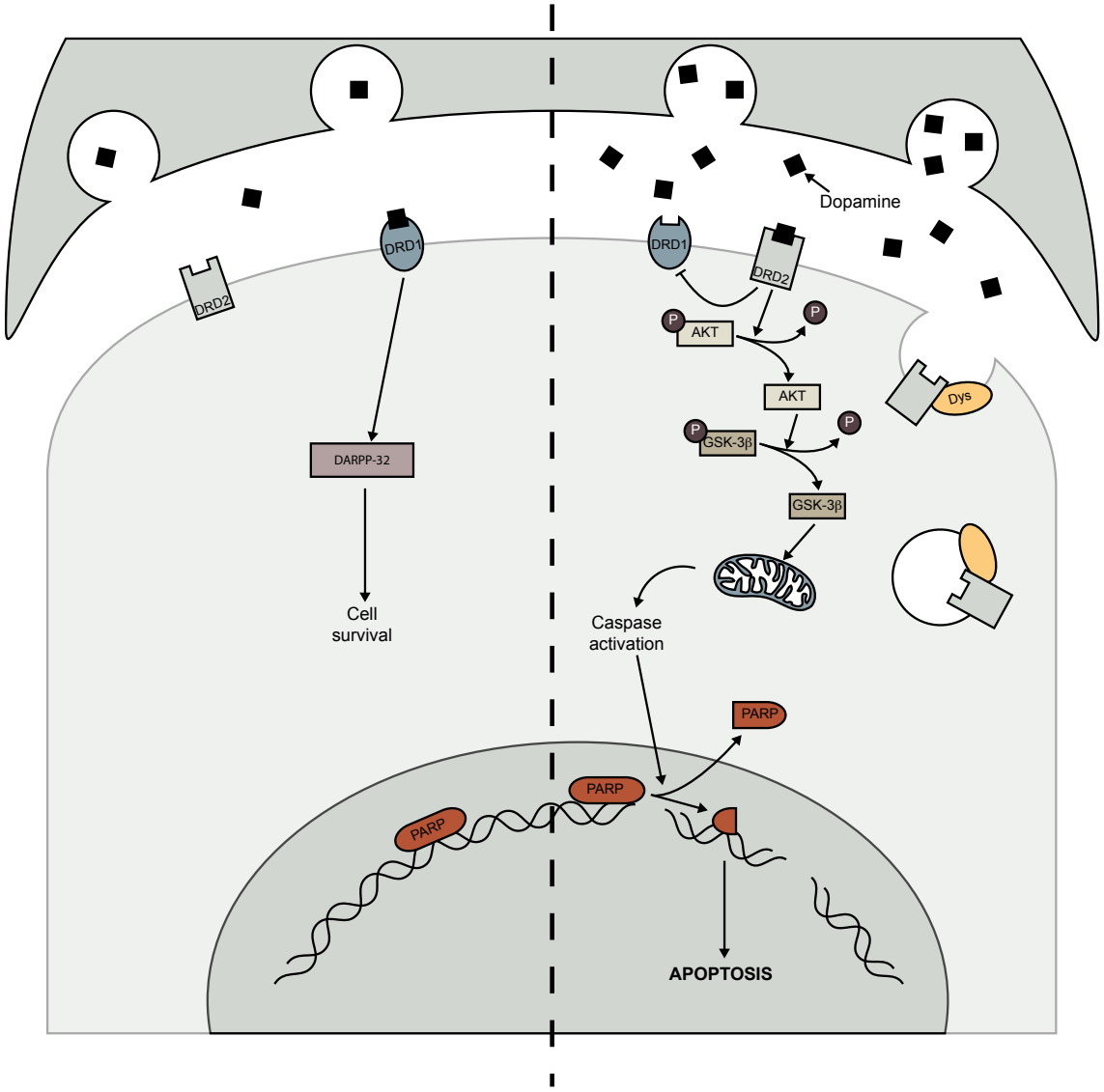

Figure 6. Schematic representation of the mechanisms of cell apoptosis induced by dopamine in our model. Under normal conditions, dopamine activates its type 1 receptors (DRD1, left part of the figure). The increased release of dopamine (right part of the figure) activates type 2 dopamine receptors (DRD2), resulting in decreased activation of Akt (i.e., decreased Akt pS473/pThr308) and therefore decreased inhibition of GSK3β (i.e., decreased GSK3β pS9). The resulting activation of GSK3β triggers the intrinsic apoptotic pathway. Mitochondria are damaged and caspases activated. In the final steps of this cascade, PARP-1 is cleaved and a 89-kDa fragment is released from the nucleus into the cytoplasm. Cleaved PARP-1 is unable to maintain its DNA repairing capabilities, resulting in apoptosis.

Acknowledgments

The authors thank Carlos López-Otín and Ana Gutiérrez-Fernández for their support during the realization of this project. This Project has been supported by Instituto de Salud Carlos III (FIS PI 10-00606). A.G.L. is the recipient of a grant from Universidad de Oviedo (UNOV-09-pf). A. A. And I.L.A are recipients of a grant from Instituto Universitario de Oncología del Principado de Asturias. E.B.S is the recipient of a grant from Fundación para el Fomento en Asturias de la Investigación Científica Aplicada y la Tecnología (FICYT, COF-11-40). GMA is the recipient of a grant from Instituto de Salud Carlos III (Intensificación de la Actividad Investigadora-INT 12/007).

References.

1. Jones SF, Pisani MA. Icu delirium: An update. *Curr Opin Crit Care* 2012;18:146-151.
2. Girard TD. Brain dysfunction in patients with chronic critical illness. *Respir Care* 2012;57:947-955; discussion 955-947.
3. Pun BT, Ely EW. The importance of diagnosing and managing icu delirium. *Chest* 2007;132:624-636.
4. Ely EW, Shintani A, Truman B, Speroff T, Gordon SM, Harrell FE, Jr., Inouye SK, Bernard GR, Dittus RS. Delirium as a predictor of mortality in mechanically ventilated patients in the intensive care unit. *JAMA* 2004;291:1753-1762.
5. Morandi A, Rogers BP, Gunther ML, Merkle K, Pandharipande P, Girard TD, Jackson JC, Thompson J, Shintani AK, Geevarghese S, Miller RR, 3rd, Canonico A, Cannistraci CJ, Gore JC, Ely EW, Hopkins RO. The relationship between delirium duration, white matter integrity, and cognitive impairment in intensive care unit survivors as determined by diffusion tensor imaging: The visions prospective cohort magnetic resonance imaging study*. *Crit Care Med* 2012;40:2182-2189.
6. Girard TD, Jackson JC, Pandharipande PP, Pun BT, Thompson JL, Shintani AK, Gordon SM, Canonico AE, Dittus RS, Bernard GR, Ely EW. Delirium as a predictor of long-term cognitive impairment in survivors of critical illness. *Crit Care Med* 2010;38:1513-1520.
7. Jacobi J, Fraser GL, Coursin DB, Riker RR, Fontaine D, Wittbrodt ET, Chalfin DB, Masica MF, Bjerke HS, Coplin WM, Crippen DW, Fuchs BD, Kelleher RM, Marik PE, Nasraway SA, Jr., Murray MJ, Peruzzi WT, Lumb PD. Clinical practice guidelines for the sustained use of sedatives and analgesics in the critically ill adult. *Crit Care Med* 2002;30:119-141.
8. Beaulieu JM, Sotnikova TD, Marion S, Lefkowitz RJ, Gainetdinov RR, Caron MG. An akt/beta-arrestin 2/pp2a signaling complex mediates dopaminergic neurotransmission and behavior. *Cell* 2005;122:261-273.
9. Li YC, Gao WJ. Gsk-3beta activity and hyperdopamine-dependent behaviors. *Neurosci Biobehav Rev* 2011;35:645-654.

10. Beaulieu JM, Gainetdinov RR, Caron MG. The akt-gsk-3 signaling cascade in the actions of dopamine. *Trends Pharmacol Sci* 2007;28:166-172.
11. Fuster-Matanzo A, Llorens-Martin M, de Barreda EG, Avila J, Hernandez F. Different susceptibility to neurodegeneration of dorsal and ventral hippocampal dentate gyrus: A study with transgenic mice overexpressing gsk3beta. *PLoS One* 2011;6:e27262.
12. Gomez-Sintes R, Hernandez F, Lucas JJ, Avila J. Gsk-3 mouse models to study neuronal apoptosis and neurodegeneration. *Frontiers in molecular neuroscience* 2011;4:45.
13. Song MS, Salmena L, Pandolfi PP. The functions and regulation of the pten tumour suppressor. *Nat Rev Mol Cell Biol* 2012;13:283-296.
14. Iizuka Y, Sei Y, Weinberger DR, Straub RE. Evidence that the bloc-1 protein dysbindin modulates dopamine d2 receptor internalization and signaling but not d1 internalization. *The Journal of neuroscience : the official journal of the Society for Neuroscience* 2007;27:12390-12395.
15. Ji Y, Yang F, Papaleo F, Wang HX, Gao WJ, Weinberger DR, Lu B. Role of dysbindin in dopamine receptor trafficking and cortical gaba function. *Proc Natl Acad Sci U S A* 2009;106:19593-19598.
16. Voisey J, Swagell CD, Hughes IP, Connor JP, Lawford BR, Young RM, Morris CP. A polymorphism in the dysbindin gene (dtnbp1) associated with multiple psychiatric disorders including schizophrenia. *Behavioral and brain functions : BBF* 2010;6:41.
17. Ely EW, Inouye SK, Bernard GR, Gordon S, Francis J, May L, Truman B, Speroff T, Gautam S, Margolin R, Hart RP, Dittus R. Delirium in mechanically ventilated patients: Validity and reliability of the confusion assessment method for the intensive care unit (cam-icu). *JAMA* 2001;286:2703-2710.
18. dos Santos CC, Slutsky AS. The contribution of biophysical lung injury to the development of biotrauma. *Annu Rev Physiol* 2006;68:585-618.
19. Quilez ME, Fuster G, Villar J, Flores C, Marti-Sistac O, Blanch L, Lopez-Aguilar J. Injurious mechanical ventilation affects neuronal activation in ventilated rats. *Crit Care* 2011;15:R124.
20. dos Santos CC, Shan Y, Akram A, Slutsky AS, Haitsma JJ. Neuroimmune regulation of ventilator-induced lung injury. *Am J Respir Crit Care Med* 2011;183:471-482.
21. Gonzalez-Lopez A, Astudillo A, Garcia-Prieto E, Fernandez-Garcia MS, Lopez-Vazquez A, Batalla-Solis E, Taboada F, Fueyo A, Albaiceta GM. Inflammation and matrix remodeling during repair of ventilator-induced lung injury. *Am J Physiol Lung Cell Mol Physiol* 2011;301:L500-509.
22. Molz S, Dal-Cim T, Budni J, Martin-de-Saavedra MD, Egea J, Romero A, del Barrio L, Rodrigues AL, Lopez MG, Tasca CI. Neuroprotective effect of guanosine against glutamate-induced cell death in rat hippocampal slices is mediated by the phosphatidylinositol-3 kinase/akt/ glycogen synthase kinase 3beta pathway activation and inducible nitric oxide synthase inhibition. *Journal of neuroscience research* 2011;89:1400-1408.
23. Livak KJ, Schmittgen TD. Analysis of relative gene expression data using real-time quantitative pcr and the 2(-delta delta c(t)) method. *Methods* 2001;25:402-408.
24. Wiener CM, Booth G, Semenza GL. In vivo expression of mrnas encoding hypoxia-inducible factor 1. *Biochem Biophys Res Commun* 1996;225:485-488.

25. Talbot K, Ong WY, Blake DJ, Tang J, Louneva N, Carlson GC. Dysbindin-1 and its protein familiy with special attention to the potential role of dysbindin-1 in neuronal functions and the pathophysiology of schizophrenia. In: Javitt D, Kantorowitz J, editors. Handbook of neurochemistry and molecular neurobiology. New York: Springer; 2009. p. 107 - 241.
26. Cavallazzi R, Saad M, Marik PE. Delirium in the icu: An overview. *Annals of intensive care* 2012;2:49.
27. Janz DR, Abel TW, Jackson JC, Gunther ML, Heckers S, Ely EW. Brain autopsy findings in intensive care unit patients previously suffering from delirium: A pilot study. *J Crit Care* 2010;25:538 e537-512.
28. Gunther ML, Morandi A, Krauskopf E, Pandharipande P, Girard TD, Jackson JC, Thompson J, Shintani AK, Geevarghese S, Miller RR, 3rd, Canonico A, Merkle K, Cannistraci CJ, Rogers BP, Gatenby JC, Heckers S, Gore JC, Hopkins RO, Ely EW. The association between brain volumes, delirium duration, and cognitive outcomes in intensive care unit survivors: The visions cohort magnetic resonance imaging study*. *Crit Care Med* 2012;40:2022-2032.
29. Semmler A, Frisch C, Debeir T, Ramanathan M, Okulla T, Klockgether T, Heneka MT. Long-term cognitive impairment, neuronal loss and reduced cortical cholinergic innervation after recovery from sepsis in a rodent model. *Experimental neurology* 2007;204:733-740.
30. Castle M, Comoli E, Loewy AD. Autonomic brainstem nuclei are linked to the hippocampus. *Neuroscience* 2005;134:657-669.
31. Gourine AV, Dale N, Korsak A, Llaudet E, Tian F, Huckstepp R, Spyer KM. Release of atp and glutamate in the nucleus tractus solitarii mediate pulmonary stretch receptor (breuer-hering) reflex pathway. *The Journal of physiology* 2008;586:3963-3978.
32. Mello-Carpes PB, Izquierdo I. The nucleus of the solitary tract-->nucleus paragigantocellularis-->locus coeruleus-->ca1 region of dorsal hippocampus pathway is important for consolidation of object recognition memory. *Neurobiology of learning and memory* 2012;100C:56-63.
33. Abi-Dargham A, Moore H. Prefrontal da transmission at d1 receptors and the pathology of schizophrenia. *The Neuroscientist : a review journal bringing neurobiology, neurology and psychiatry* 2003;9:404-416.
34. Dzirasa K, Ramsey AJ, Takahashi DY, Stapleton J, Potes JM, Williams JK, Gainetdinov RR, Sameshima K, Caron MG, Nicolelis MA. Hyperdopaminergia and nmda receptor hypofunction disrupt neural phase signaling. *The Journal of neuroscience : the official journal of the Society for Neuroscience* 2009;29:8215-8224.
35. Simpson EH, Kellendonk C, Kandel E. A possible role for the striatum in the pathogenesis of the cognitive symptoms of schizophrenia. *Neuron* 2010;65:585-596.
36. Beaulieu JM, Del'guidice T, Sotnikova TD, Lemasson M, Gainetdinov RR. Beyond camp: The regulation of akt and gsk3 by dopamine receptors. *Frontiers in molecular neuroscience* 2011;4:38.
37. Jope RS. Glycogen synthase kinase-3 in the etiology and treatment of mood disorders. *Frontiers in molecular neuroscience* 2011;4:16.
38. Krishnan V, Han MH, Mazei-Robison M, Iniguez SD, Ables JL, Vialou V, Berton O, Ghose S, Covington HE, 3rd, Wiley MD, Henderson RP, Neve RL, Eisch AJ, Tamminga CA, Russo SJ, Bolanos CA, Nestler EJ. Akt signaling within the ventral

tegmental area regulates cellular and behavioral responses to stressful stimuli. *Biol Psychiatry* 2008;64:691-700.
39. Chen S, Owens GC, Edelman DB. Dopamine inhibits mitochondrial motility in hippocampal neurons. *PLoS One* 2008;3:e2804.
40. Beurel E, Jope RS. The paradoxical pro- and anti-apoptotic actions of gsk3 in the intrinsic and extrinsic apoptosis signaling pathways. *Progress in neurobiology* 2006;79:173-189.
41. Zhang L, Yang H, Zhao H, Zhao C. Calcium-related signaling pathways contributed to dopamine-induced cortical neuron apoptosis. *Neurochemistry international* 2011;58:281-294.
42. Larner SF, McKinsey DM, Hayes RL, KK WW. Caspase 7: Increased expression and activation after traumatic brain injury in rats. *J Neurochem* 2005;94:97-108.
43. Chaitanya GV, Steven AJ, Babu PP. Parp-1 cleavage fragments: Signatures of cell-death proteases in neurodegeneration. *Cell communication and signaling : CCS* 2010;8:31.
44. Soldani C, Lazze MC, Bottone MG, Tognon G, Biggiogera M, Pellicciari CE, Scovassi AI. Poly(adp-ribose) polymerase cleavage during apoptosis: When and where? *Experimental cell research* 2001;269:193-201.
45. Tang J, LeGros RP, Louneva N, Yeh L, Cohen JW, Hahn CG, Blake DJ, Arnold SE, Talbot K. Dysbindin-1 in dorsolateral prefrontal cortex of schizophrenia cases is reduced in an isoform-specific manner unrelated to dysbindin-1 mrna expression. *Human molecular genetics* 2009;18:3851-3863.
46. Talbot K, Louneva N, Cohen JW, Kazi H, Blake DJ, Arnold SE. Synaptic dysbindin-1 reductions in schizophrenia occur in an isoform-specific manner indicating their subsynaptic location. *PLoS One* 2011;6:e16886.
47. Wang W, Li HL, Wang DX, Zhu X, Li SL, Yao GQ, Chen KS, Gu XE, Zhu SN. Haloperidol prophylaxis decreases delirium incidence in elderly patients after noncardiac surgery: A randomized controlled trial*. *Crit Care Med* 2012;40:731-739.
48. Morimoto K, Miyatake R, Nakamura M, Watanabe T, Hirao T, Suwaki H. Delusional disorder: Molecular genetic evidence for dopamine psychosis. *Neuropsychopharmacology : official publication of the American College of Neuropsychopharmacology* 2002;26:794-801.
49. Blasi G, Napolitano F, Ursini G, Taurisano P, Romano R, Caforio G, Fazio L, Gelao B, Di Giorgio A, Iacovelli L, Sinibaldi L, Popolizio T, Usiello A, Bertolino A. Drd2/akt1 interaction on d2 c-amp independent signaling, attentional processing, and response to olanzapine treatment in schizophrenia. *Proc Natl Acad Sci U S A* 2011;108:1158-1163.

Supplementary data

Figure S1. Effects of mechanical ventilation on hippocampal formation autophagy.

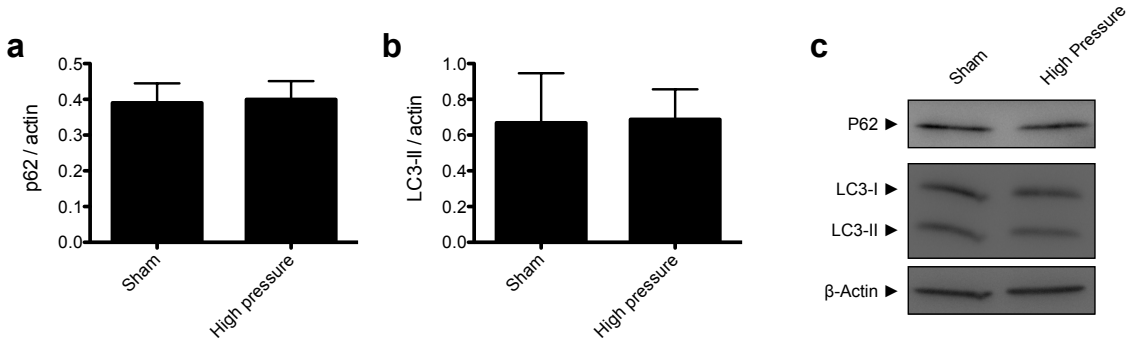

Mechanical ventilation does not modify autophagic activity in the hippocampal formation. As autophagy may be closely related to cell death, levels of p62 (a specific substrate of autophagy, panel a) and LC3-II (the lipidated form of LC3, an essential component of the autophagosomal membrane, panel b) were measured in hippocampal formation homogenates. There were no differences between ventilated and sham groups. Panel c shows representative western blots.

Figure S2. Expression of *Hif1α* in hippocampal formation homogenates.

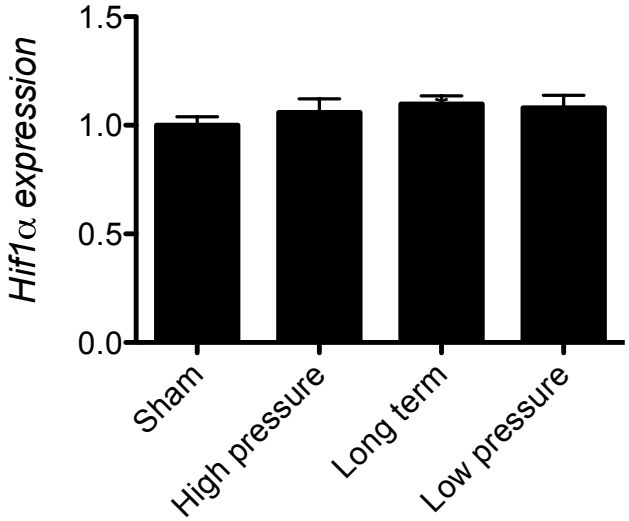

To test the possibility that hypoxia may explain the ventilation effects observed in this study, expression of the *Hif1α* gene was measured. This gene shows a fast response during hypoxia. No such differences were found among the experimental groups, however.

Figure S3. Measurement of Dysbindin-1A.

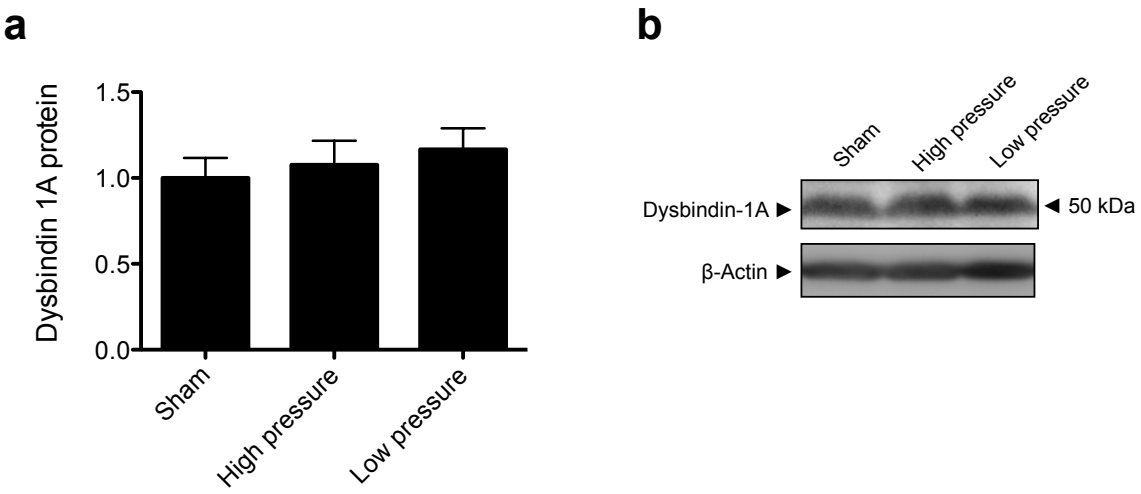

The levels of the dysbindin-1A isoform were measured in hippocampal formation homogenates. There were no significant differences among the experimental groups (panel a). Panel b shows a western blot of these homogenates (also shown in the main results section).

Supplemental Table 1. Clinical data from patients included in the study. HIV: Human immunodeficiency virus. AIDS: Acquired immunodeficiency syndrome.

	Age	Sex	Diagnosis	Days of ventilation
1	58	Male	Severe pneumonia	4
2	49	Male	H1N1 influenza	2
3	53	Male	Severe pneumonia	35
4	74	Female	Intestinal ischemia Sepsis	2
5	39	Male	Aortic replacement. Postoperative multiorgan failure	7
6	47	Female	Acute leukemia Alveolar hemorrhage	17
7	73	Female	Lupus Sepsis of unknown origin	9
8	63	Male	Bone marrow transplantation Respiratory failure	2
9	41	Male	Cirrhosis Aspiration pneumonia, sepsis	10
10	68	Male	Dilated cardiomyopathy	-
11	45	Male	HIV infection, AIDS Sepsis	-
12	73	Male	Kidney failure	-
13	71	Male	Pneumonia and sepsis	-
14	24	Female	Fulminant hepatitis	-

There were no differences in age between ventilated and non-ventilated patients (56±21 *vs* 55±13 years respectively, p=0.92).

DISCUSIÓN

El síndrome de daño pulmonar definido bajo el término de distrés respiratorio agudo se caracteriza por la presencia de inflamación, hipoxia, edema pulmonar de origen no cardiogénico y aumento en el trabajo respiratorio. A pesar de los numerosos estudios experimentales y ensayos clínicos llevados a cabo, no existe ninguna terapia eficaz más allá del tratamiento de la causa inicial de la lesión o de proveer de soporte vital mediante ventilación mecánica. Este hecho ha provocado que tras décadas de estudio la mortalidad del SDRA siga siendo elevada (30-70%) y que la calidad de vida de los supervivientes se siga viendo mermada. Por ello, la adquisición de un conocimiento profundo de los procesos moleculares desencadenados durante el SDRA y su regulación puede ser de gran utilidad para el desarrollo de terapias encaminadas tanto a disminuir la lesión pulmonar y el fallo multiorgánico como a mejorar los procesos de reparación tisular.

La pérdida de integridad de la barrera alveolo capilar durante el SDRA implica tanto una desestructuración de la matriz extracelular como una la afectación de las uniones celulares de la barrera epitelial y del endotelio subyacente. Independientemente de si la causa del SDRA es una agresión directa o indirecta al parénquima pulmonar, el infiltrado leucocitario que llega al tejido procedente de la circulación periférica compromete aun más al pulmón mediante la liberación de distintos mediadores inflamatorios. Esta respuesta inflamatoria supone un mecanismo lesivo adicional que agrava la pérdida de la arquitectura pulmonar y la función respiratoria. En este contexto las MMPs parecen candidatas idóneas para el estudio del SDRA. Esta familia de proteasas posee un amplio catálogo de funciones que van desde el procesado del conjunto de la matriz extracelular, la liberación de cualquier molécula bioactiva unida no covalentemente a ella o su generación (Lin y col., 2008), el procesamiento de proteínas de membrana y la modulación de la actividad de mediadores inmunes, entre otras (Loffek y col., 2011). La implicación de las MMPs en la fisiopatología del distrés respiratorio se ha documentado tanto en estudios clínicos como experimentales. Se han detectado niveles elevados de MMPs en el fluido broncoalveolar de pacientes con distrés respiratorio (Ricou y col., 1996; Lanchou y col., 2003; Brand y col., 2012; Capone y col., 2012) y en los últimos años, distintos modelos experimentales de lesión pulmonar aguda han avalado esta asociación (Foda y col.,

2001; Oyaizu y col., 2012). Sin embargo, el papel específico de cada MMP en el desarrollo de la lesión pulmonar ha de ser estudiado por separado dada la complejidad de sus funciones. El uso de ratones modificados genéticamente deficientes para una MMP específica se constituye por tanto como una herramienta prometedora para su estudio. Así por ejemplo, el uso de ratones *Mmp9*$^{-/-}$ ha servido para demostrar el papel protector de esta proteasa en modelos de daño pulmonar inducido por ventilación mecánica (Albaiceta y col., 2008), ozono (Yoon y col., 2007) o displasia pulmonar (Lukkarinen y col., 2009).

El interés de esta tesis doctoral por la MMP-8 como posible regulador del SDRA viene dado por la presencia de niveles elevados de esta proteasa en el tejido pulmonar de pacientes con este síndrome (Fligiel y col., 2006) o enfermedad pulmonar obstructiva crónica (Vernooy y col., 2004). Por otro lado, aunque los ratones deficientes en MMP-8 no muestran anomalías en el desarrollo embrionario ni en la vida adulta bajo condiciones normales, sí presentan grandes diferencias fenotípicas cuando son expuestos a distintos modelos experimentales (Balbin y col., 2003). Estos hechos denotan que el papel de esta molécula en procesos no patológicos o bien no es significativo o bien es compensado por otras MMPs, pero que juega un papel determinante en el desarrollo de patologías. Concretamente, nos llamó la atención la respuesta inflamatoria anormal provocada por la deficiencia en esta MMP, caracterizada por retrasos tanto en el desarrollo inicial del infiltrado neutrofílico como en el aclaramiento posterior del mismo debido, entre otros mecanismos, a una menor apoptosis. Estos hechos generan un estado inflamatorio prolongado que se traduce en un retraso en el cierre de heridas (Gutierrez-Fernandez y col., 2007) y una mayor susceptibilidad tumoral en un modelo de carcinogénesis experimental (Balbin y col., 2003). Esta capacidad moduladora, unida a la descripción de un creciente número de sustratos procesados por esta MMP (Van Lint and Libert, 2006), nos hizo preguntarnos por su papel en los procesos del daño pulmonar en los que la inflamación es un mecanismo patogenético tan relevante.

Como primera aproximación a su estudio nos quisimos centrar en un modelo de lesión pulmonar aguda inducida por ventilación mecánica. La práctica totalidad de

los enfermos de SDRA ingresados en las unidades de cuidados intensivos necesitan el soporte ventilatorio con presión positiva. A pesar de que esta técnica permite el mantenimiento del intercambio gaseoso en estos pacientes, se asocia, tal y como se ha descrito previamente, a la producción o empeoramiento del daño pulmonar (Terragni y col., 2007). La reducción de la lesión asociada a ventilación mecánica ha resultado ser uno de los pilares del manejo de los pacientes con SDRA, de tal manera que las únicas estrategias terapéuticas que han logrado disminuir la mortalidad de este síndrome son aquellas dirigidas a evitar la lesión adicional del parénquima.

Los modelos experimentales de lesión inducida por ventilación se basan en el uso de presiones inspiratorias elevadas, capaces de generar una respuesta inflamatoria con características similares a la observada durante el SDRA. Nuestros datos muestran un incremento significativo en los niveles de MMP-8 tanto en tejido pulmonar como el lavado broncoalveolar de ratones *Mmp8*$^{+/+}$ sometidos a ventilación mecánica con presión elevada, de forma congruente con estudios recientes en MMP-8 (Dolinay y col., 2008) y con el incremento observado en otras MMPs en modelos similares (Foda y col., 2001; Haseneen y col., 2003; Hasaneen y col., 2005).

Más interesante es el hecho de que los ratones deficientes en MMP-8 mostraron una menor lesión inducida por ventilación tras dos horas de ventilación, con una mejor oxigenación sanguínea y menor edema pulmonar, daño histológico, afectación de la permeabilidad alveolar e infiltrado leucocitario comparado con los ratones *Mmp8*$^{+/+}$. Este hecho se confirmó mediante el estudio de pérdida de función de MMP-8 mediante inhibición farmacológica en ratones *Mmp8*$^{+/+}$. La ausencia de diferencias tanto en las poblaciones leucocitarias circulantes como en el contenido de colágeno entre genotipos, aun con el incremento característico de colágeno asociado a la ventilación encontrado también en otros estudios (de Carvalho y col., 2007), nos llevaron a pensar que las diferencias observadas entre genotipos podían deberse al papel modulador de MMP-8 sobre mediadores inflamatorios. Evaluamos esta posible vía mediante la cuantificación de distintas cito- y quimiocinas tanto en homogeneizados pulmonares como en BALF. Tras la ventilación con presiones elevadas, los animales *Mmp8*$^{-/-}$ mostraron menores niveles de MIP-2 y LIX. Ambas moléculas,

pertenecientes a la familia de las quimiocinas CXC, son potentes quimioatrayentes de neutrófilos. Un retraso inicial de los niveles de MIP-2 durante el proceso inflamatorio ha sido descrito con anterioridad en estos animales, sin embargo esta prórroga podría ser causante a medio plazo de la persistencia en la inflamación observada en otros modelos (Gutierrez-Fernandez y col., 2007). Con respecto a la quimiocina LIX, se ha descrito que MMP-8 es capaz de procesarla generando una forma más activa (Tester y col., 2007) y se ha propuesto que es capaz de liberarla de su unión a elementos de la matriz aumentando su biodisponibilidad (Van Lint y col., 2005), lo que podría explicar no sólo el menor infiltrado encontrado en los ratones *Mmp8*$^{-/-}$ sino también por qué sólo se encontraron diferencias significativas en el BALF. Aunque se ha descrito un aumento en la expresión de IL-1β en modelos crónicos de artritis utilizando ratones deficientes en MMP-8 (Garcia y col., 2010), la ausencia de diferencias en nuestro modelo hace pensar que el papel de MMP-8 en los estadios iniciales de la inflamación no parece involucrar una modulación anormal de las citoquinas proinflamatorias de respuesta rápida. Sin embargo, sí que parece regular la respuesta antiinflamatoria dados los niveles incrementados de IL-4 e IL-10, hecho observado también en un modelo de encefalomielitis autoinmune (Folgueras y col., 2008). Si bien los niveles elevados de IL-4 podrían ser favorables en las primeras fases de la inflamación, es también cierto que se han propuesto como posible causa del defectuoso aclaramiento por apoptosis de los neutrófilos una vez establecido el infiltrado (Gueders y col., 2005; Gutierrez-Fernandez y col., 2007; Cox y col., 2010). De mayor interés nos pareció el incremento en los niveles de IL-10, la única de las citoquinas que se mostró también incrementada tras la terapia inhibitoria. Otros estudios ya han mostrado los beneficios de una respuesta antiinflamatoria mediada por IL-10 durante la lesión inducida por ventilación (Donnelly y col., 1996; Lee y col., 2008; Pedreira y col., 2008; Hoegl y col., 2009). Este contexto nos llevó a intentar comprobar el mecanismo de regulación de MMP-8 sobre IL-10, hecho que discutiremos en párrafos posteriores.

Tras comprobar que la ausencia de MMP-8 se traducía en una menor inflamación en el modelo de lesión pulmonar por ventilación mecánica, nos planteamos estudiar su efecto en un modelo de lesión de causa extrapulmonar como es el de endotoxemia. La administración de LPS es un modelo de inflamación sistémica,

en el que todas las fases de la respuesta inflamatoria, incluyendo la migración leucocitaria, se ven alteradas. La exacerbada liberación de quimioatrayentes durante la sepsis provoca una menor expresión de receptores de quimiocinas CXC (LIX, KC y MIP-2) (Cummings y col., 1999), en parte por internalización de receptores ocupados y en parte vía activación de receptores TLR (Alves-Filho y col., 2009). Además, se ha demostrado que dosis elevadas de algunos PAMPs provocan la desensibilización de sus receptores provocando un aumento en la liberación de especies reactivas de oxígeno (ROS) en detrimento de la quimiotaxis (Bohrer y col., 1991). La pérdida de la respuesta a quimiocinas durante la endotoxemia, unido al aumento tanto de la lesión histológica como del infiltrado inflamatorio en los ratones deficientes en MMP-8, veinticuatro horas tras la inyección intraperitoneal de LPS, nos sugirió que otros factores podrían estar interviniendo en el reclutamiento leucocitario a distancia. El incremento en los niveles de MIP-1α encontrado en ratones *Mmp8*$^{-/-}$, importante mediador proinflamatorio pulmonar en estos animales que se ha visto es inactivado por esta MMP (Quintero y col., 2010) podría explicar, al menos en parte, este aumento del infiltrado. Sin embargo, los modelos utilizados en este estudio fueron de lesión local donde puede existir un gradiente claro de MIP-1α. Por esta razón, consideramos que deberían existir otros factores que explicasen las diferencias existentes en el modelo de afectación sistémica.

Con el objetivo de identificar otros posibles mediadores de la respuesta inflamatoria regulados por MMP-8, llevamos a cabo una aproximación proteómica mediante un análisis 2D-DIGE en homogeneizados pulmonares de animales de ambos genotipos sometidos a endotoxemia. La deficiencia en MMP-8 se tradujo en una acumulación de las alarminas S100A8 y S100A9. Estas proteínas pertenecientes a los DAMPs, representan entre el 30 y el 60% del contenido citoplasmático total en neutrófilos y entre el 1 al 5% en monocitos (Edgeworth y col., 1991). Han sido consideradas tradicionalmente como desencadenantes de respuestas proinflamatorias a través de la activación de la vía de NFκB mediante su unión a receptores TLR-4 y RAGE (Ehlermann y col., 2006; Vogl y col., 2007; Boyd y col., 2008) y su expresión está regulada por estímulos proinflamatorios como TNFα, IL-1, IFNγ y LPS. Estos atributos, unidos a su capacidad de unión al heparán sulfato (Robinson y col., 2002), las dotan de

una preferencia por el tejido pulmonar, altamente vascularizado y con una considerable población de macrófagos residentes y de receptores RAGE y TLR dada su constante exposición a patógenos ambientales. Experimentos funcionales en distintos modelos inflamatorios han demostrado la implicación de estas alarminas en la modulación de la migración leucocitaria mediante el aumento en los niveles de expresión y activación de Mac-1 en neutrófilos y de ICAM-1 y VCAM-1 en células endoteliales, induciendo la adhesión y migración transendotelial de neutrófilos hacia la zona inflamada (Ryckman y col., 2003; Vandal y col., 2003; Raquil y col., 2008). Por otro lado, la activación de receptores RAGE induce una respuesta quimiotáctica mediada por la vía p52-NFκB (Penzo y col., 2010). Nuestros datos muestran la activación de este factor de transcripción en ratones *Mmp8*$^{-/-}$. Se ha descrito que este tipo de activación conlleva una retroalimentación positiva (Gebhardt y col., 2008), lo que podría justificar la persistencia del infiltrado inflamatorio en los animales deficientes en MMP-8.

Algunos autores han relacionado la expresión de proteínas S100A8 y S100A9 con la infiltración tisular por las denominadas células mieloides supresoras, que a su vez son capaces de secretarlas (Sinha y col., 2008). Sin embargo, no encontramos ninguna diferencia en las subpoblaciones leucocitarias en los infiltrados pulmonares de animales *Mmp8*$^{+/+}$ y *Mmp8*$^{-/-}$. La causa de esta ausencia de diferencias podría deberse a que el modelo de endotoxemia no es el más adecuado para estudiar este efecto concreto, dado que se trata de un modelo agudo cuya señal decae rápidamente a partir de las 24 horas (Rojas y col., 2005). Un modelo crónico de infección por patógenos gram-negativos viables podría tener mejores resultados dado que se asemejaría más a las condiciones de inflamación crónicas (Brudecki y col., 2012).

Recientemente, se ha descubierto que IL-10 es capaz de inducir la expresión de ambas S100 (Endoh y col., 2009; Diercks y col., 2013), a la par que se encuentra incrementada en modelos de sepsis polimicrobiana en ratones deficientes en MMP-8 (Solan y col., 2012). Dado el papel modulador de MMP-8 sobre IL-10 parece razonable pensar que la acumulación observada en los animales *Mmp8*$^{-/-}$ podría deberse a una mayor expresión de ambas alarminas. Sin embargo, el análisis de su expresión mediante PCR cuantitativa no mostró diferencias entre genotipos tras el tratamiento

con LPS. En la misma línea, tampoco encontramos diferencias en sus niveles en proteína ni en suero sanguíneo ni en bazo. Esto nos sugiere que la acumulación de S100A8 y S100A9 observada en pulmón no es la manifestación de una diferencia sistémica en los niveles de alarminas sino un fenómeno localizado, y que su causa no viene dada por una mayor expresión sino por una eliminación reducida del parénquima pulmonar. En este sentido, existen diferentes resultados que apoyan el papel regulador que las MMPs ejercen sobre S100A8 y S100A9. MMP-2 y MMP-9 son responsables de la proteólisis de ambas alarminas (Greenlee y col., 2006) y MMP-1a y MMP-8 son capaces de procesar S100A8 (Fanjul-Fernandez y col., 2013)(Dra. Gutiérrez-Fernández, Dr. López-Otín, datos no publicados). La ausencia de cambios compensatorios en MMP-2 y MMP-9 refuerza el papel de MMP-8 en las diferencias observadas entre genotipos.

Si bien es cierto que nuestros resultados muestran que la ausencia de MMP-8 actúa en detrimento de la arquitectura pulmonar, aumentando el daño histológico y la infiltración leucocitaria, acorde con modelos de instilación intratraqueal de LPS (Owen y col., 2004; Quintero y col., 2010); es también cierto que no encontramos diferencias significativas en la supervivencia. En contraposición a este resultado, en los últimos años han aparecido estudios clínicos que muestran no sólo la presencia de niveles elevados de MMP-8 en diversas enfermedades infecciosas (Yazdan-Ashoori y col., 2011; Brand y col., 2012; Haberlandt y col., 2013) sino también su correlación positiva con el grado de severidad de la enfermedad y la mortalidad (Hu y col., 2005; Lauhio y col., 2011). A esto hay que añadirle que diversos estudios experimentales muestran claramente que la inhibición de MMP-8 mejora significativamente la supervivencia tanto en modelos de shock endotóxico como en modelos de sepsis polimicrobiana por ligación- punción cecal (Hu y col., 2005; Vandenbroucke y col., 2012). Ante estos datos, aparentemente contradictorios con el mayor daño histológico observado, cabe plantearse varias explicaciones: La primera es el propio modelo de inflamación sistémica, en el que la mortalidad depende no sólo de la lesión pulmonar sino del desarrollo de fallo multiorgánico. A este respecto hay que destacar que esta disfunción multiorgánica es la principal causa de muerte de los pacientes con sepsis y distrés, mientras que la lesión pulmonar irreversible sólo es responsable de menos de un 30%

de las muertes (Montgomery y col., 1985). Otro ejemplo de la implicación multiorgánica en la sepsis es el desarrollo de disfunción cerebral que sufren hasta un 70% de los pacientes con sepsis (Ebersoldt y col., 2007). En este contexto, MMP-8 ha mostrado tener un papel patogenético tanto en modelos de encefalomielitis autoinmune como en encefalopatías sépticas, al comprometer la integridad de las barreras hematoencefálica mediante degradación proteolítica (Folgueras y col., 2008; Vandenbroucke y col., 2012), hecho que podría explicar la mayor supervivencia de los ratones deficientes en esta MMP.

Otra explicación podría venir de la propia acumulación de S100A8 y S100A9 observada en los ratones *Mmp8*$^{-/-}$. Aunque, como hemos comentado, estas moléculas han sido clasificadas clásicamente como mediadores proinflamatorios, algunos estudios recientes arrojan datos sobre su papel protector y de recuperación de la homeostasis tisular. En primer lugar por su papel antimicrobiano (Steinbakk y col., 1990; Swangchan-Uthai y col., 2012), que podría tener un efecto protector en modelos de sepsis polimicrobiana, aunque no en nuestro modelo de shock endotóxico que carece de carga bacteriana. De mayor interés parecen ser las modificaciones post-translacionales a las que pueden verse sometidos estos mediadores dependiendo de su entorno. Durante la sepsis se produce la liberación de especies reactivas de oxígeno por parte de los neutrófilos con el fin de eliminar la infección. Este aumento del estrés oxidativo puede producir además una mayor inflamación pulmonar, de tal manera que el desequilibrio entre especies oxidantes y reductoras se asocia a un peor pronóstico en pacientes (Ritter y col., 2003). S100A8 y S100A9 han mostrado ser potentes agentes reductores con una enorme susceptibilidad a la oxidación (Sroussi y col., 2012), contribuyendo a recuperar la homeostasis redox en pacientes asmáticos (Gomes y col., 2012). Esta oxidación puede ser transitoria (Lim y col., 2011) y conlleva la pérdida de su capacidad quimiotáctica (Harrison y col., 1999). De manera similar, la nitrosilación de S100A8 parece actuar como un sistema de estabilización de NO, adquiriendo propiedades antiinflamatorias, suprimiendo la adhesión y extravasación de leucocitos (Lim y col., 2009). Por otro lado se ha propuesto que el heterodímero S100A8/A9 podría unirse a las citoquinas proinflamatorias IL-1β, IL-6 y TNFα inhibiendo su actividad (Ikemoto y col., 2007). En conjunto estos hechos podrían explicar por qué

la liberación inicial de S100A8 y S100A9 en forma reducida durante las primeras fases del shock endotóxico favorecería un mayor infiltrado en el pulmón. Su posterior oxidación potencialmente reversible y nitrosilación, favorecerían la respuesta antiinflamatoria encaminada a una mejor resolución, que explicaría tanto la mayor supervivencia observada en otros estudios como la persistencia leucocitaria característica de los *Mmp8*$^{-/-}$.

Continuando con los dos primeros artículos de la presente tesis doctoral, nos planteamos si el papel inmunomodulador de MMP-8 podría tener algún efecto en el desarrollo de la fase fibrótica asociada al SDRA. La desregulación de los procesos de reparación alveolar, destinados a recuperar la función y arquitectura pulmonares, pueden conllevar una cicatrización aberrante caracterizada por un exceso en la síntesis y acumulación de elementos de la matriz extracelular. En estos casos, incluso las maniobras de soporte vital como la ventilación mecánica han demostrado ser, por si solas, desencadenantes de fibrosis al inducir síntesis de colágeno (Armstrong y col., 1999) y procesos de transición epitelio-mesénquima (Cabrera-Benitez y col., 2012). La fibrosis pulmonar resultante genera una pérdida en la elasticidad pulmonar que muy frecuentemente desemboca en un fallo respiratorio progresivo de consecuencias fatales (Rafii y col., 2013). Basado en modelos animales que muestran que la pan-inhibición de MMPs es capaz de disminuir la fibrosis pulmonar inducida por bleomicina (Fujita y col., 2011), se ha propuesto a estas proteasas como posible diana terapéutica en pacientes (Mishra y col., 2011). Sin embargo, aunque se ha documentado que la ausencia de MMPs específicas como MMP-7 protege frente a esta patología mediante la disminución de la biodisponibilidad de TGF-β y la reducción del crecimiento y migración de fibroblastos (Zuo y col., 2002; Dancer y col., 2011), también se ha observado un efecto protector en otras como la MMP-9 o la MMP-19 (Cabrera y col., 2007; Yu y col., 2012). Esta contraposición de efectos subraya la necesidad de estudiar y entender el papel que desempeña cada MMP de manera individual durante el proceso de fibrosis.

Nuestros resultados mostraron un incremento significativo de los niveles de MMP-8 en el tejido pulmonar tanto a 3 días como a 3 semanas tras la administración

de bleomicina. Además, la ausencia de esta metaloproteasa tuvo un efecto antifibrótico no relacionado con alteraciones en la capacidad colagenolítica total. Es interesante ver que, de modo similar a lo que observábamos en el modelo de shock endotóxico, los ratones *Mmp8*$^{-/-}$ presentaron una inflamación pulmonar persistente, atestiguado tanto por el mayor daño histológico como por la mayor presencia de infiltrado neutrofílico positivo para mieloperoxidasa, que a su vez se asocia a mayores niveles de MMP-9 y una menor deposición de fibras de colágeno. Estos hechos que en modelos de heridas cutáneas se traducen en un retraso perjudicial en el proceso de cicatrización (Gutierrez-Fernandez y col., 2007), en el pulmón podrían resultar en una menor fibrosis. Se ha propuesto que la sobreexpresión de MMP-9 tiene un efecto antifibrótico relacionado con la degradación del factor profibrótico IGFBP-3 (del inglés *insulin-like growth factor binding protein-3*)(Cabrera y col., 2007), mecanismo que podría actuar en beneficio de estos animales.

La ausencia de MMP-8 se tradujo en una menor síntesis de colágeno a las 3 semanas, acorde con niveles de actividad reducidos de TGF-β. Esta citoquina antiinflamatoria y con potente actividad profibrótica (Zhou y col., 2012) promueve tanto la síntesis de colágeno como la proliferación de fibroblastos y su diferenciación en miofibroblastos (Todd y col., 2012), encontrándose elevada en pacientes con fibrosis pulmonar (Khalil and Greenberg, 1991). La relación entre un patrón de mayor inflamación y menor fibrosis con niveles reducidos de actividad de TGF-β ha sido previamente observada en un modelo similar en el que utilizaban ratones deficientes en la integrina $\alpha_v\beta_6$, activador de TGF-β latente (Munger y col., 1999). Estos datos nos condujeron al estudio de IL-10, citoquina involucrada en la regulación de la respuesta inflamatoria, con demostrados efectos antifibróticos tanto *in vitro* como *in vivo* (Arai y col., 2000; Garantziotis y col., 2006; Fueki y col., 2007) y capaz de regular tanto la expresión como la activación de TGF- β (Nakagome y col., 2006). Parte de los efectos inhibitorios de IL-10 sobre TGF-β son causados por una disminución en los niveles de expresión de la integrina $\alpha_v\beta_6$. Sin embargo, este no parece ser el único mecanismo responsable de los niveles reducidos de TFG-β en los ratones mutantes, dado que estos animales muestran niveles inferiores antes incluso del incremento de IL-10. Aunque se ha dicho que los ratones *Mmp8*$^{-/-}$ tienen alterada la ruta de señalización de

TGF-β, los mecanismos subyacentes a esta alteración no han sido completamente dilucidados (Gutierrez-Fernandez y col., 2007). Si bien es cierto que existen informes de un papel profibrótico de IL-10 a través de un incremento de la respuesta inmune Th2 en la fibrosis pulmonar inducida por sílice (Barbarin y col., 2005), estos trabajos carecen de estudios histológicos que evalúen el daño del modelo, dando pie a conjeturar que la causa de esta desavenencia en los resultados sea el hecho de que la sobreexpresión de IL-10 en ausencia de un proceso fibrótico marcado puede inducir la activación alternativa de macrófagos y generar, *per se,* fibrosis pulmonar (Sun y col., 2011).

Muchos de los resultados observados en modelos experimentales que utilizan ratones deficientes en MMPs son debidos a diferencias en el procesamiento de citoquinas o quimiocinas que ven alterada su actividad. El aumento de los niveles en proteína de IL-10, similar al que habíamos encontrado previamente en ratones *Mmp8* $^{-/-}$ sometidos a lesión pulmonar inducida por ventilación mecánica, la ausencia de diferencias en su expresión e incluso el descenso de la misma coincidiendo con el pico a nivel de proteína a las tres semanas, que se ha descrito ejerce una retroalimentación negativa (Giambartolomei y col., 2002), nos hizo plantearnos si IL-10 podría ser sustrato de MMP-8. En los ensayos *in vitro* de digestión enzimática por MMP-8, tanto de la IL-10 recombinante murina como la humana, observamos la aparición de una banda de menor peso molecular tras la incubación con MMP-8 que se correspondía con una forma procesada de IL-10 y se veía inhibida por la presencia del inhibidor de MMP-8 TIMP-1. El análisis western blot de homogeneizados pulmonares de ratones 3 días y 3 semanas tras la instilación con bleomicina mostró la misma banda de procesamiento, así como un aumento en el porcentaje de IL-10 intacta en los ratones deficientes en MMP-8. El estudio de la significación funcional de este procesamiento lo llevamos a cabo mediante un ensayo de actividad de IL-10 en cultivos primarios de fibroblastos *Mmp8*$^{-/-}$ y *Mmp8*$^{+/+}$ tratados con bleomicina. La ausencia de MMP-8 se tradujo tanto en un menor procesamiento como en una mayor actividad de IL-10, y por tanto en una menor síntesis de colágeno, lo que sugiere que el efecto antifibrótico observado en nuestros ratones mutantes es dependiente de IL-10. Colectivamente, estos resultados son consistentes con un modelo como el representado en la **Figura 4**,

en el cual la ausencia de MMP-8 provocaría un incremento en la inflamación tras la instilación de bleomicina, pero también en un incremento en los niveles de IL-10. Los neutrófilos reclutados liberarían MMP-9, enzima protectora ante la fibrosis a través del procesamiento de mediadores potencialmente profibrótico como IGFBP-3. De manera simultánea, la IL-10 intacta, ya sea directamente o mediante una disminución de TGF-beta, disminuiría el proceso fibrótico, traduciéndose el conjunto en una resistencia al desarrollo de fibrosis pulmonar.

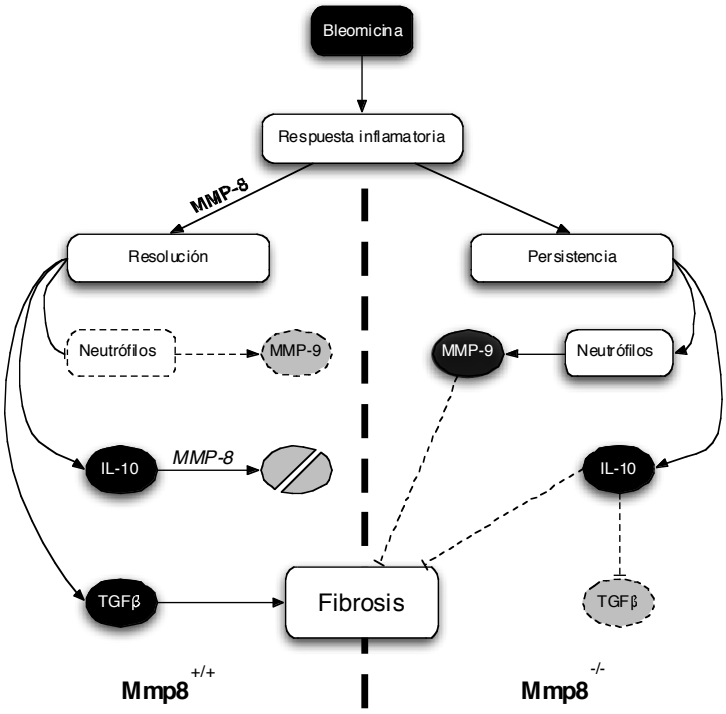

Figura 4. Mecanismo de reducción de la fibrosis pulmonar mediado por MMP-8

En conclusión, los primeros tres trabajos de la presente tesis doctoral demuestran que el papel de MMP-8 durante el proceso inflamatorio es complejo y está altamente orquestado, lo que hace difícil predecir por adelantado los efectos que conllevaría tanto su inhibición farmacológica como su sobreexpresión. Existe además una variabilidad considerable en la bibliografía en los distintos modelos experimentales, atribuible a las características propias de cada tejido, el estímulo involucrado y el tiempo en el que se midieron sus efectos. Así, el menor infiltrado y daño histológico encontrado en los animales deficientes en MMP-8 tras dos horas de ventilación mecánica es consecuente con el retraso inflamatorio inicial que ha

mostrado ser beneficioso en un modelo hepático de daño hiperagudo inducido por TNF/Galactosamina (Van Lint y col., 2005), en el que la mortalidad comienza a partir de las 6-8 horas. La duración de este retraso varía dependiendo del tipo de tejido y del estímulo utilizado. En el caso del pulmón, su alta vascularización, su fina matriz extracelular y su monocapa epitelial podrían acortar este periodo. La más que posible persistencia del infiltrado a largo plazo mostrada tanto en la bibliografía como en nuestros modelos de LPS y bleomicina podría acortar el potencial terapéutico de este enzima durante la lesión por ventilación mecánica y restringirlo a una posible utilización durante periodos de ventilación con presiones elevadas, como pueden ser las maniobras de reclutamiento alveolar. En este sentido, Dolinay y colaboradores han mostrado en un modelo de ventilación de 8 horas que la ausencia de MMP-8 no se traduce ya en diferencias en el contaje de neutrófilos en el BALF (Dolinay y col., 2008). Si bien su trabajo carece de un estudio histológico en profundidad sí parece aportar indicios que acotarían a unas pocas horas el efecto beneficioso mostrado en nuestro modelo. Respecto a la posible inhibición terapéutica de MMP-8 en sepsis, la falta de consenso en el desarrollo de los modelos experimentales hace que nos encontremos también discrepancias en la lesión pulmonar dependiendo de si el estímulo utilizado es LPS o sepsis polimicrobiana por punción-ligación cecal (Quintero y col., 2010; Solan y col., 2012; Vandenbroucke y col., 2012) .Sin embargo, incluso con una mayor inflamación pulmonar, los estudios apuntan a una mejora en la supervivencia del mismo modo que apuntan a una menor fibrosis en nuestro modelo de bleomicina. Aunque parece tentador sugerir la inhibición terapéutica de MMP-8, hay que tener en cuenta que la sepsis no es sólo una de las causas más importantes del SDRA, sino que pacientes con una afectación pulmonar preexistente pueden desarrollar sepsis como consecuencia de la ventilación mecánica. La persistencia del infiltrado inflamatorio podría provocar agravar la situación clínica en pacientes con pulmones que se encuentren ya inmersos en un proceso inflamatorio. En la fibrosis pulmonar nos encontraríamos con un caso similar, complicado además por el riesgo incrementado a desarrollar cáncer de pulmón en estos pacientes (Ozawa y col., 2009) para lo cual la inhibición tanto de MMP-8 como de TGF-β, ambos con capacidades antitumorales, sería potencialmente peligrosa (Pardali and Moustakas, 2007; Noel y col., 2012). Dada la naturaleza multifactorial del SDRA, extensible a las complicaciones causadas por su

tratamiento, es difícil predecir de forma generalizada cuál sería el efecto de dicha inhibición. Serán necesarios por tanto estudios clínicos en subgrupos muy específicos de pacientes o el desarrollo de técnicas de diagnóstico que permitan un estudio individualizado de la situación de cada paciente.

El aparente beneficio a largo plazo, o al menos la ausencia de perjuicio de una mayor inflamación en los modelos de LPS y bleomicina, nos hizo interesarnos por los procesos de reparación pulmonar. Quisimos desarrollar un modelo murino de lesión-reparación dentro del contexto del daño pulmonar inducido por ventilación mecánica, que sirviese para llevar a cabo estudios futuros encaminados a la búsqueda de mediadores de los procesos de reparación. Los estudios experimentales se han centrado normalmente en tratar de identificar y bloquear las vías involucradas en la respuesta proinflamatoria, con el fin de reducir el daño pulmonar. Sin embargo ninguna de estas estrategias ha sido aplicada con éxito en la práctica clínica. La hipótesis planteada fue que, si bien la inflamación desencadena inicialmente la pérdida de la homeostasis pulmonar, sacrificando parcialmente la integridad y funcionalidad del tejido en beneficio de una respuesta rápida frente al agente agresor; los mecanismos moleculares encaminados a recuperar esa homeostasis como la proliferación celular, el remodelado de matriz extracelular, la resolución del edema e incluso de la propia inflamación podrían iniciarse en estas fases tempranas de la respuesta al daño. El solapamiento temporal y la dualidad de funciones de algunos mediadores hacen que su bloqueo pueda prevenir el daño pulmonar si es llevado a cabo tempranamente, pero pueda actuar en detrimento de la reparación posterior. La búsqueda de indicadores de procesos de reparación podría tener un gran interés como valor pronóstico en pacientes con SDRA. Sin embargo la medida de estos mediadores adolece de un problema fundamental: Si un paciente muestra niveles elevados de un marcador en concreto, ¿es debido a que están teniendo lugar fenómenos de reparación y por tanto conlleva un mejor pronóstico? o por el contrario ¿es debido a la presencia de una mayor lesión y por tanto de una respuesta inflamatoria exacerbada? Podemos encontrar ejemplos de esta doble interpretación de los marcadores en la bibliografía. Niveles elevados de procolágeno en el fluido alveolar de pacientes con SDRA se relacionan con un mayor riesgo de mortalidad (Chesnutt y col., 1997) y sin

embargo la presencia de fibroblastos en el mismo fluido con niveles elevados de colágeno tipo I muestran una menor respuesta inflamatoria y un mejor pronóstico, sugiriendo el establecimiento de los procesos de reparación alveolar (Quesnel y col., 2010). De manera similar, niveles elevados de los factores de crecimiento HGF y KGF reflejan un peor pronóstico, a pesar de que estos mediadores promueven la proliferación celular, la diferenciación y en última instancia la reparación alveolar. En este estudio, los autores ya discutían que los niveles elevados de ambos factores en los no supervivientes podían ser debidos a un daño más severo (Verghese y col., 1998).

Pocos estudios se han centrado en la reparación tras el daño pulmonar inducido por ventilación mecánica. En el primero, llevado a cabo por Nin y colaboradores, se sometió a ratas Sprague-Dawley a ventilación mecánica durante una hora, restableciendo posteriormente la respiración espontánea durante varios días para permitir la reparación. Los estudios histológicos mostraron una reducción significativa en la congestión capilar, el edema intersticial, la necrosis de neumocitos tipo I y la formación de membranas hialinas tras 72 horas, demostrando que el VILI puede ser potencialmente reversible en un corto periodo de tiempo (Nin y col., 2008). Este modelo ha sido recientemente utilizado con éxito para el estudio de los efectos de la terapia celular en el VILI (Curley y col., 2013). Nuestro modelo confirma estos hallazgos, mediante la inducción de daño pulmonar durante 90 minutos de ventilación con presiones elevadas seguido de una recuperación de 4 horas utilizando una estrategia ventilatoria de baja presión. Tras este periodo de recuperación observamos una restauración parcial de la homeostasis tisular caracterizada por una reducción del daño histológico y una rápida disminución de la permeabilidad alveolocapilar, identificada por el rápido descenso en el contenido proteico del BALF. También encontramos que la ventilación prolongada con bajas presiones, tradicionalmente denominada no lesiva o protectora, es capaz también de inducir un daño pulmonar moderado, probablemente debido a una adaptación fisiológica al proceso artificial de la ventilación mecánica, pero a tener en cuenta en el desarrollo de modelos más complejos. En lo referente a la respuesta inflamatoria, la elevación de las citoquinas proinflamatorias TNFα e IFNγ y el descenso de las antiinflamatorias como IL-10 durante la fase lesiva es acorde a lo descrito en estudios anteriores (Pedreira y col.,

2008). La rápida normalización en las citoquinas proinflamatorias durante la fase de reparación podría ser parte de la cinética normal de las mismas durante la respuesta inflamatoria. Sin embargo, otros estudios que han utilizado ventilaciones con presión elevada durante periodos de tiempo prolongados han mostrado elevaciones mantenidas en los niveles de TNFα (Hong y col., 2008). El incremento del infiltrado leucocitario positivo para MPO observado en la histología y su persistencia durante la fase de reparación es acorde con el mantenimiento de los niveles elevados de la quimiocina MIP-2 y de MMP-2 y MMP-9, tanto en BALF como en homogeneizados pulmonares. Este aumento del infiltrado leucocitario intrapulmonar contrasta con el menor contaje de leucocitos en el BALF, y se justifica tanto por la dilución causada por el incremento del edema como por la adhesión de las células al epitelio alveolar (Imanaka y col., 2001; Frank y col., 2006). Para tratar de explicar los mecanismos responsables de la supervivencia en nuestro modelo, comparamos, dentro del grupo de reparación, aquellos animales que sobrevivieron las 4 horas extra de ventilación con baja presión frente a aquellos que no. Si bien los animales supervivientes mostraron mayor puntuación en el daño histológico, este aumento fue debido a una mayor presencia de infiltrado inflamatorio y a un incremento en la proliferación celular, demostrada por la presencia de neumocitos positivos para Ki-67. Este aumento en la celularidad podría venir explicado por los elevados niveles de MIP-2 en los supervivientes, ya que esta quimiocina es mitógeno de células epiteliales (Driscoll y col., 1995) y ha mostrado tener un papel el desarrollo del VILI (Belperio y col., 2002), nuestro modelo sugiere que también tiene un papel en la reparación pulmonar. El efecto dual de la inflamación durante el VILI podría explicar porqué los efectos beneficiosos observados con el uso de fármacos antiinflamatorios como los esteroides en modelos experimentales (Nin y col., 2006) no se han traducido en beneficios al trasladarlos a la práctica clínica (Steinberg y col., 2006). En contraste con estos datos, los pulmones de los animales supervivientes mostraron una menor afectación en la permeabilidad alveolar, una reducción en los niveles de colágeno y un aumento en los niveles de MMP-2. En conjunto, estos hecho apoyan la hipótesis de que, en el caso del VILI, los procesos encaminados a la recuperación de la homeostasis tisular pasan por el establecimiento temprano de una respuesta inflamatoria y un remodelado de la matriz extracelular adecuados.

Con el fin de encontrar posibles mediadores del proceso de reparación epitelial, decidimos realizar estudios en un modelo de cierre de heridas en cultivos tanto de neumocitos murinos suplementados con BALF de animales en fase de reparación, como de neumocitos humanos suplementados con BALF de pacientes con SDRA. Este modelo permite la realización de experimentos de inhibición para identificar los factores implicados en el cierre del epitelio. Encontramos que la inhibición de MMP-2 se traducía en una reducción en la velocidad de cierre tanto en los cultivos humanos como murinos. Esta gelatinasa es secretada constitutivamente por una gran variedad de células, incluido el epitelio alveolar, y también en respuesta a fenómenos de estiramiento (Haseneen y col., 2003). Su papel en la migración celular descrito en otros modelos de lesión (Buckley y col., 2001; Lechapt-Zalcman y col., 2006) y su localización en áreas de fibroproliferación y de disrupción de la membrana basal (Selman y col., 2000) apoya nuestros datos de que juega un papel en la reepitelización celular tras el VILI. Otros estudios han identificado varias proteasas en procesos similares de reparación. A modo de ejemplo, se ha descrito que MMP-14 regula el proceso de reparación alveolar a través de la activación de MMP-2 (Ghosh y col., 2012). En un modelo de daño pulmonar inducido por naftaleno se demostró que MMP-7 es liberada tras el daño pulmonar y tiene un papel esencial en los fenómenos de reepitelización (Chen y col., 2009; Gharib y col., 2012).

Aunque la pan-inhibición de MMPs ha mostrado tener un valor profiláctico frente al VILI (Doroszko y col., 2010), su bloqueo durante la fase de reparación puede ser perjudicial, como se extrae del retraso en la velocidad de cierre del modelo *in vitro* y de que el tratamiento con doxiciclina una vez establecido el daño pulmonar provoca una mayor afectación pulmonar. Estos efectos opuestos ilustran la relación entre el remodelado tisular, el daño inicial y la subsiguiente reparación y subrayan la importancia crítica del tiempo cuando nos decidimos a actuar sobre estos procesos. Por otro lado, la sobreexpresión de estos enzimas podría ser de interés en el contexto del daño pulmonar y la ventilación mecánica. Hay distintas drogas que pueden promover la expresión de MMPs. El Salbutanol incrementa la expresión de MMP-9 en neutrófilos y facilita la reabsorción del edema pulmonar (O'Kane y col., 2009). MMP-2 puede ser secretado en respuesta a TFG-β o el oxido nítrico (Lechapt-Zalcman y col.,

2006; Chen y col., 2008), pero su uso terapéutico en la reparación pulmonar aun no ha sido estudiado. En conclusión, hemos desarrollado un modelo válido de lesión-reparación inducida por ventilación mecánica que podría servir tanto para la búsqueda de mediadores tempranos involucrados en la reparación pulmonar como para evaluar el efecto de tratamientos farmacológicos o celulares encaminados a promoverla.

Continuando con el último objetivo de esta tesis doctoral, centramos nuestro interés en el efecto de la ventilación mecánica a nivel cerebral. Los estudios clínicos previos han hecho evidente la relación existente entre el uso de esta técnica de soporte vital y el desarrollo de desórdenes neurológicos (Ely y col., 2001; Jones and Pisani, 2012). Estos desórdenes abarcan desde el delirio hasta afectaciones cognitivas severas a largo plazo. Estas alteraciones neurocognitivas suponen un riesgo añadido de mortalidad de los pacientes ingresados en las unidades de cuidados intensivos así como una merma en su calidad de vida. La gravedad de las alteraciones a largo plazo se ha relacionado con la intensidad del delirio agudo (Girard y col., 2010), lo que hace presuponer que comparten algún mecanismo patogenético. Aunque las causas de esta disfunción siguen aun sin dilucidarse, se ha propuesto la existencia de un desequilibrio en la liberación de neurotransmisores, con un incremento en la liberación de dopamina (Figueroa-Ramos y col., 2009). Esta idea está soportada por el valor profiláctico y terapéutico del haloperidol, inhibidor de receptores de dopamina tipo 2 (DRD2) (Jacobi y col., 2002). Nuestros resultados muestran que la ventilación con presiones positivas desencadena la activación de la vía intrínseca de la apoptosis en neuronas del hipocampo. Este hallazgo se corresponde con estudios clínicos que muestran pérdida de volumen y presencia de lesiones en el hipocampo de pacientes con delirio sometidos a ventilación mecánica en la UCI (Janz y col., 2010; Gunther y col., 2012). Los hallazgos son similares a los encontrados en animales con encefalitis séptica, en los cuales se relacionaba el aumento en la apoptosis neuronal en el hipocampo con peores resultados en los test de comportamiento y de memoria (Semmler y col., 2007). Dado el papel del hipocampo en la integración y contextualización de la información sensorial para consolidar la memoria, la apoptosis neuronal observada podría ser la base de los desórdenes del comportamiento observados en los pacientes sometidos a ventilación mecánica.

La inhibición de la vía de Akt tras la ventilación mecánica, junto con una activación/defosforilación concomitante de GSK3β, inductor de la activación de la vía apoptótica intrínseca (Beurel and Jope, 2006) apuntan a un efecto excitotóxico por aumento en la actividad dopaminérgica. En estas situaciones, el incremento en la liberación de este neurotransmisor dirige su señalización hacia los receptores DRD2, que a través de un sistema mediado por β-Arrestina y Fosfatasa-2 provocan la defosforilación de la vía de AKT similar a la observada en el hipocampo de los animales ventilados (Beaulieu y col., 2005; Beaulieu y col., 2007; Fuster-Matanzo y col., 2011; Gomez-Sintes y col., 2011; Li and Gao, 2011). El descenso en la fosforilación de PTEN resulta en la activación de este enzima, inhibiendo la actividad de la PI3K, bloqueando la fosforilación de Akt y contribuyendo por tanto a la defosforilación de la vía (Diaz-Ruiz y col., 2009). La inducción de la vía intrínseca de la apoptosis por GSK3β resulta en la activación de la caspasa 7, importante mediador del daño agudo en hipocampo (Larner y col., 2005), que lleva al procesamiento de PARP-1 y a la acumulación de su fragmento de 89 kDa en el citoplasma observado en la inmunofluorescencia, y descrito previamente en estudios de excitotoxicidad por glutamato y neurodegeneración. (Soldani y col., 2001; Gilliams-Francis y col., 2003; Chaitanya y col., 2010). Nuestros resultados encajan con esta ruta, la cual también se ha observado tanto en estudios *in vitro* como clínicos versados en comportamientos dependientes de dopamina (Chen y col., 2008; Krishnan y col., 2008; Jope, 2011; Li and Gao, 2011). Se ha atribuido a la hiperdopaminergia el desarrollo de desórdenes neurológicos como la esquizofrenia, el síndrome bipolar o la depresión (Abi-Dargham and Moore, 2003; Dzirasa y col., 2009; Simpson y col., 2010).

El tratamiento previo con haloperidol o la realización de la vagotomía cervical bilateral inhibieron tanto la defosforilación de la vía de Akt como la apoptosis neuronal. A esto se une que el incremento observado en la expresión de TH tras la ventilación mecánica, enzima limitante de la síntesis de dopamina que a su vez se sobreexpresa en presencia de la misma (Magal y col., 1993), no aumenta tras la vagotomía pero si tras el tratamiento con haloperidol. Esto refuerza la hipótesis de que el mecanismo principal de daño cerebral en nuestro modelo es la señalización neuronal dirigida por vía vagal. Las fibras nerviosas de diferentes órganos, incluidos los pulmones, pueden

alcanzar el hipocampo a través del nervio vago tras una conexión sináptica en el tronco del encéfalo (Castle y col., 2005). El *núcleo del tracto solitario* es el principal núcleo vagal en esta zona, y la activación de mecanoreceptores pulmonares ha mostrado incrementar su activación mediante la liberación de neurotransmisores como el glutamato (Gourine y col., 2008). Desde aquí, las fibras alcanzan el hipocampo a través de una ruta multisináptica que incluye neuronas catecolaminérgicas (Mello-Carpes and Izquierdo, 2012).

Finalmente, observamos un incremento en la expresión de Disbindina 1C tras 90 min de ventilación mecánica, que se tradujo en un aumento en sus niveles de proteína a las 5 horas. La Disbindina forma parte del sistema regulador de tráfico intracelular denominado BLOC-1 (del inglés *biogénesis of lysosome-related organelles complex 1*) y ha sido relacionada directamente en los procesos internalización de los receptores DRD2 postsinápticos y dirección de los mismos hacia su degradación en los lisosomas (Ji y col., 2009; Marley and von Zastrow, 2010). Respecto a su transcrito -1C, se encuentra principalmente en la zona postsináptica (Talbot y col., 2011) y diversos estudios clínicos han relacionado niveles reducidos del mismo con desórdenes del comportamiento como la esquizofrenia (Tang y col., 2009; Talbot y col., 2011). El tratamiento con haloperidol, tanto en el modelo animal como *in vitro*, y la vagotomía cervical bilateral abolieron el aumento de expresión de esta isoforma. En conjunto, estos datos sugieren que la Disbindina actúa como un mecanismo de compensación destinado a disminuir los efectos perjudiciales de la hiperdopaminergia. La observación de niveles incrementados de Disbindina en los estudios inmunohistoquímicos de hipocampos de pacientes ventilados sugiere que esta proteína podría tener un papel en la regulación de la respuesta cerebral a la ventilación mecánica.

Los hallazgos anteriormente descritos abren la puesta a la realización de estudios genéticos en este campo. La existencia de polimorfismos genéticos relacionados con estados de hiperdopaminergia, tanto en el gen de la Disbindina (Voisey y col., 2010) como en los de DRD2 (Morimoto y col., 2002) y Akt (Blasi y col., 2011), podrían ser un factor de riesgo adicional al desarrollo del delirio o de

afectaciones cognitivas y podría ayudar a identificar pacientes susceptibles a intervenciones profilácticas.

En conclusión, nuestros resultados describen un mecanismo de excitotoxicidad por dopamina que podría justificar los efectos perniciosos de la ventilación mecánica en el cerebro, válido para explicar el desarrollo de desórdenes neurológicos en pacientes sometidos a ventilación mecánica y para desarrollar estrategias terapéuticas encaminadas a mejorar su pronóstico.

CONCLUSIONS

1. MMP-8 modulates different aspects of lung injury due to its ability to catalyze various inflammatory mediators. This enzyme plays different roles depending on the experimental model and the timing of the study:
    a. MMP-8 has a proinflammatory role by facilitating acute neutrophilic infiltration during ventilator-induced lung injury.
    b. MMP-8 has an anti-inflammatory role during endotoxic shock, preventing the massive influx of leukocytes and promoting their clearance from lung parenchyma by modulating alarmins and chemokines.
    c. MMP-8 has a profibrotic role after bleomycin treatment, both *in vivo* and *in vitro*. This effect is not related to alterations in total collagenolytic capacity, but to the ability of MMP-8 to cleave and inactivate the anti-fibrotic and anti-inflammatory cytokine IL-10.

2. Ventilator-induced lung injury is reversible in a short period of time after restoration of a ventilatory strategy with low pressures and moderate PEEP. This repair process depends on both an adequate and sufficient inflammatory response and remodelling of extracellular matrix. Regarding to the latter, MMP-2 promotes lung repair by facilitating epithelial migration, necessary for alveolar restoration.

3. Mechanical ventilation triggers neuronal apoptosis into hippocampus, as a result of a hyperdopaminergic state in response to vagal signalling. The increase in dysbindin-1C may have a compensatory effect, aimed to reduce the availability of dopamine receptors in the cell membrane.

CONCLUSIONES

1. La MMP-8 modula diferentes aspectos de la lesión pulmonar por su papel en la catálisis de diferentes mediadores inflamatorios, con efectos diferentes dependiendo del modelo experimental y el momento de estudio:
    a. Tiene un papel proinflamatorio al facilitar la infiltración neutrofílica aguda durante la lesión inducida por ventilación mecánica.
    b. Tiene un papel antiinflamatorio durante el shock endotóxico, evitando la llegada masiva de leucocitos y promoviendo su aclaramiento del parénquima pulmonar mediante la modulación de alarminas y quimiocinas.
    c. Tiene un papel profibrótico como consecuencia de la presencia de bleomicina tanto *in vivo* como *in vitro.* Este efecto no está relacionado con alteraciones en la capacidad colagenolítica total, sino con la habilidad de MMP-8 de procesar e inactivar a la citoquina antiinflamatoria y antifibrótica IL-10.

2. La lesión pulmonar inducida por ventilación mecánica es reversible en un corto periodo de tiempo tras la instauración de una estrategia ventilatoria con presiones bajas y PEEP moderada. Este proceso de reparación depende tanto de una adecuada y suficiente respuesta inflamatoria como del remodelado de la matriz extracelular. A este respecto, MMP-2 es capaz de promover la reparación pulmonar facilitando la migración epitelial necesaria para la reconstitución alveolar.

3. La ventilación mecánica desencadena apoptosis neuronal en el hipocampo como resultado de un estado de hiperdopaminergia en respuesta a una señalización vagal. El aumento de disbindina-1C concomitante podría tener un efecto compensatorio, con el objetivo de disminuir la disponibilidad de receptores dopaminérgicos en la membrana celular.

BIBLIOGRAFÍA

Abi-Dargham, A. and H. Moore (2003). Prefrontal DA transmission at D1 receptors and the pathology of schizophrenia. Neuroscientist 9(5): 404-416.

Agrawal, S., P. Anderson, M. Durbeej, N. van Rooijen, F. Ivars, G. Opdenakker and L. M. Sorokin (2006). Dystroglycan is selectively cleaved at the parenchymal basement membrane at sites of leukocyte extravasation in experimental autoimmune encephalomyelitis. J Exp Med 203(4): 1007-1019.

Albaiceta, G. M., A. Gutierrez-Fernandez, D. Parra, A. Astudillo, E. Garcia-Prieto, F. Taboada and A. Fueyo (2008). Lack of matrix metalloproteinase-9 worsens ventilator-induced lung injury. Am J Physiol Lung Cell Mol Physiol 294(3): L535-543.

Alves-Filho, J. C., A. Freitas, F. O. Souto, F. Spiller, H. Paula-Neto, J. S. Silva, R. T. Gazzinelli, M. M. Teixeira, S. H. Ferreira and F. Q. Cunha (2009). Regulation of chemokine receptor by Toll-like receptor 2 is critical to neutrophil migration and resistance to polymicrobial sepsis. Proc Natl Acad Sci U S A 106(10): 4018-4023.

Arai, T., K. Abe, H. Matsuoka, M. Yoshida, M. Mori, S. Goya, H. Kida, K. Nishino, T. Osaki, I. Tachibana, Y. Kaneda and S. Hayashi (2000). Introduction of the interleukin-10 gene into mice inhibited bleomycin-induced lung injury in vivo. Am J Physiol Lung Cell Mol Physiol 278(5): L914-922.

Armstrong, L., D. R. Thickett, J. P. Mansell, M. Ionescu, E. Hoyle, R. C. Billinghurst, A. R. Poole and A. B. Millar (1999). Changes in collagen turnover in early acute respiratory distress syndrome. Am J Respir Crit Care Med 160(6): 1910-1915.

Ashbaugh, D. G., D. B. Bigelow, T. L. Petty and B. E. Levine (1967). Acute respiratory distress in adults. Lancet 2(7511): 319-323.

Ashcroft, T., J. M. Simpson and V. Timbrell (1988). Simple method of estimating severity of pulmonary fibrosis on a numerical scale. J Clin Pathol 41(4): 467-470.

Atabai, K. and M. A. Matthay (2002). The pulmonary physician in critical care. 5: Acute lung injury and the acute respiratory distress syndrome: definitions and epidemiology. Thorax 57(5): 452-458.

Bai, C., N. Fukuda, Y. Song, T. Ma, M. A. Matthay and A. S. Verkman (1999). Lung fluid transport in aquaporin-1 and aquaporin-4 knockout mice. J Clin Invest 103(4): 555-561.

Balbin, M., A. Fueyo, A. M. Tester, A. M. Pendas, A. S. Pitiot, A. Astudillo, C. M. Overall, S. D. Shapiro and C. Lopez-Otin (2003). Loss of collagenase-2 confers increased skin tumor susceptibility to male mice. Nat Genet 35(3): 252-257.

Banerjee, E. R. and W. R. Henderson, Jr. (2012). Characterization of lung stem cell niches in a mouse model of bleomycin-induced fibrosis. Stem Cell Res Ther 3(3): 21.

Barbarin, V., Z. Xing, M. Delos, D. Lison and F. Huaux (2005). Pulmonary overexpression of IL-10 augments lung fibrosis and Th2 responses induced by silica particles. Am J Physiol Lung Cell Mol Physiol 288(5): L841-848.

Beaulieu, J. M., R. R. Gainetdinov and M. G. Caron (2007). The Akt-GSK-3 signaling cascade in the actions of dopamine. Trends Pharmacol Sci 28(4): 166-172.

Beaulieu, J. M., T. D. Sotnikova, S. Marion, R. J. Lefkowitz, R. R. Gainetdinov and M. G. Caron (2005). An Akt/beta-arrestin 2/PP2A signaling complex mediates dopaminergic neurotransmission and behavior. Cell 122(2): 261-273.

Bein, T., S. Weber-Carstens, A. Goldmann, T. Muller, T. Staudinger, J. Brederlau, R. Muellenbach, R. Dembinski, B. M. Graf, M. Wewalka, A. Philipp, K. D. Wernecke, M. Lubnow and A. S. Slutsky (2013). Lower tidal volume strategy (approximately 3 ml/kg) combined with extracorporeal CO(2) removal versus 'conventional' protective ventilation (6 ml/kg) in severe ARDS : The prospective randomized Xtravent-study. Intensive Care Med.

Belperio, J. A., M. P. Keane, M. D. Burdick, V. Londhe, Y. Y. Xue, K. Li, R. J. Phillips and R. M. Strieter (2002). Critical role for CXCR2 and CXCR2 ligands during the pathogenesis of ventilator-induced lung injury. J Clin Invest 110(11): 1703-1716.

Bernard, G. R., A. Artigas, K. L. Brigham, J. Carlet, K. Falke, L. Hudson, M. Lamy, J. R. Legall, A. Morris and R. Spragg (1994). The American-European Consensus Conference on ARDS. Definitions, mechanisms, relevant outcomes, and clinical trial coordination. Am J Respir Crit Care Med 149(3 Pt 1): 818-824.

Beurel, E. and R. S. Jope (2006). The paradoxical pro- and anti-apoptotic actions of GSK3 in the intrinsic and extrinsic apoptosis signaling pathways. Prog Neurobiol 79(4): 173-189.

Bhattacharya, S., N. Sen, M. T. Yiming, R. Patel, K. Parthasarathi, S. Quadri, A. C. Issekutz and J. Bhattacharya (2003). High tidal volume ventilation induces

proinflammatory signaling in rat lung endothelium. Am J Respir Cell Mol Biol 28(2): 218-224.

Bianchi, M. E. (2007). DAMPs, PAMPs and alarmins: all we need to know about danger. J Leukoc Biol 81(1): 1-5.

Biasone, A., P. Tortorella, C. Campestre, M. Agamennone, S. Preziuso, M. Chiappini, E. Nuti, P. Carelli, A. Rossello, F. Mazza and C. Gallina (2007). alpha-Biphenylsulfonylamino 2-methylpropyl phosphonates: enantioselective synthesis and selective inhibition of MMPs. Bioorg Med Chem 15(2): 791-799.

Blasi, G., F. Napolitano, G. Ursini, P. Taurisano, R. Romano, G. Caforio, L. Fazio, B. Gelao, A. Di Giorgio, L. Iacovelli, L. Sinibaldi, T. Popolizio, A. Usiello and A. Bertolino (2011). DRD2/AKT1 interaction on D2 c-AMP independent signaling, attentional processing, and response to olanzapine treatment in schizophrenia. Proc Natl Acad Sci U S A 108(3): 1158-1163.

Bohrer, H., M. Schick, R. Schonstedt and A. Bach (1991). Marked decrease in arterial oxygen tension associated with continuous intravenous nifedipine administration. Anaesthesia 46(10): 856-858.

Boyd, J. H., B. Kan, H. Roberts, Y. Wang and K. R. Walley (2008). S100A8 and S100A9 mediate endotoxin-induced cardiomyocyte dysfunction via the receptor for advanced glycation end products. Circ Res 102(10): 1239-1246.

Brand, K. H., I. M. Ahout, R. de Groot, A. Warris, G. Ferwerda and P. W. Hermans (2012). Use of MMP-8 and MMP-9 to assess disease severity in children with viral lower respiratory tract infections. J Med Virol 84(9): 1471-1480.

Brudecki, L., D. A. Ferguson, C. E. McCall and M. El Gazzar (2012). Myeloid-derived suppressor cells evolve during sepsis and can enhance or attenuate the systemic inflammatory response. Infect Immun 80(6): 2026-2034.

Buckley, S., B. Driscoll, W. Shi, K. Anderson and D. Warburton (2001). Migration and gelatinases in cultured fetal, adult, and hyperoxic alveolar epithelial cells. Am J Physiol Lung Cell Mol Physiol 281(2): L427-434.

Cabrera, S., M. Gaxiola, J. L. Arreola, R. Ramirez, P. Jara, J. D'Armiento, T. Richards, M. Selman and A. Pardo (2007). Overexpression of MMP9 in macrophages attenuates pulmonary fibrosis induced by bleomycin. Int J Biochem Cell Biol 39(12): 2324-2338.

Cabrera-Benitez, N. E., M. Parotto, M. Post, B. Han, P. M. Spieth, W. E. Cheng, F. Valladares, J. Villar, M. Liu, M. Sato, H. Zhang and A. S. Slutsky (2012). Mechanical stress induces lung fibrosis by epithelial-mesenchymal transition. Crit Care Med 40(2): 510-517.

Capone, F., E. Guerriero, A. Sorice, P. Maio, G. Colonna, G. Castello and S. Costantini (2012). Characterization of metalloproteinases, oxidative status and inflammation levels in the different stages of fibrosis in HCV patients. Clin Biochem 45(7-8): 525-529.

Castle, M., E. Comoli and A. D. Loewy (2005). Autonomic brainstem nuclei are linked to the hippocampus. Neuroscience 134(2): 657-669.

Cavallazzi, R., M. Saad and P. E. Marik (2012). Delirium in the ICU: an overview. Ann Intensive Care 2(1): 49.

Chaitanya, G. V., A. J. Steven and P. P. Babu (2010). PARP-1 cleavage fragments: signatures of cell-death proteases in neurodegeneration. Cell Commun Signal 8: 31.

Chen, J. H., H. H. Lin, T. A. Chiang, J. D. Hsu, H. H. Ho, Y. C. Lee and C. J. Wang (2008). Gaseous nitrogen oxide promotes human lung cancer cell line A549 migration, invasion, and metastasis via iNOS-mediated MMP-2 production. Toxicol Sci 106(2): 364-375.

Chen, L., E. E. Tredget, P. Y. Wu and Y. Wu (2008). Paracrine factors of mesenchymal stem cells recruit macrophages and endothelial lineage cells and enhance wound healing. PLoS One 3(4): e1886.

Chen, P., L. E. Abacherli, S. T. Nadler, Y. Wang, Q. Li and W. C. Parks (2009). MMP7 shedding of syndecan-1 facilitates re-epithelialization by affecting alpha(2)beta(1) integrin activation. PLoS One 4(8): e6565.

Chen, S., G. C. Owens and D. B. Edelman (2008). Dopamine inhibits mitochondrial motility in hippocampal neurons. PLoS One 3(7): e2804.

Chertcoff, F. J., S. Quadrelli, E. D. Soloaga, M. L. Chertcoff, J. Poliszuk and F. Perez Prieto (2011). [Mechanical ventilation. Influence of the age in the outcome]. Medicina (B Aires) 71(1): 27-32.

Chesnutt, A. N., M. A. Matthay, F. A. Tibayan and J. G. Clark (1997). Early detection of type III procollagen peptide in acute lung injury. Pathogenetic and prognostic significance. Am J Respir Crit Care Med 156(3 Pt 1): 840-845.

Cheung, A. M., C. M. Tansey, G. Tomlinson, N. Diaz-Granados, A. Matte, A. Barr, S. Mehta, C. D. Mazer, C. B. Guest, T. E. Stewart, F. Al-Saidi, A. B. Cooper, D. Cook, A. S. Slutsky and M. S. Herridge (2006). Two-year outcomes, health care use, and costs of survivors of acute respiratory distress syndrome. Am J Respir Crit Care Med 174(5): 538-544.

Cox, J. H., A. E. Starr, R. Kappelhoff, R. Yan, C. R. Roberts and C. M. Overall (2010). Matrix metalloproteinase 8 deficiency in mice exacerbates inflammatory arthritis through delayed neutrophil apoptosis and reduced caspase 11 expression. Arthritis Rheum 62(12): 3645-3655.

Crandall, E. D. and M. A. Matthay (2001). Alveolar epithelial transport. Basic science to clinical medicine. Am J Respir Crit Care Med 163(4): 1021-1029.

Cummings, C. J., T. R. Martin, C. W. Frevert, J. M. Quan, V. A. Wong, S. M. Mongovin, T. R. Hagen, K. P. Steinberg and R. B. Goodman (1999). Expression and function of the chemokine receptors CXCR1 and CXCR2 in sepsis. J Immunol 162(4): 2341-2346.

Curley, G. F., B. Ansari, M. Hayes, J. Devaney, C. Masterson, A. Ryan, F. Barry, T. O'Brien, D. O. Toole and J. G. Laffey (2013). Effects of Intratracheal Mesenchymal Stromal Cell Therapy during Recovery and Resolution after Ventilator-induced Lung Injury. Anesthesiology.

Curley, G. F., M. Hayes, B. Ansari, G. Shaw, A. Ryan, F. Barry, T. O'Brien, D. O'Toole and J. G. Laffey (2012). Mesenchymal stem cells enhance recovery and repair following ventilator-induced lung injury in the rat. Thorax 67(6): 496-501.

Curley, M. A., P. L. Hibberd, L. D. Fineman, D. Wypij, M. C. Shih, J. E. Thompson, M. J. Grant, F. E. Barr, N. Z. Cvijanovich, L. Sorce, P. M. Luckett, M. A. Matthay and J. H. Arnold (2005). Effect of prone positioning on clinical outcomes in children with acute lung injury: a randomized controlled trial. JAMA 294(2): 229-237.

D'Agostino, B., N. Sullo, D. Siniscalco, A. De Angelis and F. Rossi (2010). Mesenchymal stem cell therapy for the treatment of chronic obstructive pulmonary disease. Expert Opin Biol Ther 10(5): 681-687.

D'Mello, C., T. Le and M. G. Swain (2009). Cerebral microglia recruit monocytes into the brain in response to tumor necrosis factoralpha signaling during peripheral organ inflammation. J Neurosci 29(7): 2089-2102.

Dancer, R. C., A. M. Wood and D. R. Thickett (2011). Metalloproteinases in idiopathic pulmonary fibrosis. Eur Respir J 38(6): 1461-1467.

Dantzer, R. (2001). Cytokine-induced sickness behavior: mechanisms and implications. Ann N Y Acad Sci 933: 222-234.

de Carvalho, M. E., M. Dolhnikoff, S. I. Meireles, L. F. Reis, M. A. Martins and D. Deheinzelin (2007). Effects of overinflation on procollagen type III expression in experimental acute lung injury. Crit Care 11(1): R23.

Diaz-Ruiz, O., A. Zapata, L. Shan, Y. Zhang, A. C. Tomac, N. Malik, F. de la Cruz and C. M. Backman (2009). Selective deletion of PTEN in dopamine neurons leads to trophic effects and adaptation of striatal medium spiny projecting neurons. PLoS One 4(9): e7027.

Diercks, B. P., I. Hauschildt, F. Stab, H. Wenck, O. Doring and N. Peters (2013). IL-10 Promotes Secretion of S100A8/A9 from Human Monocytes Trough an Inclusion in Plasma Membranes. Scand J Immunol 77(2): 169-170.

Dobbs, L. G., M. C. Williams and A. E. Brandt (1985). Changes in biochemical characteristics and pattern of lectin binding of alveolar type II cells with time in culture. Biochim Biophys Acta 846(1): 155-166.

Dolinay, T., W. Wu, N. Kaminski, E. Ifedigbo, A. M. Kaynar, M. Szilasi, S. C. Watkins, S. W. Ryter, A. Hoetzel and A. M. Choi (2008). Mitogen-activated protein kinases regulate susceptibility to ventilator-induced lung injury. PLoS One 3(2): e1601.

Donnelly, S. C., R. M. Strieter, P. T. Reid, S. L. Kunkel, M. D. Burdick, I. Armstrong, A. Mackenzie and C. Haslett (1996). The association between mortality rates and decreased concentrations of interleukin-10 and interleukin-1 receptor antagonist in the lung fluids of patients with the adult respiratory distress syndrome. Ann Intern Med 125(3): 191-196.

Doroszko, A., T. S. Hurst, D. Polewicz, J. Sawicka, J. Fert-Bober, D. H. Johnson and G. Sawicki (2010). Effects of MMP-9 inhibition by doxycycline on proteome of lungs in high tidal volume mechanical ventilation-induced acute lung injury. Proteome Sci 8: 3.

dos Santos, C. C., S. Murthy, P. Hu, Y. Shan, J. J. Haitsma, S. H. Mei, D. J. Stewart and W. C. Liles (2012). Network analysis of transcriptional responses induced by mesenchymal stem cell treatment of experimental sepsis. Am J Pathol 181(5): 1681-1692.

Driscoll, K. E., D. G. Hassenbein, B. W. Howard, R. J. Isfort, D. Cody, M. H. Tindal, M. Suchanek and J. M. Carter (1995). Cloning, expression, and functional characterization of rat MIP-2: a neutrophil chemoattractant and epithelial cell mitogen. J Leukoc Biol 58(3): 359-364.

Dzirasa, K., A. J. Ramsey, D. Y. Takahashi, J. Stapleton, J. M. Potes, J. K. Williams, R. R. Gainetdinov, K. Sameshima, M. G. Caron and M. A. Nicolelis (2009). Hyperdopaminergia and NMDA receptor hypofunction disrupt neural phase signaling. J Neurosci 29(25): 8215-8224.

Ebersoldt, M., T. Sharshar and D. Annane (2007). Sepsis-associated delirium. Intensive Care Med 33(6): 941-950.

Edgeworth, J., M. Gorman, R. Bennett, P. Freemont and N. Hogg (1991). Identification of p8,14 as a highly abundant heterodimeric calcium binding protein complex of myeloid cells. J Biol Chem 266(12): 7706-7713.

Effros, R. M., C. Darin, E. R. Jacobs, R. A. Rogers, G. Krenz and E. E. Schneeberger (1997). Water transport and the distribution of aquaporin-1 in pulmonary air spaces. J Appl Physiol 83(3): 1002-1016.

Egli, M., H. Duplain, M. Lepori, S. Cook, P. Nicod, E. Hummler, C. Sartori and U. Scherrer (2004). Defective respiratory amiloride-sensitive sodium transport predisposes to pulmonary oedema and delays its resolution in mice. J Physiol 560(Pt 3): 857-865.

Ehlermann, P., K. Eggers, A. Bierhaus, P. Most, D. Weichenhan, J. Greten, P. P. Nawroth, H. A. Katus and A. Remppis (2006). Increased proinflammatory endothelial response to S100A8/A9 after preactivation through advanced glycation end products. Cardiovasc Diabetol 5: 6.

Ely, E. W., S. K. Inouye, G. R. Bernard, S. Gordon, J. Francis, L. May, B. Truman, T. Speroff, S. Gautam, R. Margolin, R. P. Hart and R. Dittus (2001). Delirium in mechanically ventilated patients: validity and reliability of the confusion

assessment method for the intensive care unit (CAM-ICU). JAMA 286(21): 2703-2710.

Ely, E. W., A. Shintani, B. Truman, T. Speroff, S. M. Gordon, F. E. Harrell, Jr., S. K. Inouye, G. R. Bernard and R. S. Dittus (2004). Delirium as a predictor of mortality in mechanically ventilated patients in the intensive care unit. JAMA 291(14): 1753-1762.

Endoh, Y., Y. M. Chung, I. A. Clark, C. L. Geczy and K. Hsu (2009). IL-10-dependent S100A8 gene induction in monocytes/macrophages by double-stranded RNA. J Immunol 182(4): 2258-2268.

Fanjul-Fernandez, M., A. R. Folgueras, S. Cabrera and C. Lopez-Otin (2010). Matrix metalloproteinases: evolution, gene regulation and functional analysis in mouse models. Biochim Biophys Acta 1803(1): 3-19.

Fanjul-Fernandez, M., A. R. Folgueras, A. Fueyo, M. Balbin, M. F. Suarez, M. S. Fernandez-Garcia, S. D. Shapiro, J. M. Freije and C. Lopez-Otin (2013). Matrix metalloproteinase Mmp-1a is dispensable for normal growth and fertility in mice and promotes lung cancer progression by modulating inflammatory responses. J Biol Chem.

Figueroa-Ramos, M. I., C. M. Arroyo-Novoa, K. A. Lee, G. Padilla and K. A. Puntillo (2009). Sleep and delirium in ICU patients: a review of mechanisms and manifestations. Intensive Care Med 35(5): 781-795.

Fligiel, S. E., T. Standiford, H. M. Fligiel, D. Tashkin, R. M. Strieter, R. L. Warner, K. J. Johnson and J. Varani (2006). Matrix metalloproteinases and matrix metalloproteinase inhibitors in acute lung injury. Hum Pathol 37(4): 422-430.

Foda, H. D., E. E. Rollo, M. Drews, C. Conner, K. Appelt, D. R. Shalinsky and S. Zucker (2001). Ventilator-induced lung injury upregulates and activates gelatinases and EMMPRIN: attenuation by the synthetic matrix metalloproteinase inhibitor, Prinomastat (AG3340). Am J Respir Cell Mol Biol 25(6): 717-724.

Folgueras, A. R., A. Fueyo, O. Garcia-Suarez, J. Cox, A. Astudillo, P. Tortorella, C. Campestre, A. Gutierrez-Fernandez, M. Fanjul-Fernandez, C. J. Pennington, D. R. Edwards, C. M. Overall and C. Lopez-Otin (2008). Collagenase-2 deficiency or inhibition impairs experimental autoimmune encephalomyelitis in mice. J Biol Chem 283(14): 9465-9474.

Fowler AA, W. S., Giclas PC, et al. (1982). Characterization of antiprotease activity in the adult respiratory distress syndrome

. Chest 81: 50S-51S.

Frank, J. A., C. M. Wray, D. F. McAuley, R. Schwendener and M. A. Matthay (2006). Alveolar macrophages contribute to alveolar barrier dysfunction in ventilator-induced lung injury. Am J Physiol Lung Cell Mol Physiol 291(6): L1191-1198.

Fudala, R., A. Krupa, D. Stankowska, T. C. Allen and A. K. Kurdowska (2008). Anti-interleukin-8 autoantibody:interleukin-8 immune complexes in acute lung injury/acute respiratory distress syndrome. Clin Sci (Lond) 114(6): 403-412.

Fueki, N., H. Sagara, K. Akimoto, M. Ota, T. Okada, K. Sugiyama, M. Fueki, S. Makino and T. Fukuda (2007). Interleukin-10 regulates transforming growth factor-beta signaling in cultured human bronchial epithelial cells. Respiration 74(4): 454-459.

Fujita, H., N. Sakamoto, Y. Ishimatsu, T. Kakugawa, S. Hara, A. Hara, M. Amenomori, H. Ishimoto, T. Nagata, H. Mukae and S. Kohno (2011). Effects of doxycycline on production of growth factors and matrix metalloproteinases in pulmonary fibrosis. Respiration 81(5): 420-430.

Fuster-Matanzo, A., M. Llorens-Martin, E. G. de Barreda, J. Avila and F. Hernandez (2011). Different susceptibility to neurodegeneration of dorsal and ventral hippocampal dentate gyrus: a study with transgenic mice overexpressing GSK3beta. PLoS One 6(11): e27262.

Gando, S., T. Kameue, S. Nanzaki, T. Hayakawa and Y. Nakanishi (1997). Increased neutrophil elastase, persistent intravascular coagulation, and decreased fibrinolytic activity in patients with posttraumatic acute respiratory distress syndrome. J Trauma 42(6): 1068-1072.

Garantziotis, S., D. M. Brass, J. Savov, J. W. Hollingsworth, E. McElvania-TeKippe, K. Berman, J. K. Walker and D. A. Schwartz (2006). Leukocyte-derived IL-10 reduces subepithelial fibrosis associated with chronically inhaled endotoxin. Am J Respir Cell Mol Biol 35(6): 662-667.

Garcia, S., J. Forteza, C. Lopez-Otin, J. J. Gomez-Reino, A. Gonzalez and C. Conde (2010). Matrix metalloproteinase-8 deficiency increases joint inflammation and

bone erosion in the K/BxN serum-transfer arthritis model. Arthritis Res Ther 12(6): R224.

Gattinoni, L., A. Pesenti, L. Avalli, F. Rossi and M. Bombino (1987). Pressure-volume curve of total respiratory system in acute respiratory failure. Computed tomographic scan study. Am Rev Respir Dis 136(3): 730-736.

Gebhardt, C., A. Riehl, M. Durchdewald, J. Nemeth, G. Furstenberger, K. Muller-Decker, A. Enk, B. Arnold, A. Bierhaus, P. P. Nawroth, J. Hess and P. Angel (2008). RAGE signaling sustains inflammation and promotes tumor development. J Exp Med 205(2): 275-285.

Geerts, L., P. G. Jorens, J. Willems, M. De Ley and H. Slegers (2001). Natural inhibitors of neutrophil function in acute respiratory distress syndrome. Crit Care Med 29(10): 1920-1924.

Gharib, S. A., W. A. Altemeier, L. S. Van Winkle, C. G. Plopper, S. Y. Schlesinger, C. A. Buell, R. Brauer, V. Lee, W. C. Parks and P. Chen (2012). MMP7 Coordinates Airway Epithelial Injury Response and Differentiation of Ciliated Cells. Am J Respir Cell Mol Biol.

Ghosh, M. C., P. S. Makena, V. Gorantla, S. E. Sinclair and C. M. Waters (2012). CXCR4 regulates migration of lung alveolar epithelial cells through activation of Rac1 and matrix metalloproteinase-2. Am J Physiol Lung Cell Mol Physiol 302(9): L846-856.

Giambartolomei, G. H., V. A. Dennis, B. L. Lasater, P. K. Murthy and M. T. Philipp (2002). Autocrine and exocrine regulation of interleukin-10 production in THP-1 cells stimulated with Borrelia burgdorferi lipoproteins. Infect Immun 70(4): 1881-1888.

Gilliams-Francis, K. L., A. A. Quaye and J. R. Naegele (2003). PARP cleavage, DNA fragmentation, and pyknosis during excitotoxin-induced neuronal death. Exp Neurol 184(1): 359-372.

Girard, T. D., J. C. Jackson, P. P. Pandharipande, B. T. Pun, J. L. Thompson, A. K. Shintani, S. M. Gordon, A. E. Canonico, R. S. Dittus, G. R. Bernard and E. W. Ely (2010). Delirium as a predictor of long-term cognitive impairment in survivors of critical illness. Crit Care Med 38(7): 1513-1520.

Gomes, L. H., M. J. Raftery, W. Xing Yan, J. D. Goyette, P. S. Thomas and C. L. Geczy (2012). S100A8 and S100A9-oxidant scavengers in inflammation. Free Radic Biol Med.

Gomez-Sintes, R., F. Hernandez, J. J. Lucas and J. Avila (2011). GSK-3 Mouse Models to Study Neuronal Apoptosis and Neurodegeneration. Front Mol Neurosci 4: 45.

Gonzalez, R. F., L. Allen and L. G. Dobbs (2009). Rat alveolar type I cells proliferate, express OCT-4, and exhibit phenotypic plasticity in vitro. Am J Physiol Lung Cell Mol Physiol 297(6): L1045-1055.

Gourine, A. V., N. Dale, A. Korsak, E. Llaudet, F. Tian, R. Huckstepp and K. M. Spyer (2008). Release of ATP and glutamate in the nucleus tractus solitarii mediate pulmonary stretch receptor (Breuer-Hering) reflex pathway. J Physiol 586(16): 3963-3978.

Greenlee, K. J., D. B. Corry, D. A. Engler, R. K. Matsunami, P. Tessier, R. G. Cook, Z. Werb and F. Kheradmand (2006). Proteomic identification of in vivo substrates for matrix metalloproteinases 2 and 9 reveals a mechanism for resolution of inflammation. J Immunol 177(10): 7312-7321.

Grembowicz, K. P., D. Sprague and P. L. McNeil (1999). Temporary disruption of the plasma membrane is required for c-fos expression in response to mechanical stress. Mol Biol Cell 10(4): 1247-1257.

Gueders, M. M., M. Balbin, N. Rocks, J. M. Foidart, P. Gosset, R. Louis, S. Shapiro, C. Lopez-Otin, A. Noel and D. D. Cataldo (2005). Matrix metalloproteinase-8 deficiency promotes granulocytic allergen-induced airway inflammation. J Immunol 175(4): 2589-2597.

Gunther, M. L., A. Morandi, E. Krauskopf, P. Pandharipande, T. D. Girard, J. C. Jackson, J. Thompson, A. K. Shintani, S. Geevarghese, R. R. Miller, 3rd, A. Canonico, K. Merkle, C. J. Cannistraci, B. P. Rogers, J. C. Gatenby, S. Heckers, J. C. Gore, R. O. Hopkins and E. W. Ely (2012). The association between brain volumes, delirium duration, and cognitive outcomes in intensive care unit survivors: the VISIONS cohort magnetic resonance imaging study*. Crit Care Med 40(7): 2022-2032.

Gutierrez-Fernandez, A., M. Inada, M. Balbin, A. Fueyo, A. S. Pitiot, A. Astudillo, K. Hirose, M. Hirata, S. D. Shapiro, A. Noel, Z. Werb, S. M. Krane, C. Lopez-Otin

and X. S. Puente (2007). Increased inflammation delays wound healing in mice deficient in collagenase-2 (MMP-8). FASEB J 21(10): 2580-2591.

Haberlandt, E., M. Rauchenzauner, M. Morass, P. Wondrak, S. S. Burgi, K. Rostasy and D. Karall (2013). Matrix-metalloproteinases and proinflammatory cytokines in children with febrile convulsions and epilepsy-Cause or consequence? Epilepsy Res.

Harrison, C. A., M. J. Raftery, J. Walsh, P. Alewood, S. E. Iismaa, S. Thliveris and C. L. Geczy (1999). Oxidation regulates the inflammatory properties of the murine S100 protein S100A8. J Biol Chem 274(13): 8561-8569.

Hasaneen, N. A., S. Zucker, J. Cao, C. Chiarelli, R. A. Panettieri and H. D. Foda (2005). Cyclic mechanical strain-induced proliferation and migration of human airway smooth muscle cells: role of EMMPRIN and MMPs. FASEB J 19(11): 1507-1509.

Haseneen, N. A., G. G. Vaday, S. Zucker and H. D. Foda (2003). Mechanical stretch induces MMP-2 release and activation in lung endothelium: role of EMMPRIN. Am J Physiol Lung Cell Mol Physiol 284(3): L541-547.

Headley, A. S., E. Tolley and G. U. Meduri (1997). Infections and the inflammatory response in acute respiratory distress syndrome. Chest 111(5): 1306-1321.

Hoegl, S., K. A. Boost, H. Czerwonka, A. Dolfen, P. Scheiermann, H. Muhl, B. Zwissler and C. Hofstetter (2009). Inhaled IL-10 reduces biotrauma and mortality in a model of ventilator-induced lung injury. Respir Med 103(3): 463-470.

Hoffman, A. M. and E. P. Ingenito (2012). Alveolar Epithelial Stem and Progenitor Cells: Emerging Evidence for their Role in Lung Regeneration. Curr Med Chem 19(35): 6003-6008.

Hong, S. B., Y. Huang, L. Moreno-Vinasco, S. Sammani, J. Moitra, J. W. Barnard, S. F. Ma, T. Mirzapoiazova, C. Evenoski, R. R. Reeves, E. T. Chiang, G. D. Lang, A. N. Husain, S. M. Dudek, J. R. Jacobson, S. Q. Ye, Y. A. Lussier and J. G. Garcia (2008). Essential role of pre-B-cell colony enhancing factor in ventilator-induced lung injury. Am J Respir Crit Care Med 178(6): 605-617.

Hu, J., P. E. Van den Steen, C. Dillen and G. Opdenakker (2005). Targeting neutrophil collagenase/matrix metalloproteinase-8 and gelatinase B/matrix metalloproteinase-9 with a peptidomimetic inhibitor protects against endotoxin shock. Biochem Pharmacol 70(4): 535-544.

Hummler, E., P. Barker, J. Gatzy, F. Beermann, C. Verdumo, A. Schmidt, R. Boucher and B. C. Rossier (1996). Early death due to defective neonatal lung liquid clearance in alpha-ENaC-deficient mice. Nat Genet 12(3): 325-328.

Ikemoto, M., H. Murayama, H. Itoh, M. Totani and M. Fujita (2007). Intrinsic function of S100A8/A9 complex as an anti-inflammatory protein in liver injury induced by lipopolysaccharide in rats. Clin Chim Acta 376(1-2): 197-204.

Imai, Y., J. Parodo, O. Kajikawa, M. de Perrot, S. Fischer, V. Edwards, E. Cutz, M. Liu, S. Keshavjee, T. R. Martin, J. C. Marshall, V. M. Ranieri and A. S. Slutsky (2003). Injurious mechanical ventilation and end-organ epithelial cell apoptosis and organ dysfunction in an experimental model of acute respiratory distress syndrome. JAMA 289(16): 2104-2112.

Imanaka, H., M. Shimaoka, N. Matsuura, M. Nishimura, N. Ohta and H. Kiyono (2001). Ventilator-induced lung injury is associated with neutrophil infiltration, macrophage activation, and TGF-beta 1 mRNA upregulation in rat lungs. Anesth Analg 92(2): 428-436.

Isakson, B. E., R. L. Lubman, G. J. Seedorf and S. Boitano (2001). Modulation of pulmonary alveolar type II cell phenotype and communication by extracellular matrix and KGF. Am J Physiol Cell Physiol 281(4): C1291-1299.

Jacobi, J., G. L. Fraser, D. B. Coursin, R. R. Riker, D. Fontaine, E. T. Wittbrodt, D. B. Chalfin, M. F. Masica, H. S. Bjerke, W. M. Coplin, D. W. Crippen, B. D. Fuchs, R. M. Kelleher, P. E. Marik, S. A. Nasraway, Jr., M. J. Murray, W. T. Peruzzi and P. D. Lumb (2002). Clinical practice guidelines for the sustained use of sedatives and analgesics in the critically ill adult. Crit Care Med 30(1): 119-141.

Janz, D. R., T. W. Abel, J. C. Jackson, M. L. Gunther, S. Heckers and E. W. Ely (2010). Brain autopsy findings in intensive care unit patients previously suffering from delirium: a pilot study. J Crit Care 25(3): 538 e537-512.

Jensen-Taubman, S. M., S. M. Steinberg and R. I. Linnoila (1998). Bronchiolization of the alveoli in lung cancer: pathology, patterns of differentiation and oncogene expression. Int J Cancer 75(4): 489-496.

Ji, Y., F. Yang, F. Papaleo, H. X. Wang, W. J. Gao, D. R. Weinberger and B. Lu (2009). Role of dysbindin in dopamine receptor trafficking and cortical GABA function. Proc Natl Acad Sci U S A 106(46): 19593-19598.

Jones, S. F. and M. A. Pisani (2012). ICU delirium: an update. Curr Opin Crit Care 18(2): 146-151.

Jope, R. S. (2011). Glycogen synthase kinase-3 in the etiology and treatment of mood disorders. Front Mol Neurosci 4: 16.

Khalil, N. and A. H. Greenberg (1991). The role of TGF-beta in pulmonary fibrosis. Ciba Found Symp 157: 194-207; discussion 207-111.

Korpos, E., C. Wu and L. Sorokin (2009). Multiple roles of the extracellular matrix in inflammation. Curr Pharm Des 15(12): 1349-1357.

Kreda, S. M., M. C. Gynn, D. A. Fenstermacher, R. C. Boucher and S. E. Gabriel (2001). Expression and localization of epithelial aquaporins in the adult human lung. Am J Respir Cell Mol Biol 24(3): 224-234.

Krishnan, V., M. H. Han, M. Mazei-Robison, S. D. Iniguez, J. L. Ables, V. Vialou, O. Berton, S. Ghose, H. E. Covington, 3rd, M. D. Wiley, R. P. Henderson, R. L. Neve, A. J. Eisch, C. A. Tamminga, S. J. Russo, C. A. Bolanos and E. J. Nestler (2008). AKT signaling within the ventral tegmental area regulates cellular and behavioral responses to stressful stimuli. Biol Psychiatry 64(8): 691-700.

Kubo, H. (2011). Molecular basis of lung tissue regeneration. Gen Thorac Cardiovasc Surg 59(4): 231-244.

Kuljeet SA, V. D. (2012). Hippocampus in health and disease: An overview. Official journal of accademy of neurology 15(4): 239-246.

Lanchou, J., M. Corbel, M. Tanguy, N. Germain, E. Boichot, N. Theret, B. Clement, V. Lagente and Y. Malledant (2003). Imbalance between matrix metalloproteinases (MMP-9 and MMP-2) and tissue inhibitors of metalloproteinases (TIMP-1 and TIMP-2) in acute respiratory distress syndrome patients. Crit Care Med 31(2): 536-542.

Larner, S. F., D. M. McKinsey, R. L. Hayes and W. W. KK (2005). Caspase 7: increased expression and activation after traumatic brain injury in rats. J Neurochem 94(1): 97-108.

Lauhio, A., J. Hastbacka, V. Pettila, T. Tervahartiala, S. Karlsson, T. Varpula, M. Varpula, E. Ruokonen, T. Sorsa and E. Kolho (2011). Serum MMP-8, -9 and TIMP-1 in sepsis: high serum levels of MMP-8 and TIMP-1 are associated with

fatal outcome in a multicentre, prospective cohort study. Hypothetical impact of tetracyclines. Pharmacol Res 64(6): 590-594.

Lechapt-Zalcman, E., V. Pruliere-Escabasse, D. Advenier, S. Galiacy, C. Charriere-Bertrand, A. Coste, A. Harf, M. P. d'Ortho and E. Escudier (2006). Transforming growth factor-beta1 increases airway wound repair via MMP-2 upregulation: a new pathway for epithelial wound repair? Am J Physiol Lung Cell Mol Physiol 290(6): L1277-1282.

Lee, H. S., Y. Wang, B. S. Maciejewski, K. Esho, C. Fulton, S. Sharma and J. Sanchez-Esteban (2008). Interleukin-10 protects cultured fetal rat type II epithelial cells from injury induced by mechanical stretch. Am J Physiol Lung Cell Mol Physiol 294(2): L225-232.

Leite-Junior, J. H., C. S. Garcia, A. B. Souza-Fernandes, P. L. Silva, D. S. Ornellas, A. P. Larangeira, H. C. Castro-Faria-Neto, M. M. Morales, E. M. Negri, V. L. Capelozzi, W. A. Zin, P. Pelosi, P. T. Bozza and P. R. Rocco (2008). Methylprednisolone improves lung mechanics and reduces the inflammatory response in pulmonary but not in extrapulmonary mild acute lung injury in mice. Crit Care Med 36(9): 2621-2628.

Lesur, O., A. Kokis, C. Hermans, T. Fulop, A. Bernard and D. Lane (2000). Interleukin-2 involvement in early acute respiratory distress syndrome: relationship with polymorphonuclear neutrophil apoptosis and patient survival. Crit Care Med 28(12): 3814-3822.

Li, Y. C. and W. J. Gao (2011). GSK-3beta activity and hyperdopamine-dependent behaviors. Neurosci Biobehav Rev 35(3): 645-654.

Lim, S. Y., M. J. Raftery and C. L. Geczy (2011). Oxidative modifications of DAMPs suppress inflammation: the case for S100A8 and S100A9. Antioxid Redox Signal 15(8): 2235-2248.

Lim, S. Y., M. J. Raftery, J. Goyette, K. Hsu and C. L. Geczy (2009). Oxidative modifications of S100 proteins: functional regulation by redox. J Leukoc Biol 86(3): 577-587.

Lin, M., P. Jackson, A. M. Tester, E. Diaconu, C. M. Overall, J. E. Blalock and E. Pearlman (2008). Matrix metalloproteinase-8 facilitates neutrophil migration

through the corneal stromal matrix by collagen degradation and production of the chemotactic peptide Pro-Gly-Pro. Am J Pathol 173(1): 144-153.

Lindsay, C. D. (2011). Novel therapeutic strategies for acute lung injury induced by lung damaging agents: the potential role of growth factors as treatment options. Hum Exp Toxicol 30(7): 701-724.

Livak, K. J. and T. D. Schmittgen (2001). Analysis of relative gene expression data using real-time quantitative PCR and the 2(-Delta Delta C(T)) Method. Methods 25(4): 402-408.

Loffek, S., O. Schilling and C. W. Franzke (2011). Series "matrix metalloproteinases in lung health and disease": Biological role of matrix metalloproteinases: a critical balance. Eur Respir J 38(1): 191-208.

Lopez-Otin, C. and J. S. Bond (2008). Proteases: multifunctional enzymes in life and disease. J Biol Chem 283(45): 30433-30437.

Lukkarinen, H., A. Hogmalm, U. Lappalainen and K. Bry (2009). Matrix metalloproteinase-9 deficiency worsens lung injury in a model of bronchopulmonary dysplasia. Am J Respir Cell Mol Biol 41(1): 59-68.

Magal, E., P. Burnham, S. Varon and J. C. Louis (1993). Convergent regulation by ciliary neurotrophic factor and dopamine of tyrosine hydroxylase expression in cultures of rat substantia nigra. Neuroscience 52(4): 867-881.

Manicone, A. M. and J. K. McGuire (2008). Matrix metalloproteinases as modulators of inflammation. Semin Cell Dev Biol 19(1): 34-41.

Marley, A. and M. von Zastrow (2010). Dysbindin promotes the post-endocytic sorting of G protein-coupled receptors to lysosomes. PLoS One 5(2): e9325.

Matute-Bello, G., W. C. Liles, F. Radella, 2nd, K. P. Steinberg, J. T. Ruzinski, M. Jonas, E. Y. Chi, L. D. Hudson and T. R. Martin (1997). Neutrophil apoptosis in the acute respiratory distress syndrome. Am J Respir Crit Care Med 156(6): 1969-1977.

McQuibban, G. A., J. H. Gong, J. P. Wong, J. L. Wallace, I. Clark-Lewis and C. M. Overall (2002). Matrix metalloproteinase processing of monocyte chemoattractant proteins generates CC chemokine receptor antagonists with anti-inflammatory properties in vivo. Blood 100(4): 1160-1167.

Meade, M. O., D. J. Cook, G. H. Guyatt, A. S. Slutsky, Y. M. Arabi, D. J. Cooper, A. R. Davies, L. E. Hand, Q. Zhou, L. Thabane, P. Austin, S. Lapinsky, A. Baxter, J. Russell, Y. Skrobik, J. J. Ronco and T. E. Stewart (2008). Ventilation strategy using low tidal volumes, recruitment maneuvers, and high positive end-expiratory pressure for acute lung injury and acute respiratory distress syndrome: a randomized controlled trial. JAMA 299(6): 637-645.

Meduri, G. U., S. Headley, G. Kohler, F. Stentz, E. Tolley, R. Umberger and K. Leeper (1995). Persistent elevation of inflammatory cytokines predicts a poor outcome in ARDS. Plasma IL-1 beta and IL-6 levels are consistent and efficient predictors of outcome over time. Chest 107(4): 1062-1073.

Mello-Carpes, P. B. and I. Izquierdo (2012). The Nucleus of the Solitary Tract-->Nucleus Paragigantocellularis-->Locus Coeruleus-->CA1 region of dorsal hippocampus pathway is important for consolidation of object recognition memory. Neurobiol Learn Mem 100C: 56-63.

Menezes, S. L., P. T. Bozza, H. C. Neto, A. P. Laranjeira, E. M. Negri, V. L. Capelozzi, W. A. Zin and P. R. Rocco (2005). Pulmonary and extrapulmonary acute lung injury: inflammatory and ultrastructural analyses. J Appl Physiol 98(5): 1777-1783.

Milbrandt, E. B., S. Deppen, P. L. Harrison, A. K. Shintani, T. Speroff, R. A. Stiles, B. Truman, G. R. Bernard, R. S. Dittus and E. W. Ely (2004). Costs associated with delirium in mechanically ventilated patients. Crit Care Med 32(4): 955-962.

Mishra, A., P. Bhattacharya, S. Paul, R. Paul and S. Swarnakar (2011). An alternative therapy for idiopathic pulmonary fibrosis by doxycycline through matrix metalloproteinase inhibition. Lung India 28(3): 174-179.

Montgomery, A. B., M. A. Stager, C. J. Carrico and L. D. Hudson (1985). Causes of mortality in patients with the adult respiratory distress syndrome. Am Rev Respir Dis 132(3): 485-489.

Morandi, A., B. P. Rogers, M. L. Gunther, K. Merkle, P. Pandharipande, T. D. Girard, J. C. Jackson, J. Thompson, A. K. Shintani, S. Geevarghese, R. R. Miller, 3rd, A. Canonico, C. J. Cannistraci, J. C. Gore, E. W. Ely and R. O. Hopkins (2012). The relationship between delirium duration, white matter integrity, and cognitive impairment in intensive care unit survivors as determined by diffusion tensor

imaging: the VISIONS prospective cohort magnetic resonance imaging study*. Crit Care Med 40(7): 2182-2189.

Morimoto, K., R. Miyatake, M. Nakamura, T. Watanabe, T. Hirao and H. Suwaki (2002). Delusional disorder: molecular genetic evidence for dopamine psychosis. Neuropsychopharmacology 26(6): 794-801.

Munger, J. S., X. Huang, H. Kawakatsu, M. J. Griffiths, S. L. Dalton, J. Wu, J. F. Pittet, N. Kaminski, C. Garat, M. A. Matthay, D. B. Rifkin and D. Sheppard (1999). The integrin alpha v beta 6 binds and activates latent TGF beta 1: a mechanism for regulating pulmonary inflammation and fibrosis. Cell 96(3): 319-328.

Muscedere, J. G., J. B. Mullen, K. Gan and A. S. Slutsky (1994). Tidal ventilation at low airway pressures can augment lung injury. Am J Respir Crit Care Med 149(5): 1327-1334.

Nakagome, K., M. Dohi, K. Okunishi, R. Tanaka, J. Miyazaki and K. Yamamoto (2006). In vivo IL-10 gene delivery attenuates bleomycin induced pulmonary fibrosis by inhibiting the production and activation of TGF-beta in the lung. Thorax 61(10): 886-894.

Naruse, K. and M. Sokabe (1993). Involvement of stretch-activated ion channels in Ca2+ mobilization to mechanical stretch in endothelial cells. Am J Physiol 264(4 Pt 1): C1037-1044.

Neves, G., S. F. Cooke and T. V. Bliss (2008). Synaptic plasticity, memory and the hippocampus: a neural network approach to causality. Nat Rev Neurosci 9(1): 65-75.

Nin, N., J. A. Lorente, M. de Paula, M. El Assar, S. Vallejo, O. Penuelas, P. Fernandez-Segoviano, A. Ferruelo, A. Sanchez-Ferrer and A. Esteban (2008). Rats surviving injurious mechanical ventilation show reversible pulmonary, vascular and inflammatory changes. Intensive Care Med 34(5): 948-956.

Nin, N., O. Penuelas, M. de Paula, J. A. Lorente, P. Fernandez-Segoviano and A. Esteban (2006). Ventilation-induced lung injury in rats is associated with organ injury and systemic inflammation that is attenuated by dexamethasone. Crit Care Med 34(4): 1093-1098.

No-authors-listed (2000). Ventilation with lower tidal volumes as compared with traditional tidal volumes for acute lung injury and the acute respiratory distress

syndrome. The Acute Respiratory Distress Syndrome Network. N Engl J Med 342(18): 1301-1308.

Noel, A., A. Gutierrez-Fernandez, N. E. Sounni, N. Behrendt, E. Maquoi, I. K. Lund, S. Cal, G. Hoyer-Hansen and C. Lopez-Otin (2012). New and paradoxical roles of matrix metalloproteinases in the tumor microenvironment. Front Pharmacol 3: 140.

O'Kane, C. M., S. W. McKeown, G. D. Perkins, C. R. Bassford, F. Gao, D. R. Thickett and D. F. McAuley (2009). Salbutamol up-regulates matrix metalloproteinase-9 in the alveolar space in the acute respiratory distress syndrome. Crit Care Med 37(7): 2242-2249.

Ochs, M., J. R. Nyengaard, A. Jung, L. Knudsen, M. Voigt, T. Wahlers, J. Richter and H. J. Gundersen (2004). The number of alveoli in the human lung. Am J Respir Crit Care Med 169(1): 120-124.

Owen, C. A., Z. Hu, C. Lopez-Otin and S. D. Shapiro (2004). Membrane-bound matrix metalloproteinase-8 on activated polymorphonuclear cells is a potent, tissue inhibitor of metalloproteinase-resistant collagenase and serpinase. J Immunol 172(12): 7791-7803.

Oyaizu, T., S. Y. Fung, A. Shiozaki, Z. Guan, Q. Zhang, C. C. dos Santos, B. Han, M. Mura, S. Keshavjee and M. Liu (2012). Src tyrosine kinase inhibition prevents pulmonary ischemia-reperfusion-induced acute lung injury. Intensive Care Med 38(5): 894-905.

Ozawa, Y., T. Suda, T. Naito, N. Enomoto, D. Hashimoto, T. Fujisawa, Y. Nakamura, N. Inui, H. Nakamura and K. Chida (2009). Cumulative incidence of and predictive factors for lung cancer in IPF. Respirology 14(5): 723-728.

Panos, R. J., P. M. Bak, W. S. Simonet, J. S. Rubin and L. J. Smith (1995). Intratracheal instillation of keratinocyte growth factor decreases hyperoxia-induced mortality in rats. J Clin Invest 96(4): 2026-2033.

Panoskaltsis-Mortari, A., D. H. Ingbar, P. Jung, I. Y. Haddad, P. B. Bitterman, O. D. Wangensteen, C. L. Farrell, D. L. Lacey and B. R. Blazar (2000). KGF pretreatment decreases B7 and granzyme B expression and hastens repair in lungs of mice after allogeneic BMT. Am J Physiol Lung Cell Mol Physiol 278(5): L988-999.

Pardali, K. and A. Moustakas (2007). Actions of TGF-beta as tumor suppressor and pro-metastatic factor in human cancer. Biochim Biophys Acta 1775(1): 21-62.

Parsons, P. E. (1998). Interleukin-10: the ambiguity in sepsis continues. Crit Care Med 26(5): 818-819.

Pedreira, P. R., E. Garcia-Prieto, D. Parra, A. Astudillo, E. Diaz, F. Taboada and G. M. Albaiceta (2008). Effects of melatonin in an experimental model of ventilator-induced lung injury. Am J Physiol Lung Cell Mol Physiol 295(5): L820-827.

Penzo, M., R. Molteni, T. Suda, S. Samaniego, A. Raucci, D. M. Habiel, F. Miller, H. P. Jiang, J. Li, R. Pardi, R. Palumbo, E. Olivotto, R. R. Kew, M. E. Bianchi and K. B. Marcu (2010). Inhibitor of NF-kappa B kinases alpha and beta are both essential for high mobility group box 1-mediated chemotaxis [corrected]. J Immunol 184(8): 4497-4509.

Pun, B. T. and E. W. Ely (2007). The importance of diagnosing and managing ICU delirium. Chest 132(2): 624-636.

Qiao, R., W. Yan, C. Clavijo, R. Mehrian-Shai, Q. Zhong, K. J. Kim, D. Ann, E. D. Crandall and Z. Borok (2008). Effects of KGF on alveolar epithelial cell transdifferentiation are mediated by JNK signaling. Am J Respir Cell Mol Biol 38(2): 239-246.

Quesnel, C., L. Nardelli, P. Piednoir, V. Lecon, J. Marchal-Somme, S. Lasocki, L. Bouadma, I. Philip, P. Soler, B. Crestani and M. Dehoux (2010). Alveolar fibroblasts in acute lung injury: biological behaviour and clinical relevance. Eur Respir J 35(6): 1312-1321.

Quilez, M. E., G. Fuster, J. Villar, C. Flores, O. Marti-Sistac, L. Blanch and J. Lopez-Aguilar (2011). Injurious mechanical ventilation affects neuronal activation in ventilated rats. Crit Care 15(3): R124.

Quintero, P. A., M. D. Knolle, L. F. Cala, Y. Zhuang and C. A. Owen (2010). Matrix metalloproteinase-8 inactivates macrophage inflammatory protein-1 alpha to reduce acute lung inflammation and injury in mice. J Immunol 184(3): 1575-1588.

Raaberg, L., E. Nexo, S. Buckley, W. Luo, M. L. Snead and D. Warburton (1992). Epidermal growth factor transcription, translation, and signal transduction by rat type II pneumocytes in culture. Am J Respir Cell Mol Biol 6(1): 44-49.

Rafii, R., M. M. Juarez, T. E. Albertson and A. L. Chan (2013). A review of current and novel therapies for idiopathic pulmonary fibrosis. J Thorac Dis 5(1): 48-73.

Ranieri, V. M., G. D. Rubenfeld, B. T. Thompson, N. D. Ferguson, E. Caldwell, E. Fan, L. Camporota and A. S. Slutsky (2012). Acute respiratory distress syndrome: the Berlin Definition. JAMA 307(23): 2526-2533.

Ranieri, V. M., P. M. Suter, C. Tortorella, R. De Tullio, J. M. Dayer, A. Brienza, F. Bruno and A. S. Slutsky (1999). Effect of mechanical ventilation on inflammatory mediators in patients with acute respiratory distress syndrome: a randomized controlled trial. JAMA 282(1): 54-61.

Raquil, M. A., N. Anceriz, P. Rouleau and P. A. Tessier (2008). Blockade of antimicrobial proteins S100A8 and S100A9 inhibits phagocyte migration to the alveoli in streptococcal pneumonia. J Immunol 180(5): 3366-3374.

Rawlins, E. L., L. E. Ostrowski, S. H. Randell and B. L. Hogan (2007). Lung development and repair: contribution of the ciliated lineage. Proc Natl Acad Sci U S A 104(2): 410-417.

Reijerkerk, A., G. Kooij, S. M. van der Pol, S. Khazen, C. D. Dijkstra and H. E. de Vries (2006). Diapedesis of monocytes is associated with MMP-mediated occludin disappearance in brain endothelial cells. FASEB J 20(14): 2550-2552.

Reynolds, S. D., A. Giangreco, J. H. Power and B. R. Stripp (2000). Neuroepithelial bodies of pulmonary airways serve as a reservoir of progenitor cells capable of epithelial regeneration. Am J Pathol 156(1): 269-278.

Ricou, B., L. Nicod, S. Lacraz, H. G. Welgus, P. M. Suter and J. M. Dayer (1996). Matrix metalloproteinases and TIMP in acute respiratory distress syndrome. Am J Respir Crit Care Med 154(2 Pt 1): 346-352.

Ritter, C., M. Andrades, M. Guerreiro, L. Zavaschi, D. P. Gelain, L. F. Souza, C. A. Ribeiro, N. Clausell, S. Menna-Barreto, J. C. Moreira and F. Dal-Pizzol (2003). Plasma oxidative parameters and mortality in patients with severe burn injury. Intensive Care Med 29(8): 1380-1383.

Robinson, M. J., P. Tessier, R. Poulsom and N. Hogg (2002). The S100 family heterodimer, MRP-8/14, binds with high affinity to heparin and heparan sulfate glycosaminoglycans on endothelial cells. J Biol Chem 277(5): 3658-3665.

Rojas, M., C. R. Woods, A. L. Mora, J. Xu and K. L. Brigham (2005). Endotoxin-induced lung injury in mice: structural, functional, and biochemical responses. Am J Physiol Lung Cell Mol Physiol 288(2): L333-341.

Ryckman, C., K. Vandal, P. Rouleau, M. Talbot and P. A. Tessier (2003). Proinflammatory activities of S100: proteins S100A8, S100A9, and S100A8/A9 induce neutrophil chemotaxis and adhesion. J Immunol 170(6): 3233-3242.

Sage, E. K., M. R. Loebinger, J. Polak and S. M. Janes (2008). The role of bone marrow-derived stem cells in lung regeneration and repair.

Schubert-Unkmeir, A., C. Konrad, H. Slanina, F. Czapek, S. Hebling and M. Frosch (2010). Neisseria meningitidis induces brain microvascular endothelial cell detachment from the matrix and cleavage of occludin: a role for MMP-8. PLoS Pathog 6(4): e1000874.

Selman, M., V. Ruiz, S. Cabrera, L. Segura, R. Ramirez, R. Barrios and A. Pardo (2000). TIMP-1, -2, -3, and -4 in idiopathic pulmonary fibrosis. A prevailing nondegradative lung microenvironment? Am J Physiol Lung Cell Mol Physiol 279(3): L562-574.

Semmler, A., C. Frisch, T. Debeir, M. Ramanathan, T. Okulla, T. Klockgether and M. T. Heneka (2007). Long-term cognitive impairment, neuronal loss and reduced cortical cholinergic innervation after recovery from sepsis in a rodent model. Exp Neurol 204(2): 733-740.

Simon R.H, W. P. A. (1992). Adult respiratory distress syndrome. Inflammation: Basic principles and clinical correlates. 2 ed. New York, Raven Press: 999-1012.

Simpson, E. H., C. Kellendonk and E. Kandel (2010). A possible role for the striatum in the pathogenesis of the cognitive symptoms of schizophrenia. Neuron 65(5): 585-596.

Sinha, P., C. Okoro, D. Foell, H. H. Freeze, S. Ostrand-Rosenberg and G. Srikrishna (2008). Proinflammatory S100 proteins regulate the accumulation of myeloid-derived suppressor cells. J Immunol 181(7): 4666-4675.

Slutsky, A. S. and L. N. Tremblay (1998). Multiple system organ failure. Is mechanical ventilation a contributing factor? Am J Respir Crit Care Med 157(6 Pt 1): 1721-1725.

Solan, P. D., K. E. Dunsmore, A. G. Denenberg, K. Odoms, B. Zingarelli and H. R. Wong (2012). A novel role for matrix metalloproteinase-8 in sepsis. Crit Care Med 40(2): 379-387.

Soldani, C., M. C. Lazze, M. G. Bottone, G. Tognon, M. Biggiogera, C. E. Pellicciari and A. I. Scovassi (2001). Poly(ADP-ribose) polymerase cleavage during apoptosis: when and where? Exp Cell Res 269(2): 193-201.

Song, Y., N. Fukuda, C. Bai, T. Ma, M. A. Matthay and A. S. Verkman (2000). Role of aquaporins in alveolar fluid clearance in neonatal and adult lung, and in oedema formation following acute lung injury: studies in transgenic aquaporin null mice. J Physiol 525 Pt 3: 771-779.

Sroussi, H. Y., Y. Lu, D. Villines and Y. Sun (2012). The down regulation of neutrophil oxidative metabolism by S100A8 and S100A9: implication of the protease-activated receptor-2. Mol Immunol 50(1-2): 42-48.

Stamenkovic, I. (2003). Extracellular matrix remodelling: the role of matrix metalloproteinases. J Pathol 200(4): 448-464.

Stefanidakis, M. and E. Koivunen (2006). Cell-surface association between matrix metalloproteinases and integrins: role of the complexes in leukocyte migration and cancer progression. Blood 108(5): 1441-1450.

Steinbakk, M., C. F. Naess-Andresen, E. Lingaas, I. Dale, P. Brandtzaeg and M. K. Fagerhol (1990). Antimicrobial actions of calcium binding leucocyte L1 protein, calprotectin. Lancet 336(8718): 763-765.

Steinberg, K. P., L. D. Hudson, R. B. Goodman, C. L. Hough, P. N. Lanken, R. Hyzy, B. T. Thompson and M. Ancukiewicz (2006). Efficacy and safety of corticosteroids for persistent acute respiratory distress syndrome. N Engl J Med 354(16): 1671-1684.

Sun, L., M. C. Louie, K. M. Vannella, C. A. Wilke, A. M. LeVine, B. B. Moore and T. P. Shanley (2011). New concepts of IL-10-induced lung fibrosis: fibrocyte recruitment and M2 activation in a CCL2/CCR2 axis. Am J Physiol Lung Cell Mol Physiol 300(3): L341-353.

Suzuki, T., T. J. Moraes, E. Vachon, H. H. Ginzberg, T. T. Huang, M. A. Matthay, M. D. Hollenberg, J. Marshall, C. A. McCulloch, M. T. Abreu, C. W. Chow and G. P. Downey (2005). Proteinase-activated receptor-1 mediates elastase-induced

apoptosis of human lung epithelial cells. Am J Respir Cell Mol Biol 33(3): 231-247.

Swangchan-Uthai, T., C. R. Lavender, Z. Cheng, A. A. Fouladi-Nashta and D. C. Wathes (2012). Time course of defense mechanisms in bovine endometrium in response to lipopolysaccharide. Biol Reprod 87(6): 135.

Talbot, K., N. Louneva, J. W. Cohen, H. Kazi, D. J. Blake and S. E. Arnold (2011). Synaptic dysbindin-1 reductions in schizophrenia occur in an isoform-specific manner indicating their subsynaptic location. PLoS One 6(3): e16886.

Tang, J., R. P. LeGros, N. Louneva, L. Yeh, J. W. Cohen, C. G. Hahn, D. J. Blake, S. E. Arnold and K. Talbot (2009). Dysbindin-1 in dorsolateral prefrontal cortex of schizophrenia cases is reduced in an isoform-specific manner unrelated to dysbindin-1 mRNA expression. Hum Mol Genet 18(20): 3851-3863.

Taniguchi, L. U., E. G. Caldini, I. T. Velasco and E. M. Negri (2010). Cytoskeleton and mechanotransduction in the pathophysiology of ventilator-induced lung injury. J Bras Pneumol 36(3): 363-371.

Terragni, P. P., G. Rosboch, A. Tealdi, E. Corno, E. Menaldo, O. Davini, G. Gandini, P. Herrmann, L. Mascia, M. Quintel, A. S. Slutsky, L. Gattinoni and V. M. Ranieri (2007). Tidal hyperinflation during low tidal volume ventilation in acute respiratory distress syndrome. Am J Respir Crit Care Med 175(2): 160-166.

Tester, A. M., J. H. Cox, A. R. Connor, A. E. Starr, R. A. Dean, X. S. Puente, C. Lopez-Otin and C. M. Overall (2007). LPS responsiveness and neutrophil chemotaxis in vivo require PMN MMP-8 activity. PLoS One 2(3): e312.

Todd, N. W., I. G. Luzina and S. P. Atamas (2012). Molecular and cellular mechanisms of pulmonary fibrosis. Fibrogenesis Tissue Repair 5(1): 11.

Tomashefski, J. F., Jr. (2000). Pulmonary pathology of acute respiratory distress syndrome. Clin Chest Med 21(3): 435-466.

Tremblay, L., F. Valenza, S. P. Ribeiro, J. Li and A. S. Slutsky (1997). Injurious ventilatory strategies increase cytokines and c-fos m-RNA expression in an isolated rat lung model. J Clin Invest 99(5): 944-952.

Uhlig, S. and U. Uhlig (2004). Pharmacological interventions in ventilator-induced lung injury. Trends Pharmacol Sci 25(11): 592-600.

Unroe, M., J. M. Kahn, S. S. Carson, J. A. Govert, T. Martinu, S. J. Sathy, A. S. Clay, J. Chia, A. Gray, J. A. Tulsky and C. E. Cox (2010). One-year trajectories of care and resource utilization for recipients of prolonged mechanical ventilation: a cohort study. Ann Intern Med 153(3): 167-175.

Van den Steen, P. E., S. J. Husson, P. Proost, J. Van Damme and G. Opdenakker (2003). Carboxyterminal cleavage of the chemokines MIG and IP-10 by gelatinase B and neutrophil collagenase. Biochem Biophys Res Commun 310(3): 889-896.

Van Lint, P. and C. Libert (2006). Matrix metalloproteinase-8: cleavage can be decisive. Cytokine Growth Factor Rev 17(4): 217-223.

Van Lint, P. and C. Libert (2007). Chemokine and cytokine processing by matrix metalloproteinases and its effect on leukocyte migration and inflammation. J Leukoc Biol 82(6): 1375-1381.

Van Lint, P., B. Wielockx, L. Puimege, A. Noel, C. Lopez-Otin and C. Libert (2005). Resistance of collagenase-2 (matrix metalloproteinase-8)-deficient mice to TNF-induced lethal hepatitis. J Immunol 175(11): 7642-7649.

Vandal, K., P. Rouleau, A. Boivin, C. Ryckman, M. Talbot and P. A. Tessier (2003). Blockade of S100A8 and S100A9 suppresses neutrophil migration in response to lipopolysaccharide. J Immunol 171(5): 2602-2609.

Vandenbroucke, R. E., E. Dejonckheere, P. Van Lint, D. Demeestere, E. Van Wonterghem, I. Vanlaere, L. Puimege, F. Van Hauwermeiren, R. De Rycke, C. Mc Guire, C. Campestre, C. Lopez-Otin, P. Matthys, G. Leclercq and C. Libert (2012). Matrix metalloprotease 8-dependent extracellular matrix cleavage at the blood-CSF barrier contributes to lethality during systemic inflammatory diseases. J Neurosci 32(29): 9805-9816.

Vasilevskis, E. E., A. Morandi, L. Boehm, P. P. Pandharipande, T. D. Girard, J. C. Jackson, J. L. Thompson, A. Shintani, S. M. Gordon, B. T. Pun and E. Wesley Ely (2011). Delirium and sedation recognition using validated instruments: reliability of bedside intensive care unit nursing assessments from 2007 to 2010. J Am Geriatr Soc 59 Suppl 2: S249-255.

Verghese, G. M., K. McCormick-Shannon, R. J. Mason and M. A. Matthay (1998). Hepatocyte growth factor and keratinocyte growth factor in the pulmonary

edema fluid of patients with acute lung injury. Biologic and clinical significance. Am J Respir Crit Care Med 158(2): 386-394.

Vernooy, J. H., J. H. Lindeman, J. A. Jacobs, R. Hanemaaijer and E. F. Wouters (2004). Increased activity of matrix metalloproteinase-8 and matrix metalloproteinase-9 in induced sputum from patients with COPD. Chest 126(6): 1802-1810.

Villar, J., J. Blanco, J. M. Anon, A. Santos-Bouza, L. Blanch, A. Ambros, F. Gandia, D. Carriedo, F. Mosteiro, S. Basaldua, R. L. Fernandez and R. M. Kacmarek (2011). The ALIEN study: incidence and outcome of acute respiratory distress syndrome in the era of lung protective ventilation. Intensive Care Med 37(12): 1932-1941.

Vogl, T., K. Tenbrock, S. Ludwig, N. Leukert, C. Ehrhardt, M. A. van Zoelen, W. Nacken, D. Foell, T. van der Poll, C. Sorg and J. Roth (2007). Mrp8 and Mrp14 are endogenous activators of Toll-like receptor 4, promoting lethal, endotoxin-induced shock. Nat Med 13(9): 1042-1049.

Voisey, J., C. D. Swagell, I. P. Hughes, J. P. Connor, B. R. Lawford, R. M. Young and C. P. Morris (2010). A polymorphism in the dysbindin gene (DTNBP1) associated with multiple psychiatric disorders including schizophrenia. Behav Brain Funct 6: 41.

Ware, L. B. and M. A. Matthay (2000). The acute respiratory distress syndrome. N Engl J Med 342(18): 1334-1349.

Waszak, P., R. Alphonse, A. Vadivel, L. Ionescu, F. Eaton and B. Thebaud (2012). Preconditioning enhances the paracrine effect of mesenchymal stem cells in preventing oxygen-induced neonatal lung injury in rats. Stem Cells Dev 21(15): 2789-2797.

Webb, H. H. and D. F. Tierney (1974). Experimental pulmonary edema due to intermittent positive pressure ventilation with high inflation pressures. Protection by positive end-expiratory pressure. Am Rev Respir Dis 110(5): 556-565.

Weed FW, M. L. (1927). Wound shock. The Medical Department of the United States Army in the World War II: 185-213.

Williams, M. C. (2003). Alveolar type I cells: molecular phenotype and development. Annu Rev Physiol 65: 669-695.

Wolf, K., R. Muller, S. Borgmann, E. B. Brocker and P. Friedl (2003). Amoeboid shape change and contact guidance: T-lymphocyte crawling through fibrillar collagen is independent of matrix remodeling by MMPs and other proteases. Blood 102(9): 3262-3269.

Woodfin, A., M. B. Voisin and S. Nourshargh (2010). Recent developments and complexities in neutrophil transmigration. Curr Opin Hematol 17(1): 9-17.

Xu, Y. L., Y. L. Liu, Q. Wang, G. Li, X. D. Lu and B. Kong (2012). Intravenous transplantation of mesenchymal stem cells attenuates oleic acid induced acute lung injury in rats. Chin Med J (Engl) 125(11): 2012-2018.

Yazdan-Ashoori, P., P. Liaw, L. Toltl, B. Webb, G. Kilmer, D. E. Carter and D. D. Fraser (2011). Elevated plasma matrix metalloproteinases and their tissue inhibitors in patients with severe sepsis. J Crit Care 26(6): 556-565.

Yilmaz, S., N. Inandiklioglu, D. Yildizdas, C. Subasi, A. Acikalin, Y. Kuyucu, I. Bayram, A. Topak, A. Tanyeli, G. Duruksu and E. Karaoz (2012). Mesenchymal Stem Cell: Does it Work in an Experimental Model with Acute Respiratory Distress Syndrome? Stem Cell Rev.

Yoon, H. K., H. Y. Cho and S. R. Kleeberger (2007). Protective role of matrix metalloproteinase-9 in ozone-induced airway inflammation. Environ Health Perspect 115(11): 1557-1563.

Yu, G., E. Kovkarova-Naumovski, P. Jara, A. Parwani, D. Kass, V. Ruiz, C. Lopez-Otin, I. O. Rosas, K. F. Gibson, S. Cabrera, R. Ramirez, S. A. Yousem, T. J. Richards, L. J. Chensny, M. Selman, N. Kaminski and A. Pardo (2012). Matrix metalloproteinase-19 is a key regulator of lung fibrosis in mice and humans. Am J Respir Crit Care Med 186(8): 752-762.

Zahm, J. M., M. Chevillard and E. Puchelle (1991). Wound repair of human surface respiratory epithelium. Am J Respir Cell Mol Biol 5(3): 242-248.

Zhou, Y., J. Y. Lee, C. M. Lee, W. K. Cho, M. J. Kang, J. L. Koff, P. O. Yoon, J. Chae, H. O. Park, J. A. Elias and C. G. Lee (2012). Amphiregulin, an epidermal growth factor receptor ligand, plays an essential role in the pathogenesis of transforming growth factor-beta-induced pulmonary fibrosis. J Biol Chem 287(50): 41991-42000.

Zuo, F., N. Kaminski, E. Eugui, J. Allard, Z. Yakhini, A. Ben-Dor, L. Lollini, D. Morris, Y. Kim, B. DeLustro, D. Sheppard, A. Pardo, M. Selman and R. A. Heller (2002). Gene expression analysis reveals matrilysin as a key regulator of pulmonary fibrosis in mice and humans. Proc Natl Acad Sci U S A 99(9): 6292-6297.